

Assessment of antibiotic resistance in soil and its link to different land use types and intensities

Dissertation

for the award of the degree

“Doctor rerum naturalium” (Dr. rer. nat.)

of the Georg-August-Universität Göttingen

within the doctoral program Biology

of the Georg-August University School of Science (GAUSS)

submitted by

Inka Marie Willms

from Westerstede

Göttingen, 2020

Thesis Committee

Dr. Heiko Nacke, Department of Genomic and Applied Microbiology, Institute of Microbiology and Genetics, Georg-August University Göttingen

PD. Dr. Michael Hoppert, Department of General Microbiology, Institute of Microbiology and Genetics, Georg-August University Göttingen

Members of the Examination Board

Referent: **Dr. Heiko Nacke**, Department of Genomic and Applied Microbiology, Institute of Microbiology and Genetics, Georg-August University Göttingen

Coreferent: **PD. Dr. Michael Hoppert**, Department of General Microbiology, Institute of Microbiology and Genetics, Georg-August University Göttingen

Further Members of the Examination Board

Prof. Dr. Rolf Daniel, Department of Genomic and Applied Microbiology, Institute of Microbiology and Genetics, Georg-August University Göttingen

Prof. Dr. Jörg Stülke, Department of General Microbiology, Institute of Microbiology and Genetics, Georg-August University Göttingen

Prof. Dr. Stefanie Pöggeler, Department of Genetics of Eukaryotic Microorganisms, Institute of Microbiology and Genetics, Georg-August University Göttingen

Prof. Dr. Kai Heimel, Department of Molecular Microbiology and Genetics, Institute of Microbiology and Genetics, Georg-August University Göttingen

Date of oral examination: 26.05.2020

“Wisdom comes out of dialogue.

You have to develop a capacity to expose your own ignorance
so that they may discover their own wisdom.”

John Goodenough

Table of contents

1. Summary	1
2. Introduction.....	3
2.1. Antibiotic synthesis and resistance in the soil microbiome.....	3
2.2. Antibiotic resistance crisis and the influence of land use practices.....	6
2.3. <i>Candidatus</i> Udaeobacter's relevance for the soil bacterial resistome	10
2.4. The Biodiversity Exploratories research project	11
2.5. Aim of the thesis	13
2.6. Literature.....	14
3. Distribution of Medically Relevant Antibiotic Resistance Genes and Mobile Genetic Elements in Soils of Temperate Forests and Grasslands Varying in Land Use	20
3.1. Supplemental information for chapter three	39
4. Discovery of Novel Antibiotic Resistance Determinants in Forest and Grassland Soil Metagenomes	54
4.1. Supplemental information for chapter four	66
5. Globally abundant <i>Candidatus</i> Udaeobacter benefits from release of antibiotics in soil and potentially performs trace gas scavenging	69
5.1. Supplemental information for chapter five	102
6. Discussion	119
6.1. Anthropogenic and natural effectors of the soil resistome	120
6.2. Novel sulfonamide and tetracycline resistance genes from forest and grassland soils	124
6.3. Antibiotic resistance properties and lifestyle features of <i>Ca. Udaeobacter</i>	128
6.4. Literature.....	133
7. Appendix	140
7.1. Declaration of plagiarism	140
7.2. Danksagung.....	141
7.3. Curriculum Vitae of Inka Marie Willms.....	143

1. Summary

Nowadays, bacterial infections pose a serious risk for human health again, due to multi-resistant pathogens insensitive to antibiotic treatment. Some of the antibiotic resistance genes (ARGs) carried by these pathogens were most likely acquired through horizontal gene transfer (HGT), as this is a more efficient means to adapt to exposition to antibiotics than the invention of protective mechanisms by mutational changes. Many of the ARGs, identified in human pathogens, are believed to originate from microorganisms colonizing soil, where antibiotic synthesis and resistance development have co-evolved for millions of years, leading to an inconceivable variety of resistance genes, also termed the soil resistome. Due to knowledge gaps in this field, the soil resistome was investigated in three different work packages within this thesis.

First, anthropogenic effectors influencing the distribution of medically relevant ARGs and mobile genetic elements (MGEs) in 300 different soils with divergent land use history were analyzed. In this context, it was determined that, except for the considered beta-lactamase genes, all target ARGs and MGEs were more frequently detected in grassland soils which are in closer proximity to human activities than the investigated forest soils. The macrolide resistance gene *mefA* and the sulfonamide resistance gene *su12* showed higher abundances in grassland soils that experienced organic fertilization. To potentially reduce the influence of organic fertilizers, which can originate from animals treated with antimicrobial compounds, it was proposed that the frequent veterinary utilization of macrolide preparations with long elimination half-lives should be limited and the prescription range of veterinary utilized sulfonamides reconsidered. However, the input of veterinary antibiotics, ARGs and antibiotic-resistant bacteria into the soil microbial community may be limited best, by reducing factory farming. This would decrease the infection frequency of livestock and thereby the amount of utilized antibiotics. Besides a significant effect of organic fertilization on *mefA* and *su12*, the abundance of the aminoglycoside resistance gene *aac(6')-Ib* increased with mowing frequency in grassland soil and a positive correlation between the beta-lactamase gene *bla_{IMP-12}* and fungal diversity was detected in beech forest soil.

In the second work package, parts of the so far unexplored variety of resistances against tetracyclines and the synthetic sulfonamides were investigated using function-based screenings of

grassland and forest soil metagenomic libraries. Thereby, four major facilitator superfamily (MFS) efflux pumps conferring tetracycline resistance and four dihydropteroate synthases (DHPS) conferring sulfonamide resistance, were identified. The DHPS genes were detected in metagenomic libraries from forest soils without a history of antibiotic exposure. They support the hypothesis that resistance genes against synthetic antibiotics naturally occur in complex microbial communities and are most likely caused by mutational changes which confer resistance as a side effect. This confirms that the soil resistome is a probable source of resistance mechanisms against novel synthetic or semisynthetic antibiotics and underlines the necessity for further screenings with respect to genes conferring resistance against critically important antibiotics.

Throughout the third work package, a globally abundant soil verrucomicrobial genus, *Candidatus Udaeobacter*, was analyzed as the composition of the bacterial community is considered the primary determinant of the composition of the soil resistome. Thereby, it was found that these largely unexplored soil bacteria show multi-resistance and benefit from the release of antibiotics in soil. A metagenome assembled genome (MAG) from a *Ca. Udaeobacter* representative that showed increased growth upon antibiotics release, was analyzed in terms of features explaining this observed behavior as well as its global distribution in soil. In this context, vitamin and amino acid transporter as well as several vitamin salvage pathways were detected. This indicates that *Ca. Udaeobacter* efficiently utilizes nutrients which are released by other soil bacteria as a consequence of antibiotic-driven cell lysis. Furthermore, a variety of different ARGs are encoded on the investigated MAG, including several multidrug and macrolide resistance pumps as well as beta-lactam resistance genes. Considering the globally high abundance of *Ca. Udaeobacter* in soil, its ARG repertoire constitutes a huge fraction of the soil resistome. Components of this repertoire can potentially be mobilized and transferred to clinically relevant strains. These mobilization events may be fostered by environmental antibiotic pollution, especially as *Ca. Udaeobacter* shows increased growth upon antibiotic exposure which further increases the proportion of the respective ARGs in the resistome. The MAG further indicated that these bacteria are able to perform hydrogen scavenging and are protected against acidic conditions which also may have contributed to the dissemination of *Ca. Udaeobacter* in soils worldwide.

2. Introduction

2.1. Antibiotic synthesis and resistance in the soil microbiome

Soil is “*the most complicated biomaterial on the planet*” (Surette and Wright 2017; Young and Crawford 2004). It is characterized by spatially and temporally fluctuating conditions including changes in soil moisture, oxygen saturation, pH, salinity, temperature, accessible nitrogen or organic carbon concentration (Fierer 2017; Heuer and Smalla 2012). This high variability across small spatial scales causes the formation of innumerable microhabitats with divergent living conditions, explaining the tremendous microbial diversity in soil. In fact, estimates of the bacterial species number per gram of soil range between 10^3 to 10^5 whereas the bacterial cell count can exceed 10^{10} (Gans, Wolinsky, and Dunbar 2005; Heuer and Smalla 2012; Schloss and Handelsman 2006; Roesch et al. 2007). As a consequence of this dense colonization by a diverse prokaryotic community, different bacterial taxa compete with each other for living space and limited resources (Hibbing et al. 2010). Since competition is a strong selection pressure, the involved players must constantly adapt to their neighbors, producing a continuously evolving, highly interdependent soil bacterial community (Hibbing et al. 2010). In this context, survival strategies such as biofilm production, motility or toxin excretion can be advantageous to prevail in many different microhabitats or to conquer specific environmental niches.

Regarding toxin excretion, synthesis of antibiotics is of special interest, as these microbial secondary metabolites have become important compounds with respect to the treatment of bacterial infections throughout the past century. They are synthesized not only by bacteria but also by fungi which further increase the selection pressure and the need for adaptation within the soil bacterial community. Besides *Penicillium*, the fungal genus which synthesizes the first discovered natural antibiotic (penicillin) (Houbraken, Frisvad, and Samson 2011; Fleming 1929), *Actinobacteria*, and in particular the genus *Streptomyces*, are notorious for the vast variety of antibiotic classes they produce. For example, *S. clavuligerus* is known to synthesize different cephalosporins which belong to the beta-lactam antibiotics, *S. aureofaciens* produces tetracycline and *Saccharopolyspora erythraea*, formerly known as *Streptomyces erythraea*, synthesizes the macrolide erythromycin (de Lima Procópio et al. 2012).

Different antibiotic classes are characterized by distinct modes of action, allowing their producers to kill rivals (bactericidal) or to inhibit their growth (bacteriostatic). Beta-lactam antibiotics for instance target the bacterial cell wall. In this context, the antibiotic binds to penicillin-binding proteins (PBPs). These enzymes represent transpeptidases which are responsible for the 4–3 cross-linkages between *N*-acetylmuramic acids, one of the two major building blocks of peptidoglycan (Macheboeuf et al. 2006). Since cell-growth is achieved through a balance between transpeptidases and autolysins, the binding of beta-lactam antibiotics to PBPs causes an imbalance in this interactive process and consequently cell lysis (Cho, Uehara, and Bernhardt 2014; Finch and Roger 2010). In contrast to beta-lactam antibiotics, tetracyclines and macrolides function bacteriostatic by inhibiting protein synthesis. Tetracyclines interact with the 30S ribosomal subunit and prevent aminoacyl-tRNAs from binding to the A-site of the ribosome, whereas macrolides block the exit path of the growing peptide chain, located on the 50S ribosomal subunit (Finch and Roger 2010). These compounds probably only make up a small part of the various antibiotics that are naturally produced in soil. However, new compounds are rarely discovered nowadays, probably because they are synthesized by uncultivable species, making the screening process more complicated, labor-intensive and thereby unprofitable (Ling et al. 2015).

Soil bacterial communities can adapt to selective pressure, generated by antibiotic production via development of defense mechanisms encoded on antibiotic resistance genes (ARGs). Considering that this co-evolution has been taking place for millions of years, soil bacteria have had plenty of time to evolve an inconceivable variety of ARGs, the so-called soil bacterial resistome, which still conceals a vast array of unknown resistance mechanisms. In fact, novel ARGs are frequently discovered within soils by functional screenings based on metagenomic DNA or via bioinformatic analysis of metagenomic data (Lau et al. 2017; Arango-Argoty et al. 2018; Berglund et al. 2019). The corresponding resistance mechanisms either comprise intrinsic properties, allowing a general response to toxic molecules, or are received through horizontal gene transfer (HGT) and typically target specific antibiotics which is termed acquired resistance (Surette and Wright 2017). Intrinsic features constitute permeability barriers of the cell envelope which restrict antimicrobial access to target sites (e.g. the outer membrane of gram-negative bacteria), broad spectrum efflux pumps, chromosomally encoded antibiotic degradation mechanisms and the upregulation of mutational changes throughout the complete chromosome (Surette and Wright 2017; Zgurskaya, López, and Gnanakaran 2015). Acquired resistance mechanisms

include the expression of alternative target proteins, enzymes which degrade the antimicrobial agent and compound specific efflux pumps (Surette and Wright 2017; van Hoek et al. 2011). These resistance mechanisms are often encoded on mobile genetic elements (MGEs) which enable transmission via HGT throughout bacterial communities. Intrinsic resistance genes can also become acquired ARGs through integration into MGEs, referred to as gene mobilization (Bengtsson-Palme, Kristiansson, and Larsson 2018; Hall et al. 2017). A recent example for this phenomenon is the novel mobile sulfonamide resistance gene *sul4* that encodes an alternative dihydropteroate synthase and was detected within a class 1 integron (Razavi et al. 2017). The difference between intrinsic and acquired resistance mechanisms and the role of MGEs is depicted in Figure 1.

Three types of MGEs, known to be relevant with respect to the spread of ARGs, are conjugative plasmids, transposons and integrons. A well-known group of conjugative broad-host range plasmids are the members of the incompatibility group 1, also called IncP-1 plasmids. These plasmids can spread amongst virtually all gram-negative bacterial phyla and have also been detected in some gram-positive species (Popowska and Krawczyk-Balska 2013, Musovic et al. 2006). They are broadly distributed throughout all sorts of environments, including hospitals, wastewater treatment plants, manure as well as soil. They can encode a large variety of different accessory genes, including diverse families of ARGs (Popowska and Krawczyk-Balska 2013). Interactions between different types of MGEs can increase the efficiency of HGT (Dionisio, Zilhão, and Gama 2019). For instance, the IncP-1 plasmids pTB11 and pSP21 encode the transposon Tn402 which contains a class 1 integron, carrying aminoglycoside resistance genes (Popowska and Krawczyk-Balska 2013; Schlüter et al. 2007). Transposons are elements, which can translocate DNA between plasmids and chromosomes, via transposases and terminal inverted repeat regions (Partridge et al. 2018). Integrons are immobile, except when integrated into a transposon or plasmid. They capture gene cassettes into an attachment site downstream of a promoter with the action of an encoded integrase (Partridge et al. 2018).

In general, MGEs allow by far more efficient adaptation to environmental challenges than the invention of novel resistance mechanisms via mutational changes (Jain et al. 2003; Hermisson and Pennings 2005; Heuer and Smalla 2012).

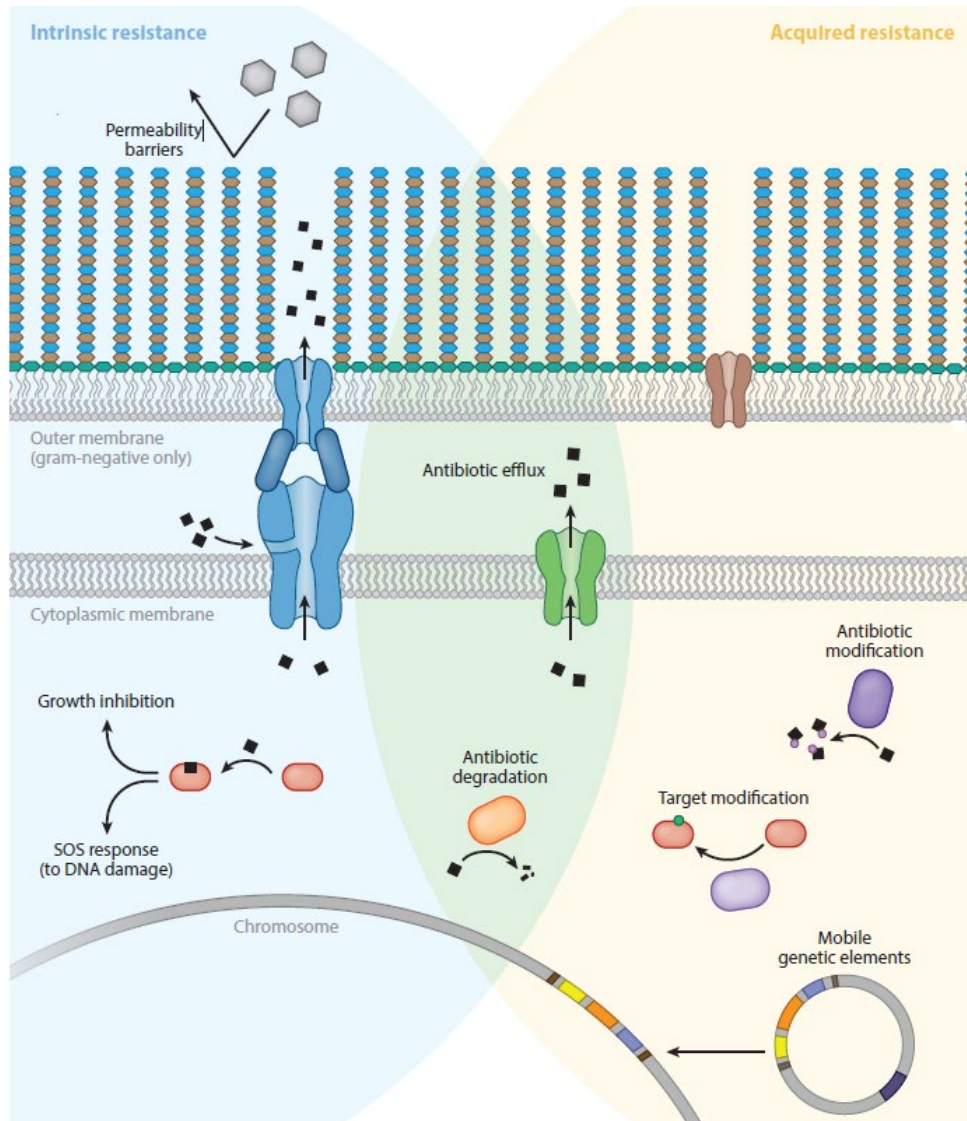


Figure 1 The intrinsic and acquired antibiotic resistomes. Intrinsic mechanisms, include drug permeability, efflux, degradation, and upregulation of genomic mutation. Acquired resistance includes altered targets, drug inactivation and efflux. The latter were mostly received through horizontal gene transfer from other species and genera. Adapted from Surette and Wright, 2017.

2.2. Antibiotic resistance crisis and the influence of land use practices

Nowadays, we are in an antibiotic resistance crisis as antibiotic-resistant bacteria (ARBs) have become a medical priority problem. Infections that were treatable in the past cause acute problems today and, in increasing numbers, even death. In fact, it is estimated that ARBs are responsible for 670,000 infections in Europe per year, whereof 33,000 lead to the patient's death (Cassini et al. 2019). Furthermore, they are the cause for 870,000 years under disability adjusted conditions and lead in

Europe to health care associated costs of 1.5 billion Euro, yearly (Cassini et al. 2019, Antofianzas and Goossens 2019). Bacterial pathogens are often not only drug resistant but can contain MGEs stocked with several different resistance mechanisms, rendering them multidrug resistant (MDR) (Partridge et al. 2018). Examples for bacteria that are frequently MDR are the ESKAPEE pathogens *Enterococcus faecium*, *Staphylococcus aureus*, *Klebsiella pneumoniae*, *Acinetobacter baumannii*, *Pseudomonas aeruginosa*, *Enterobacter spp.* and *Escherichia coli* (Santajit and Indrawattana 2016; Partridge et al. 2018). Another name that should be mentioned in this context is MDR *Clostridium difficile* which can cause infections of the gastro-intestinal tract as a consequence of an imbalance in the intestinal microflora, due to antibiotic treatment (Spigaglia, Mastrantonio, and Barbanti 2018). The ESKAPEE pathogens as well as *C. difficile* are notorious with respect to globally occurring nosocomial (hospital acquired) infections which are extremely difficult to treat and therefore a serious threat to human health.

Even though the highest density of ARGs is prevalent in bacteria from clinical settings (Surette and Wright 2017), the true origin of the respective genes is in most cases still unclear. As outlined above, the soil bacterial resistome comprises an inconceivably large variety of resistance genes which is very likely the origin of many pathogen encoded ARGs. This theory is supported by the mentioned fact that intrinsic resistance mechanisms can be mobilized and acquisition of ARGs through HGT is by far more efficient than the invention of novel resistance mechanisms via mutational changes. In fact, it has been discovered that specific ARGs which are encoded by known human pathogens, such as *K. pneumoniae* or *Salmonella typhimurium*, show 100% identity to genes of soil bacteria (Forsberg et al. 2012). Furthermore, evidence suggests that ARGs can be transferred from harmless soil bacteria to hazardous pathogens via HGT events (Forsberg et al. 2012; Pärnänen et al. 2016). Therefore, it can be concluded that ARGs and ARBs can spread to humans through direct or indirect contact with the soil microbial community (EMA 2018; Forsberg et al. 2012; Canteón 2009). These circumstances underline the importance of the in depth study of the soil resistome in order to identify unknown resistance mechanisms that may become problematic in the future.

The occurrence of MDR pathogens is closely linked to human use of antibiotics since the middle of the 20th century (Surette and Wright 2017). An accumulation of ARGs in MGEs and their efficient spread over species borders probably occurs much more frequently nowadays because of the selection

pressure, established through anthropogenic antibiotic pollution (Bengtsson-Palme, Kristiansson, and Larsson 2018). Particularly relevant in this regard is the treatment of livestock in agriculture, a practice that is quite common, due to the prevalent factory farming and the associated higher infection risk of farm animals. A major fraction of all human diseases develops in animals (van Doorn 2014) that are potentially colonized by bacteria which have evolved resistance mechanisms as a result of continuous antibiotic exposure. Humans can pick up these antibiotic resistant pathogens via the food chain and fall sick with hard-to-treat infections. An example for such a food-borne infection is campylobacteriosis, a gastro-intestinal disease that is caused by *Campylobacter* species which are very frequently resistant to fluoroquinolones (EFSA and ECDC 2019) (bacteriocidal antibiotics that inhibit DNA replication). Another reason why antibiotic treatment of livestock is problematic is the large proportion of antibiotics that are excreted functionally by the treated animals. Consequently, manure is often enriched with the active compounds as well as with bacteria that have developed resistance against these harmful substances (Berendsen et al. 2015). When manure is applied as organic fertilizer, an increase in the abundance of medically relevant ARGs and MGEs within the soil microbial community can occur (Graham et al. 2016; Jechalke et al. 2014; Binh et al. 2007). Additionally, antibiotics, ARBs and ARGs can disseminate throughout the environment via surface water run offs, dust and migrating wild animals (Allen et al. 2010). This leads to a circulation of ARGs between soil, human and livestock, driven by the evolutionary pressure established through antibiotic application or pollution (Figure 2).

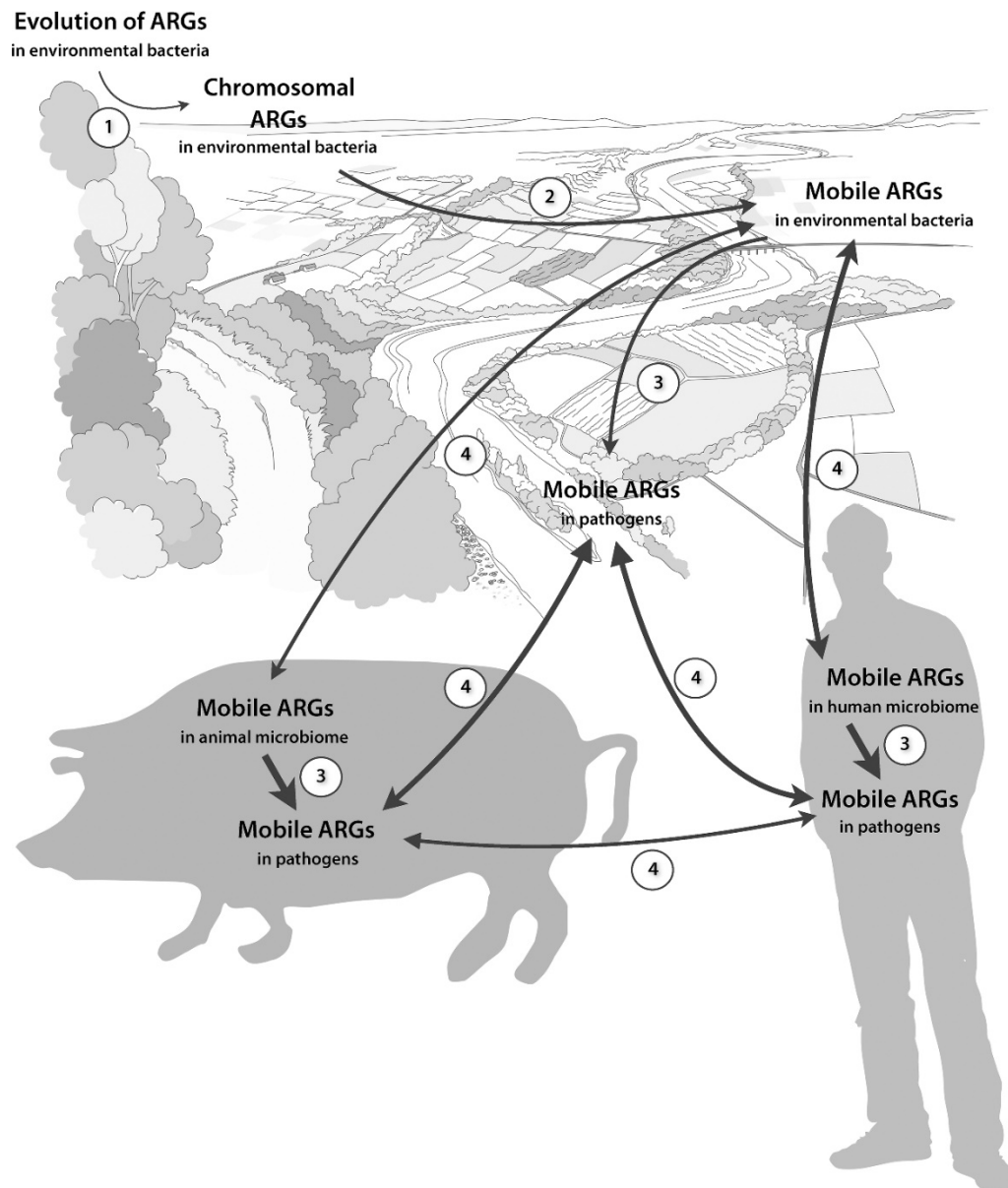


Figure 2. The role of the environment in the recruitment of antibiotic resistance genes (ARGs) to human pathogens. This takes place in four major steps: (1) emergence of novel resistance factors in the environment, (2) mobilization onto mobile genetic elements, (3) transfer of ARGs to human pathogens, and (4) dissemination of ARGs into the human microbiome. The arrow widths approximately mirror the estimated frequency of each event. Adapted from Bengtsson-Palme, Kristiansson, and Larsson 2018.

To find ways to counteract the dissemination of ARGs, it is necessary to consider the contribution of a variety of parameters, many of which are presently still elusive. For example, detailed information on the overall contribution of land use types and intensities that influence the development and transmission of ARGs in soil microbiomes need to be evaluated. Currently, most studies that address this issue focus on a small number of study plots, or set up microcosms from just one or two

soils, and simulate land use by e.g. spiking manure with antibiotics. However, data from various soil sites over a large spatial scale with a variety of realistic land use histories is still lacking. This would allow a deeper understanding of the effect of different land use types and intensities on the abundance and transmission of ARGs and MGEs throughout soil ecosystems which could be, together with data on other environmental resistomes, useful for the development of approaches to overcome the antibiotic resistance crisis.

2.3. *Candidatus Udaeobacter*'s relevance for the soil bacterial resistome

A metagenomic survey conducted by Forsberg et al. (2014) indicates that bacterial community composition is the primary determinant of ARG content in soil. Understanding how different bacterial species are involved in shaping soil resistomes requires knowledge about their lifestyle, genetic content and global abundance. Nevertheless, soil microbiomes are very challenging to study and even referred to as a black box (Tiedje et al. 1999; Cortois and De Deyn 2012). The interdependence within the soil microbial community and the diverse abiotic conditions in soil ecosystems are important reasons why the majority of soil bacteria are still uncultivated. Furthermore, due to soil microdiversity, assigning metagenomic data precisely to distinct species is very complex and bioinformatically challenging.

It is estimated that only 1% of microbial soil species have been cultivated so far (Gans, Wolinsky, and Dunbar 2005; Pedrós-Alió and Manrubia 2016). One example for an uncultivable soil bacterial genus is *Candidatus Udaeobacter* (Brewer et al. 2016). Even though soil bacterial communities are commonly very diverse in response to parameters like oxygen availability, soil texture, soil moisture and pH (Kaiser et al. 2016; Delgado-Baquerizo et al. 2018), *Ca. Udaeobacter* was found to be amongst the 2% of bacterial phylotypes accounting for almost half of the soil bacterial communities globally (Delgado-Baquerizo et al. 2018). However, bacteria of the respective phylum (*Verrucomicrobia*) have long been excluded from studies uncovering the composition of soil microbial communities, due to primer-template mismatches (Bergmann et al. 2011). Therefore, only very limited information about the distribution of these bacteria is available. Nonetheless, based on a recently published metagenome assembled genome (MAG) from *Ca. Udaeobacter copiosus* (Brewer et al. 2016), insights into the genetic content and possible lifestyle features were revealed. The MAG indicated that *Ca. Udaeobacter copiosus* exhibits auxotrophies for many putative vitamin and costly amino acid synthesis pathways.

Furthermore, the complete genome of this species is estimated to encode approximately 2.81 Mbp (Brewer et al. 2016). Typically, ubiquitous soil bacteria encode for larger genomes enabling flexibility toward rapidly changing conditions within their complex habitat (Barberán et al. 2014; Konstantinidis and Tiedje 2004). However, *Ca. Udaeobacter* seems to compensate for its limited genetic content with efficient uptake mechanisms comprising a high density of encoded peptide and amino acid transporters (Brewer et al. 2016). Hence, this species probably favors uptake of essential metabolites over synthesis. Being dependent on extracellular metabolites in a densely colonized ecosystem such as soil (Fierer 2017), likely entails increased influx and therefore vulnerability to toxic agents secreted by microorganisms competing for scarce nutrients (Leisner, Jørgensen, and Middelboe 2016). Therefore, a strategy for protection against harmful substances becomes advantageous and has potentially contributed to the evolutionary success of *Ca. Udaeobacter*. This theory is supported by the enrichment of beta-lactam resistance genes, identified through functional metagenomic screening, within the phylum *Verrucomicrobia* (Forsberg et al. 2014). However, the actual response of *Ca. Udaeobacter* to antibiotics release has so far not been studied and therefore remains unclear. If the propagated hypothesis about its antibiotic resistance properties holds true, *Ca. Udaeobacter* is an important player to consider when analyzing the abundance and spread of ARGs due to its high occurrence in soils globally.

2.4. The Biodiversity Exploratories research project

To evaluate the interconnectedness between different species, the influence of biodiversity on ecosystem processes and the effects of land use change on biodiversity, three large scale research sites, termed Biodiversity Exploratories, were established in 2006. They serve as study regions for scientific working groups covering various research fields such as microbiology, zoology and botany, and therefore allow comprehensive interdisciplinary research (Fischer et al. 2010). The UNESCO Biosphere Reserve Schorfheide-Chorin in Brandenburg, the National Park Hainich and surrounding areas (Hainich-Dün) in Thuringia and the UNESCO Biosphere Reserve Schwäbische-Alb in Baden-Württemberg, constitute the three exploratories which are distributed on a north-east to south-west gradient (Figure 3) (Fischer et al. 2010). The Schorheide-Chorin exploratory comprises a postglacial landscape with many wetlands, the hilly Hainich-Dün exploratory is characterized by the largest

contiguous deciduous forest in Germany, and the Schwäbische Alb contains sub-montane to montane plateaus and a higher proportion of grasslands than forests (Fischer et al. 2010; BEO 2019).

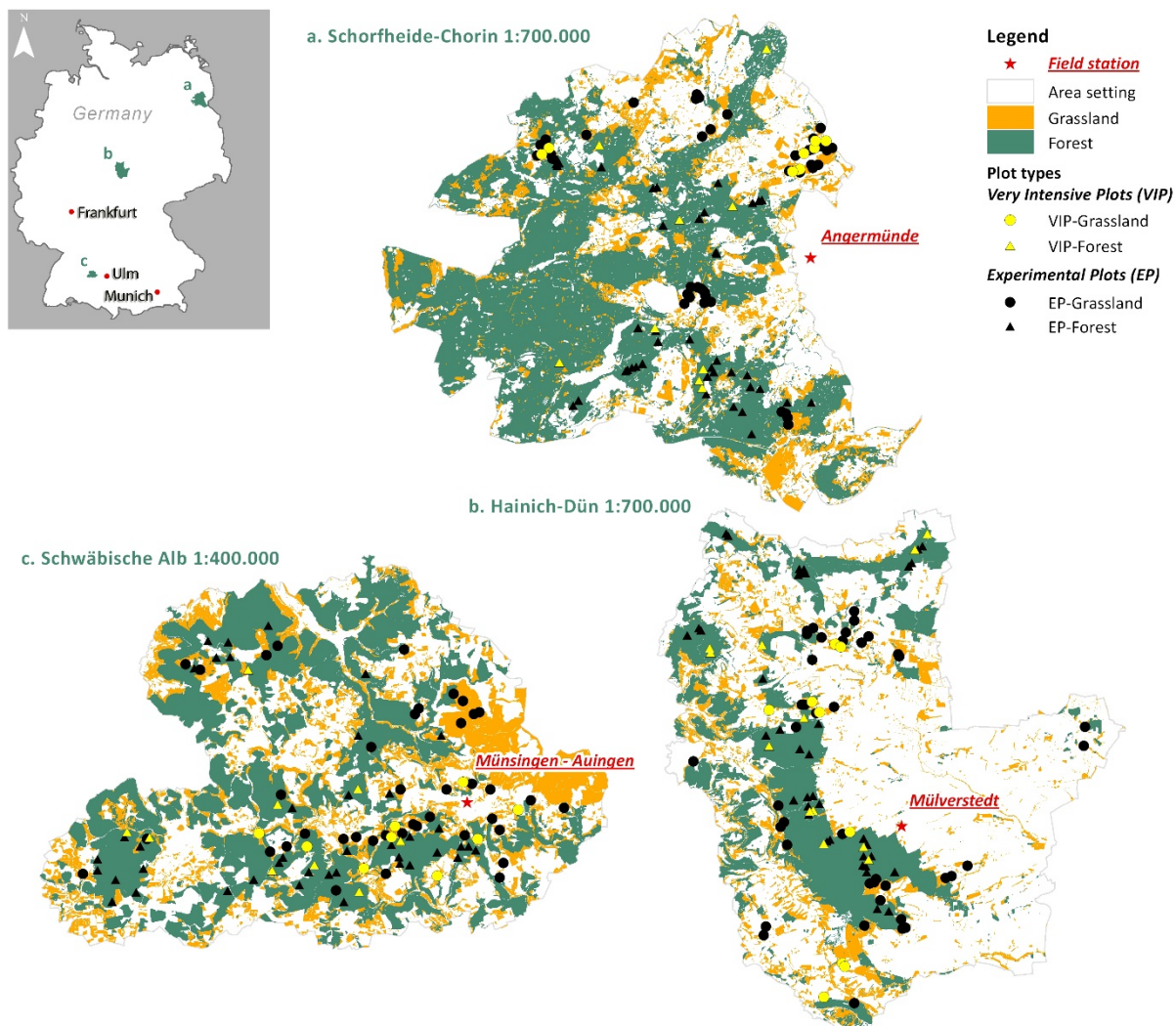


Figure 3 Locations, landscapes and sample plots of the three Biodiversity Exploratories. The figure was generated by the coordination office of the Biodiversity Exploratories (BEO).

All three exploratories have unique features that distinguish them from each other and together reflect a variety of different landscapes, soil parameters as well as land use types and intensities. Each exploratory is subdivided into 50 grassland (50 m x 50 m) and 50 forest (100 m x 100 m) experimental plots (EPs). The ten most intensively studied grassland and forest EPs of each exploratory are further referred to as very intensive plots (VIPs). Since 2008, a soil sampling campaign has taken place in all exploratories every three years, which enables comparability of the research results from the participating scientific groups. In this context, 14 soil cores from the upper mineral soil were collected

at each EP along two 20 m (grassland EPs) or 40 m transects (forest EPs) (Solly et al. 2014). Furthermore, the landowners of the grassland EPs are interviewed annually about the kind and number of grazing animals, mowing frequencies as well as about the type, amount and frequency of fertilizer application (Vogt et al. 2019). Characteristics like the predominant tree species and management type of the forest EPs are determined, as well. The evaluated information is standardized and available to all participating researchers. This enables a multidisciplinary data interpretation and underlines the advantages of the Biodiversity Exploratories.

2.5. Aim of the thesis

This work was aimed at identifying previously unknown ARGs as well as gaining a deeper understanding on the factors that influence the transmission and accumulation of ARGs in the soil microbiome. In this context, a major focus is the globally abundant soil bacterial genus *Ca. Udaeobacter*, which potentially affects soil resistomes worldwide.

Three projects, comprising an array of appropriate molecular methods, were designed to address the mentioned objectives. In the first project, the occurrence and abundance of medically relevant ARGs and MGEs was determined in soil DNA from 300 forest and grassland plots via quantitative real-time PCR. The corresponding data were evaluated with respect to correlations with land use types and intensities as well as plot characteristics such as pH, water content or dominant tree species. In the second project, functional screenings of forest and grassland soil metagenomic libraries were conducted to identify novel ARGs. Importantly, besides natural antibiotics also synthetic antimicrobials were used as selective compounds during screening. The third project was focused on *Ca. Udaeobacter* and its response to antibiotics release. In this context, lifestyle characteristics of this largely unexplored verrucomicrobial genus were evaluated in terms of antibiotic resistance and other specific strategies that potentially have contributed to its high and widespread occurrence in soils and thus have influenced the global soil resistance pattern.

2.6. Literature

- Allen HK, Donato J, Wang HH, Cloud-Hansen KA, Davies J, Handelsman J. 2010. Call of the wild: antibiotic resistance genes in natural environments. *Nat Rev Microbiol* 8:251–259.
- Antoñanzas F, Goossens H. 2019. The economics of antibiotic resistance: a claim for personalised treatments. *Eur J Heal Econ* 20:483–485.
- Arango-Argoty G, Garner E, Pruden A, Heath LS, Vikesland P, Zhang L. 2018. DeepARG: a deep learning approach for predicting antibiotic resistance genes from metagenomic data. *Microbiome* 6:23.
- Barberán A, Ramirez KS, Leff JW, Bradford MA, Wall DH, Fierer N. 2014. Why are some microbes more ubiquitous than others? Predicting the habitat breadth of soil bacteria. *Ecol Lett* 17:794–802.
- Bengtsson-Palme J, Kristiansson E, Larsson DGJ. 2018. Environmental factors influencing the development and spread of antibiotic resistance. *FEMS Microbiol Rev* 42:fx053.
- BEO. 2019. Exploratories. Accessed December 12, 2019. <https://www.biodiversity-exploratories.de/1/exploratories/>.
- Berendsen BJA, Wegh RS, Memelink J, Zuidema T, Stolker LAM. 2015. The analysis of animal faeces as a tool to monitor antibiotic usage. *Talanta* 132:258–268.
- Berglund F, Österlund T, Boulund F, Marathe NP, Larsson DGJ, Kristiansson E. 2019. Identification and reconstruction of novel antibiotic resistance genes from metagenomes. *Microbiome* 7:52.
- Bergmann GT, Bates ST, Eilers KG, Lauber CL, Caporaso JG, Walters WA, Knight R, Fierer N. 2011. The under-recognized dominance of *Verrucomicrobia* in soil bacterial communities. *Soil Biol Biochem* 43:1450–1455.
- Binh CTT, Heuer H, Gomes NCM, Kotzerke A, Fulle M, Wilke B-M, Schlöter M, Smalla K. 2007. Short-term effects of amoxicillin on bacterial communities in manured soil. *FEMS Microbiol Ecol* 62:290–302.
- Brewer TE, Handley KM, Carini P, Gilbert JA, Fierer N. 2016. Genome reduction in an abundant and

- ubiquitous soil bacterium '*Candidatus Udaeobacter copiosus*'. Nat Microbiol 2:16198.
- Canteón R. 2009. Antibiotic resistance genes from the environment: a perspective through newly identified antibiotic resistance mechanisms in the clinical setting. Clin Microbiol Infect 15:20–25.
- Cassini A, Högberg LD, Plachouras D, Quattrocchi A, Hoxha A, Simonsen GS, Colomb-Cotinat M, Kretzschmar ME, Devleeschauwer B, Cecchini M, Ouakrim DA, Oliveira TC, Struelens MJ, Suetens C, Monnet DL and the Burden of AMR Collaborative Group. 2019. Attributable deaths and disability-adjusted life-years caused by infections with antibiotic-resistant bacteria in the EU and the European Economic Area in 2015: a population-level modelling analysis. Lancet Infect Dis 19:56–66.
- Cho H, Uehara T, Bernhardt TG. 2014. Beta-Lactam Antibiotics Induce a Lethal Malfunctioning of the Bacterial Cell Wall Synthesis Machinery. Cell 159: 1300–1311.
- Cortois R, De Deyn GB. 2012. The curse of the black box. Plant Soil 350:27–33.
- Delgado-Baquerizo M, Oliverio AM, Brewer TE, Benavent-González A, Eldridge DJ, Bardgett RD, Maestre FT, Singh BK, Fierer N. 2018. A global atlas of the dominant bacteria found in soil. Science 359:320–325.
- Dionisio F, Zilhão R, Gama JA. 2019. Interactions between plasmids and other mobile genetic elements affect their transmission and persistence. Plasmid 102:29–36.
- Van Doorn HR. 2014. Emerging infectious diseases. Medicine (Abingdon) 42:60–63.
- EFSA, ECDC. 2019. The European Union summary report on antimicrobial resistance in zoonotic and indicator bacteria from humans, animals and food in 2017. EFSA J 17:e05598.
- EMA. 2018. Antimicrobial resistance in the environment: considerations for current and future risk assessment of veterinary medicinal products.
- Fierer N. 2017. Embracing the Unknown: Disentangling the Complexities of the Soil Microbiome. Nature Reviews Microbiology 15:579–90.
- Finch RG, Greenwood D, Whitley R, Norrby SR. 2010. Antibiotic and Chemotherapy : Anti-Infective Agents and Their Use in Therapy. 9th ed. Saunders, Edinburgh, NY.

- Fischer M, Bossdorf O, Gockel S, Hänsel F, Hemp A, Hessenmöller D, Korte G, Nieschulze J, Pfeiffer S, Prati D, Renner S, Schöning I, Schumacher U, Wells K, Buscot F, Kalko EKV, Linsenmair KE, Schulze E-D, Weisser WW. 2010. Implementing large-scale and long-term functional biodiversity research: The Biodiversity Exploratories. *Basic Appl Ecol* 11:473–485.
- Fleming A. 1929. On the Antibacterial Action of Cultures of a *Penicillium*, with Special Reference to Their Use in the Isolation of *B. Influenzae*. *Br. J. Exp. Pathol.* 10: 226–36.
- Forsberg KJ, Patel S, Gibson MK, Lauber CL, Knight R, Fierer N, Dantas G. 2014. Bacterial phylogeny structures soil resistomes across habitats. *Nature* 509:612–616.
- Forsberg KJ, Reyes A, Wang B, Selleck EM, Sommer MOA, Dantas G. 2012. The shared antibiotic resistome of soil bacteria and human pathogens. *Science* 337:1107–11.
- Gans J, Wolinsky M, Dunbar J. 2005. Computational Improvements Reveal Great Bacterial Diversity and High Metal Toxicity in Soil. *Science* 309: 1387–90.
- Graham DW, Knapp CW, Christensen BT, McCluskey S, Dolfing J. 2016. Appearance of β -lactam Resistance Genes in Agricultural Soils and Clinical Isolates over the 20th Century. *Sci Rep* 6:21550.
- Hall JPJ, Williams D, Paterson S, Harrison E, Brockhurst MA. 2017. Positive selection inhibits gene mobilization and transfer in soil bacterial communities. *Nat Ecol Evol* 1:1348–1353.
- Hermisson J, Pennings PS. 2005. Soft Sweeps : Molecular Population Genetics of Adaptation From Standing Genetic Variation. *Genetics* 169:2335–2352.
- Heuer H, Smalla K. 2012. Plasmids Foster Diversification and Adaptation of Bacterial Populations in Soil. *FEMS Microbiol. Rev* 36: 1083–1104.
- Hibbing ME, Fuqua C, Parsek MR, Peterson SB. 2010. Bacterial Competition: Surviving and Thriving in the Microbial Jungle. *Nat. Rev. Microbiol* 8:15–25.
- Van Hoek AHAM, Mevius D, Guerra B, Mullany P, Roberts AP, Aarts HJM. 2011. Acquired Antibiotic Resistance Genes: An Overview. *Front Microbiol* 2:203.
- Houbraken J, Frisvad JC, Samson RA. 2011. Fleming's Penicillin Producing Strain Is Not *Penicillium*

Chrysogenum but *P. Rubens*. IMA Fungus 2: 87–95.

Jain R, Rivera MC, Moore JE, Lake JA. 2003. Horizontal Gene Transfer Accelerates Genome Innovation and Evolution. Mol Biol Evol 20:1598–1602.

Jechalke S, Heuer H, Siemens J, Amelung W, Smalla K. 2014. Fate and effects of veterinary antibiotics in soil. Trends Microbiol 22:536-545.

Kaiser K, Wemheuer B, Korolkow V, Wemheuer F, Nacke H, Schöning I, Schrumpf M, Daniel R. 2016. Driving forces of soil bacterial community structure, diversity, and function in temperate grasslands and forests. Sci Rep 6:33696.

Konstantinidis KT, Tiedje JM. 2004. Trends between gene content and genome size in prokaryotic species with larger genomes. Proc Natl Acad Sci U S A 101:3160–3165.

Lau CH-F, van Engelen K, Gordon S, Renaud J, Topp E. 2017. Novel Antibiotic Resistance Determinants from Agricultural Soil Exposed to Antibiotics Widely Used in Human Medicine and Animal Farming. Appl Environ Microbiol 83:e00989-17.

Leisner JJ, Jørgensen NOG, Middelboe M. 2016. Predation and selection for antibiotic resistance in natural environments. Evol Appl 9:427–434.

De Lima Procópio RE, da Silva IR, Martins MK, de Azevedo JL, de Araújo JM. 2012. Antibiotics Produced by *Streptomyces*. Bras J Infect Dis 16:466–71.

Ling LL, Schneider T, Peoples AJ, Spoering AL, Engels I, Conlon BP, Mueller A, Schäberle TF, Hughes DE, Epstein S, Jones M, Lazarides L, Steadman VA, Cohen DR, Felix CR, Fetterman KA, Millett WP, Nitti AG, Zullo AM, Chen C, Lewis K. 2015. A new antibiotic kills pathogens without detectable resistance. Nature 517:455–459.

Macheboeuf P, Contreras-Martel C, Job V, Dideberg O, Dessen A. 2006. Penicillin Binding Proteins: Key Players in Bacterial Cell Cycle and Drug Resistance Processes. FEMS Microbiol Rev 30:673–91.

Musovic S, Oregaard G, Kroer N, Sørensen SJ. 2006. Cultivation-Independent Examination of Horizontal Transfer and Host Range of an IncP-1 Plasmid among Gram-Positive and Gram-

- Negative Bacteria Indigenous to the Barley Rhizosphere. *Appl Environ Microbiol* 72:6687–6692.
- Pärnänen K, Karkman A, Tamminen M, Lyra C, Hultman J, Paulin L, Virta M. 2016. Evaluating the mobility potential of antibiotic resistance genes in environmental resistomes without metagenomics. *Sci Rep* 6:35790.
- Partridge SR, Kwong SM, Firth N, Jensen SO. 2018. Mobile Genetic Elements Associated with Antimicrobial Resistance. *Clin Microbiol Rev* 31:e00088-17.
- Pedrós-Alió C, Manrubia S. 2016. The vast unknown microbial biosphere. *Proc Natl Acad Sci U S A* 113:6585–7.
- Popowska M, Krawczyk-Balska A. 2013. Broad-host-range IncP-1 plasmids and their resistance potential. *Front Microbiol* 4:44.
- Razavi M, Marathe NP, Gillings MR, Flach C-F, Kristiansson E, Joakim Larsson DG. 2017. Discovery of the fourth mobile sulfonamide resistance gene. *Microbiome* 5:160.
- Roesch LFW, Fulthorpe RR, Riva A, Casella G, Hadwin AKM, Kent AD, Daroub SH, Camargo FAO, Farmerie WG, Triplett EW. 2007. Pyrosequencing enumerates and contrasts soil microbial diversity. *ISME J* 1: 283–290.
- Santajit S, Indrawattana N. 2016. Mechanisms of Antimicrobial Resistance in ESKAPE Pathogens. *Biomed Res Int* 2016:1–8.
- Schloss PD, Handelsman J. 2006. Toward a Census of Bacteria in Soil. *PLOS Comput Biol* 2:e92.
- Schlüter A, Szczepanowski R, Pühler A, Top EM. 2007. Genomics of IncP-1 antibiotic resistance plasmids isolated from wastewater treatment plants provides evidence for a widely accessible drug resistance gene pool. *FEMS Microbiol Rev* 31:449–477.
- Solly EF, Schöning I, Boch S, Kandeler E, Marhan S, Michalzik B, Müller J, Zscheischler J, Trumbore SE, Schrumpf M. 2014. Factors controlling decomposition rates of fine root litter in temperate forests and grasslands. *Plant Soil* 382:203–218.
- Spigaglia P, Mastrantonio P, Barbanti F. 2018. Antibiotic resistances of *Clostridium difficile*. *Adv in Exp Med Biol* 1050:137-159.

- Surette MD., Wright GD. 2017. Lessons from the Environmental Antibiotic Resistome. *Annu. Rev. Microbiol* 71:309–29.
- Tiedje JM, Asuming-Brempong S, Nüsslein K, Marsh TL, Flynn SJ. 1999. Opening the black box of soil microbial diversity. *Appl Soil Ecol* 13:109-122.
- Vogt J, Klaus VH, Both S, Fürstenau C, Gockel S, Gossner MM, Heinze J, Hemp A, Hölzel N, Jung K, Kleinebecker T, Lauterbach R, Lorenzen K, Ostrowski A, Otto N, Prati D, Renner S, Schumacher U, Seibold S, Simons N, Steitz I, Teuscher M, Thiele J, Weithmann S, Wells K, Wiesner K, Ayasse M, Blüthgen N, Fischer M, Weisser WW. 2019. Eleven years' data of grassland management in Germany. *Biodivers data J* 7:e36387.
- Young IM, Crawford JW. 2004. Interactions and Self-Organization in the Soil-Microbe Complex. *Science* 304:1634–1637.
- Zgurskaya HI, López CA, Gnanakaran S. 2015. Permeability Barrier of Gram-Negative Cell Envelopes and Approaches To Bypass It. *ACS Infect Dis* 1:512–522.

3. Distribution of Medically Relevant Antibiotic Resistance Genes and Mobile Genetic Elements in Soils of Temperate Forests and Grasslands Varying in Land Use

Inka M. Willms¹, Jingyue Yuan¹, Caterina Penone², Kezia Goldmann³, Juliane Vogt⁴, Tesfaye Wubet^{5,6}, Ingo Schöning⁷, Marion Schrumpf⁷, François Buscot^{3,6} and Heiko Nacke^{1*}

¹ Department of Genomic and Applied Microbiology and Göttingen Genomics Laboratory, Institute of Microbiology and Genetics, Georg-August University of Göttingen, D-37077 Göttingen, Germany

² Institute of Plant Sciences, University of Bern, CH-3013 Bern, Switzerland

³ Department of Soil Ecology, UFZ – Helmholtz Centre for Environmental Research, D-06120 Halle-Saale, Germany

⁴ Terrestrial Ecology Research Group, Department of Ecology and Ecosystem Management, Technical University of Munich, D-85354 Freising, Germany

⁵ Department of Community Ecology, UFZ – Helmholtz Centre for Environmental Research, D-06120 Halle-Saale, Germany

⁶ German Centre for Integrative Biodiversity Research (iDiv) Halle-Jena-Leipzig, D-04103 Leipzig, Germany

⁷ Max Planck Institute for Biogeochemistry, D-07745 Jena, Germany





Genes (2020), 11:150

Author contribution to the work:

Conceptualization, I.M.W and H.N.; formal analysis, I.M.W, J.Y, C.P. and H.N.; investigation, I.M.W, J.Y, K.G.; resources, H.N., M.S., T.W. and F.B.; data curation, I.M.W, K.G., I.S. J.V. ;writing—original draft preparation, I.M.W and H.N.; writing—review and editing, I.M.W, H.N., K.G., J.V., I.S., M.S., T.W. and F.B. ; visualization, I.M.W; supervision, I.M.W and H.N.; project administration, H.N.; funding acquisition, H.N.

Article

Distribution of Medically Relevant Antibiotic Resistance Genes and Mobile Genetic Elements in Soils of Temperate Forests and Grasslands Varying in Land Use

Inka M. Willms ¹, Jingyue Yuan ¹, Caterina Penone ² , Kezia Goldmann ³ , Juliane Vogt ⁴, Tesfaye Wubet ^{5,6}, Ingo Schöning ⁷ , Marion Schruppf ⁷, François Buscot ^{3,6}  and Heiko Nacke ^{1,*}

- ¹ Department of Genomic and Applied Microbiology and Göttingen Genomics Laboratory, Institute of Microbiology and Genetics, Georg-August University of Göttingen, D-37077 Göttingen, Germany; inka.willms@uni-goettingen.de (I.M.W.); jingyue.yuan@stud.uni-goettingen.de (J.Y.)
- ² Institute of Plant Sciences, University of Bern, CH-3013 Bern, Switzerland; caterina.penone@ips.unibe.ch
- ³ Department of Soil Ecology, UFZ—Helmholtz Centre for Environmental Research, D-06120 Halle-Saale, Germany; kezia.goldmann@ufz.de (K.G.); francois.buscot@ufz.de (F.B.)
- ⁴ Terrestrial Ecology Research Group, Department of Ecology and Ecosystem Management, Technical University of Munich, D-85354 Freising, Germany; juliane.vogt@tum.de
- ⁵ Department of Community Ecology, UFZ—Helmholtz Centre for Environmental Research, D-06120 Halle-Saale, Germany; tesfaye.wubet@ufz.de
- ⁶ German Centre for Integrative Biodiversity Research (iDiv) Halle-Jena-Leipzig, D-04103 Leipzig, Germany
- ⁷ Max Planck Institute for Biogeochemistry, D-07745 Jena, Germany; Ingo.Schoening@bgc-jena.mpg.de (I.S.); mschrumpf@bgc-jena.mpg.de (M.S.)
- * Correspondence: hnacke@gwdg.de; Tel.: +49-551-3933841

Received: 18 December 2019; Accepted: 24 January 2020; Published: 30 January 2020



Abstract: Antibiotic-resistant pathogens claim the lives of thousands of people each year and are currently considered as one of the most serious threats to public health. Apart from clinical environments, soil ecosystems also represent a major source of antibiotic resistance determinants, which can potentially disseminate across distinct microbial habitats and be acquired by human pathogens via horizontal gene transfer. Therefore, it is of global importance to retrieve comprehensive information on environmental factors, contributing to an accumulation of antibiotic resistance genes and mobile genetic elements in these ecosystems. Here, medically relevant antibiotic resistance genes, class 1 integrons and IncP-1 plasmids were quantified via real time quantitative PCR in soils derived from temperate grasslands and forests, varying in land use over a large spatial scale. The generated dataset allowed an analysis, decoupled from regional influences, and enabled the identification of land use practices and soil characteristics elevating the abundance of antibiotic resistance genes and mobile genetic elements. In grassland soils, the abundance of the macrolide resistance gene *mefA* as well as the sulfonamide resistance gene *sul2* was positively correlated with organic fertilization and the abundance of *aac(6′)-Ib*, conferring resistance to different aminoglycosides, increased with mowing frequency. With respect to forest soils, the beta-lactam resistance gene *bla_{IMP-12}* was significantly correlated with fungal diversity which might be due to the fact that different fungal species can produce beta-lactams. Furthermore, except *bla_{IMP-5}* and *bla_{IMP-12}*, the analyzed antibiotic resistance genes as well as IncP-1 plasmids and class-1 integrons were detected less frequently in forest soils than in soils derived from grassland that are commonly in closer proximity to human activities.

Keywords: antibiotic resistance genes; mobile genetic elements; land use; fertilization; mowing; horizontal gene transfer; forest; grassland; class 1 integrons; IncP-1 plasmids

1. Introduction

Bacterial infections are still a major concern for human health due to the increasing number of antibiotic-resistant pathogens. According to a recent review on antimicrobial resistance, the number of deaths from infections with antibiotic-resistant bacteria (ARBs) might even exceed those from cancer in 2050 [1]. To counteract this prediction, a reduction of antibiotic use to a minimum is necessary. However, antibacterial preparations are still widely overused globally and sufficient knowledge on the various products is frequently lacking [2–4]. In recent years, efforts have been made to control the spread of antibiotic resistance genes (ARGs) by agencies such as the World Health Organization (WHO), the European Union agency for Disease Prevention and Control (ECDC), the European Medicines Agency (EMA) and the European Food Safety Authority (EFSA) [5]. In this context, the WHO published a report on critically important antibiotics for human medicine, based on which risk management strategies for antimicrobial use in food-producing animals can be formulated [6]. This is of high importance as a major fraction of all human diseases develop in animals [7], potentially harboring bacteria that acquired resistance as a result of exposure to antibiotics. Some of these bacteria pose risks to public health as they might cause difficult to treat infections [8]. Therefore, the European Union banned the use of antibiotic growth promoters in agriculture in 2006 [9], allowing antibiotic application only for veterinary purposes. Nevertheless, it remains questionable whether this is sufficient to significantly limit the spread of ARBs and ARGs, as veterinary antibiotics are widely used due to prevalent factory farming and the associated higher infection risk of farm animals [10,11].

Although high densities of ARGs can be found in bacteria from clinical settings, the original sources of the respective genes remain largely unknown. ARGs and ARBs can potentially spread to humans through direct or indirect contact with the soil microbial community [12–14], which comprises numerous antibiotic producers but also bacteria which evolved resistance mechanisms against these harmful substances. This co-evolution resulted in an inconceivably large variety of resistance genes [15]. Moreover, the selection pressure, established through anthropogenic antibiotic pollution, can even increase the ARG abundance in soil [15–17]. Antibiotic pollution of soil is partly due to agricultural land use practices such as application of organic fertilizers (e.g., manure) [17–19]. Through antibiotic treatment of livestock, a selection pressure is established which leads to a higher proportion of resistant bacteria in the gut microbial community of the animals [20]. Additionally, antibiotics are to a large extent eliminated functionally through feces and accumulate in manure [21]. As a consequence, ARGs harbored by bacteria in organic fertilizers as well as the antibiotics themselves potentially cause the pronounced development of resistance genes in soil [22,23]. These ARGs can be encoded on mobile genetic elements (MGEs) such as IncP-1 plasmids or class 1 integrons and potentially spread to human pathogens via horizontal gene transfer (HGT) [24].

Many studies on the distribution of ARGs in non-clinical environments were focused on grassland soils. In contrast, almost no comprehensive surveys on antibiotic resistance profiles of forest soils are available [25], even though they provide information about the natural abundance and spread of resistance genes in habitats with comparably low anthropogenic influence. As grasslands are often affected by agricultural land use and typically in closer proximity to human activities than forests, direct comparisons between resistomes derived from these ecosystems are necessary to predict possible consequences of anthropogenic impacts. Furthermore, forest soil resistomes are of great interest, as effects of environmental parameters can be analyzed in natural settings. These parameters include the diversity of fungi, some of which are known to produce antibiotics such as penicillin [26], and dominant tree species as it has been shown that they can shape soil microbial communities [27,28].

Here, 150 grassland and 150 forest soil samples from three geographic regions in Germany, located up to 700 km apart, were analyzed for the abundance of medically relevant ARGs. In addition, class 1 integrons and IncP-1 plasmids, which can contribute to the spread of antibiotic resistance, were quantified. With respect to the analyzed grassland plots, land use comprises livestock grazing, fertilization as well as mowing, and the forest plots harbor different dominant broad-leaved and coniferous tree species.

Our comprehensive dataset allowed an analysis, decoupled from regional influences, and enabled the identification of general land use practices and soil properties increasing the abundance of ARGs and MGEs over a large spatial scale. Additionally, the study was conducted in Germany, a country, which prohibits antibiotic growth promotion in agriculture. This allowed gaining information about potential impacts of antibiotics, used for veterinary purposes but not as growth promoters, on the ARG and MGE abundance level in soil.

2. Materials and Methods

2.1. Sampling, Soil Characteristics and DNA Extraction

Samples from the upper mineral soil (0–10 cm without the organic layer) were derived from 300 experimental plots of the Biodiversity Exploratories Schorfheide-Chorin (northeastern Germany), Hainich-Dün (central Germany), and Schwäbische Alb (southwestern Germany) [29] in May 2017, as described by Solly et al. [30]. Each study region covers the land use types grassland and forest. Grassland plots are 50 m × 50 m and forest plots are 100 m × 100 m in size. The pH of each soil was determined as described by Solly et al. [30]. Furthermore, soil moisture was assessed daily at ten cm below surface with the ML2X soil Humidity Probe (Delta-T Devices, Ltd., Cambridge, UK) and the mean with respect to measurements in May 2017 was calculated. Information about organic and mineral fertilization in grasslands were derived as described by Vogt et al. [31], based on interviews with the land users. Nitrogen contents of mineral fertilizer were directly determined according to manufacturer specifications, and for organic fertilizer calculated by conversion factors according to the amount and type of slurry or manure. Furthermore, mowing frequency equates to the number of cuts per year and grazing intensity is composed of the number and type of livestock multiplied with the grazing days on a hectare. Based on these three grassland management compounds a Land Use Index (LUI) was developed by Blüthgen et al. [32] to reflect the management intensity with respect to the study plots. Detailed information on soil characteristics and land use is given in Table S1.

Microbial community DNA was isolated from the 300 soil samples by using the DNeasy PowerSoil Kit (Qiagen, Hilden, Germany) according to the manufacturer's instructions. DNA concentrations were determined using a NanoDrop ND-1000 UV-Vis Spectrophotometer (NanoDrop Technologies, Wilmington, NC, USA) as recommended by the manufacturer. Additionally, for real time quantitative PCR (qPCR) DNA concentrations were determined in quadruplicate by using the Microplate reader Synergy2 (BioTek, Winooski, VT, USA) and the QuantiFluor dsDNA System (Promega, Mannheim, Germany) following the manufacturer's instructions. Outliers were detected and discarded via the Dixon's Q-test [33].

2.2. Soil Fungal Diversity

The assessment of fungal diversity was based on the internal transcribed spacer (ITS) region 2. We amplified fungal ITS DNA by using proofreading Kapa Hifi polymerase (Kapa Biosystems, Boston, MA, USA) and the primers fITS7 (5'-GTGARTCATCGAATCTTTG-3') [34] and ITS4 (5'-TCCTCCGCTTATTGATATGC-3') [35] which contained Illumina adapter sequences. The PCR reactions were initiated at 95 °C (3 min) followed by 30 cycles of 98 °C (20 s), 56 °C (20 s) and 72 °C (20 s), and ended with incubation at 72 °C for 5 min. Each PCR reaction was carried out in triplicate and the created amplicons were checked by gel electrophoresis and purified with an Agencourt AMPure XP kit (Beckman Coulter, Krefeld, Germany). Illumina Nextera XT Indices were added in an additional PCR and subsequently products were purified with AMPure beads (Beckmann Coulter, Vienna, Austria). Libraries were quantified by performing PicoGreen assays (Molecular Probes, Eugene, OR, USA) and pooled to provide equimolar representation. Fragment sizes and quality of the libraries were checked using an Agilent 2100 Bioanalyzer (Agilent Technologies, Palo Alto, CA, USA). Sequencing was carried out using an Illumina MiSeq sequencer (Illumina Inc., San Diego, CA, USA) in paired-end mode and the MiSeq Reagent kit v3.

Fungal amplicon sequencing data processing was carried out using a customized bioinformatics pipeline, mainly based on MOTHUR [36] and OBITools [37]. Prior to running this pipeline, Illumina adaptors, indices and primer sequences were removed by the software provided by Illumina. The resulting paired-end reads were merged with a minimum overlap of 20 bp using PandaSeq [38]. Subsequently, sequences shorter than 200 bp and those containing ambiguous nucleotides or homopolymers were removed. The average quality trimming parameter was set to Phred score 22. Potential chimeric reads were detected and removed from each sample using the UCHIME algorithm [39]. De-replicated reads were clustered into operational taxonomic units (OTUs) using the vsearch algorithm [40]. Afterwards, OTU-representative sequences were taxonomically assigned based on reference sequences provided by the Unite.v7.2 database [41]. Only OTUs affiliated to Fungi were used for further analysis. Singleton, doubleton and tripton sequences were discarded. Remaining representative sequences were additionally checked with ITSx [42] to finally exclude non-ITS2 sequences from the dataset.

The datasets were rarefied to the smallest number of sequences per sample (12,532) using the package phyloseq [43] in R version 3.5.3 [44]. This resulted in a total of 36,655 fungal OTUs in 300 soil samples. Based on this final OTU matrix, the fungal Shannon H' diversity index was calculated using the R package vegan [45].

2.3. Quantification of 16S rRNA Genes, IncP-1 Plasmids and Class 1 Integrins

All quantifications were conducted with an iQ5 real-time PCR detection system (Bio-Rad, Hercules, CA, USA). Quantification of 16S rRNA genes was performed by using 12 ng template DNA, 0.4 µM of the primers BACT1369F (5'-CGGTGAATACGTTTCYCGG-3') and PROK1492R (5'-GGWTA CCTTGTACGACTT-3'), and 0.2 µM of the TaqMan probe TM1389F ([FAM] 5'-CTTGTACA CACCGCCCGTC-3' [TAM]) [46]. A DNA fragment obtained via PCR using the BACT1369F and PROK1492R primer set was cloned into the vector pCR4-TOPO (Thermo Fisher Scientific, Braunschweig, Germany), as recommended by the manufacturer, to serve as standard. To quantify IncP-1 plasmids 18 ng template DNA, 0.4 µM of each of the primers F (5'-TCATCGACAACGAC TACAACG-3'), R (5'-TTCTTCTTGCCCTTCGCCAG-3'), Fz (5'-TCGTGGATAACGACTACAACG-3'), Rge (5'-TTYTTCYTGCCCTTGCCAG-3'), and Rd (5'-TTCTTGACTCCCTTCGCCAG-3'), and 0.2 µM of the TaqMan probe P ([Fam] 5'-TCAGYTCRTTGCGYTGCAGGTTCTCVAT-3' [Tam]) were used [47]. The pCR2.1-TOPO vector (Thermo Fisher Scientific) comprising an insert, amplified with the F and R primers targeting the *korB* gene of the RP4 plasmid [48], served as standard throughout quantification. The class 1 integron-integrase gene *intI1* was quantified using 18.5 ng template DNA, 0.4 µM of each of the primers *intI1*-LC1 (5'-GCCTTGATGTTACCCGAGAG-3') and *intI1*-LC5 (5'-GATCGGTGCGAATGCGTGT-3'), and 0.2 µM of the *intI1*-probe ([FAM] 5'-ATTCCTGGCC GTGGTTCTGGGTTTT-3' [BHQ1]) [49]. Quantification of 16S rRNA genes, IncP-1 plasmids and class 1 integrons was conducted using the QuantiNova Probe PCR Kit. The cycler program for the quantification of these three targets started with an initial activation step at 95 °C for 2 min followed by 40 cycles of denaturation at 95 °C for 6 sec and a combined annealing and extension step at 60 °C for 6 s. To get comparable results from all reaction plates of the class 1 integron quantifications, four selected DNA samples were included into each of the plates, based on which the base lines were standardized.

2.4. Detection of Antibiotic Resistance Genes via qPCR Array

Comprehensive qPCR arrays including a total of 84 ARGs were performed based on DNA, extracted from a subset of collected soil samples. These soil samples were derived from grassland (AEG8, AEG21, HEG7, HEG21 SEG32, and SEG43) and forest (AEW2, AEW7, HEW3, HEW5, and SEW6) experimental plots located in the Schwäbische Alb, Hainich-Dün, and Schorfheide-Chorin exploratory. We selected the experimental plots as they cover different land use types and intensities as well as variations in soil properties (e.g., soil pH). Quantification of ARGs was conducted by using the Antibiotic Resistance Genes qPCR Array for microbial DNA testing (BAID-1901Z, QIAGEN). This array

allows the quantification of 84 different ARGs in a single qPCR run (primers and probes are supplied in each well of the qPCR array). More precisely, five aminoglycoside, 57 β -lactam, 14 erythromycin, five macrolide, two tetracycline and two vancomycin resistance genes were analyzed. Each reaction mixture (final volume, 25 μ L) contained 12.5 μ L 2 \times microbial qPCR master mix (QIAGEN), 6.5 μ L microbial DNA-free water, and 12 ng template DNA. A control reaction plate was set up with 10 mM Tris buffer instead of template DNA. The following cycling conditions were used: 95 $^{\circ}$ C for 10 min and 40 cycles of 95 $^{\circ}$ C for 15 s and combined annealing and extension at 60 $^{\circ}$ C for 2 min. Based on the threshold cycle (C_T) values of all detected genes, seven ARGs were selected for quantification in soil samples of all 300 experimental plots.

2.5. Quantification of ARGs in Soils Derived from 300 Study Plots

The aminoglycoside resistance genes *aac(6')-Ib* and *aacC1*, the β -lactam resistance genes *bla_{IMP-12}* and *bla_{IMP-5}*, the macrolide-lincosamide-streptogramin B (MLS) resistance gene *ermB*, the macrolide resistance gene *mefA* as well as the tetracycline resistance gene *tetA* were quantified based on soil DNA derived from all 300 experimental plots by using a customized qPCR array kit (QIAGEN). Each customized qPCR array contained quantification reactions of the seven selected ARGs in 11 different soil DNA samples and a negative control. Positive control reactions were included to test for the presence of inhibitors. The reaction mixture (final volume, 25 μ L) contained 12.5 μ L 2 \times microbial qPCR master mix (QIAGEN) and 25 ng template DNA. In case of negative controls, buffer was added instead of DNA. The cycling conditions were the same as for the qPCR arrays mentioned above.

The reactions were standardized by adjusting the baseline manually to the level of the 12 positive control reactions in each array across all qPCR runs.

Besides the seven ARGs that were selected based on comprehensive qPCR arrays, we quantified the sulfonamide resistance gene *sul2*. For the quantification of *sul2*, the QuantiNova SYBR Green PCR Kit (Qiagen), 19 ng template DNA, and 0.7 μ M of each of the primers *sul2*-forward (5'-TCATCTGCCAACTCGTCGTTA-3') and *sul2*-reverse (5'-GTCAAAGAACGCCGCAATGT-3') [50,51] were used. Results of the quantifications from different reaction plates were standardized by including four selected samples into each plate, based on which the baseline was adjusted. The cycler program comprised an initial activation step at 95 $^{\circ}$ C for 10 min followed by 40 cycles of 95 $^{\circ}$ C for 5 s and a combined annealing and extension step at 60 $^{\circ}$ C for 10 s. A melting curve analysis was conducted to determine the specificity of amplification during PCR. Reactions with aberrant melting curves were designated as not accessible (NA).

2.6. Statistical Analysis

With respect to all conducted quantification reactions, samples that did not exceed the baseline before the 37th cycle, were regarded as non-detects as described by Hu et al. and Zhao et al. [52,53].

The abundance and occurrence of IncP-1 plasmids, class 1 integrons and the eight selected ARGs were analyzed with R. In order to identify soil characteristics as well as land use practices affecting the quantified genes, two regression approaches were carried out:

(1) A binomial regression approach to analyze the distribution of positive quantifications against non-detects. In this context, the original C_T values were transformed into binary data. More precisely, C_T values < 37 were replaced with a one and C_T values \geq 37 with a zero.

(2) A left censored regression analysis was performed with the tobit function of the R package AER [54] to address the differential relative gene abundance in all sample plots without having to substitute or discard non-detects. For this purpose, ΔC_T values were calculated as follows:

$$C_{T(\text{Reference Gene})} - C_{T(\text{Target Gene})} = \Delta C_T \quad (1)$$

where C_T values from the 16S rRNA gene quantifications served as $C_{T(\text{Reference Gene})}$. The ΔC_T values of all target sequences are listed in Table S2. They were used for tobit regression analysis, where large

ΔC_T values indicate high gene abundance. Furthermore, the lowest ΔC_T value of a positive reaction reduced by 0.01 was assigned to quantifications of specific genes, which resulted in non-detects. The non-detect ΔC_T value was used as left limit for the censored dependent variable in the tobit formula. In case of all tobit models, a Gaussian distribution was applied.

For the statistical analysis, independent variables were scaled and centered with the basic scale function of R and checked for collinearity with the basic R function `rcorr` and the `corrplot` function of the R package `corrplot` [55]. Afterwards, it was tested whether specific genes occur notably more often in grassland than in forest soil. In this context, the occurrence (binomial model) or relative abundance (tobit model) of the respective genes, which showed less than 80% non-detects (80% censoring), were modeled against the two independent variables forest (1 or 0) and exploratory (Schorfheide-Chorin, Hainich-Dün or Schwäbische Alb). The $2^{\Delta C_T}$ values of targets that were less than 80% censored (IncP-1 plasmids, class 1 integrons, *mefA*, *aac(6')-Ib*, *sul2*, *tetA*, *bla_{IMP-12}* and *bla_{IMP-5}*) were visualized with the `cenboxplot` function of the NADA package [56] with a range of 1.5 for forests, grasslands and each exploratory. When insufficient numbers of uncensored observations were available to estimate the distribution below the censoring threshold in the respective area (*mefA*, *aac(6')-Ib*, *tetA* and class 1 integrons in forest plots), the `boxplot` function of basic R was utilized which does not allow an estimation for the censored values. The highest censoring threshold of all candidate genes was indicated with a horizontal red line. Everything below this line was calculated based on the proportion of censored data and the values of uncensored data with `cenros` of NADA.

When targets were less than 70% censored in grassland plots, the impact of agricultural land use such as mowing, fertilization, and grazing was analyzed. This analysis comprised the LUI. The pH or the mean soil moisture in %, determined in May 2017, was added as independent variable in the models for the grassland soils to account for the different soil characteristics of the 300 experimental plots, because they turned out to be the best soil descriptors for the analyzed genes. Due to variable collinearity, only one of these two parameters was chosen, based on quality comparisons of the respective gene models. In the first step, only one land use variable along with the pH or the soil moisture was modeled at a time, to evade the influence of collinearity between the different land use practices onto the model output. Based on these preliminary models, final models were derived, containing the most influential land use variables.

Regarding forest soils, the influence of the tree type and the fungal Shannon diversity on the abundance and occurrence of the two β -lactamase genes was statistically analyzed.

The residuals of all tobit models were tested for normality and constant variance with quantile-quantile plots and residual plots. Furthermore, in order to compare the influence of variable exchange on model quality, the McFadden's pseudo- R^2 [57] was determined for all generated models. With respect to the final models for analysis of land use effects in grassland or forest, either the binomial or tobit approach was supposed to construct a model with an R^2 of at least 0.1. Furthermore, the two approaches were supposed to reveal the same correlation (positive or negative) and yield similar p-values. When final models explained less than 10% of the variance with respect to the dependent variable for both approaches (binomial and tobit) or only the binomial approach was applicable due to too high censoring, no conclusions with respect to the impact of land use were drawn.

3. Results

3.1. Selection of Targets for ARG Quantification in Forest and Grassland Soils

A total of 84 ARGs were quantified in a subset of soil samples derived from three different geographic regions in Germany (Hainich-Dün, Schorfheide-Chorin and Schwäbische Alb). This subset covers beech and spruce forest soils as well as grassland soils affected by different land use intensities. The very low C_T values and detection frequencies with respect to the majority of the 84 ARGs restricted the selection of targets for qPCR-based analysis comprising DNA extracted from each of the 300 experimental plots. The aminoglycoside resistance genes *aac(6')-Ib* and *aacC1*, the beta-lactam resistance

genes *bla*_{IMP-12} and *bla*_{IMP-5}, the MLS resistance gene *ermB*, the macrolide resistance gene *mefA* and the tetracycline resistance gene *tetA*, were chosen for this analysis, which allowed the identification of factors significantly shaping forest and grassland soil resistomes. The analyzed factors comprise land use practices (fertilization, grazing and mowing) as well as dominant tree species and soil fungal diversity. Furthermore, besides resistances to representatives of the mentioned antibiotic classes, the sulfonamide resistance gene *sul2* was considered.

3.2. IncP-1 Plasmids, *mefA* and *sul2* Are More Abundant in Grassland than in Forest Soils

In order to identify differences in occurrence and relative abundance of the selected ARGs, IncP-1 plasmids as well as class 1 integrons between forest and grassland soils, statistical analysis was carried out. Binomial generalized linear models revealed that the occurrence of *aac(6′)-Ib*, *mefA*, *sul2*, *tetA*, IncP-1 plasmids and class 1 integrons was significantly negatively correlated with forest soils (*p*-values: 4.29×10^{-6} , 4.62×10^{-11} , 1.81×10^{-6} , 0.00145, 2.27×10^{-15} and 0.00159, respectively; estimates: −4.7632, −4.01039, −1.5767, −3.2825, −2.2824 and −3.2585, respectively; R^2 : 0.39, 0.33, 0.09, 0.20, 0.21 and 0.17, respectively). This trend could be validated for *mefA*, *sul2* and the IncP-1 plasmids by modelling their relative abundances based on censored tobit models. Again, a statistically significant negative impact of forest soils on *mefA*, *sul2* and IncP-1 plasmid abundance could be determined (*p*-values: 7.85×10^{-14} , 3.08×10^{-7} and $<2 \times 10^{-16}$, respectively; estimates: −5.45, −5.56 and −3.74, respectively; R^2 : 0.19, 0.06, and 0.09, respectively). Due to a very low abundance of *aac(6′)-Ib*, *tetA* and class 1 integrons in forest soils, increasing the proportional number of censored samples to over 80%, statistical analysis was restricted to binomial generalized models with respect to these genes.

Both, the occurrence and relative abundance, of the two β -lactamase genes *bla*_{IMP-12} and *bla*_{IMP-5} did not significantly differ between grassland and forest soils. This was revealed by the binomial model approach (*p*-values: 0.79 and 0.78, respectively; estimate: 0.06 and 0.08, respectively; R^2 : 0.05 and 0.1, respectively) and the tobit models (*p*-values: 0.98 and 0.7, respectively; estimate: 0.01 and −0.17, respectively; R^2 : 0.03 and 0.06, respectively). The relative abundance of the quantified ARGs and MGEs in forest and grassland soils is depicted in censored boxplots (Figure 1). As *ermB* and *aacC1* were only detected in 13 and 5 of the 300 soil samples, respectively, they could not be considered in the statistical analysis.

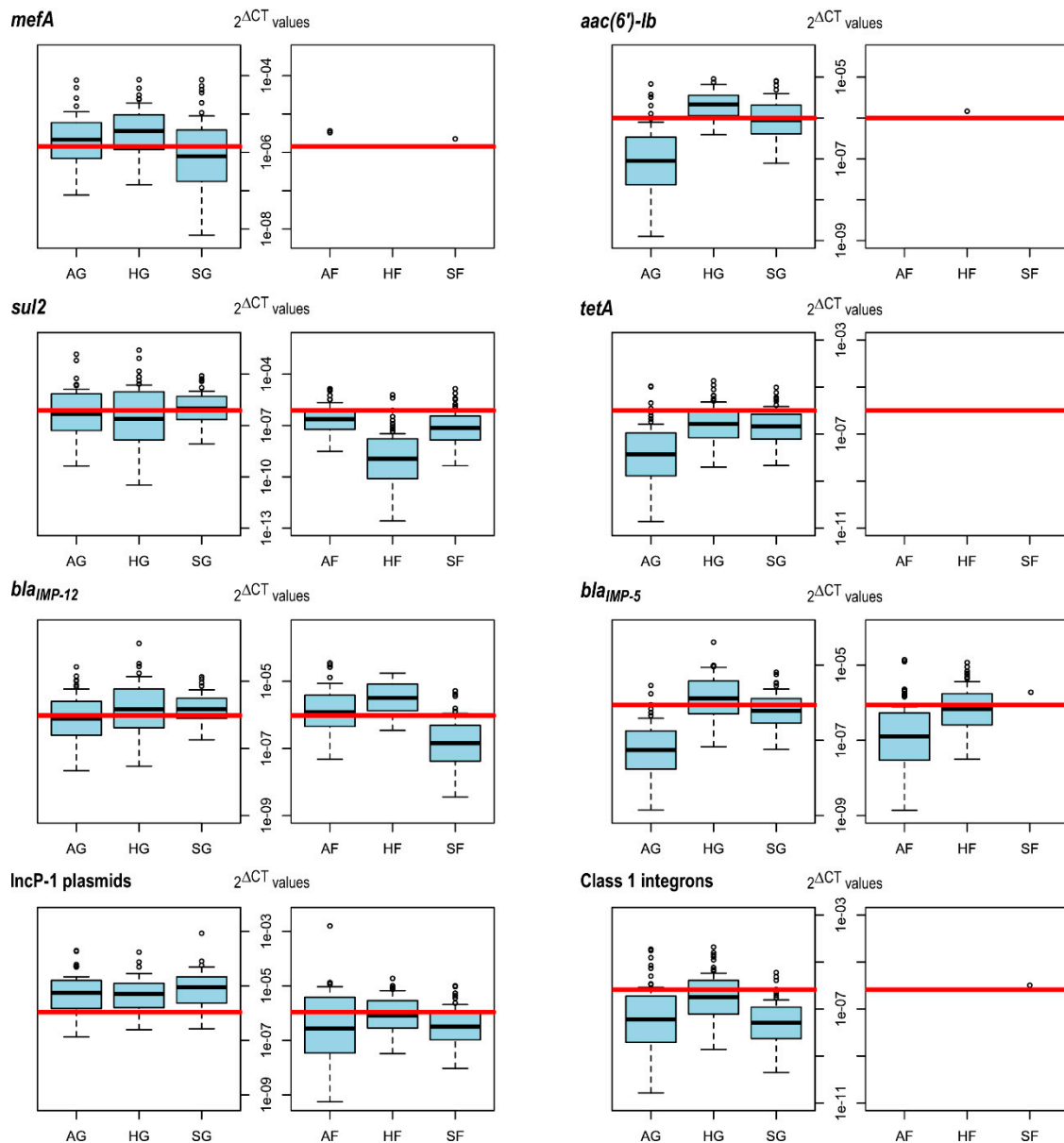


Figure 1. Censored boxplots depicting $2^{\Delta CT}$ values of quantified antibiotic resistance genes and mobile genetic elements. The red horizontal line indicates the highest censoring threshold. Everything below this line was estimated. The whiskers represent 1.5 times the outer quartile range. AG, HG and SG represent Schwäbische-Alb, Hainich-Dün and Schorfheide-Chorin grassland soils, respectively, whereas AF, HF and SF represent Schwäbische-Alb, Hainich-Dün and Schorfheide-Chorin forest soils, respectively.

3.3. Land Use Practices in Grassland Affect the Abundances of *aac(6')-lb*, *mefA* and *sul2*

With respect to the occurrence and relative abundance of *aac(6')-lb*, *mefA* and *sul2* in grassland soils, statistically significant correlations with land use were identified (Table 1). The occurrence of *aac(6')-lb* is positively correlated with the mowing frequency and soil pH (p -values: 0.03 and 7.4×10^{-7} ; estimate: 0.45 and 1.74; R^2 : 0.21). This trend could be validated with the tobit model focusing on the relative gene abundance (p -values: 0.044 and 1.5×10^{-7} ; estimate 0.37 and 1.65; R^2 : 0.12). Furthermore, the occurrence of *mefA* is positively influenced by nitrogen input from organic fertilizers and negatively influenced by the soil moisture content (p -values: 9.4×10^{-4} and 3×10^{-3} , estimate: 1.14 and -0.68 ; R^2 : 0.24), which was again validated by the tobit model (p -values: 3.9×10^{-3} and 9.2×10^{-5} ; estimate: 0.64 and -1.01 ; R^2 : 0.11). The occurrence and relative abundance of the *sul2* gene is also significantly

more pronounced in grassland soils, which experienced high nitrogen input from organic fertilizers (binomial model: p -value: 0.01; estimate: 0.53; R^2 : 0.1; tobit model: p -value: 2.2×10^{-3} ; estimate: 1.6; R^2 : 0.08).

Table 1. Final regression models of the occurrence (binomial model: A) or relative abundance (tobit model: B) of antibiotic resistance genes. At least one of the two models was supposed to explain $\geq 10\%$ of the variance (R^2) and p values < 0.05 were considered significant (highlighted in bold). The outer left column lists the dependent (shown in bold) and independent variables of each model (also intercept is considered with respect to each model). The models below the dashed bar focus on *bla*_{IMP-12} in forest soils and the other models focus on *aac*(6′)-*lb*, *mefA* and *sul2* in grassland soils. Est. is the abbreviation for estimate, Moisture for soil moisture, Shan-H for fungal diversity as assessed by Shannon index, Df stands for degrees of freedom and Null/Resid. for the null or residual deviance, respectively.

A						B				
	p	Est.	R^2	Df	Null/Resid.	p	Est.	R^2	Df	Null/Resid.
<i>aac</i>(6′)-<i>lb</i>			0.21	143	191.3/152			0.12	142	333.7/292.7
Intercept	3.8×10^{-7}	−12.29				$<2 \times 10^{-16}$	−31.49			
Mowing	0.03	0.45				4.4×10^{-2}	0.37			
pH	7.4×10^{-7}	1.74				1.5×10^{-7}	1.65			
<i>mefA</i>			0.24	140	198.6/163			0.11	141	198.6/178.5
Intercept	0.02	0.52				$<2 \times 10^{-16}$	−18.81			
Mowing	0.13	0.33				8.1×10^{-2}	0.41			
Org. N	9.4×10^{-4}	1.14				3.9×10^{-3}	0.64			
Moisture	3.0×10^{-3}	−0.68				9.2×10^{-5}	−1.01			
<i>sul2</i>			0.1	140	182.5/171.6			0.08	140	182.5/177.9
Intercept	9.3×10^{-4}	−0.62				$<2 \times 10^{-16}$	−22.18			
Org. N	0.01	0.53				2.2×10^{-3}	1.60			
Moisture	0.10	−0.37				8.9×10^{-2}	−1.14			
<i>bla</i>_{IMP-12}			0.17	133	188.5/155.6			0.09	132	417.1/380.7
Intercept	8.4×10^{-4}	−1.64				$<2 \times 10^{-16}$	−21.93			
Beech	7.0×10^{-5}	2.13				7.4×10^{-6}	2.75			
Shan-H	4.6×10^{-3}	0.65				2.4×10^{-3}	0.73			

With respect to *tetA* and class 1 integrons, statistical analysis was restricted to binomial models (Table S3) as both genes were over 70% censored in grassland samples. Only the binomial model comprising the LUI indicated a significantly positive correlation with the gene occurrence of *tetA* (p -value: 0.03; estimate: 0.48; R^2 : 0.11). Moreover, the class 1 integrons seem to be affected by a number of land use variables. The occurrence of these MGEs was positively correlated with grazing and negatively correlated with mowing, fertilization, mineral N input, organic N input and LUI.

When analyzing IncP-1 plasmids as well as *bla*_{IMP12} and *bla*_{IMP5} in grassland soils, none of the two approaches (binomial and tobit model approach) revealed a statistically significant influence of a land use variable with a sufficient R^2 (Table S3).

3.4. The Abundance of *bla*_{IMP-12} Increases with Fungal Diversity in Forest Soil

The gene *bla*_{IMP-12} could be detected more frequently in beech forest and at sites with a high fungal diversity compared to other considered forest sites (p -values: 7×10^{-5} and 4.6×10^{-3} ; estimate: 2.13 and 0.65; R^2 : 0.17) (Table 1). The tobit approach, modelling the relative abundance of this gene, supports this finding (p -values: 7.4×10^{-6} and 2.4×10^{-3} ; estimate: 2.75 and 0.73; R^2 : 0.09). With respect to *bla*_{IMP-5} the same trend could be detected, but the model quality is below the quality threshold (Table S3). In general, *bla*_{IMP-12} and *bla*_{IMP-5} were the only analyzed genes, which were not significantly more abundant in grassland than in forest soils. Regarding the grassland soils, no environmental parameter could be identified which impacts the abundance of these genes.

4. Discussion

In this study, a general difference between grassland and forest soils with respect to the occurrence of selected ARGs and MGEs was visible. All selected ARGs, except the two β -lactamase genes *bla*_{IMP-12} and *bla*_{IMP-5}, as well as IncP-1 plasmids and class 1 integrons were more frequently detected in grassland than in forest soils (Figure 1). This might partly be due to differences in soil bacterial community composition between forest and grassland, which were detected in a previous study comprising all analyzed experimental plots [58]. In accordance with this theory, Forsberg et al. [59] identified bacterial community composition as a major determinant of antibiotic resistance gene content based on metagenomic analysis of agricultural and grassland soil. The lower pH in forest soils (Table S1) potentially contributes to variations in ARG as well as MGE abundance as this abiotic parameter has previously been shown to be a key driver of soil bacterial community composition [58,60,61]. This assumption is supported by the identified significant positive correlation between pH and the abundance of the *aac(6')-lb* gene in grassland soil. Another possible explanation for the identified differences between forest and grassland ecosystems might be proximity to anthropogenic activities with respect to grassland sites, which comprise the use of antibiotics in human and veterinary medicine as well as associated ARBs, ARGs and MGEs [62]. When the two ecosystems were analyzed separately, we determined a statistically sound relationship between land use and the abundance of the medically relevant ARGs *mefA*, *sul2* and *aac(6')-lb* in grassland soil. Additionally, it was possible to identify factors controlling the abundance of the β -lactamase gene *bla*_{IMP-12} in forest soil (Table 2).

Table 2. Summary of factors significantly affecting target antibiotic resistance genes and mobile genetic elements in soil ecosystems analyzed in this study. Targets showing increased occurrence as well as relative abundance in grassland compared to forest soil are depicted. Furthermore, factors significantly influencing the occurrence as well as relative abundance of targets in grassland (mowing frequency and organic nitrogen input) or forest soil (fungal diversity and beech as dominant tree species) are depicted.

Target	Occurrence and Relative Abundance Significantly Increased in Grassland Compared to Forest Soil	Factors Significantly Influencing Target Occurrence and Relative Abundance in Grassland Soil	Factors Significantly Influencing Target Occurrence and Relative Abundance in Forest Soil
IncP-1	Yes	-	-
<i>aac(6')-lb</i>	Further analysis required *	Mowing frequency and pH	-
<i>mefA</i>	Yes	Organic nitrogen input	-
<i>sul2</i>	Yes	Organic nitrogen input and soil moisture	-
<i>bla</i> _{IMP-12}	No	-	Fungal diversity and beech as dominant tree species

* Due to a very low abundance of *aac(6')-lb* in forest soils, increasing the proportional number of censored samples to over 80%, statistical analysis was restricted to binomial generalized models with respect to these genes. “-” indicates that no influential factor was identified.

4.1. *sul2* and *mefA*

Both, the occurrence as well as the relative abundance of *sul2* and *mefA* were affected by organic fertilizer application in grassland. The sulfonamide resistance gene *sul2* encodes an alternative dihydropteroate synthase and is often located on small promiscuous plasmids of the IncQ incompatibility group [63,64]. These plasmids allow the dissemination of *sul2* among gram-positive and gram-negative bacterial hosts [65]. They have already been identified in a variety of different species including the pathogenic *Enterobacteriaceae* *Salmonella enterica* [66], *Klebsiella pneumoniae* [67] and *Escherichia coli*, isolated from German cattle [68]. Based on communications with veterinarians working in the study regions, it was confirmed that sulfonamides together with trimethoprim are frequently used to treat cattle, as the authorization for corresponding pharmaceutical preparations

have a broad spectrum, including infections of the gastrointestinal tract, the urinary- and reproductive system as well as the skin, joints and hoof.

The quantified resistance gene *mefA* encodes an efflux protein of the major facilitator superfamily class which extrudes 14- and 15-membered macrolides (e.g., erythromycin or tulathromycin) out of the bacterial cell [69]. It has originally been identified in *Streptococcus pyogenes*, which causes infections of the upper respiratory tract and the skin as well as a variety of systemic infections in humans [70], but also in the pathogen *Streptococcus pneumoniae* [71]. In fact, *mefA* can be carried by conjugative transposons like Tn1207.3, which enable its spread among different streptococcal species [72,73]. Despite the recent categorization of macrolides as critically important in veterinary medicine according to the World Organization for Animal Health (OIE) [74], especially tulathromycin is still frequently applied for bovine respiratory diseases of calves and young cattle [75], which was confirmed by the contacted veterinarians. When several animals from a group of calves purchased from different sources fall ill, it is also common to treat the entire group. This procedure is called metaphylactic treatment. Organic cattle farms usually forego metaphylactic applications with tulathromycin, but individual treatments of calves with respiratory diseases are still conducted when necessary. A reason for the frequent application of tulathromycin is its functionality against mycoplasma species, one of the major causative agents for respiratory infections in calves [76]. As these bacteria lack a cell wall, they are intrinsically resistant against β -lactam antibiotics. Tulathromycin has to be administered only once due to a consistently high drug-level over longer times. It has an elimination half time in cattle of approximately 90 h, which is far higher than that of erythromycin (3–16 h) [75,77]. Macrolides with longer elimination half times are suspected to promote higher resistance development due to longer exposure of bacteria to sub-inhibitory drug concentrations [78]. Therefore, the frequent usage of tulathromycin in bovine agriculture could promote the resistance development of different *Streptococci* species within animal microbiomes.

As *Streptococci* species are also part of the gastrointestinal microbiome in cattle [79], resistant strains in manure, which is frequently applied as organic fertilizer with respect to the analyzed grassland plots, could get in contact with the soil microbiome, whereby HGT events can potentially take place. This might also be the case for bacteria in manure harboring the *sul2* gene, especially as this ARG is known to be frequently encoded by *Enterobacteriaceae*. It has been shown in a microcosm study by Hu et al. [52], that application of manure, which has not been treated with antibiotics, increases the ARG abundance in soil notably. However, as only 50% of the tulathromycin, 17.9% of sulfadimethoxine and 11–37% of sulfamethazine, used for treatment, are eliminated functionally by cattle [80,81], it seems probable, that besides ARB along with their ARGs also the antibiotics themselves are transferred to the soil through organic fertilization. Thus, besides other manure constituents, this antibiotic input into soil could also increase the *mefA* and *sul2* abundance due to selective pressure.

4.2. *aac(6′)-Ib*

The gene *aac(6′)-Ib* confers resistance to different aminoglycosides and is of clinical importance as it is predominantly harbored by MGEs of gram-negative bacteria [82]. Importantly, mutations in this gene can lead to resistance toward representatives of a second class of antibiotics, the fluoroquinolones [82–84].

According to contacted veterinarians, aminoglycosides are not very often used to treat cattle present in the analyzed study region. However, they are sometimes byproducts of antimicrobial preparations to treat acute udder diseases and to prevent udder infections during dry period. As all lactating cows from conventional dairy farms go through the about six weeks lasting dry period before each calving, it is a considerable factor that could influence cattle resistomes notably [85]. Apart from the aminoglycosides, fluoroquinolones are also used to treat febrile udder diseases of cattle. As the WHO declared them as critically important antimicrobials, it is required that fluoroquinolones are only used when susceptibility testing identifies the drug as only treatment option [86]. Since febrile udder diseases are very serious and, if not treated effectively, usually lead to death, animals often receive fluoroquinolones before the result of the susceptibility test is available [87,88]. This inevitably leads to

the treatment of some bacterial infections with fluoroquinolones that would have been sensitive to other antimicrobial agents.

Although *aac(6′)-Ib* was not correlated with nitrogen input from organic fertilizers, manure could contribute to transfer of fluoroquinolones and aminoglycosides into soils, as surface water run-offs, dust or wild animals could distribute the antibiotics or ARB into different areas [62,89–91]. This might partly explain the frequent detection of *aac(6′)-Ib* in grassland soils with and without history of organic fertilization.

With respect to the applied land use practices in grasslands of the study region, a clear correlation between mowing and the abundance of the *aac(6′)-Ib* gene could be identified. Plants have been shown to be a potential reservoir of ARB, due to uptake and accumulation of antibiotics [92,93]. Hence, mowing could increase the contact between antibiotic-resistant endophytes and the soil community, and thereby promote HGT, which would explain the positive influence of the mowing frequency on ARG abundance in soil. In addition, mowing might induce changes in release of potentially toxic aromatic compounds from degradation processes as well as plant exudates such as specialized antimicrobial compounds (e.g., phytoalexins and flavonoids) and signaling molecules, which could increase expression of antibiotic resistance in soil [94,95].

4.3. *bla*_{IMP-12}, *bla*_{IMP-5} and MGEs

The IMP enzymes represent broad-spectrum metallo-β-lactamases, rapidly spreading globally among the gram-negative bacteria including *Enterobacteriaceae*, *Pseudomonas* and *Acinetobacter* species as they are mainly encoded on class 1 integrons within transferable plasmids [96–100]. The β-lactamase *bla*_{IMP-12} was originally identified in a clinical *Pseudomonas putida* isolate and its preferred substrates include aminopenicillins, cephalosporins and carbapenems [98].

β-Lactam antibiotics (penicillins, aminopenicillins and cephalosporins of the first to fourth generation) are the most commonly applied substances in veterinary medicine, which was also confirmed for the study regions based on communication with veterinarians. They are applied against mastitis, during the beginning of the dry period of dairy cows and are a first treatment option for a series of different infections, including the respiratory tract, the digestive tract and the urinary and reproductive system of cattle. However, despite their frequent use in veterinary medicine, no statistically sound difference in *bla*_{IMP-12} and *bla*_{IMP-5} abundance between grassland and forest plots was identified. An explanation for this observation could be their fast hydrolytic degradation which can take place, depending on the soil moisture, within hours to a few days [101,102]. The rapid β-lactam hydrolysis and the concordant loss in selective pressure could promote the development of sensitive strains due to e.g., the loss of resistance plasmids [103]. This might be the reason for similar *bla*_{IMP-12} and *bla*_{IMP-5} abundances in forest as well as grassland soil and potentially explains why land use practices showed no clear effect on the distribution of these genes. Nevertheless, it is also possible that both genes efficiently spread across distinct ecosystems, as they were detected as part of mobile genetic elements [98,104], and protect phylogenetically diverse bacteria against the lethal effect of several beta lactam antibiotics which are naturally produced by soil microorganisms.

Strikingly, the *bla*_{IMP-12} gene showed a significant positive correlation with beech forest plots as well as soil fungal diversity. This is most probably due to the connectedness between soil fungal communities and tree species [105]. Furthermore, as penicillins and cephalosporins are synthesized by the filamentous fungi *Penicillium rubens* [106,107] and *Acremonium chrysogenum* (priorily *Cephalosporium acremonium*) [108,109], it is not surprising, that the soil fungal community has a significant impact on *bla*_{IMP-12} abundance. It is possible that soil fungi intensify the synthesis of β-lactams to compete for scarce resources or to receive access to nutrients released due to lysis of sensitive bacteria when fungal diversity in soil increases. This potentially explains the pronounced occurrence and abundance of *bla*_{IMP-12} in soils with a higher fungal diversity.

An effect of land use practices on the abundance of IncP-1 plasmids, class 1 integrons and *tetA*, which would explain their pronounced occurrence in grassland sites was not found. The

IncP-1 plasmids have been shown to encode a variety of different ARGs and heavy metal resistance genes [110–112]. Therefore, several environmental parameters can potentially impact their occurrence in soil. With respect to class 1 integrons and the tetracycline efflux pump-encoding gene *tetA*, we could not untangle statistically sound correlations between their abundance and land use practices as they were only detected in a small fraction of the analyzed soils.

Supplementary Materials: The following are available online at <http://www.mdpi.com/2073-4425/11/2/150/s1>, Table S1: Plot characteristics and soil properties of all 300 experimental plots, Table S2: ΔC_t values of all analyzed target sequences in the 300 experimental plots, Table S3: Preliminary binomial (A) or tobit regression models (B).

Author Contributions: Conceptualization, I.M.W. and H.N.; formal analysis, I.M.W., J.Y., C.P. and H.N.; investigation, I.M.W., J.Y., K.G.; resources, H.N., M.S., T.W. and F.B.; data curation, I.M.W., K.G., I.S., J.V.; writing—original draft preparation, I.M.W. and H.N.; writing—review and editing, I.M.W., H.N., K.G., J.V., I.S., M.S., T.W. and F.B.; visualization, I.M.W.; supervision, I.M.W. and H.N.; project administration, H.N.; funding acquisition, H.N. All authors have read and agreed to the published version of the manuscript.

Funding: This research was funded by the DFG Priority Program 1374 “Infrastructure-Biodiversity-Exploratories” (NA 848/2-1).

Acknowledgments: We thank the managers of the three Exploratories, Kirsten Reichel-Jung, Iris Steitz, Sandra Weithmann, Florian Straub, Katrin Lorenzen, Miriam Teuscher and all former managers for their work in maintaining the plot and project infrastructure; Christiane Fischer and Jule Mangels for giving support through the central office, Andreas Ostrowski for managing the central data base, and Markus Fischer, Eduard Linsenmair, Dominik Hessenmöller, Daniel Prati, Ernst-Detlef Schulze, Wolfgang W. Weisser and the late Elisabeth Kalko for their role in setting up the Biodiversity Exploratories project. Furthermore, we would like to thank Jochen Wilhelm, for providing feedback about statistical procedures. Special thanks goes to the veterinarians that were willing to answer our questions. In this context, Andrea Lawall has provided particularly valuable information about common practices of veterinarians in Germany and we are very grateful for this contribution. Without this first hand information about common farm veterinary practices in Germany it would have been much more difficult to interpret the results and the evaluation would probably not have been so detailed. Field work permits were issued by the responsible state environmental offices of Baden-Württemberg, Thüringen, and Brandenburg. We acknowledge support by the Open Access Publication Funds of the University of Göttingen.

Conflicts of Interest: The authors declare no conflict of interest. The funders had no role in the design of the study; in the collection, analyses, or interpretation of data; in the writing of the manuscript, or in the decision to publish the results.

References

1. O'Neill, J. *Tackling Drug-Resistant Infections Globally: Final Report and Recommendations*; Review on Antimicrobial Resistance: London, UK, 2016.
2. Auta, A.; Hadi, M.A.; Oga, E.; Adewuyi, E.O.; Abdu-Aguye, S.N.; Adedoye, D.; Strickland-Hodge, B.; Morgan, D.J. Global access to antibiotics without prescription in community pharmacies: A systematic review and meta-analysis. *J. Infect.* **2019**, *78*, 8–18. [CrossRef] [PubMed]
3. Versporten, A.; Bolokhovets, G.; Ghazaryan, L.; Abilova, V.; Pyshnik, G.; Spasojevic, T.; Korinteli, I.; Raka, L.; Kambaralieva, B.; Cizmovic, L.; et al. Antibiotic use in eastern Europe: A cross-national database study in coordination with the WHO regional office for Europe. *Lancet Infect. Dis.* **2014**, *14*, 381–387. [CrossRef]
4. WHO Regional Office for Europe. *Assessing Non-Prescription and Inappropriate Use of Antibiotics: Report on Survey*; WHO: Copenhagen, Denmark, 2019.
5. Anderson, M.; Clift, C.; Schulze, K.; Sagan, A.; Nahrgang, S.; Ait Ouakrim, D.; Mossialos, E. Averting the AMR crisis: What are the avenues for policy action for countries in Europe? In *European Observatory Policy Briefs*; European Observatory on Health Systems and Policies: Copenhagen, Denmark, 2019.
6. World Health Organization. *Critically Important Antibacterial Agents for Human Medicine for Risk Management Strategies of Non-Human Use: Report of a WHO Working Group Consultation*; World Health Organization: Canberra, Australia, 2005.
7. Van Doorn, H.R. Emerging infectious diseases. *Medicine* **2014**, *42*, 60–63. [CrossRef]
8. World Health Organization. Of All Human Diseases, 60% Originate in Animals—“One Health” Is the Only Way to Keep Antibiotics Working. Available online: <http://www.euro.who.int/en/health-topics/disease-prevention/food-safety/news/news/2018/11/of-all-human-diseases,-60-originate-in-animals-one-health-is-the-only-way-to-keep-antibiotics-working> (accessed on 28 August 2019).

9. European Union. Ban on Antibiotics as Growth Promoters in Animal Feed Enters into Effect. Available online: https://europa.eu/rapid/press-release_IP-05-1687_en.htm (accessed on 22 November 2019).
10. Anomaly, J. What's wrong with factory farming? *Public Health Ethics* **2015**, *8*, 246–254. [[CrossRef](#)]
11. Pluhar, E.B. Meat and morality: Alternatives to factory farming. *J. Agric. Environ. Ethics* **2010**, *23*, 455–468. [[CrossRef](#)]
12. EMA. *Antimicrobial Resistance in the Environment: Considerations for Current and Future Risk Assessment of Veterinary Medicinal Products*; European Medicines Agency: Amsterdam, The Netherlands, 2018.
13. Forsberg, K.J.; Reyes, A.; Wang, B.; Selleck, E.M.; Sommer, M.O.A.; Dantas, G. The shared antibiotic resistome of soil bacteria and human pathogens. *Science* **2012**, *337*, 1107–1111. [[CrossRef](#)]
14. Canteón, R. Antibiotic resistance genes from the environment: A perspective through newly identified antibiotic resistance mechanisms in the clinical setting. *Clin. Microbiol. Infect.* **2009**, *15*, 20–25. [[CrossRef](#)]
15. Surette, M.D.; Wright, G.D. Lessons from the environmental antibiotic resistome. *Annu. Rev. Microbiol.* **2017**, *71*, 309–329. [[CrossRef](#)]
16. Knapp, C.W.; Doling, J.; Ehlert, P.A.I.; Graham, D.W. Evidence of increasing antibiotic resistance gene abundances in archived soils since 1940. *Environ. Sci. Technol.* **2010**, *44*, 580–587. [[CrossRef](#)]
17. Heuer, H.; Schmitt, H.; Smalla, K. Antibiotic resistance gene spread due to manure application on agricultural fields. *Curr. Opin. Microbiol.* **2011**, *14*, 236–243. [[CrossRef](#)] [[PubMed](#)]
18. Graham, D.W.; Knapp, C.W.; Christensen, B.T.; McCluskey, S.; Doling, J. Appearance of β -lactam resistance genes in agricultural soils and clinical isolates over the 20th century. *Sci. Rep.* **2016**, *6*, 21550. [[CrossRef](#)] [[PubMed](#)]
19. Wang, F.; Xu, M.; Stedtfeld, R.D.; Sheng, H.; Fan, J.; Liu, M.; Chai, B.; Soares de Carvalho, T.; Li, H.; Li, Z.; et al. Long-term effect of different fertilization and cropping systems on the soil antibiotic resistome. *Environ. Sci. Technol.* **2018**, *52*, 13037–13046. [[CrossRef](#)] [[PubMed](#)]
20. DeFrancesco, K.A.; Cobbold, R.N.; Rice, D.H.; Besser, T.E.; Hancock, D.D. Antimicrobial resistance of commensal *Escherichia coli* from dairy cattle associated with recent multi-resistant salmonellosis outbreaks. *Vet. Microbiol.* **2004**, *98*, 55–61. [[CrossRef](#)]
21. Berendsen, B.J.A.; Wegh, R.S.; Memelink, J.; Zuidema, T.; Stolker, L.A.M. The analysis of animal faeces as a tool to monitor antibiotic usage. *Talanta* **2015**, *132*, 258–268. [[CrossRef](#)]
22. Guo, T.; Lou, C.; Zhai, W.; Tang, X.; Hashmi, M.Z.; Murtaza, R.; Li, Y.; Liu, X.; Xu, J. Increased occurrence of heavy metals, antibiotics and resistance genes in surface soil after long-term application of manure. *Sci. Total Environ.* **2018**, *635*, 995–1003. [[CrossRef](#)]
23. Peng, S.; Feng, Y.; Wang, Y.; Guo, X.; Chu, H.; Lin, X. Prevalence of antibiotic resistance genes in soils after continually applied with different manure for 30 years. *J. Hazard. Mater.* **2017**, *340*, 16–25. [[CrossRef](#)]
24. Jechalke, S.; Schreiter, S.; Wolters, B.; Dealtry, S.; Heuer, H.; Smalla, K. Widespread dissemination of class 1 integron components in soils and related ecosystems as revealed by cultivation-independent analysis. *Front. Microbiol.* **2014**, *4*, 420. [[CrossRef](#)]
25. Hu, H.-W.; Wang, J.-T.; Singh, B.K.; Liu, Y.-R.; Chen, Y.-L.; Zhang, Y.-J.; He, J.-Z. Diversity of herbaceous plants and bacterial communities regulates soil resistome across forest biomes. *Environ. Microbiol.* **2018**, *20*, 3186–3200. [[CrossRef](#)]
26. Clardy, J.; Fischbach, M.; Currie, C. The natural history of antibiotics. *Curr. Biol.* **2009**, *11*, R437–R441. [[CrossRef](#)]
27. Urbanová, M.; Šnajdr, J.; Baldrian, P. Composition of fungal and bacterial communities in forest litter and soil is largely determined by dominant trees. *Soil Biol. Biochem.* **2015**, *84*, 53–64. [[CrossRef](#)]
28. Nacke, H.; Goldmann, K.; Schöning, I.; Pfeiffer, B.; Kaiser, K.; Castillo-Villamizar, G.A.; Schrumpf, M.; Buscot, F.; Daniel, R.; Wubet, T. Fine spatial scale variation of soil microbial communities under European beech and Norway spruce. *Front. Microbiol.* **2016**, *7*, 2067. [[CrossRef](#)] [[PubMed](#)]
29. Fischer, M.; Bossdorf, O.; Gockel, S.; Hänsel, F.; Hemp, A.; Hessenmöller, D.; Korte, G.; Nieschulze, J.; Pfeiffer, S.; Prati, D.; et al. Implementing large-scale and long-term functional biodiversity research: The biodiversity exploratories. *Basic Appl. Ecol.* **2010**, *11*, 473–485. [[CrossRef](#)]
30. Solly, E.F.; Schöning, I.; Boch, S.; Kandeler, E.; Marhan, S.; Michalzik, B.; Müller, J.; Zscheischler, J.; Trumbore, S.E.; Schrumpf, M. Factors controlling decomposition rates of fine root litter in temperate forests and grasslands. *Plant Soil* **2014**, *382*, 203–218. [[CrossRef](#)]

31. Vogt, J.; Klaus, V.H.; Both, S.; Fürstenau, C.; Gockel, S.; Gossner, M.M.; Heinze, J.; Hemp, A.; Hölzel, N.; Jung, K.; et al. Eleven years' data of grassland management in Germany. *Biodivers. Data J.* **2019**, *7*, e36387. [\[CrossRef\]](#)
32. Blüthgen, N.; Dormann, C.F.; Prati, D.; Klaus, V.H.; Kleinebecker, T.; Hölzel, N.; Alt, F.; Boch, S.; Gockel, S.; Hemp, A.; et al. A quantitative index of land-use intensity in grasslands: Integrating mowing, grazing and fertilization. *Basic Appl. Ecol.* **2012**, *13*, 207–220. [\[CrossRef\]](#)
33. Dean, R.B.; Dixon, W.J. Simplified statistics for small numbers of observations. *Anal. Chem.* **1951**, *23*, 636–638. [\[CrossRef\]](#)
34. Ihrmark, K.; Bödeker, I.T.M.; Cruz-Martinez, K.; Friberg, H.; Kubartova, A.; Schenck, J.; Strid, Y.; Stenlid, J.; Brandström-Durling, M.; Clemmensen, K.E.; et al. New primers to amplify the fungal ITS2 region—Evaluation by 454-sequencing of artificial and natural communities. *FEMS Microbiol. Ecol.* **2012**, *82*, 666–677. [\[CrossRef\]](#)
35. Gardes, M.; Bruns, T.D. ITS primers with enhanced specificity for basidiomycetes—Application to the identification of mycorrhizae and rusts. *Mol. Ecol.* **1993**, *2*, 113–118. [\[CrossRef\]](#)
36. Schloss, P.D.; Westcott, S.L.; Ryabin, T.; Hall, J.R.; Hartmann, M.; Hollister, E.B.; Lesniewski, R.A.; Oakley, B.B.; Parks, D.H.; Robinson, C.J.; et al. Introducing mothur: Open-Source, platform-independent, community-supported software for describing and comparing microbial communities. *Appl. Environ. Microbiol.* **2009**, *75*, 7537–7541. [\[CrossRef\]](#)
37. Boyer, F.; Mercier, C.; Bonin, A.; Le Bras, Y.; Taberlet, P.; Coissac, E. OBITOOLS: A UNIX-inspired software package for DNA metabarcoding. *Mol. Ecol. Resour.* **2016**, *16*, 176–182. [\[CrossRef\]](#)
38. Masella, A.P.; Bartram, A.K.; Truszkowski, J.M.; Brown, D.G.; Neufeld, J.D. PANDAseq: Paired-end assembler for illumina sequences. *BMC Bioinform.* **2012**, *13*, 31. [\[CrossRef\]](#)
39. Edgar, R.C.; Haas, B.J.; Clemente, J.C.; Quince, C.; Knight, R. UCHIME improves sensitivity and speed of chimera detection. *Bioinformatics* **2011**, *27*, 2194–2200. [\[CrossRef\]](#)
40. Rognes, T.; Flouri, T.; Nichols, B.; Quince, C.; Mahé, F. VSEARCH: A versatile open source tool for metagenomics. *PeerJ* **2016**, *4*, e2584. [\[CrossRef\]](#)
41. Nilsson, R.H.; Larsson, K.-H.; Taylor, A.F.S.; Bengtsson-Palme, J.; Jeppesen, T.S.; Schigel, D.; Kennedy, P.; Picard, K.; Glöckner, F.O.; Tedersoo, L.; et al. The UNITE database for molecular identification of fungi: Handling dark taxa and parallel taxonomic classifications. *Nucleic Acids Res.* **2019**, *47*, D259–D264. [\[CrossRef\]](#)
42. Bengtsson-Palme, J.; Ryberg, M.; Hartmann, M.; Branco, S.; Wang, Z.; Godhe, A.; De Wit, P.; Sánchez-García, M.; Ebersberger, I.; de Sousa, F.; et al. Improved software detection and extraction of ITS1 and ITS2 from ribosomal ITS sequences of fungi and other eukaryotes for analysis of environmental sequencing data. *Methods Ecol. Evol.* **2013**, *4*, 914–919. [\[CrossRef\]](#)
43. McMurdie, P.J.; Holmes, S. phyloseq: An R package for reproducible interactive analysis and graphics of microbiome census data. *PLoS ONE* **2013**, *8*, e61217. [\[CrossRef\]](#)
44. R Core Team. *R: A Language and Environment for Statistical Computing*; R Foundation for Statistical Computing: Vienna, Austria, 2019.
45. Oksanen, J.; Blanchet, F.G.; Friendly, M.; Kindt, R.; Legendre, P.; McGlinn, D.; Michin, P.R.; O'Hara, R.B.; Simpson, G.L.; Solymos, P.; et al. *Vegan: Community Ecology Package*; R Foundation for Statistical Computing: Vienna, Austria, 2019.
46. Suzuki, M.T.; Taylor, L.T.; DeLong, E.F. Quantitative analysis of small-subunit rRNA genes in mixed microbial populations via 5'-nuclease assays. *Appl. Environ. Microbiol.* **2000**, *66*, 4605–4614. [\[CrossRef\]](#)
47. Jechalke, S.; Dealtry, S.; Smalla, K.; Heuer, H. Quantification of IncP-1 plasmid prevalence in environmental Samples. *Appl. Environ. Microbiol.* **2013**, *79*, 1410–1413. [\[CrossRef\]](#)
48. Pansegrau, W.; Lanka, E.; Barth, P.T.; Figurski, D.H.; Guiney, D.G.; Haas, D.; Helinski, D.R.; Schwab, H.; Stanisich, V.A.; Thomas, C.M. Complete nucleotide sequence of Birmingham IncPα plasmids. *J. Mol. Biol.* **1994**, *239*, 623–663. [\[CrossRef\]](#)
49. Barraud, O.; Baclet, M.C.; Denis, F.; Ploy, M.C. Quantitative multiplex real-time PCR for detecting class 1, 2 and 3 integrons. *J. Antimicrob. Chemother.* **2010**, *65*, 1642–1645. [\[CrossRef\]](#)
50. Zhu, Y.-G.; Johnson, T.A.; Su, J.-Q.; Qiao, M.; Guo, G.-X.; Stedtfeld, R.D.; Hashsham, S.A.; Tiedje, J.M. Diverse and abundant antibiotic resistance genes in Chinese swine farms. *Proc. Natl. Acad. Sci. USA* **2013**, *110*, 3435–3440. [\[CrossRef\]](#)

51. Looft, T.; Johnson, T.A.; Allen, H.K.; Bayles, D.O.; Alt, D.P.; Stedtfeld, R.D.; Sul, W.J.; Stedtfeld, T.M.; Chai, B.; Cole, J.R.; et al. In-feed antibiotic effects on the swine intestinal microbiome. *Proc. Natl. Acad. Sci. USA* **2012**, *109*, 1691–1696. [\[CrossRef\]](#)
52. Hu, H.-W.; Han, X.-M.; Shi, X.-Z.; Wang, J.-T.; Han, L.-L.; Chen, D.; He, J.-Z. Temporal changes of antibiotic-resistance genes and bacterial communities in two contrasting soils treated with cattle manure. *FEMS Microbiol. Ecol.* **2016**, *92*, fiv169. [\[CrossRef\]](#)
53. Zhao, Z.; Wang, J.; Han, Y.; Chen, J.; Liu, G.; Lu, H.; Yan, B.; Chen, S. Nutrients, heavy metals and microbial communities co-driven distribution of antibiotic resistance genes in adjacent environment of mariculture. *Environ. Pollut.* **2017**, *220*, 909–918. [\[CrossRef\]](#)
54. Kleiber, C.; Zeileis, A. *Applied Econometrics with R*; Springer New York: New York, NY, USA, 2008; ISBN 978-0-387-77316-2.
55. We, T.; Simko, V. *R Package “corrplot”: Visualization of a Correlation Matrix*; R Foundation for Statistical Computing: Vienna, Austria, 2017.
56. Lopaka, L. *NADA: Nondetects and Data Analysis for Environmental Data*; R Foundation for Statistical Computing: Vienna, Austria, 2017.
57. Mcfadden, D. Conditional logit analysis of qualitative choice behavior. In *Frontiers in Econometrics*; Zarembka, P., Ed.; Academic Press: New York, NY, USA, 1974; pp. 105–142.
58. Kaiser, K.; Wemheuer, B.; Korolkow, V.; Wemheuer, F.; Nacke, H.; Schöning, I.; Schrumpf, M.; Daniel, R. Driving forces of soil bacterial community structure, diversity, and function in temperate grasslands and forests. *Sci. Rep.* **2016**, *6*, 33696. [\[CrossRef\]](#)
59. Forsberg, K.J.; Patel, S.; Gibson, M.K.; Lauber, C.L.; Knight, R.; Fierer, N.; Dantas, G. Bacterial phylogeny structures soil resistomes across habitats. *Nature*. **2014**, *509*, 612–616. [\[CrossRef\]](#)
60. Lauber, C.L.; Hamady, M.; Knight, R.; Fierer, N. Pyrosequencing-based assessment of soil pH as a predictor of soil bacterial community structure at the continental scale. *Appl. Environ. Microbiol.* **2009**, *75*, 5111–5120. [\[CrossRef\]](#)
61. Rousk, J.; Bååth, E.; Brookes, P.C.; Lauber, C.L.; Lozupone, C.; Caporaso, J.G.; Knight, R.; Fierer, N. Soil bacterial and fungal communities across a pH gradient in an arable soil. *ISME J.* **2010**, *4*, 1340–1351. [\[CrossRef\]](#)
62. Allen, H.K.; Donato, J.; Wang, H.H.; Cloud-Hansen, K.A.; Davies, J.; Handelsman, J. Call of the wild: Antibiotic resistance genes in natural environments. *Nat. Rev. Microbiol.* **2010**, *8*, 251–259. [\[CrossRef\]](#)
63. Sköld, O. Sulfonamide resistance: Mechanisms and trends. *Drug Resist. Updat.* **2000**, *3*, 155–160. [\[CrossRef\]](#)
64. Sköld, O. Resistance to trimethoprim and sulfonamides. *Vet. Res.* **2001**, *32*, 261–273. [\[CrossRef\]](#)
65. Rawlings, D.E.; Tietze, E. Comparative biology of IncQ and IncQ-like plasmids. *Microbiol. Mol. Biol. Rev.* **2001**, *65*, 481–496. [\[CrossRef\]](#)
66. Antunes, P.; Machado, J.; Sousa, J.C.; Peixe, L. Dissemination of sulfonamide resistance genes (*sul1*, *sul2*, and *sul3*) in Portuguese *Salmonella enterica* strains and relation with integrons. *Antimicrob. Agents Chemother.* **2005**, *49*, 836–839. [\[CrossRef\]](#)
67. Seiffert, S.N.; Marschall, J.; Perreten, V.; Carattoli, A.; Furrer, H.; Endimiani, A. Emergence of *Klebsiella pneumoniae* co-producing NDM-1, OXA-48, CTX-M-15, CMY-16, QnrA and ArmA in Switzerland. *Int. J. Antimicrob. Agents* **2014**, *44*, 260–262. [\[CrossRef\]](#)
68. Guerra, B.; Junker, E.; Schroeter, A.; Malorny, B.; Lehmann, S.; Helmuth, R. Phenotypic and genotypic characterization of antimicrobial resistance in German *Escherichia coli* isolates from cattle, swine and poultry. *J. Antimicrob. Chemother.* **2003**, *52*, 489–492. [\[CrossRef\]](#)
69. Leclercq, R.; Courvalin, P. Resistance to macrolides and related antibiotics in *Streptococcus pneumoniae*. *Antimicrob. Agents Chemother.* **2002**, *46*, 2727–2734. [\[CrossRef\]](#)
70. Griffith, F. The serological classification of *Streptococcus pyogenes*. *Epidemiol. Infect.* **1934**, *34*, 542–584. [\[CrossRef\]](#)
71. Oster, P.; Zanchi, A.; Cresti, S.; Lattanzi, M.; Montagnani, F.; Cellesi, C.; Rossolini, G.M. Patterns of macrolide resistance determinants among community-acquired *Streptococcus pneumoniae* isolates over a 5-year period of decreased macrolide susceptibility rates. *Antimicrob. Agents Chemother.* **1999**, *43*, 2510–2512. [\[CrossRef\]](#)
72. Santagati, M.; Iannelli, F.; Cascone, C.; Campanile, F.; Oggioni, M.R.; Stefani, S.; Pozzi, G. The novel conjugative transposon Tn 1207.3 carries the macrolide efflux gene *mef* (A) in *Streptococcus pyogenes*. *Microb. Drug Resist.* **2003**, *9*, 243–247. [\[CrossRef\]](#)

73. Haenni, M.; Saras, E.; Bertin, S.; Leblond, P.; Madec, J.-Y.; Payot, S. Diversity and mobility of integrative and conjugative elements in bovine isolates of *Streptococcus agalactiae*, *S. dysgalactiae* subsp. *dysgalactiae*, and *S. uberis*. *Appl. Environ. Microbiol.* **2010**, *76*, 7957–7965. [CrossRef]
74. Collignon, P.; Powers, J.H.; Chiller, T.M.; Aidara-Kane, A.; Aarestrup, F.M. World Health Organization ranking of antimicrobials according to their importance in human medicine: A critical step for developing risk management strategies for the use of antimicrobials in food production animals. *Clin. Infect. Dis.* **2009**, *49*, 132–141. [CrossRef]
75. Giguère, S. *Antimicrobial Therapy in Veterinary Medicine*; John Wiley & Sons Inc.: Hoboken, NJ, USA, 2013. [CrossRef]
76. Bartram, D.J.; Moyaert, H.; Vanimisetti, B.H.; Ramage, C.P.; Reddick, D.; Stegemann, M.R. Comparative efficacy of tulathromycin and tildipirosin for the treatment of experimental *Mycoplasma bovis* infection in calves. *Vet. Med. Sci.* **2016**, *2*, 170–178. [CrossRef]
77. Baggot, J.D.; Gingerich, D.A. Pharmacokinetic interpretation of erythromycin and tylosin activity in serum after intravenous administration of a single dose to cows. *Res. Vet. Sci.* **1976**, *21*, 318–323. [CrossRef]
78. Blondeau, J. Differential impact of macrolide compounds in the selection of macrolide nonsusceptible *Streptococcus pneumoniae*. *Therapy* **2005**, *2*, 813–818. [CrossRef]
79. Kim, M.; Park, T.; Yu, Z. Metagenomic investigation of gastrointestinal microbiome in cattle. *Asian Australasian J. Anim. Sci.* **2017**, *30*, 1515. [CrossRef]
80. Holman, D.B.; Yang, W.; Alexander, T.W. Antibiotic treatment in feedlot cattle: A longitudinal study of the effect of oxytetracycline and tulathromycin on the fecal and nasopharyngeal microbiota. *Microbiome* **2019**, *7*, 86. [CrossRef]
81. United States Pharmacopeial Convention. *The United States Pharmacopeia 31: The National Formulary 26*; United States Pharmacopeial Convention: Rockville, MD, USA, 2007.
82. Ramirez, M.S.; Nikolaidis, N.; Tolmasky, M.E. Rise and dissemination of aminoglycoside resistance: The *aac(6′)-Ib* paradigm. *Front. Microbiol.* **2013**, *4*, 121. [CrossRef]
83. Lambert, T.; Ploy, M.-C.; Courvalin, P. A spontaneous point mutation in the *aac(6′)-Ib′* gene results in altered substrate specificity of aminoglycoside 6′-N-acetyltransferase of a *Pseudomonas fluorescens* strain. *FEMS Microbiol. Lett.* **1994**, *115*, 297–303. [CrossRef]
84. Robicsek, A.; Strahilevitz, J.; Jacoby, G.A.; Macielag, M.; Abbanat, D.; Hye Park, C.; Bush, K.; Hooper, D.C. Fluoroquinolone-modifying enzyme: A new adaptation of a common aminoglycoside acetyltransferase. *Nat. Med.* **2006**, *12*, 83–88. [CrossRef]
85. Wallmann, J. *Erfahrungen und Schlussfolgerungen aus der Antibiotikaabgabefassung in der Veterinärmedizin*; BVL: Berlin, Germany, 2014.
86. Aidara-Kane, A.; Angulo, F.J.; Conly, J.M.; Minato, Y.; Silbergeld, E.K.; McEwen, S.A.; Collignon, P.J.; WHO guideline development group. World Health Organization (WHO) guidelines on use of medically important antimicrobials in food-producing animals. *Antimicrob. Resist. Infect. Control.* **2018**, *7*, 7. [CrossRef]
87. Ruegg, P.L. Responsible Use of Antibiotics for Treatment of Clinical Mastitis—DAIReXNET. Available online: <https://dairy-cattle.extension.org/responsible-use-of-antibiotics-for-treatment-of-clinical-mastitis/> (accessed on 10 November 2019).
88. Persson, Y.; Katholm, J.; Landin, H.; Mörk, M.J. Efficacy of enrofloxacin for the treatment of acute clinical mastitis caused by *Escherichia coli* in dairy cows. *Vet. Rec.* **2015**, *176*, 673. [CrossRef]
89. Kemper, N. Veterinary antibiotics in the aquatic and terrestrial environment. *Ecol. Indic.* **2008**, *8*, 1–13. [CrossRef]
90. Thiele-Bruhn, S. Pharmaceutical antibiotic compounds in soils—A review. *J. Plant Nutr. Soil Sci.* **2003**, *166*, 145–167. [CrossRef]
91. Schulz, J.; Kemper, N.; Hartung, J.; Janusch, F.; Mohring, S.A.I.; Hamscher, G. Analysis of fluoroquinolones in dusts from intensive livestock farming and the co-occurrence of fluoroquinolone-resistant *Escherichia coli*. *Sci. Rep.* **2019**, *9*, 5117. [CrossRef]
92. Lillenberg, M.; Litvin, S.V.; Nei, L.; Roasto, M.; Sepp, K.I. Enrofloxacin and ciprofloxacin uptake by plants from soil. *Agron. Res.* **2010**, *8*, 807–814.
93. Hu, X.; Zhou, Q.; Luo, Y. Occurrence and source analysis of typical veterinary antibiotics in manure, soil, vegetables and groundwater from organic vegetable bases, northern China. *Environ. Pollut.* **2010**, *158*, 2992–2998. [CrossRef]

94. Alonso, A.; Sanchez, P.; Martinez, J.L. Environmental selection of antibiotic resistance genes. *Environ. Microbiol.* **2001**, *3*, 1–9. [[CrossRef](#)]
95. Yergeau, E.; Sanschagrin, S.; Maynard, C.; St-Arnaud, M.; Greer, C.W. Microbial expression profiles in the rhizosphere of willows depend on soil contamination. *ISME J.* **2014**, *8*, 344–358. [[CrossRef](#)]
96. Diene, S.M.; Rolain, J.-M. Carbapenemase genes and genetic platforms in Gram-negative bacilli: *Enterobacteriaceae*, *Pseudomonas* and *Acinetobacter* species. *Clin. Microbiol. Infect.* **2014**, *20*, 831–838. [[CrossRef](#)]
97. Cornaglia, G.; Giamarellou, H.; Rossolini, G.M. Metallo- β -lactamases: A last frontier for β -lactams? *Lancet Infect. Dis.* **2011**, *11*, 381–393. [[CrossRef](#)]
98. Docquier, J.-D.; Riccio, M.L.; Mugnaioli, C.; Luzzaro, F.; Endimiani, A.; Toniolo, A.; Amicosante, G.; Rossolini, G.M. IMP-12, a new plasmid-encoded metallo-beta-lactamase from a *Pseudomonas putida* clinical isolate. *Antimicrob. Agents Chemother.* **2003**, *47*, 1522–1528. [[CrossRef](#)] [[PubMed](#)]
99. Zhao, W.-H.; Chen, G.; Ito, R.; Kimura, S.; Hu, Z.-Q. Identification of a plasmid-borne *bla*_{IMP-11} gene in clinical isolates of *Escherichia coli* and *Klebsiella pneumoniae*. *J. Med. Microbiol.* **2012**, *61*, 246–251. [[CrossRef](#)] [[PubMed](#)]
100. Wang, S.; Zhou, K.; Xiao, S.; Xie, L.; Gu, F.; Li, X.; Ni, Y.; Sun, J.; Han, L. A multidrug resistance Plasmid pIMP26, carrying *bla*_{IMP-26}, *fosA5*, *bla*_{DHA-1}, and *qnrB4* in *Enterobacter cloacae*. *Sci. Rep.* **2019**, *9*, 10212. [[CrossRef](#)]
101. Braschi, I.; Blasioli, S.; Fellet, C.; Lorenzini, R.; Garelli, A.; Pori, M.; Giacomini, D. Persistence and degradation of new β -lactam antibiotics in the soil and water environment. *Chemosphere* **2013**, *93*, 152–159. [[CrossRef](#)]
102. Jechalke, S.; Heuer, H.; Siemens, J.; Amelung, W.; Smalla, K. Fate and effects of veterinary antibiotics in soil. *Trends Microbiol.* **2014**, *9*, 536–545. [[CrossRef](#)]
103. Chen, S.; Larsson, M.; Robinson, R.C.; Chen, S.L. Direct and convenient measurement of plasmid stability in lab and clinical isolates of *E. coli*. *Sci. Rep.* **2017**, *7*, 4788. [[CrossRef](#)]
104. Da Silva, G.; Correia, M.; Vital, C.; Ribeiro, G.; Sousa, J.C.; Leitão, R.; Peixe, L.; Duarte, A. Molecular characterization of *bla*_{IMP-5}, a new integrons-borne metallo- β -lactamase gene from an *Acinetobacter baumannii* nosocomial isolate in Portugal. *FEMS Microbiol. Lett.* **2002**, *215*, 33–39. [[CrossRef](#)]
105. Goldmann, K.; Schöning, I.; Buscot, F.; Wubet, T. Forest management type influences diversity and community composition of soil fungi across temperate forest ecosystems. *Front. Microbiol.* **2015**, *6*, 1300. [[CrossRef](#)]
106. Fleming, A. On the antibacterial action of cultures of a penicillium, with special reference to their use in the isolation of *B. influenzae*. *Br. J. Exp. Pathol.* **1929**, *10*, 226–236. [[CrossRef](#)]
107. Houbaken, J.; Frisvad, J.C.; Samson, R.A. Fleming's penicillin producing strain is not *Penicillium chrysogenum* but *P. rubens*. *IMA Fungus* **2011**, *2*, 87–95. [[CrossRef](#)] [[PubMed](#)]
108. Burton, H.S.; Abraham, E.P. Isolation of antibiotics from a species of *Cephalosporium*. Cephalosporins P₁, P₂, P₃, P₄ and P₅. *Biochem. J.* **1951**, *50*, 168–174. [[CrossRef](#)] [[PubMed](#)]
109. Pöggeler, S.; Hoff, B.; Kück, U. Asexual cephalosporin C producer *Acremonium chrysogenum* carries a functional mating type locus. *Appl. Environ. Microbiol.* **2008**, *74*, 6006–6016. [[CrossRef](#)] [[PubMed](#)]
110. Heuer, H.; Smalla, K. Plasmids foster diversification and adaptation of bacterial populations in soil. *FEMS Microbiol. Rev.* **2012**, *36*, 1083–1104. [[CrossRef](#)]
111. Popowska, M.; Krawczyk-Balska, A. Broad-host-range IncP-1 plasmids and their resistance potential. *Front. Microbiol.* **2013**, *4*, 44. [[CrossRef](#)]
112. Sen, D.; Van der Auwera, G.A.; Rogers, L.M.; Thomas, C.M.; Brown, C.J.; Top, E.M. Broad-host-range plasmids from agricultural soils have IncP-1 backbones with diverse accessory genes. *Appl. Environ. Microbiol.* **2011**, *77*, 7975–7983. [[CrossRef](#)]



3.1. Supplemental information for chapter three

Table S1: Plot characteristics and soil properties of all 300 experimental plots.

Table S2: ΔC_t values of all analyzed target sequences in the 300 experimental plots. The non-detect ΔC_t values are marked in grey.

Table S3: Preliminary binomial (A) or tobit regression models (B).

Table S1: Plot characteristics and soil properties of all 300 experimental plots. Graz., Mow., Fert., LUI, Org. N and Min. N represent grazing, mowing, the general fertilization frequency, the land use intensity index as described in Blüthgen et al. (2012), the organic nitrogen input from organic fertilizers and the nitrogen input from mineral fertilizers from the years 2006-2016. Tree describes the dominant tree type and Moist. the mean soil moisture in May 2017. Shannon H represents fungal diversity as assessed by Shannon index.

Plot ID	Graz.	Mow.	Fert.	Org. N	Min. N	LUI	Tree	pH	Moist.	Shannon H
SEG1	0.0	2.0	1.9	0.0	64.4	2.0	NA	7.5	44.1	4.6
SEG2	0.4	1.5	1.8	52.0	63.5	1.9	NA	7.5	49.0	4.5
SEG3	0.5	1.7	1.8	0.0	52.9	2.0	NA	7.6	50.2	4.4
SEG4	0.3	0.7	0.0	18.1	1.8	1.0	NA	7.5	24.7	4.7
SEG5	0.1	1.1	0.0	11.1	6.8	1.1	NA	7.6	39.0	4.2
SEG6	1.7	0.4	0.0	0.0	6.8	1.4	NA	5.5	36.7	3.9
SEG7	2.6	0.1	0.0	0.0	0.0	1.7	NA	7.5	32.8	4.1
SEG8	0.8	1.0	0.6	9.5	0.0	1.5	NA	7.5	29.2	3.9
SEG9	2.9	0.2	0.0	0.0	0.0	1.8	NA	6.6	55.6	4.6
SEG10	0.6	1.4	1.8	0.0	52.9	2.0	NA	7.5	43.9	4.4
SEG11	0.6	1.2	1.8	0.0	59.7	1.9	NA	7.5	34.5	4.6
SEG12	0.0	2.0	1.9	0.0	64.4	2.0	NA	7.5	51.7	4.5
SEG13	0.2	1.8	0.6	8.9	25.2	1.6	NA	5.5	20.0	4.2
SEG14	0.6	0.7	0.0	44.2	7.7	1.2	NA	7.5	51.8	4.3
SEG15	0.0	1.3	0.0	32.0	7.3	1.2	NA	7.5	52.2	4.6
SEG16	1.0	0.7	0.0	0.0	0.0	1.3	NA	7.4	39.1	4.5
SEG17	0.8	1.1	0.0	3.9	0.0	1.4	NA	5.4	34.5	4.5
SEG18	0.0	1.8	0.0	32.5	7.7	1.3	NA	4.9	26.2	3.6
SEG19	0.8	0.6	0.0	0.0	6.8	1.2	NA	7.5	43.4	4.8
SEG20	2.2	0.3	0.0	0.0	0.0	1.6	NA	6.4	20.9	4.5
SEG21	2.6	0.1	0.0	19.1	0.0	1.6	NA	5.3	20.9	4.5
SEG22	2.8	0.0	0.0	3.5	0.0	1.7	NA	7.5	39.7	4.6
SEG23	0.0	2.1	1.0	23.7	0.0	1.8	NA	5.2	35.2	3.8
SEG24	0.0	1.2	0.0	18.5	0.0	1.1	NA	7.5	54.5	4.4
SEG25	0.0	2.0	0.0	0.0	0.0	1.4	NA	6.5	48.6	4.6
SEG26	0.0	2.0	1.0	22.3	0.0	1.7	NA	7.2	41.2	4.6
SEG27	0.0	1.1	0.0	0.0	0.0	1.0	NA	6.1	26.1	4.3
SEG28	0.0	1.3	0.0	0.0	0.0	1.2	NA	7.5	52.6	4.2
SEG29	0.1	0.8	0.0	0.0	0.0	0.9	NA	7.6	53.8	4.7
SEG30	0.0	1.7	0.0	0.0	0.0	1.3	NA	7.0	27.1	3.7
SEG31	0.0	1.7	0.0	0.0	0.0	1.3	NA	6.0	31.4	3.7
SEG32	0.0	1.7	0.0	0.0	0.0	1.3	NA	5.7	14.6	4.1
SEG33	2.1	0.3	0.9	18.3	12.0	1.8	NA	5.7	33.8	4.1
SEG34	1.2	0.5	1.6	27.5	23.1	1.8	NA	5.8	29.5	4.3
SEG35	1.0	0.7	1.6	33.5	29.9	1.8	NA	6.2	27.3	3.8
SEG36	2.1	0.1	0.0	6.0	6.8	1.5	NA	6.3	28.4	4.6
SEG37	2.7	0.2	0.0	17.3	6.4	1.7	NA	4.7	15.2	4.1
SEG38	4.3	0.9	0.0	4.5	0.0	2.3	NA	5.2	13.5	4.0
SEG39	0.8	0.7	0.2	6.7	12.0	1.3	NA	7.4	29.6	4.1
SEG40	4.1	0.0	0.0	6.7	6.4	2.0	NA	6.1	22.8	3.7
SEG41	4.1	0.2	0.0	32.0	4.6	2.1	NA	6.1	24.4	4.4
SEG42	5.2	0.0	2.2	23.5	2.7	2.7	NA	5.0	18.2	4.3
SEG43	2.5	0.0	1.8	6.8	0.0	2.1	NA	6.5	24.7	4.6
SEG44	2.1	0.0	0.3	0.0	0.0	1.5	NA	5.5	24.5	4.5
SEG45	1.8	0.0	0.0	9.8	0.0	1.3	NA	5.9	19.7	4.6
SEG46	4.4	0.1	0.0	0.0	0.0	2.1	NA	7.1	20.9	4.5

Table S1 continued:

Plot ID	Graz.	Mow.	Fert.	Org. N	Min. N	LUI	Tree	pH	Moist.	Shannon H
SEG47	2.3	0.2	0.0	0.0	0.0	1.6	NA	5.7	28.7	4.6
SEG48	3.0	0.1	0.0	0.0	0.0	1.7	NA	6.7	18.4	4.4
SEG49	2.7	0	0	0	0	1.6	NA	6.4	NA	4.2
SEG50	2.1	0	0	2.2	0	1.5	NA	5.4	11.2	4.4
SEW1	NA	NA	NA	NA	NA	NA	Pine	3.6	11.9	3.9
SEW2	NA	NA	NA	NA	NA	NA	Pine	3.5	10.5	4.5
SEW3	NA	NA	NA	NA	NA	NA	Pine	3.4	15.3	4
SEW4	NA	NA	NA	NA	NA	NA	Pine	3.5	18.1	3.5
SEW5	NA	NA	NA	NA	NA	NA	Beech	3.4	14.2	3.4
SEW6	NA	NA	NA	NA	NA	NA	Beech	3.7	15.8	4.1
SEW7	NA	NA	NA	NA	NA	NA	Beech	3.8	17.9	4.3
SEW8	NA	NA	NA	NA	NA	NA	Beech	3.4	12.8	4.2
SEW9	NA	NA	NA	NA	NA	NA	Beech	3.5	17.8	3.4
SEW10	NA	NA	NA	NA	NA	NA	Pine	3.7	10.2	3.8
SEW11	NA	NA	NA	NA	NA	NA	Pine	3.7	15.2	3.9
SEW12	NA	NA	NA	NA	NA	NA	Pine	3.5	9.2	3.1
SEW13	NA	NA	NA	NA	NA	NA	Pine	3.3	17.3	4.2
SEW14	NA	NA	NA	NA	NA	NA	Pine	3.4	NA	4.1
SEW15	NA	NA	NA	NA	NA	NA	Pine	3.7	10.4	3.9
SEW16	NA	NA	NA	NA	NA	NA	Pine	3.6	13.2	3.4
SEW17	NA	NA	NA	NA	NA	NA	Pine	3.3	15.0	3.1
SEW18	NA	NA	NA	NA	NA	NA	Pine	3.3	10.4	3.5
SEW19	NA	NA	NA	NA	NA	NA	Pine	3.6	11.8	3
SEW20	NA	NA	NA	NA	NA	NA	Pine	3.6	10.6	4.2
SEW21	NA	NA	NA	NA	NA	NA	Pine	3.3	10.8	4
SEW22	NA	NA	NA	NA	NA	NA	Oak	3.6	17.2	4.4
SEW23	NA	NA	NA	NA	NA	NA	Oak	3.5	14.5	3.9
SEW24	NA	NA	NA	NA	NA	NA	Oak	3.7	18.5	4.4
SEW25	NA	NA	NA	NA	NA	NA	Oak	3.7	15.4	4.3
SEW26	NA	NA	NA	NA	NA	NA	Oak	3.7	14.1	4.3
SEW27	NA	NA	NA	NA	NA	NA	Oak	3.4	15.6	4.1
SEW28	NA	NA	NA	NA	NA	NA	Oak	3.5	14.8	4.2
SEW29	NA	NA	NA	NA	NA	NA	Pine	3.3	12.1	3.8
SEW30	NA	NA	NA	NA	NA	NA	Pine	3.4	13.9	3.3
SEW31	NA	NA	NA	NA	NA	NA	Pine	3.4	NA	4.1
SEW32	NA	NA	NA	NA	NA	NA	Pine	3.5	11.7	3.9
SEW33	NA	NA	NA	NA	NA	NA	Pine	3.4	11.8	3.1
SEW34	NA	NA	NA	NA	NA	NA	Pine	3.5	15.9	2.9
SEW35	NA	NA	NA	NA	NA	NA	Beech	3.6	11.9	4.1
SEW36	NA	NA	NA	NA	NA	NA	Beech	3.3	13.2	3.4
SEW37	NA	NA	NA	NA	NA	NA	Beech	3.6	17.0	4
SEW38	NA	NA	NA	NA	NA	NA	Beech	3.4	15.9	3.9
SEW39	NA	NA	NA	NA	NA	NA	Beech	3.7	11.7	4.1
SEW40	NA	NA	NA	NA	NA	NA	Beech	3.8	16.7	4.5
SEW41	NA	NA	NA	NA	NA	NA	Beech	3.8	18.5	4.3
SEW42	NA	NA	NA	NA	NA	NA	Beech	3.8	16.1	4.3
SEW43	NA	NA	NA	NA	NA	NA	Beech	3.7	NA	3.7
SEW44	NA	NA	NA	NA	NA	NA	Beech	3.7	20.1	3.9
SEW45	NA	NA	NA	NA	NA	NA	Beech	3.7	15.9	3.9
SEW46	NA	NA	NA	NA	NA	NA	Beech	3.5	13.9	3.7
SEW47	NA	NA	NA	NA	NA	NA	Beech	3.5	10.0	3.9

Table S1 continued:

Plot ID	Graz.	Mow.	Fert.	Org. N	Min. N	LUI	Tree	pH	Moist.	Shannon H
SEW48	NA	NA	NA	NA	NA	NA	Beech	3.7	16.4	4.2
SEW49	NA	NA	NA	NA	NA	NA	Beech	3.5	12.6	4
SEW50	NA	NA	NA	NA	NA	NA	Beech	3.7	NA	3.9
HEG1	0.3	2.3	5.4	34.5	101	2.8	NA	6.6	41.4	3.4
HEG2	0.1	2.2	3.7	0	106	2.5	NA	7.3	20.6	4.6
HEG3	0.1	2.8	4.3	0	97.9	2.7	NA	7.3	25.8	4.6
HEG4	0.7	1.7	2.9	8	42	2.3	NA	6.5	26.4	5
HEG5	0.9	2	3.5	17.5	64.1	2.5	NA	7.2	35.9	4.6
HEG6	0.4	1.5	1.9	68.7	0	2	NA	5.9	NA	4.4
HEG7	2.4	0.2	0	7.6	0	1.6	NA	7	28.1	4.7
HEG8	1.8	0.1	0	15.6	0	1.4	NA	7	32.6	4.7
HEG9	0.6	0.1	0	0	0	0.8	NA	7.1	32.9	4.7
HEG10	0.2	1.1	1.2	48.2	0	1.6	NA	6.5	33.0	3.8
HEG11	0.2	1	0.9	48.2	0	1.4	NA	7.3	25.8	3
HEG12	7.3	0.3	1.3	0	28.5	3	NA	7	30.6	4.2
HEG13	0.4	2.5	0.3	8.8	5.5	1.8	NA	7.2	29.1	4.1
HEG14	0.4	1.2	3.3	60.6	50.5	2.2	NA	6.4	27.7	3.6
HEG15	0.3	1.2	3.1	19.3	61.9	2.2	NA	7.1	23.4	4.2
HEG16	1.3	0	0	0	0	1.1	NA	6.8	35.7	4.4
HEG17	0.4	0.1	0	0	0	0.7	NA	6.9	32.7	3.4
HEG18	0.4	0.2	0	0	0	0.8	NA	7.4	28.5	4.5
HEG19	0.4	0	0	0	0	0.7	NA	6.6	36.9	3.6
HEG20	0.8	0.1	0	0	0	1	NA	5.5	29.0	1.9
HEG21	0.5	0.1	0	0	0	0.8	NA	7.3	31.2	4
HEG22	0.3	1.7	0.2	0	0	1.5	NA	6.9	19.0	4.5
HEG23	0.7	1.1	0	8	0	1.3	NA	7.3	34.4	3.4
HEG24	1.2	1.1	0	0	0	1.5	NA	6.8	30.0	4.7
HEG25	1.4	0.6	0	0	0	1.4	NA	7.3	21.4	3.2
HEG26	0	1.2	0.6	25.8	4.6	1.3	NA	7.4	31.7	4.3
HEG27	0.1	1.2	2	0	44.7	1.8	NA	7.2	28.4	4
HEG28	0.1	1.5	1.4	2	38.4	1.7	NA	7.3	36.8	3.3
HEG29	0.3	1.6	1.2	2	39.9	1.7	NA	7.2	35.0	4.3
HEG30	0.2	2.6	3.1	10.5	65	2.4	NA	7.2	30.3	4
HEG31	0.5	1.3	1.9	0	49.6	1.9	NA	7.2	30.6	2.6
HEG32	1.1	1	1.9	0	42	2	NA	5.6	28.8	4
HEG33	1	1.2	1.2	0	34.4	1.8	NA	5.3	23.6	4.1
HEG34	0.4	1.5	2.2	68.8	0	2	NA	7	37.2	4.1
HEG35	1.6	1	2.1	55	13.7	2.2	NA	7	24.5	4.5
HEG36	0.6	1.3	3.2	34.5	57.3	2.3	NA	7.3	27.9	3.9
HEG37	0.6	1.6	3.6	24.2	53	2.4	NA	7.3	16.3	4.3
HEG38	3.2	0.2	0	0	0	1.9	NA	7.3	NA	3.6
HEG39	1.2	0.4	0	0	0	1.3	NA	6.5	35.9	4.8
HEG40	2.6	0	0	0	0	1.6	NA	6.6	32.6	4.3
HEG41	0.8	0.1	0	0	0	1	NA	7.2	22.3	4.3
HEG42	0.4	0	0	2.6	0	0.7	NA	7.2	40.3	3.4
HEG43	0.6	0.4	0	15.8	0	1	NA	7.1	33.9	4.1
HEG44	0.5	0.3	0	10.5	0	0.9	NA	7.1	26.3	3.5
HEG45	0.5	0.1	0	0	0	0.8	NA	7	35.9	2.9
HEG46	0.6	0.3	0	0	0	0.9	NA	7.4	20.8	4.1
HEG47	0.8	1.2	0.3	0	0	1.5	NA	7.2	29.5	3.5
HEG48	0.7	1.2	0.3	0	0	1.5	NA	7	NA	3.4

Table S1 continued:

Plot ID	Graz.	Mow.	Fert.	Org. N	Min. N	LUI	Tree	pH	Moist.	Shannon H
HEG49	0.2	1.4	1.2	43.3	0	1.7	NA	6.7	31.5	4.1
HEG50	0.3	1	1.5	40.7	0	1.7	NA	6.9	33.2	3.7
HEW1	NA	NA	NA	NA	NA	NA	Spruce	6.2	30.0	4
HEW3	NA	NA	NA	NA	NA	NA	Spruce	5.1	15.0	4.3
HEW4	NA	NA	NA	NA	NA	NA	Beech	6.1	33.8	4.9
HEW5	NA	NA	NA	NA	NA	NA	Beech	5.3	33.3	3.1
HEW6	NA	NA	NA	NA	NA	NA	Beech	4.4	30.0	4.2
HEW7	NA	NA	NA	NA	NA	NA	Beech	4.1	44.2	4.3
HEW8	NA	NA	NA	NA	NA	NA	Beech	5.7	NA	3.9
HEW9	NA	NA	NA	NA	NA	NA	Beech	4.4	36.2	3.2
HEW10	NA	NA	NA	NA	NA	NA	Beech	4.9	NA	4.4
HEW11	NA	NA	NA	NA	NA	NA	Beech	4.9	NA	4.6
HEW12	NA	NA	NA	NA	NA	NA	Beech	4.1	25.9	4.6
HEW13	NA	NA	NA	NA	NA	NA	Spruce	6.8	31.2	3.9
HEW14	NA	NA	NA	NA	NA	NA	Beech	5.1	37.5	2.7
HEW15	NA	NA	NA	NA	NA	NA	Beech	4	30.7	4.5
HEW16	NA	NA	NA	NA	NA	NA	Beech	4.9	NA	4.9
HEW17	NA	NA	NA	NA	NA	NA	Beech	3.9	27.4	3.9
HEW18	NA	NA	NA	NA	NA	NA	Beech	5.6	30.2	4.8
HEW19	NA	NA	NA	NA	NA	NA	Beech	4.6	34.0	4.5
HEW20	NA	NA	NA	NA	NA	NA	Beech	6.7	36.1	4.5
HEW21	NA	NA	NA	NA	NA	NA	Beech	6.3	48.3	4.2
HEW22	NA	NA	NA	NA	NA	NA	Beech	4.8	34.5	4.1
HEW23	NA	NA	NA	NA	NA	NA	Beech	4.7	33.6	4
HEW24	NA	NA	NA	NA	NA	NA	Beech	4	32.8	4
HEW25	NA	NA	NA	NA	NA	NA	Beech	4.7	33.0	4.7
HEW26	NA	NA	NA	NA	NA	NA	Beech	4.3	29.4	4.2
HEW27	NA	NA	NA	NA	NA	NA	Beech	6	42.7	4.6
HEW28	NA	NA	NA	NA	NA	NA	Beech	6.2	41.3	3.8
HEW29	NA	NA	NA	NA	NA	NA	Beech	4.1	NA	4.5
HEW30	NA	NA	NA	NA	NA	NA	Beech	4.1	25.4	3.2
HEW31	NA	NA	NA	NA	NA	NA	Beech	4.1	28.3	4.6
HEW32	NA	NA	NA	NA	NA	NA	Beech	3.9	26.0	4.2
HEW33	NA	NA	NA	NA	NA	NA	Beech	4.8	37.1	4.4
HEW34	NA	NA	NA	NA	NA	NA	Beech	4.7	29.5	4.8
HEW35	NA	NA	NA	NA	NA	NA	Beech	4.4	33.1	4.5
HEW36	NA	NA	NA	NA	NA	NA	Beech	4.7	45.6	4.3
HEW37	NA	NA	NA	NA	NA	NA	Beech	4.4	31.6	4.2
HEW38	NA	NA	NA	NA	NA	NA	Beech	5.4	33.2	4.2
HEW39	NA	NA	NA	NA	NA	NA	Beech	4.5	32.5	4.6
HEW40	NA	NA	NA	NA	NA	NA	Beech	5.4	38.2	4.7
HEW41	NA	NA	NA	NA	NA	NA	Beech	4.6	NA	4.3
HEW42	NA	NA	NA	NA	NA	NA	Beech	4.2	31.2	4.6
HEW43	NA	NA	NA	NA	NA	NA	Beech	6.7	42.6	4.9
HEW44	NA	NA	NA	NA	NA	NA	Beech	5.4	38.7	4.2
HEW45	NA	NA	NA	NA	NA	NA	Beech	7.2	NA	3.6
HEW46	NA	NA	NA	NA	NA	NA	Beech	4.2	27.1	4.1
HEW47	NA	NA	NA	NA	NA	NA	Beech	4.9	34.4	4.5
HEW48	NA	NA	NA	NA	NA	NA	Beech	4.4	NA	4.4
HEW49	NA	NA	NA	NA	NA	NA	Beech	4.1	29.4	4
HEW50	NA	NA	NA	NA	NA	NA	Beech	4.8	31.4	3.8

Table S1 continued:

Plot ID	Graz.	Mow.	Fert.	Org. N	Min. N	LUI	Tree	pH	Moist.	Shannon H
HEW51	NA	NA	NA	NA	NA	NA	Spruce	6.6	41.5	3.6
AEG1	0	2	1.8	29.3	49.5	2	NA	6.8	21.6	4.3
AEG2	0	2.8	8.3	142.7	62.7	3.3	NA	6.9	34.4	4.6
AEG3	0.1	2	1.1	41.7	26.1	1.8	NA	6.1	35.6	4.2
AEG4	0.7	1	1.4	42.5	39.9	1.8	NA	5.3	43.0	4.6
AEG5	0.7	0.9	1.7	8.9	54.4	1.8	NA	6.3	38.7	4.4
AEG6	2.2	1	1.7	19.9	32.3	2.2	NA	6	34.8	4.3
AEG7	0.3	0	0	0	0	0.5	NA	7.3	32.3	2.4
AEG8	0.7	0.9	0	0	0	1.3	NA	6.6	30.4	4.6
AEG9	0.5	0	0	0	0	0.7	NA	6.6	31.9	3.4
AEG10	0	1	0	10.2	2.7	1	NA	5.9	35.3	4.2
AEG11	0	2.8	1.7	18.7	29.4	2.1	NA	5.4	37.4	3.9
AEG12	0	2.1	2.4	42.3	39.5	2.1	NA	6.6	30.0	4.6
AEG13	0	2	2.5	42.3	29.4	2.1	NA	6.3	35.1	4.7
AEG14	0	2	3.6	55.1	35.5	2.4	NA	6.6	29.6	4.6
AEG15	0	2.9	6.1	139.3	25	3	NA	5.7	43.4	3.8
AEG16	0.9	1.2	0.6	24.5	0	1.6	NA	6	34.5	4.5
AEG17	0	2.2	1.6	45.2	2.7	2	NA	6.9	38.9	4.2
AEG18	0	2.6	4.2	104.6	25	2.6	NA	6.9	31.9	3.8
AEG19	2.8	0.7	1.3	0	28.6	2.2	NA	5.8	36.8	4.7
AEG20	1.5	0	0.5	0	13.6	1.4	NA	6.7	42.4	4.9
AEG21	6.2	0.4	5.2	98	1.4	3.5	NA	5.8	32.9	4.5
AEG22	0.3	1	0.4	7	0	1.3	NA	5.7	36.9	4.1
AEG23	0	1.8	0.4	11.2	0	1.5	NA	7.1	42.8	3.6
AEG24	1	2.1	2.3	87.3	0	2.3	NA	6.1	39.9	4.4
AEG25	0.4	0	0.1	0	0	0.8	NA	7.2	36.7	3.6
AEG26	2	0	0	9.6	0	1.4	NA	6.8	NA	4
AEG27	1.2	0	0	0	9.1	1.1	NA	6	30.5	2.2
AEG28	0.8	0	0	0	0	0.9	NA	6.1	26.1	3
AEG29	0.7	1.1	0.4	48.5	0	1.5	NA	5.9	15.4	4.4
AEG30	1.3	0.8	0.3	0	18.6	1.6	NA	6.6	38.5	4.7
AEG31	1.1	0.7	0	0	4.6	1.4	NA	6.7	36.1	4.8
AEG32	0.5	0	0	0	9.1	0.7	NA	5.4	42.6	4.5
AEG33	1.2	0	0	0	0	1.1	NA	6	42.6	4.3
AEG34	1	0.5	0	13.2	3.6	1.3	NA	6.3	37.3	3.9
AEG35	0	2.1	1.4	18.5	29.1	1.9	NA	5.3	39.1	4.1
AEG36	0	2	1.7	9.4	42.6	1.9	NA	6	41.2	4
AEG37	0.1	2	1.7	35.4	47.6	1.9	NA	6.3	38.7	3.7
AEG38	0	2	0.3	9.3	3.6	1.5	NA	5.6	46.9	4
AEG39	0	2	1.9	29.9	29.5	2	NA	6	33.1	4.8
AEG40	0.2	2.4	1.8	44.2	12.7	2.1	NA	6.9	34.1	3
AEG41	0.1	2.3	4.7	95.8	19.7	2.7	NA	6.3	28.8	4.8
AEG42	1.2	1.6	2	49	2.7	2.2	NA	7.1	32.7	4.9
AEG43	1	0.9	0.8	29.8	0	1.7	NA	6.9	33.1	4.5
AEG44	2.5	0	0	0	0	1.6	NA	7.3	38.4	4.6
AEG45	0	2.3	0.1	9.8	0	1.6	NA	5.4	NA	4.5
AEG46	2.4	0	0	0	0	1.5	NA	6	42.2	4.5
AEG47	0.7	0	0	9.6	0	0.8	NA	7.5	29.4	4
AEG48	0.4	0	0	9.6	0	0.7	NA	7.6	27.1	4.2
AEG49	1	0	0	9.6	0	1	NA	6	36.3	3.9
AEG50	0	2	2.1	69	12.5	2	NA	6	33.8	4.6

Table S1 continued:

Plot ID	Graz.	Mow.	Fert.	Org. N	Min. N	LUI	Tree	pH	Moist.	Shannon H
AEW1	NA	NA	NA	NA	NA	NA	Spruce	3.3	38.7	3.6
AEW2	NA	NA	NA	NA	NA	NA	Spruce	4.8	23.4	4.5
AEW3	NA	NA	NA	NA	NA	NA	Spruce	5.6	34.6	4.1
AEW4	NA	NA	NA	NA	NA	NA	Beech	6.8	38.7	3.6
AEW5	NA	NA	NA	NA	NA	NA	Beech	4.5	NA	3.6
AEW6	NA	NA	NA	NA	NA	NA	Beech	5.6	39.9	4.1
AEW7	NA	NA	NA	NA	NA	NA	Beech	5	41.6	2.8
AEW8	NA	NA	NA	NA	NA	NA	Beech	6.4	42.9	3
AEW9	NA	NA	NA	NA	NA	NA	Beech	6.1	27.5	3.1
AEW10	NA	NA	NA	NA	NA	NA	Spruce	4.6	30.9	3.1
AEW11	NA	NA	NA	NA	NA	NA	Spruce	3.4	27.8	3.3
AEW12	NA	NA	NA	NA	NA	NA	Spruce	4.5	32.0	4.4
AEW13	NA	NA	NA	NA	NA	NA	Spruce	5.2	40.7	4
AEW14	NA	NA	NA	NA	NA	NA	Spruce	4.8	38.9	4.6
AEW15	NA	NA	NA	NA	NA	NA	Beech	6.4	36.7	4.1
AEW16	NA	NA	NA	NA	NA	NA	Beech	6.4	30.1	3.7
AEW17	NA	NA	NA	NA	NA	NA	Beech	6.5	42.6	4.1
AEW18	NA	NA	NA	NA	NA	NA	Beech	4.7	30.3	4.4
AEW19	NA	NA	NA	NA	NA	NA	Beech	5.1	32.0	4
AEW20	NA	NA	NA	NA	NA	NA	Beech	6.6	40.5	3.8
AEW21	NA	NA	NA	NA	NA	NA	Beech	6.3	28.8	5.3
AEW22	NA	NA	NA	NA	NA	NA	Beech	6.3	40.7	4
AEW23	NA	NA	NA	NA	NA	NA	Beech	5.6	20.5	3.9
AEW24	NA	NA	NA	NA	NA	NA	Beech	5.3	NA	4.6
AEW25	NA	NA	NA	NA	NA	NA	Beech	5.1	31.1	3.9
AEW26	NA	NA	NA	NA	NA	NA	Beech	5.1	39.4	3.8
AEW27	NA	NA	NA	NA	NA	NA	Beech	4.6	39.5	4
AEW28	NA	NA	NA	NA	NA	NA	Beech	4.7	33.4	4.2
AEW29	NA	NA	NA	NA	NA	NA	Beech	4.4	34.3	4.3
AEW30	NA	NA	NA	NA	NA	NA	Beech	5.8	39.6	4.4
AEW31	NA	NA	NA	NA	NA	NA	Spruce	5.6	33.6	3.9
AEW32	NA	NA	NA	NA	NA	NA	Spruce	6.9	13.4	3.8
AEW33	NA	NA	NA	NA	NA	NA	Spruce	5.8	26.6	3.9
AEW34	NA	NA	NA	NA	NA	NA	Spruce	4.9	29.5	4.4
AEW35	NA	NA	NA	NA	NA	NA	Beech	5.5	39.2	4.7
AEW36	NA	NA	NA	NA	NA	NA	Beech	6	29.4	4.5
AEW37	NA	NA	NA	NA	NA	NA	Beech	5.2	37.9	3.9
AEW38	NA	NA	NA	NA	NA	NA	Beech	6.9	31.9	4.3
AEW39	NA	NA	NA	NA	NA	NA	Beech	5.2	31.5	4.4
AEW40	NA	NA	NA	NA	NA	NA	Beech	5.3	35.4	4.5
AEW41	NA	NA	NA	NA	NA	NA	Beech	5.7	38.6	4.1
AEW42	NA	NA	NA	NA	NA	NA	Beech	6.5	21.7	4.7
AEW43	NA	NA	NA	NA	NA	NA	Beech	5.1	38.0	5
AEW44	NA	NA	NA	NA	NA	NA	Beech	6	NA	3.7
AEW45	NA	NA	NA	NA	NA	NA	Beech	5.8	26.5	4.4
AEW46	NA	NA	NA	NA	NA	NA	Beech	5.5	35.4	3.9
AEW47	NA	NA	NA	NA	NA	NA	Beech	5.2	NA	4
AEW48	NA	NA	NA	NA	NA	NA	Beech	5.8	31.6	4.2
AEW49	NA	NA	NA	NA	NA	NA	Beech	6.3	20.7	4.7
AEW50	NA	NA	NA	NA	NA	NA	Beech	5.9	27.0	3.2

Table S2: ΔC_t values of all analyzed target sequences in the 300 experimental plots. The non-detect ΔC_t values are marked in grey.

Plot ID	IncP-1.	Class 1 integrans.	<i>aac(6')-lb</i>	<i>aacC1</i>	<i>blaIMP-12</i>	<i>blaIMP-5</i>	<i>ermB</i>	<i>mefA</i>	<i>tetA</i>	<i>sul2</i>
SEG1	-17	-20.51	-18.89	-19.58	-20	-19.39	-20.02	-19.43	-19.92	-20.31
SEG2	-14.5	-20.51	-18.18	-19.58	-20	-17.43	-19.12	-19.04	-19.92	-20.31
SEG3	-15.5	-20.51	-18.31	-19.58	-20	-20.13	-20.02	-17.51	-19.92	-20.31
SEG4	-16.5	-20.51	-18.05	-19.58	-20	-20.13	-20.02	-19.43	-19.92	-20.31
SEG5	-19.81	NA	-18.28	-19.58	-16.77	-18.16	-20.02	-19.43	-19.92	-20.31
SEG6	-15.8	-20.51	-19.93	-19.58	-20	-20.13	-20.02	-19.43	-19.92	-20.31
SEG7	-17.7	-20.51	-19.93	-19.58	-17.81	-17.24	-20.02	-19.43	-19.92	-20.31
SEG8	-18.7	-20.51	-18.21	-19.58	-20	-20.13	-20.02	-17.98	-19.92	-20.31
SEG9	-18	-20.51	-19.92	-19.58	-20	-20.13	-20.02	-19.43	-19.92	-20.31
SEG10	-17.1	-20.51	-19.93	-19.58	-20	-20.13	-20.02	-19.43	-19.92	-20.31
SEG11	-18.4	-20.51	-18.92	-19.58	-20	-20.13	-20.02	-19.43	-19.92	-20.31
SEG12	-15.7	-20.51	-19.93	-19.58	-20	-20.13	-20.02	-19.43	-19.92	-14.67
SEG13	-16.3	-18.1	-19.93	-19.58	-18.21	-20.13	-20.02	-16.5	-19.92	-14.65
SEG14	-19.81	-20.51	-19.93	-19.58	-17.95	-20.13	-20.02	-19.43	-19.92	-16.79
SEG15	-15.4	-20.51	-19.93	-19.58	-20	-20.13	-20.02	-19.43	-19.92	-20.31
SEG16	-19.81	-20.51	-19.93	-19.58	-20	-20.13	-20.02	-19.43	-19.92	-20.31
SEG17	-19.81	-20.51	-19.93	-19.58	-20	-20.13	-20.02	-19.43	-19.92	NA
SEG18	-14.1	-20.51	-17.29	-19.58	-20	-20.13	-20.02	-19.43	-19.92	-14.18
SEG19	-18.1	-20.51	-19.93	-19.58	-20	-20.13	-20.02	-19.43	-19.92	-20.31
SEG20	-15.7	-20.51	-19.93	-19.58	-20	-20.13	-20.02	-19.43	-19.92	-20.31
SEG21	-16.1	-20.51	-19.93	-19.58	-20	-18.72	-20.02	-19.43	-19.92	-20.31
SEG22	-19.81	-20.51	-17.64	-19.58	-20	-20.13	-20.02	-19.43	-19.92	-20.31
SEG23	-19.81	NA	-19.93	-19.58	-19.17	-20.13	-20.02	-16.98	-19.92	-20.31
SEG24	-19.81	-20.51	-18.12	-19.58	-18.9	-20.13	-20.02	-19.43	-19.92	-20.31
SEG25	-15.9	-20.51	-19.93	-19.58	-20	-20.13	-20.02	-19.43	-19.92	-20.31
SEG26	-16.8	-20.51	-17.95	-19.58	-18.66	-20.13	-20.02	-19.22	-19.92	-17.6
SEG27	-17.4	-20.51	-19.93	-19.58	-20	-20.13	-20.02	-19.43	-19.92	-20.31
SEG28	-17.4	-20.51	-16.91	-19.58	-18.65	-18.44	-20.02	-19.43	-19.92	-20.31
SEG29	-17.4	NA	-16.96	-19.58	-17.73	-20.13	-20.02	-19.43	-19.92	-20.31
SEG30	-16	-20.51	-19.93	-19.58	-17.84	-20.13	-20.02	-19.43	-18.08	-20.31
SEG31	-18.8	-20.51	-19.93	-19.58	-18.66	-20.13	-20.02	-18.57	-19.92	-20.31
SEG32	-18.4	NA	-19.93	-19.58	-20	-20.13	-20.02	-18.65	-19.92	-20.31
SEG33	-15.2	-20.51	-19.93	-19.58	-17.45	-18.22	-20.02	-18.34	-19.16	-17.3
SEG34	-16.6	-20.5	-19.93	-19.58	-18.55	-18.72	-20.02	-17.17	-19.92	-20.31
SEG35	-15.4	-20.51	-19.93	-19.58	-18.36	-20.13	-20.02	-17.71	-17.4	-20.31
SEG36	-16.4	NA	-19.93	-19.58	-19.38	-20.13	-20.02	-19.43	-19.37	-18.7
SEG37	-10.2	-20.51	-19.93	-19.58	-20	-20.13	-20.02	-15.64	-19.92	-20.31
SEG38	-15.4	-20.51	-19.93	-19.58	-20	-19.04	-20.02	-18.31	-19.92	-18.3
SEG39	-19.81	-18.7	-19.93	-19.58	-18.36	-20.13	-20.02	-19.43	-19.92	-15.9
SEG40	-19.4	-20.51	-19.93	-19.58	-20	-20.13	-20.02	-16.78	-19.82	-17.8
SEG41	-13.6	-20.51	-19.93	-19.58	-20	-20.13	-20.02	-19.04	-18.31	-16.9
SEG42	-14.3	-20.51	-19.93	-19.58	-19.05	-20.13	-20.02	-14.52	-19.92	-20.31
SEG43	-18	-20.51	-18.57	-19.58	-16.17	-18.74	-20.02	-14.76	-16.66	-14.5
SEG44	-15.1	-20.51	-19.93	-19.58	-17.08	-20.13	-20.02	-13.64	-19.92	-16.8
SEG45	-15.5	-20.51	-19.93	-19.58	-16.38	-20.13	-20.02	-14.17	-19.92	-13.6
SEG46	-19.81	-20.51	-19.93	-19.58	-18.66	-20.13	-20.02	-18.65	-18.57	-16.6
SEG47	-19.81	-20.51	-19.93	-19.58	-17.67	-19.01	-20.02	-19.42	-19.83	-20.31
SEG48	NA	-20.51	-19.93	-19.58	-18.29	-20.13	-20.02	-18	-18.14	-20.31
SEG49	-15.5	-19.2	-19.5	-19.58	-18.76	-20.13	-20.02	-19.43	-19.92	-17.2
SEG50	-15.8	-20.51	-19.93	-19.58	-17.86	-20.13	-20.02	-19.43	-19.92	-20.31
SEW1	-19.81	-20.51	-19.93	-19.58	-20	-20.13	-20.02	-19.43	-19.92	-20.31

Table S2 continued:

Plot ID	IncP-1.	Class 1 integrans.	<i>aac(6')- lb</i>	<i>aacC1</i>	<i>bla</i> _{IMP-12}	<i>bla</i> _{IMP-5}	<i>ermB</i>	<i>mefA</i>	<i>tetA</i>	<i>sul2</i>
SEW2	-19.81	-20.51	-19.93	-19.58	-20	-20.13	-20.02	-19.43	-19.92	-20.31
SEW3	-19.81	NA	-19.93	-19.58	-20	-20.13	-20.02	-19.43	-19.92	-20.31
SEW4	-19.81	-20.51	NA	NA	NA	NA	NA	NA	NA	-20.31
SEW5	-19.81	-20.51	-19.93	-19.58	-20	-20.13	-20.02	-19.43	-19.92	-20.31
SEW6	-19.81	-20.51	-19.93	-19.58	-20	-20.13	-20.02	-19.43	-19.92	-20.31
SEW7	-19.81	-20.51	-19.93	-19.58	-19.78	-20.13	-20.02	-19.43	-19.92	-20.31
SEW8	-19.81	-20.51	-19.93	-19.58	-20	-20.13	-20.02	-19.43	-19.92	-20.31
SEW9	-19.81	-20.51	-19.93	-19.58	-20	-20.13	-20.02	-19.43	-19.92	-20.31
SEW10	-19.81	-20.51	-19.93	-19.58	-20	-20.13	-20.02	-19.43	-19.92	-20.31
SEW11	-19.81	-20.51	-19.93	-19.58	-20	-20.13	-20.02	-19.43	-19.92	-18.2
SEW12	-19.81	-20.51	-19.93	-19.58	-20	-20.13	-20.02	-19.43	-19.92	-20.31
SEW13	-19.81	-20.51	NA	NA	NA	NA	NA	NA	NA	-20.31
SEW14	-16.7	-20.51	NA	NA	NA	NA	NA	NA	NA	-20.31
SEW15	-19.81	-20.51	-19.93	-19.58	-20	-20.13	-20.02	-19.43	-19.92	-17
SEW16	-19.81	-20.51	NA	NA	NA	NA	NA	NA	NA	-20.31
SEW17	-18.1	-20.51	NA	NA	NA	NA	NA	NA	NA	-20.31
SEW18	-19.81	-20.51	NA	NA	NA	NA	NA	NA	NA	-20.31
SEW19	-19.81	-20.51	NA	NA	NA	NA	NA	NA	NA	-20.31
SEW20	-19.81	-20.51	NA	NA	NA	NA	NA	NA	NA	-20.31
SEW21	-19.81	-20.51	NA	NA	NA	NA	NA	NA	NA	-20.31
SEW22	-19.81	-20.51	-19.93	-19.58	-20	-20.13	-20.02	-19.43	-19.92	-20.31
SEW23	-19.81	-20.51	-19.93	-19.58	-20	-20.13	-20.02	-19.43	-19.92	-20.31
SEW24	-19.81	-20.51	-19.93	-19.58	-19.58	-20.13	-20.02	-19.43	-19.92	-20.31
SEW25	-19.81	-20.51	-19.93	-19.58	-17.55	-20.13	-20.02	-19.43	-19.92	-20.31
SEW26	-17.5	-20.51	-19.93	-19.58	-20	-20.13	-20.02	-19.43	-19.92	-20.31
SEW27	-19.81	-20.51	-19.93	-19.58	-20	-20.13	-20.02	-19.43	-19.92	-20.31
SEW28	-16.6	-20.51	-19.93	-19.58	-20	-20.13	-20.02	-19.43	-19.92	-20.31
SEW29	-19.81	-20.51	-19.93	-19.58	-20	-20.13	-20.02	-19.43	-19.92	-20.31
SEW30	-19.81	-20.51	NA	NA	NA	NA	NA	NA	NA	-20.31
SEW31	-18.7	-20.51	-19.93	-19.58	-20	-20.13	-20.02	-19.43	-19.92	-20.31
SEW32	-19.81	-20.51	-19.93	-19.58	-20	-20.13	-20.02	-19.43	-19.92	-20.31
SEW33	-19.81	-19.9	-19.93	-19.58	-20	-20.13	-20.02	-19.43	-19.92	-20.31
SEW34	-19.81	-20.51	-19.93	-19.58	-20	-20.13	-20.02	-19.43	-19.92	-20.31
SEW35	-19.81	-20.51	-19.93	-19.58	-20	-20.13	-20.02	-19.43	-19.92	-16.1
SEW36	-19.81	-20.51	NA	NA	NA	NA	NA	NA	NA	-20.31
SEW37	-19.81	-20.51	-19.93	-19.58	-20	-20.13	-20.02	-19.43	-19.92	-20.31
SEW38	-19.81	-20.51	-19.93	-19.58	-20	-20.13	-20.02	-19.43	-19.92	-20.31
SEW39	-19.81	-20.51	-19.93	-19.58	-20	-20.13	-20.02	-19.43	-19.92	-20.31
SEW40	-19.81	-20.51	-19.93	-19.58	-20	-20.13	-20.02	-18.76	-19.92	-20.31
SEW41	-17.8	-20.51	-19.93	-19.58	-20	-20.13	-20.01	-19.43	-19.92	-20.31
SEW42	-19.81	-20.51	-19.93	-19.58	-19.29	-20.13	-20.02	-19.43	-19.92	-20.31
SEW43	-19.81	-20.51	-19.93	-19.58	-17.87	-19.05	-20.02	-19.43	-19.92	-20.31
SEW44	-19.81	-20.51	-19.93	-19.58	-20	-20.13	-20.02	-19.43	-19.92	-20.31
SEW45	-19.81	-20.51	-19.93	-19.58	-18.08	-20.13	-20.02	-19.43	-19.92	-20.31
SEW46	-19.81	NA	-19.93	-19.58	-20	-20.13	-20.02	-19.43	-19.92	-18
SEW47	-19.81	-20.51	-19.93	-19.58	-20	-20.13	-20.02	-19.43	-19.92	-20.31
SEW48	-19.81	-20.51	-19.93	-19.58	-20	-20.13	-20.02	-19.43	-19.92	-20.31
SEW49	-19.81	-20.51	NA	NA	NA	NA	NA	NA	NA	-20.31
SEW50	-19.81	-20.51	-19.93	-19.58	-20	-20.13	-20.02	-19.43	-19.92	-20.31
HEG1	-19.4	-20.51	NA	-19.58	-19.43	-18.77	-20.02	-19.43	-19.92	-20.31
HEG2	-18.4	-20.51	-19.93	-19.58	-19.38	-18.54	-20.02	-19.43	-19.92	-19.6

Table S2 continued:

Plot ID	IncP-1.	Class 1 integrans.	<i>aac(6')- lb</i>	<i>aacC1</i>	<i>bla_{IMP-12}</i>	<i>bla_{IMP-5}</i>	<i>ermB</i>	<i>mefA</i>	<i>tetA</i>	<i>sul2</i>
HEG3	-18.6	-20.51	-17.54	-18.87	-17.24	-18.01	-20.02	-19.43	-19.92	-20.31
HEG4	-16.3	-18.2	-19.01	-19.58	-17.36	-17.34	-20.02	-16.71	-19.92	-15.9
HEG5	-19.81	-17.7	-18.69	-19.58	-16.89	-20.13	-20.02	-17.16	-17.84	-16.4
HEG6	-17.6	-14.5	-19.43	-19.58	-19.03	-17.07	-14.09	-13.64	-15.73	-8.6
HEG7	-19.81	-20.51	-19.93	-19.58	-20	-17.44	-20.02	-19.43	-19.92	-20.31
HEG8	-19.81	-20.51	-16.75	-19.58	-17.65	-17.8	-20.02	-19.43	-19.92	-18.8
HEG9	-13.7	-20.51	-19.93	-19.58	-20	-20.13	-20.02	-19.02	-19.92	-20.1
HEG10	-16.1	-20.51	-18.82	-19.58	-17.36	-20.13	-20.02	-17.59	-19.92	-17
HEG11	-16.9	-20.51	-19.93	-19.58	-20	-20.13	-20.02	-15.95	-19.92	-20.31
HEG12	-16.9	-20.51	-18.48	-18.83	-20	-16.63	-20.02	-19.43	-19.92	-20.31
HEG13	-17.6	-20.51	-17.76	-19.58	-20	-20.13	-20.02	-17.23	-19.92	-16
HEG14	-16.2	-20.51	-19.93	-19.58	-20	-20.13	-20.02	-16.67	-19.92	-20.31
HEG15	-16.4	-20.51	-18.78	-19.58	-15.81	-20.13	-20.02	-19.43	-18.48	-18.9
HEG16	-19.81	-20.51	-19.04	-19.58	-20	-20.13	-20.02	-19.43	-19.92	-20.31
HEG17	-16.4	-20.51	-18.09	-19.58	-19.38	-20.13	-20.02	-19.43	-19.92	-20.31
HEG18	-17.6	-20.51	-19.93	-19.58	-20	-20.13	-20.02	-19.43	-19.92	-20.31
HEG19	-17.6	-20.51	-19.93	-19.58	-18.43	-16.81	-20.02	-19.43	-19.92	-20.31
HEG20	-14.3	-20.51	-19.93	-19.58	-20	-20.13	-20.02	-19.43	-19.92	-20.31
HEG21	-19.81	-17.4	-19.93	-19.13	-20	-18.28	-17.42	-16.54	-18.25	-14.6
HEG22	-18.2	-20.51	-17.57	-19.58	-20	-20.13	-20.02	-17.05	-19.92	-20.31
HEG23	-19.81	-20.51	-19.93	-19.58	-18.35	-20.13	-20.02	-17.75	-19.1	-20.31
HEG24	-16.3	-20.51	-18.46	-19.58	-16.46	-18.23	-20.02	-18.42	-19.92	-20.31
HEG25	NA	-20.51	-19.49	-19.57	-20	-20.13	-19.64	-19.07	-19.92	-20.31
HEG26	-18.6	NA	-18.4	-19.58	-18.81	-20.13	-20.02	-17.16	-19.92	-20.31
HEG27	-16.7	-20.51	-19.75	-19.58	-20	-20.13	-20.02	-19.43	-19.92	-20.31
HEG28	-15.2	-20.51	-18.74	-19.58	-20	-20.13	-20.02	-14.97	-17.8	-20.31
HEG29	-17.7	-20.51	-18.58	-19.58	-20	-20.13	-20.02	-18.2	-19.92	-20.31
HEG30	NA	-20.51	-18.84	-19.58	-12.86	-17.48	-20.02	-16.16	-18.57	-20.31
HEG31	NA	-19	-17.03	-19.58	-16.37	-20.13	-20.02	-16.57	-19.92	-20.31
HEG32	-18.5	NA	-19.93	-19.58	-14.87	-17.26	-20.02	-19.43	-19.92	-20.31
HEG33	-12.5	-15.6	-19.93	-19.58	-16.68	-14.58	-17.62	-15.3	-19.92	-15.4
HEG34	-19.81	-17.9	-17.35	-19.58	-19.2	-19.01	-17.55	-16.03	-19.57	-12.7
HEG35	-15.9	-16.3	-18.59	-19.58	-20	-20.13	-16.45	-14.38	-16.34	-10.2
HEG36	-17.3	-15.9	-17.9	-19.58	-20	-20.13	-17.12	-15.82	-16.96	-13.8
HEG37	-15.1	-15.3	-18.64	-18.66	-17.88	-16.74	-17.87	-15.35	-18.74	-13.8
HEG38	-19.81	-20.51	-19.93	-19.58	-17.17	-20.13	-20.02	-18.49	-19.92	-20.31
HEG39	-19.81	-20.51	-18.05	-19.58	-17.67	-20.13	-20.02	-19.43	-19.92	-20.31
HEG40	-19.81	-20.51	-18.86	-19.58	-20	-20.13	-18.25	-19.43	-19.92	-15.2
HEG41	NA	-20.51	-19.93	-19.58	-15.14	-16.69	-20.02	-19.43	-19.92	-16.7
HEG42	-16.7	-20.51	-19.93	-19.58	-18.68	-20.13	-20.02	-19.43	-19.92	-20.31
HEG43	-15.4	-20.51	-19.93	-19.58	-20	-20.13	-20.02	-17.73	-19.92	-16.5
HEG44	-17.5	NA	-19.93	-19.58	-20	-20.13	-20.02	-17.67	-19.92	-20.31
HEG45	-17.6	-20.51	-17.21	-19.58	-20	-18.86	-20.02	-19.43	-19.92	-20.31
HEG46	NA	-20.51	-17.92	-19.58	-20	-20.13	-20.02	-19.43	-19.92	-20.31
HEG47	NA	NA	-18.72	-19.58	-20	-20.13	-20.02	-17.17	-19.92	-20.31
HEG48	-17.5	-20.51	-18.05	-19.58	-16.14	-20.13	-20.02	-17.98	-19.92	-20.31
HEG49	-16.3	-20.51	-18.19	-19.58	-18.61	-20.13	-20.02	-15.66	-19.92	-20.31
HEG50	-19.81	-20.51	-17.63	-19.58	-17.41	-16.69	-20.02	-17.61	-19.92	-20.31
HEW1	-19.81	-20.51	-19.93	-19.58	-17.82	-20.13	-20.02	-19.43	-19.92	-20.31
HEW2	-15.7	-20.51	-19.93	-19.58	-19.95	-20.12	-20.02	-19.43	-19.92	-20.3
HEW3	-18.6	-20.51	-17.54	-18.87	-17.24	-18.01	-20.02	-19.43	-19.92	-20.31

Table S2 continued:

Plot ID	IncP-1.	Class 1 integrons.	<i>aac(6')- lb</i>	<i>aacC1</i>	<i>bla</i> _{IMP-12}	<i>bla</i> _{IMP-5}	<i>ermB</i>	<i>mefA</i>	<i>tetA</i>	<i>sul2</i>
HEW4	-19.81	-20.51	-19.93	-19.58	-16.91	-20.13	-20.02	-19.43	-19.92	-20.31
HEW5	-19.81	-20.51	-19.93	-19.58	-20	-20.13	-20.02	-19.43	-19.92	-20.31
HEW6	NA	-20.51	-19.93	-19.58	-18.29	-20.13	-20.02	-19.43	-19.92	-20.31
HEW7	-18.3	-20.51	-19.93	-19.58	-19.23	-19.78	-20.02	-19.43	-19.92	-20.31
HEW8	NA	-20.51	-19.93	-19.58	-16.11	-20.13	-20.02	-19.43	-19.92	-20.31
HEW9	-19.81	-20.51	-19.93	-19.58	-19.04	-19.99	-20.02	-19.43	-19.92	-20.31
HEW10	-17.2	-20.51	-19.93	-19.58	-17.99	-19.47	-20.02	-19.43	-19.92	-20.31
HEW11	NA	-20.51	-19.93	-19.58	-16.88	-20.13	-20.02	-19.43	-19.92	-20.31
HEW12	-19.4	-20.51	-19.93	-19.58	-17.46	-16.38	-20.02	-19.43	-19.92	-20.31
HEW13	-16.9	-20.51	-19.93	-19.58	-16.87	-20.13	-20.02	-19.43	-19.92	-20.31
HEW14	-18.2	-20.51	-19.93	-19.58	-20	-20.13	-20.02	-19.43	-19.92	-20.31
HEW15	-19.81	-20.51	-19.93	-19.58	-20	-20.13	-20.02	-19.43	-19.92	-20.31
HEW16	-19.81	-20.51	-19.93	-19.58	-16.13	-17.66	-20.02	-19.43	-19.92	-20.31
HEW17	-19.81	-20.51	-19.93	-19.58	-19.79	-17.43	-20.02	-19.43	-19.92	-17.3
HEW18	-19.81	NA	-19.93	-19.58	-17.64	-20.13	-20.02	-19.43	-19.92	-20.31
HEW19	NA	-20.51	-19.93	-19.58	-17.29	-18.16	-20.02	-19.43	-19.92	-20.31
HEW20	-19.81	NA	-19.93	-19.58	-18.23	-20.13	-20.02	-19.43	-19.92	-20.31
HEW21	-18.4	-20.51	-19.93	-19.58	-17.45	-20.13	-20.02	-19.43	-19.92	-20.31
HEW22	-19.81	-20.51	-19.93	-19.58	-20	-20.13	-20.02	-19.43	-19.92	-20.31
HEW23	-19.81	-20.51	-19.93	-19.58	-18.84	-20.13	-20.02	-19.43	-19.92	-20.31
HEW24	-19.81	-20.51	-19.93	-19.58	-20	-20.13	-20.02	-19.43	-19.91	-20.31
HEW25	-19.81	-20.51	-19.93	-19.58	-20	-20.13	-20.02	-19.43	-19.92	-20.31
HEW26	-19.81	-20.51	-19.93	-19.58	-18.41	-19.15	-20.02	-19.43	-19.92	-20.31
HEW27	-16.8	-20.51	-19.93	-19.58	-18.59	-20.13	-20.02	-19.43	-19.92	-20.31
HEW28	-17	-20.51	-19.93	-19.58	-20	-20.13	-20.02	-19.43	-19.92	-20.31
HEW29	-18.4	-20.51	-19.93	-19.58	-17.28	-17.79	-20.02	-19.43	-19.92	-20.31
HEW30	-19.81	-20.51	-19.93	-19.58	-17.81	-20.13	-20.02	-19.43	-19.92	-20.31
HEW31	-19.81	-20.51	-19.93	-19.58	-16.72	-17.8	-20.02	-19.43	-19.92	-20.31
HEW32	-19.81	-20.51	-19.93	-19.58	-20	-20.13	-20.02	-19.43	-19.92	-20.31
HEW33	-19.81	-20.51	-19.93	-19.58	-15.84	-19.1	-20.02	-19.43	-19.92	-20.31
HEW34	NA	-20.51	-19.93	-19.58	-18.33	-16.77	-20.02	-19.43	-19.92	-20.31
HEW35	NA	-20.51	-19.93	-19.58	-17.64	-19.63	-20.02	-19.43	-19.92	-20.31
HEW36	NA	-20.51	-19.93	-19.58	-16.54	-20.13	-20.02	-19.43	-19.92	-20.31
HEW37	-19.81	-20.51	-19.93	-19.58	-16.33	-19.13	-20.02	-19.43	-19.92	-20.31
HEW38	-19.81	-20.51	-19.93	-19.58	-16.73	-17.15	-20.02	-19.43	-19.92	-20.31
HEW39	-19.81	-20.51	-19.93	-19.58	-16.39	-17.34	-20.02	-19.43	-19.92	-20.31
HEW40	-19.81	-20.51	-19.93	-19.58	-18.01	-20.13	-20.02	-19.43	-19.92	-20.31
HEW41	-19.81	-20.51	-19.93	-19.58	-16.29	-20.13	-20.02	-19.43	-19.92	-20.31
HEW42	NA	-20.51	-19.93	-19.58	-18.68	-19.9	-20.02	-19.43	-19.92	-20.31
HEW43	-19	-20.51	-19.93	-19.58	-18.88	-20.13	-20.02	-19.43	-19.92	-20.31
HEW44	-19.81	-20.51	-19.93	-19.58	-20	-20.13	-20.02	-19.43	-19.92	-20.31
HEW45	-18.1	-20.51	-19.93	-19.58	-18.76	-20.13	-20.02	-19.43	-19.92	-17.9
HEW46	-19.81	-20.51	-19.93	-19.58	-20	-20.13	-20.02	-19.43	-19.92	-20.31
HEW47	-16.6	-20.51	-19.93	-19.58	-16.2	-18.47	-20.02	-19.43	-19.92	-20.31
HEW48	-19.81	-20.51	-19.93	-19.58	-18.73	-18.07	-20.02	-19.43	-19.92	NA
HEW49	-19.8	-20.51	-19.93	-19.58	-15.8	-20.13	-20.02	-19.43	-19.92	NA
HEW50	-19.81	-20.51	-19.93	-19.58	-18.71	-19.36	-20.02	-19.43	-19.92	-20.31
HEW51	-17.7	-20.51	-19.38	-19.58	-20	-19.54	-20.02	-19.43	-19.92	-20.31
AEG1	-19.81	-19.7	-19.93	-19.58	-20	-20.13	-20.02	-17.51	-19.92	-20.31
AEG2	-17.5	-17.1	-19.93	-19.58	-20	-20.13	-20.02	-18.26	-19.92	-15.3
AEG3	-16.4	-20.51	-19.93	-19.58	-20	-20.13	-20.02	-19.43	-19.92	-20.31

Table S2 continued

Plot ID	IncP-1.	Class 1 integrons.	<i>aac(6')- Ib</i>	<i>aacC1</i>	<i>bla_{IMP-12}</i>	<i>bla_{IMP-5}</i>	<i>ermB</i>	<i>mefA</i>	<i>tetA</i>	<i>sul2</i>
AEG4	-14.3	-20.51	-19.93	-19.58	-20	-20.13	-20.02	-17.88	-19.92	-15.5
AEG5	-16.6	-20.51	-19.93	-19.58	-20	-20.13	-20.02	-19.43	-19.92	-17.5
AEG6	NA	-20.51	-19.93	-19.58	-20	-20.13	-20.02	-19.43	-19.92	-20.31
AEG7	-15.5	-20.51	-19.93	-19.58	-20	-20.13	-20.02	-19.43	-19.92	-20.31
AEG8	NA	-20.51	-19.93	-19.58	-20	-20.13	-20.02	-19.43	-19.92	-16.7
AEG9	-19.81	-20.51	-19.93	-19.58	-20	-20.13	-20.02	-15.23	-19.92	-20.31
AEG10	-18.1	-20.51	-19.93	-19.58	-20	-20.13	-20.02	-19.43	-19.92	-20.31
AEG11	-18.6	-20.51	-19.93	-19.58	-20	-20.13	-20.02	-19.06	-19.92	-20.31
AEG12	-18.1	-20.51	-19.93	-19.58	-18.6	-20.13	-20.02	-16.94	-19.92	-17.1
AEG13	-17.1	-20.51	-19.93	-19.58	-16.5	-20.13	-20.02	-16.42	-19.92	-20.31
AEG14	-17.6	-18.6	-19.93	-19.58	-20	-20.13	-20.02	-16.94	-19.92	-20.31
AEG15	NA	-20.51	-19.93	-19.58	-17.52	-20.13	-20.02	-17.99	-19.92	-16.8
AEG16	NA	-20.51	-19.93	-19.58	-16.98	-20.13	-20.02	-17.36	-19.92	-20.31
AEG17	-19.81	-20.51	-19.93	-19.58	-20	-19.14	-20.02	-19.43	-19.92	-20.31
AEG18	-17.9	-20.51	-19.58	-19.58	-19.2	-20.13	-20.02	-16.77	-19.92	-20.31
AEG19	-15.9	-20.51	-19.93	-19.58	-20	-20.13	-20.02	-18.63	-19.92	-20.31
AEG20	-16.1	-20.51	-19.93	-19.58	-20	-20.13	-20.02	-19.43	-19.92	-20.31
AEG21	-19.3	-20.51	-19.93	-19.58	-18.87	-20.13	-20.02	-18.18	-19.92	-16.2
AEG22	-19.81	-15	-19.93	-19.58	-19.79	-20.13	-16.73	-19.38	-16.57	-9.4
AEG23	-17.3	-17.5	-18.23	-19.58	-20	-20.13	-20.02	-19.43	-19.92	-20.31
AEG24	NA	-20.51	-19.93	-19.58	-20	-20.13	-20.02	-15.93	-18.86	-17.3
AEG25	-15.8	-20.51	-19.93	-19.58	-20	-20.13	-20.02	-19.43	-19.92	-20.31
AEG26	-18.5	-20.51	-19.93	-19.58	-20	-20.13	-20.02	-19.43	-19.92	-20.31
AEG27	-16.4	-20.51	-19.93	-19.58	-20	-18.41	-20.02	-19.43	-19.92	-17.8
AEG28	-15.7	-20.51	-19.93	-19.58	-19.53	-20.13	-20.02	-19.43	-19.92	-20.31
AEG29	-16	NA	-19.93	-19.58	-20	-20.13	-20.02	-19.43	-19.92	-20.31
AEG30	-17.8	-20.51	-19.93	-19.58	-20	-20.13	-20.02	-19.43	-19.92	-20.31
AEG31	NA	-20.51	-19.93	-19.58	-19.29	-20.13	-20.02	-19.43	-19.92	-20.31
AEG32	-12.4	-20.51	-19.93	-19.58	-16.59	-20.13	-20.02	-19.43	-19.92	-20.31
AEG33	-19.81	-20.51	-19.93	-19.58	-20	-20.13	-20.02	-17.15	-19.92	-20.31
AEG34	-19.81	-20.51	-19.93	-19.58	-20	-20.13	-20.02	-17.58	-19.92	-20.31
AEG35	-18.7	NA	-19.93	-19.58	-15.18	-20.13	-20.02	-16.76	-19.92	-16.3
AEG36	-14.2	-20.51	-19.93	-19.58	-18.73	-20.13	-20.02	-17.45	-19.92	-15.3
AEG37	-18.7	-20.51	-19.93	-19.58	-18.46	-20.13	-20.02	-13.68	-19.92	-14.1
AEG38	-14	-20.51	-19.93	-19.58	-17.45	-20.13	-20.02	-19.43	-19.92	-20.31
AEG39	-17.4	-20.51	-19.93	-19.58	-17.38	-20.13	-20.02	-14.32	-19.92	-20.31
AEG40	-19.81	-14.8	-18.92	-19.58	-20	-20.13	-20.02	-16.8	-16.48	-10.6
AEG41	-19.81	-20.51	-19.93	-19.58	-20	-20.13	-20.02	-17.41	-19.92	-20.31
AEG42	-19.81	-20.51	-17.16	-19.58	-19.06	-20.13	-20.02	-19.09	-19.92	-20.31
AEG43	-14.3	-16	-18.02	-19.58	-20	-20.13	-20.02	-18.59	-19.92	-17
AEG44	-17.1	-20.51	-19.93	-19.58	-17.88	-20.13	-20.02	-17.34	-19.92	-20.31
AEG45	-16.8	-20.51	NA	-19.58	-16.1	-20.13	-20.02	-19.43	-19.92	-20.31
AEG46	-16.9	-20.51	NA	-19.58	-18.08	-20.13	-20.02	-19.15	-19.92	-20.31
AEG47	-14.2	-20.51	NA	-19.58	-20	-20.13	-20.02	-19.43	-19.92	-20.31
AEG48	-12.3	-20.51	-19.93	-19.58	-20	-20.13	-20.02	-19.43	-19.92	-20.31
AEG49	-19.81	-20.51	-19.93	-19.58	-20	-20.13	-20.02	-18.5	-19.92	-20.31
AEG50	-19.81	NA	-19.93	-19.58	-17.15	-20.13	-20.02	-18.5	-19.92	-16.3
AEW1	-19.81	-20.51	NA	NA	NA	NA	NA	NA	NA	-20.31
AEW2	-19.81	NA	-19.93	-19.58	-20	-20.13	-20.02	-19.43	-19.92	-20.31
AEW3	-19.81	NA	-19.93	-19.58	-20	-20.13	-20.02	-19.43	-19.92	-20.31
AEW4	-19.81	-20.51	NA	-19.58	-18.75	-20.13	-20.02	-19.43	-19.92	-18.2

Table S2 continued:

Plot ID	IncP-1.	Class 1 integrons.	<i>aac(6')- Ib</i>	<i>aacC1</i>	<i>bla_{IMP-12}</i>	<i>bla_{IMP-5}</i>	<i>ermB</i>	<i>mefA</i>	<i>tetA</i>	<i>sul2</i>
AEW5	NA	-20.51	NA	-19.58	-20	-20.13	-20.02	-19.43	-19.92	-20.31
AEW6	NA	-20.51	-19.93	-19.58	-20	-19.4	-20.02	-19.43	-19.92	-17.4
AEW7	-19.81	-20.51	-19.93	-19.58	-20	-20.13	-20.02	-19.43	-19.92	-20.31
AEW8	NA	-20.51	-19.93	-19.58	-17.23	-20.13	-20.02	-19.43	-19.92	-20.31
AEW9	-19.81	-20.51	-19.93	-19.58	-18.3	-20.13	-20.02	-19.43	-19.92	-20.31
AEW10	-19.81	-20.51	-19.93	-19.58	-20	-20.13	-20.02	-19.43	-19.92	-20.31
AEW11	-16.4	-20.51	NA	NA	NA	NA	NA	NA	NA	-20.31
AEW12	-18.4	-20.51	-19.93	-19.58	-20	-20.13	-20.02	-19.43	-19.92	-20.31
AEW13	-18	-20.51	-19.93	-19.58	-20	-20.13	-20.02	-18.06	-19.92	-20.31
AEW14	-17.1	-20.51	-19.93	-19.58	-20	-20.13	-20.02	-19.43	-19.92	-18.8
AEW15	NA	-20.51	-19.93	-19.58	-20	-20.13	-20.02	-19.43	-19.92	-20.31
AEW16	NA	-20.51	-19.93	-19.58	-20	-16.3	-20.02	-19.43	-19.92	-16.3
AEW17	-19.81	-20.51	-19.93	-19.58	-20	-20.13	-20.02	-19.43	-19.92	-20.31
AEW18	NA	-20.51	-19.93	-19.58	-18.78	-18.83	-20.02	-19.43	-19.92	-20.31
AEW19	-19.81	-20.51	-19.93	-19.58	-18.03	-20.13	-20.02	-19.43	-19.92	-20.31
AEW20	-17.7	-20.51	-19.93	-19.58	-20	-20.13	-20.02	-19.43	-19.92	-20.31
AEW21	-19.81	-20.51	-19.93	-19.58	-17.6	-19.37	-20.02	-19.43	-19.92	-18.2
AEW22	-19.81	-20.51	-19.93	-19.58	-20	-20.13	-20.02	-19.43	-19.92	-16.5
AEW23	-19.81	-20.51	-19.93	-19.58	-19.26	-20.13	-20.02	-19.43	-19.92	-20.31
AEW24	NA	-20.51	-19.93	-19.58	-20	-20.13	-20.02	-19.43	-19.92	-20.31
AEW25	-17.7	-20.51	-19.93	-19.58	-16.82	-20.13	-20.02	-19.43	-19.92	-20.31
AEW26	NA	-20.51	-19.93	-19.58	-16.23	-19.14	-20.02	-19.43	-19.92	-20.31
AEW27	NA	-20.51	-19.93	-19.58	-18.73	-19.28	-20.02	-19.43	-19.92	-20.31
AEW28	-19.81	-20.51	-19.93	-19.58	-19.79	-20.13	-20.02	-19.43	-19.92	-20.31
AEW29	-19.81	-20.51	-19.93	-19.58	-18.75	-18.9	-20.02	-19.43	-19.92	-20.31
AEW30	-19.81	-20.51	-19.93	-19.58	-17.94	-20.13	-20.02	-19.43	-19.92	-20.31
AEW31	-19.81	-20.51	-19.93	-19.58	-20	-20.13	-20.02	-18.22	-19.92	-20.31
AEW32	-19.81	-20.51	-19.93	-19.58	-20	-20.13	-20.02	-19.43	-19.92	-20.31
AEW33	-19.81	-20.51	-19.93	-19.58	-20	-20.13	-20.02	-19.43	-19.92	-16.1
AEW34	NA	-20.51	-19.93	-19.58	-20	-20.13	-20.02	-19.43	-19.92	-20.31
AEW35	NA	-20.51	-19.93	-19.58	-20	-20.13	-20.02	-19.43	-19.92	-20.31
AEW36	NA	-20.51	-19.93	-19.58	-18.41	-20.13	-20.02	-19.43	-19.92	-20.31
AEW37	-19.81	-20.51	-19.93	-19.58	-14.99	-20.13	-20.02	-19.43	-19.92	-20.31
AEW38	-19.81	-20.51	-19.93	-19.58	-18.56	-20.13	-20.02	-19.43	-19.92	-20.31
AEW39	-19.81	-20.51	-19.93	-19.58	-20	-20.13	-20.02	-19.43	-19.92	-20.31
AEW40	-19.81	-20.51	-19.93	-19.58	-17.11	-20.13	-20.02	-19.43	-19.92	-20.31
AEW41	-19.81	-20.51	-19.93	-19.58	-20	-20.13	-20.02	-19.43	-19.92	-20.31
AEW42	-17.4	-20.51	-19.93	-19.58	-20	-20.13	-17.01	-19.43	-19.92	-20.31
AEW43	-16.7	-20.51	-19.93	-19.58	-15.21	-16.13	-20.02	-19.43	-19.92	-20.31
AEW44	-19.81	-20.51	-19.93	-19.58	-14.79	-18.74	-20.02	-19.43	-19.92	-20.31
AEW45	-16.2	-20.51	-19.93	-19.58	-18.08	-20.13	-20.02	-19.43	-19.92	-20.31
AEW46	-9.3	-20.51	-19.93	-19.58	-17.23	-20.13	-20.02	-19.43	-19.92	-20.31
AEW47	-18.3	-20.51	-19.93	-19.58	-18.37	-20.13	-20.02	-19.43	-19.92	-20.31
AEW48	-19.81	-20.51	-19.93	-19.58	-17.81	-20.13	-20.02	-19.43	-19.92	-20.31
AEW49	-19.81	-20.51	-19.93	-19.58	-17.18	-20.13	-20.02	-19.43	-19.92	-20.31
AEW50	-17.6	-20.51	NA	-19.58	-20	-20.13	-20.02	-19.43	-19.92	-20.31

Table S3: Preliminary binomial (A) or tobit regression models (B). The left column describes the model components including dependent variables (the target ARG, class 1 integrons or IncP-1 plasmids), fixed independent variables (pH, soil moisture or Shannon index) and interchanging independent variables (grazing, mowing, fertilization, organic N, mineral N and LUI with respect to grassland data and beech, pine, spruce and oak with respect to forest data). Significant effects (p-value < 0.05) are highlighted in orange.

	A			B		
	p	Estimate	R ²	p	Estimate	R ²
<i>aac(6')-Ib</i> with pH						
Grazing	0.84	-0.04	0.18	0.557	-0.11	0.11
Mowing	0.03	0.45	0.21	0.0435	0.37	0.12
Fertilization	0.08	0.35	0.21	0.281	0.19	0.12
Organic N	0.43	0.15	0.18	0.459	0.14	0.11
Mineral N	0.58	0.11	0.21	0.882	-0.03	0.11
LUI	0.02	0.49	0.21	0.13	0.28	0.12
<i>mefA</i> with soil moisture						
Grazing	0.91	-0.02	0.07	0.49	-0.16	0.07
Mowing	5.1E-04	0.69	0.14	5.6E-04	0.75	0.09
Fertilization	4.4E-04	0.94	0.17	3.4E-05	0.82	0.11
Organic N	6.3E-05	1.32	0.20	3.3E-05	0.83	0.10
Mineral N	0.45	0.13	0.07	0.14	0.32	0.07
LUI	4.4E-05	0.87	0.17	2.2E-05	0.90	0.10
<i>sul2</i> with soil moisture						
Grazing	0.47	0.13	0.05	0.772	0.17	0.05
Mowing	0.29	0.12	0.06	0.06	1.09	0.06
Fertilization	0.02	0.43	0.09	0.01	1.38	0.08
Organic N	0.01	0.53	0.10	2.2E-03	1.60	0.08
Mineral N	0.11	0.28	0.06	0.16	0.78	0.06
LUI	3.9E-03	0.54	0.10	3.6E-03	1.65	0.07
<i>tetA</i> with soil moisture						
Grazing	0.23	0.24	0.09			
Mowing	0.75	0.07	0.08			
Fertilization	0.16	0.29	0.10			
Organic N	0.38	0.19	0.09			
Mineral N	0.17	0.44	0.09			
LUI	0.03	0.48	0.11			
Class 1 integrons with soil						
Grazing	0.03	-1.06	0.17			
Mowing	3.8E-03	0.77	0.18			
Fertilization	1.7E-03	0.68	0.19			
Organic N	0.02	0.47	0.14			
Mineral N	0.02	0.49	0.14			
LUI	0.03	0.54	0.14			
IncP-1 plasmids with pH						
Grazing	0.59	-0.11	0.01	0.82	-0.05	0.01
Mowing	0.44	0.16	0.02	0.23	-0.26	0.02
Fertilization	0.25	0.29	0.03	0.61	-0.11	0.02
Organic N	0.45	-0.16	0.02	0.22	-0.28	0.02
Mineral N	0.01	0.80	0.07	0.16	0.30	0.02
LUI	0.51	0.14	0.02	0.23	-0.26	0.02

Table S3 continued:

	A			B		
<i>bla</i> _{IMP-12} with soil moisture	p	Estimate	R²	p	Estimate	R²
Grazing	0.78	-0.05	0.04	0.50	-0.17	0.06
Mowing	0.26	0.20	0.05	0.16	0.33	0.06
Fertilization	0.10	0.29	0.06	0.06	0.43	0.08
Organic N	0.45	0.13	0.05	0.79	0.06	0.06
Mineral N	0.11	0.51	0.04	0.21	0.29	0.06
LUI	0.10	0.28	0.06	0.09	0.40	0.07
<i>bla</i> _{IMP-5} with soil moisture						
Grazing	0.25	0.22	0.05	0.26	0.39	0.05
Mowing	0.89	-0.03	0.04	0.84	-0.07	0.04
Fertilization	0.32	0.19	0.07	0.32	0.35	0.07
Organic N	0.26	-0.30	0.05	0.21	-0.55	0.05
Mineral N	0.02	0.42	0.07	0.04	0.65	0.06
LUI	0.14	0.30	0.06	0.17	0.48	0.05
<i>bla</i> _{IMP-12} with Shannon index						
Beech	7.0E-05	2.13	0.17	7.4E-06	2.75	0.09
Pine	0.99	-17.40	0.14	0.99	-13.18	0.07
Spruce	0.04	-1.43	0.09	0.02	-1.95	0.04
Oak	0.16	-1.21	0.08	0.09	-1.90	0.04
<i>bla</i> _{IMP-5} with Shannon index						
Beech	0.03	1.70	0.09	0.01	2.28	0.07
Pine	0.99	-16.10	0.08	0.99	-11.94	0.06
Spruce	0.48	-0.56	0.05	0.30	-1.07	0.04
Oak	0.99	-16.56	0.08	1.00	-12.37	0.06

4. Discovery of Novel Antibiotic Resistance

Determinants in Forest and Grassland Soil Metagenomes

Inka Marie Willms¹, Aysha Kamran², Nils Frederik Aßmann¹, Denis Krone¹, Simon Henning Bolz¹, Fabian Fiedler¹ and Heiko Nacke^{1*}

¹ Department of Genomic and Applied Microbiology and Göttingen Genomics Laboratory, Institute of Microbiology and Genetics, Georg-August University, Göttingen, Germany

² Department of General Microbiology, Institute of Microbiology and Genetics, Georg-August University, Göttingen, Germany

Front. Microbiol. (2019), 10:460

Author Contributions to the work:

Conceptualization: H.N.; formal analysis: H.N.; investigation, I.M.W, A.K., N.F.A., D.K., S.H.B., F.F. H.N.; resources, H.N.; data curation; I.M.W., N.F.A., D.K., S.H.B., F.F. H.N.; writing—original draft preparation, I.M.W and H.N.; writing—review and editing, I.M.W, and H.N; visualization, H.N.; supervision, I.M.W. and H.N.; project administration, H.N.; funding acquisition, H.N.



Discovery of Novel Antibiotic Resistance Determinants in Forest and Grassland Soil Metagenomes

Inka Marie Willms¹, Aysha Kamran², Nils Frederik Aßmann¹, Denis Krone¹, Simon Henning Bolz¹, Fabian Fiedler¹ and Heiko Nacke^{1*}

¹ Department of Genomic and Applied Microbiology and Göttingen Genomics Laboratory, Institute of Microbiology and Genetics, Georg-August University, Göttingen, Germany, ² Department of General Microbiology, Institute of Microbiology and Genetics, Georg-August University, Göttingen, Germany

OPEN ACCESS

Edited by:

Ziad Daoud,
University of Balamand, Lebanon

Reviewed by:

Atte Von Wright,
University of Eastern Finland, Finland
Ghassan M. Matar,
American University of Beirut,
Lebanon

*Correspondence:

Heiko Nacke
hnacke@gwdg.de

Specialty section:

This article was submitted to
Antimicrobials, Resistance
and Chemotherapy,
a section of the journal
Frontiers in Microbiology

Received: 08 December 2018

Accepted: 21 February 2019

Published: 07 March 2019

Citation:

Willms IM, Kamran A, Aßmann NF,
Krone D, Bolz SH, Fiedler F and
Nacke H (2019) Discovery of Novel
Antibiotic Resistance Determinants
in Forest and Grassland Soil
Metagenomes.
Front. Microbiol. 10:460.
doi: 10.3389/fmicb.2019.00460

Soil represents a significant reservoir of antibiotic resistance genes (ARGs), which can potentially spread across distinct ecosystems and be acquired by pathogens threatening human as well as animal health. Currently, information on the identity and diversity of these genes, enabling anticipation of possible future resistance development in clinical environments and the livestock sector, is lacking. In this study, we applied functional metagenomics to discover novel sulfonamide as well as tetracycline resistance genes in soils derived from forest and grassland. Screening of soil metagenomic libraries revealed a total of eight so far unknown ARGs. The recovered genes originate from phylogenetically diverse soil bacteria (e.g., Actinobacteria, Chloroflexi, or Proteobacteria) and encode proteins with a minimum identity of 46% to other antibiotic resistance determinants. In particular forest soil ecosystems have so far been neglected in studies focusing on antibiotic resistance. Here, we detected for the first time non-mobile dihydropteroate synthase (DHPS) genes conferring resistance to sulfonamides in forest soil with no history of exposure to these synthetic drugs. In total, three sulfonamide resistant DHPs, differing in taxonomic origin, were discovered in beech or pine forest soil. This indicates that sulfonamide resistance naturally occurs in forest-resident soil bacterial communities. Besides forest soil-derived sulfonamide resistance proteins, we also identified a DHPS affiliated to Chloroflexi in grassland soil. This enzyme and the other recovered DHPs confer reduced susceptibility toward sulfamethazine, which is widely used in food animal production. With respect to tetracycline resistance, four efflux proteins affiliated to the major facilitator superfamily (MFS) were identified. Noteworthy, one of these proteins also conferred reduced susceptibility toward lincomycin.

Keywords: soil metagenome, functional metagenomics, antibiotic resistance, dihydropteroate synthase, tetracycline resistance, sulfonamide resistance

INTRODUCTION

Pathogenic bacteria resistant to multiple classes of antibiotics pose risks to public health and are considered as one of the major global challenges within the 21st century. Some of the antibiotic resistance genes (ARGs) carried by these bacteria have been traced to soil origins (Forsberg et al., 2012) and can potentially spread via e.g., groundwater or wildlife (Davies and Davies, 2010).

Nevertheless, in contrast to clinical pathogens, bacterial communities inhabiting complex environments such as soil have been rarely considered within studies focusing on antibiotic resistance (Walsh, 2013b). To assess risks of environmental resistomes and develop strategies to tackle antibiotic resistance, an improved knowledge on the ecology of resistance determinants including their origins, diversity and underlying resistance mechanisms is urgently required (Allen et al., 2009; Wang et al., 2017).

Among Earth's microbial habitats, soil harbors the highest diversity of prokaryotes including numerous multi-resistant bacteria (Delmont et al., 2011; Walsh and Duffy, 2013; Nesme and Simonet, 2015). The synthesis of antibiotics likely evolved in this habitat and promoted the development of different antimicrobial compound-specific resistance mechanisms (D'Costa et al., 2007; Walsh, 2013a). Previously unknown soil-derived ARGs were recovered from both, pristine and intensively managed sites, by function-based screening of metagenomic libraries (Allen et al., 2009; Perron et al., 2015; Lau et al., 2017). In contrast to sequence-based metagenomic library screening, this culture-independent approach is not based on conserved DNA regions and therefore allows the identification of entirely novel target genes (Nacke and Daniel, 2014; Cheng et al., 2017). For instance, a so far unknown peptide-associated macrolide resistance mechanism was uncovered by coupling function-based metagenomic library screening and high-resolution proteomics analysis (Lau et al., 2017). Besides dependence on conserved DNA regions, the fact that various resistance genes show high levels of similarity to genes encoding other cellular functions (Martínez, 2008; Perron et al., 2015) represents another limitation of sequence-based resistome analysis. An illustrative example are efflux pumps of the resistance-nodulation-division (RND) superfamily, which can confer antibiotic resistance, but can also transport proteins involved in cell division and nodulation, or both (Piddock, 2006; Perron et al., 2015).

In this study, we used function-based metagenomic library screening to identify so far unknown tetracycline and sulfonamide resistance genes in forest and grassland soil. Due to an excellent therapeutic index, few side effects, oral administration and low cost, tetracyclines belong to the most widely used classes of broad spectrum antibiotics in clinic (Thaker et al., 2010; Wang et al., 2017). After more than 60 years of excessive tetracycline usage, tetracycline resistance became one of the most abundant antibiotic resistances among clinical and commensal microbes (Wang et al., 2017). Another class of antibiotics, sulfonamides, is also commonly prescribed to people suffering from infections (Landers et al., 2012).

ARGs present in forests and grasslands, belonging to the most abundant terrestrial ecosystems worldwide, might become clinically relevant as they can potentially spread via lateral gene transfer. Here, we report the identification of four novel tetracycline and four previously unknown sulfonamide resistance genes derived from these ecosystems. Most of the proteins encoded by the novel ARGs showed low identity to already known antibiotic resistance determinants.

MATERIALS AND METHODS

Site Description, Soil Sampling, and Metagenomic Library Construction

Soil samples were derived from forest and grassland sites of the German Biodiversity Exploratories Schorfheide-Chorin and Schwäbische Alb (Fischer et al., 2010). The land use intensity index (LUI) (Blüthgen et al., 2012) was calculated for all grassland sites. To account for interannual variation in management practices, the LUI was calculated from 2006 to 2008 (sampling year) (Table 1). LUI allows separate analysis of the intensity of grazing (calculated by considering numbers of grazing cattle, horses, or sheep, and duration of grazing with respect to each site), the mowing frequency, and the intensity of fertilization. Forest plots were dominated by European beech (*Fagus sylvatica*) or Scots pine (*Pinus sylvestris*) (Table 1).

The collection of the samples was performed previously as described by Nacke et al. (2011a). Descriptions of the soil characteristics are provided in Table 2. Total microbial community DNA was isolated from collected soil by employing the PowerSoil DNA isolation kit (MoBio Laboratories, Carlsbad, CA, United States) and metagenomic libraries, named AEG2, AEG3, and SEG8 were generated as described by Nacke et al. (2011b). The metagenomic libraries AEW9, SEG6, SEW2, and SEW5 were previously constructed (Nacke et al., 2011b). Names of constructed metagenomic libraries refer to the designation of the samples from which the libraries were derived.

Antibiotic Resistance Screening and Sequence Analysis

The function-based screening was based on the ability of metagenomic library-bearing *Escherichia coli* clones to form colonies on LB agar medium containing 50 mg/L kanamycin, which selects for the screening vector pCR-XL-TOPO (Thermo Fisher Scientific, Braunschweig, Germany), and 5 mg/L tetracycline or 250 mg/L sulfamethoxazole. Colonies formed after incubation for 1–3 days at 37°C under aerobic conditions were picked for further study.

The recombinant plasmids derived from positive clones were sequenced by Microsynth SeqLab (Göttingen, Germany) using Sanger sequencing technology. All plasmid inserts were taxonomically classified using the software KAIJU (Menzel et al., 2016). An initial prediction of ORFs located on the inserts was performed by employing the ORF finder tool provided by the National Center for Biotechnology Information (NCBI) and the Artemis program (Rutherford et al., 2000; Wheeler et al., 2003). The results were verified and improved manually by e.g., GC frame plot and ribosome-binding site analysis. Subsequently, blast (Altschul et al., 1990) search against the NCBI non-redundant protein sequence database was performed. In addition, Resfams (Gibson et al., 2015), a recently generated database of protein families and associated profile hidden Markov models, representing all major ARG classes, was used for sequence comparisons. Blast searches against the ACLAME database (Leplae et al., 2010) version 0.4 and the Gypsy database (Llorens et al., 2011) release 2.0 were performed to identify

TABLE 1 | Characteristics of the study sites.

Site	Land use	Management	Treatment	Tree species	LUI (grazing, mowing, fertilization)
AEG2	Grassland	Meadow	Fertilized	NA	0.00, 2.07, 1.27
AEG3	Grassland	Meadow	Fertilized	NA	0.00, 2.76, 2.06
AEW9	Forest	Unmanaged forest	NA	Beech	NA
SEG6	Grassland	Mown pasture	Non-fertilized	NA	0.29, 1.38, 0.00
SEG8	Grassland	Pasture	Non-fertilized	NA	0.14, 0.69, 0.00
SEW2	Forest	Age class forest	NA	Pine	NA
SEW5	Forest	Age class forest	NA	Beech	NA

The table lists the sites, land use, management type, treatment, dominant tree species, and LUI, land use index (calculated for 2006–2008) for grassland samples. AEG/AEW: sites located in the Biodiversity Exploratory Schwäbische Alb; SEG/SEW: sites located in the Biodiversity Exploratory Schorfheide-Chorin.

TABLE 2 | Basic properties of soil samples.

Sample	Soil type	pH	OC (g kg ⁻¹)	Total N (g kg ⁻¹)	C:N ratio
AEG2	Leptosol	6.9	72.3	7.2	10.1
AEG3	Leptosol	6.3	53.7	5.2	10.4
AEW9	Leptosol	6.4	60.0	4.5	13.4
SEG6	Histosol	5.2	284.1	23.9	11.9
SEG8	Gleysol	7.4	73.2	7.1	10.4
SEW2	Cambisol	3.5	17.0	1.0	16.7
SEW5	Cambisol	3.1	29.6	1.6	18.3

AEG/AEW: soil samples derived from the Biodiversity Exploratory Schwäbische Alb; SEG/SEW: soil samples derived from the Biodiversity Exploratory Schorfheide-Chorin.

mobile genetic elements. Moreover, the IS finder (database from 2018-09-11) (Siguier et al., 2006) was employed for identification of bacterial insertion sequences.

A neighbor-joining phylogenetic tree was constructed in MEGA (version 7.0) (Kumar et al., 2016) based on a ClustalW (Thompson et al., 1994) alignment of dihydropteroate synthase (DHPS) sequences. A total number of 1,000 bootstrap samplings were carried out to test the tree topology. Branches corresponding to partitions reproduced in less than 50% bootstrap replicates were collapsed. The evolutionary distances were computed using the number of differences method.

Subcloning of ORFs Potentially Encoding Antibiotic Resistance

To verify if candidate ORFs encode antibiotic resistance, they were subcloned into vector pCR4-TOPO (Thermo Fisher Scientific) and subsequently introduced into *E. coli* TOP10. Two insert sequences (corresponding plasmids, pLAEG3_tet01 and pLSEG6_tet01) encoded proteins with similarity to members of the TetR family of regulators. In this case, the gene encoding the regulator as well as the potential ARG were subcloned together. In a first step, PCR was performed for amplification of candidate ORFs (including sequences potentially comprising promoters) from plasmid DNA. PCR primers are listed in **Table 3**. The PCR reaction mixture (50 µl) contained 10 µl 5-fold Phusion GC buffer, 200 µM of each of the four deoxynucleoside triphosphates, 5% DMSO, 0.2 µM of each primer, 1 U of Phusion HF DNA polymerase (Thermo Fisher Scientific), and approximately 20 ng of plasmid DNA. The following thermal cycling scheme was used: initial denaturation at 98°C for 1 min, 20 cycles of denaturation at 98°C for 1 min, annealing for

45 s (annealing temperatures, see **Table 3**), and extension at 72°C for 30 s per kb, followed by a final extension period at 72°C for 5 min. PCR products were purified using the QIAquick PCR purification kit (Qiagen, Hilden, Germany) according to the instructions of the manufacturer. Subsequently, a deoxyadenosine was added to the 3' termini of the DNA as described by Nacke et al. (2011b) to facilitate cloning by the TA method. The DNA was then purified using the QIAquick PCR purification kit (Qiagen) and inserted into vector pCR4-TOPO (Thermo Fisher Scientific) as described by the manufacturer. Transformation of resulting vectors into *E. coli* TOP10 chemically competent cells was performed according to the protocol of the manufacturer.

Antibiotic Susceptibility Analysis

Antibiotic susceptibility assays were conducted by using the 2-fold serial microtiter broth dilution method by considering the Clinical and Laboratory Standards Institute (CLSI) guidelines document M100-S24 (2014) and the MICs were recorded after 20 h of incubation at 37°C. The antibiotics cefotaxime, chloramphenicol, erythromycin, gentamicin, lincomycin, rifampicin, sulfadiazine, sulfamethoxazole, sulfamethazine, sulfisoxazole, tetracycline, and tylosin were considered. All assays were performed in duplicate. In addition, the susceptibility to different sulfonamides was further analyzed by spotting serial dilutions of cultures with starting OD₆₀₀ of 0.5 onto Iso-Sensitest agar (Thermo Fisher Scientific) supplemented with sulfamethoxazole, sulfamethazine, sulfisoxazole or sulfadiazine. *E. coli* TOP10 carrying vector pCR4-TOPO (Thermo Fisher Scientific) was used as control.

TABLE 3 | Primer sets designed in this study and corresponding templates.

Template	Oligonucleotide	Sequence (5' to 3')	Annealing temperature (°C)
pLAEG2_dhps01	AEG2_dhps01_for_150	GATACCCTAACGTAACCGC	55
	AEG2_dhps01_rev	TCAGCGCGGATTCTGTC	55
pLAEW9_dhps01	AEW9_dhps01_for_150	CCTGATCGGTCAGGTCCTTA	55
	AEW9_dhps01_rev	TTACGCCGTTTGCCCC	55
pLSEW2_dhps01	SEW2_dhps01_for_150	CCGCCCGCCGTGTG	60
	SEW2_dhps01_rev	TTATGAAGCGGCGATAGCAGTAATAAC	60
pLSEW5_dhps01	SEW5_dhps01_for_104	GGTCATCGCGACAAAGGGTG	60
	SEW5_dhps01_rev	CTATACAGGCCGTCCAGCTGC	60
pLAEG3_tet01	AEG3_tet01b_for	CTATTGCTTGACGCGATCG	55
	AEG3_tet01a_rev	CTATTCGCGCGGCTCAG	55
pLSEG6_tet01	SEG6_tet01b_for	TTATCCTCGACGCGCCTTG	60
	SEG6_tet01a_rev	TCAGCCCGGAGCCAAGG	60
pLSEG8_tet01	SEG8_tet01_for_150	GGATTGGAACAGACATATAGTG	55
	SEG8_tet01_rev	TTACCGGTTCCCCACTG	55
pLSEG8_tet02	SEG8_tet02_for_150	TTTAAGAGAATTTTCAGGATAAAG	50
	SEG8_tet02_rev	TTAACCATGCTTTGTGACG	50

Accession Numbers

The insert sequences of the plasmids carried by metagenomic library clones showing decreased susceptibility to sulfamethoxazole or tetracycline have been submitted to GenBank under accession numbers MK159018 to MK159025.

RESULTS AND DISCUSSION

In order to discover so far unknown ARGs in environmental resistomes, soil metagenomic libraries were subjected to function-based screening. As sequence information is not required before screening, this is the only strategy that bears the potential to discover entirely novel ARGs (Simon and Daniel, 2009). In addition, it is selective for full-length genes and functional gene products. The soil used for construction of metagenomic libraries was derived from forest and grassland varying in land use history. Fertilized and non-fertilized grassland sites as well as pristine and age class forest sites, harboring different dominant tree species, were considered (Table 1). This enabled the identification of ARGs in soils from hardly as well as intensively managed ecosystems.

Metagenomic libraries contained approximately 39,800–559,000 clones (Table 4). The quality of the libraries was controlled by determining the average insert sizes and the percentage of insert-bearing *E. coli* clones. The average insert sizes of metagenomic DNA-containing plasmids ranged from 2.6 to 6.0 kb and the frequency of clones carrying plasmid inserts was at least 73% (Table 4).

Novel ARGs Derived From Phylogenetically Divergent Soil Bacteria

The soil-derived metagenomic libraries were screened for resistance against tetracycline and sulfamethoxazole using selective agar medium. We recovered eight positive *E. coli* clones, harboring plasmids listed in Table 4, from functional

screens. The entire inserts of these plasmids were sequenced and taxonomically classified, which revealed in all cases a bacterial origin (Supplementary Table S1). Some of the insert sequences are affiliated to Gram-negative bacterial phyla including Bacteroidetes and Proteobacteria whereas others belong to Actinobacteria (Supplementary Table S1). Noteworthy, one of the insert sequences was affiliated to the poorly characterized candidate phylum Zixibacteria.

Forsberg et al. (2014) reported that bacterial phyla, which were abundant in soil samples as determined by 16S rRNA gene sequencing, were also well-represented among taxa inferred from antibiotic resistance-conferring metagenomic library inserts derived from the same samples. Previously, we detected Proteobacteria, Actinobacteria, Bacteroidetes, and Chloroflexi among the dominant phyla in soils of our study sites via pyrosequencing of 16S rRNA genes (Kaiser et al., 2016). These phyla were also covered by the antibiotic resistance-conferring inserts described in this study (see Supplementary Table S1). Despite their high-GC content and predicted transcriptional incompatibilities with *E. coli*, also Actinobacteria were represented with respect to inserts of positive clones reported here and by Forsberg et al. (2014). The taxonomic origins of our resistance-conferring inserts show that the metagenomic library host *E. coli* allows identification of ARGs carried by phylogenetically divergent soil bacteria.

Forest Soil Not Exposed to Synthetic Drugs Harbors Sulfonamide-Resistant DHPs

Sulfonamides are synthetic antimicrobial compounds targeting the folic acid pathway enzyme DHPs. Although all forest sites analyzed in this study exhibit no history of exposure to these synthetic compounds, three genes, *AEW9_dhps01*, *SEW2_dhps01*, and *SEW5_dhps01*, conferring sulfonamide resistance, were recovered from beech or pine forest soil (Tables 1, 5 and Figure 1). Furthermore, with respect to both

TABLE 4 | Characterization of soil metagenomic libraries and designation of plasmids harbored by positive clones.

Library	Number of clones	Average insert size (kb)	Insert frequency (%)	Estimated library size (Gb)	Plasmids of positive clones
AEG2	115965	3.6	73	0.30	pLAEG2_dhps01
AEG3	40095	5.8	85	0.20	pLAEG3_tet01
AEW9*	100950	2.6	89	0.23	pLAEW9_dhps01
SEG6*	39825	6.0	91	0.22	pLSEG6_tet01
SEG8	559000	4.8	86	2.30	pLSEG8_tet01-02
SEW2*	135240	5.7	95	0.73	pLSEW2_dhps01
SEW5*	166040	4.0	95	0.63	pLSEW5_dhps01

AEG/AEW: metagenomic libraries derived from the Biodiversity Exploratory Schwäbische Alb; SEG/SEW: metagenomic libraries derived from the Biodiversity Exploratory Schorfheide-Chorin. *Previously generated libraries. Names of constructed metagenomic libraries refer to the designation of the samples from which the libraries were derived (see **Table 2**).

forest sites (SEW2 and SEW5) located in the Schorfheide-Chorin exploratory (Northeastern Germany), as well as the forest site (AEW9) located in the Schwäbische Alb exploratory (Southwestern Germany), to our knowledge soils were not exposed to chemicals that resemble sulfonamides in their molecular structure. Especially, in case of the site AEW9 it is

unlikely that such chemicals were spread, as this site belongs to an unmanaged beech forest. Resistance to sulfonamides is commonly mediated by the mobile DHPS-encoding genes *sul1*, *sul2*, or *sul3* (Sköld, 2000; Perreten and Boerlin, 2003), which have been detected in various environments such as shrimp ponds, swine farm wastewater and manured soil

TABLE 5 | Proteins encoded by genes associated with antibiotic resistance and their observed sequence identities.

Plasmid	Gene	No. of encoded amino acids	Closest similar non-hypothetical protein, accession no. (no. of encoded amino acids), organism	E-value	Percent identity to the closest similar protein (Blast)	Percent identity to the closest similar protein (ClustalW alignment)
pLAEG2_dhps01	<i>AEG2_dhps01</i>	286	Dihydropteroate synthase, WP_116719066 (292), Anaerolineaeles bacterium	3e-151	213/282 (76%)	74%
pLAEW9_dhps01	<i>AEW9_dhps01</i>	273	Sulfonamide-resistant dihydropteroate synthase Sul3, WP_106052391 (263), Victivallales	1e-73	123/264 (47%)	46%
pLSEW2_dhps01	<i>SEW2_dhps01</i>	269	Dihydropteroate synthase, OGQ04760 (263), Deltaproteobacteria bacterium	3e-77	140/270 (52%)	52%
pLSEW5_dhps01	<i>SEW5_dhps01</i>	271	Dihydropteroate synthase, QJU07522 (270), Alphaproteobacteria bacterium 64-11	3e-99	159/259 (61%)	58%
pLAEG3_tet01	<i>AEG3_tet01a</i>	403	MFS transporter, AIA16595 (403), uncultured bacterium	0.0	398/403 (99%)	98%
	<i>AEG3_tet01b</i>	230	Bacterial regulatory protein of tetR family, AIA16695 (190), uncultured bacterium	2e-127	179/190 (94%)	94%
pLSEG6_tet01	<i>SEG6_tet01a</i>	408	MFS transporter, WP_078811785 (418), <i>Prostheobacter debontii</i>	2e-128	200/383 (52%)	49%
	<i>SEG6_tet01b</i>	197	TetR family transcriptional regulator, PZN78209 (205), Proteobacteria bacterium	4e-63	109/194 (56%)	54%
pLSEG8_tet01	<i>SEG8_tet01</i>	432	MFS transporter, WP075350247 (408), <i>Algoriphagus marinus</i>	3e-174	250/402 (62%)	61%
pLSEG8_tet02	<i>SEG8_tet02</i>	405	Tetracycline resistance MFS efflux pump, AIA16766 (418), uncultured bacterium	0.0	272/402 (68%)	67%

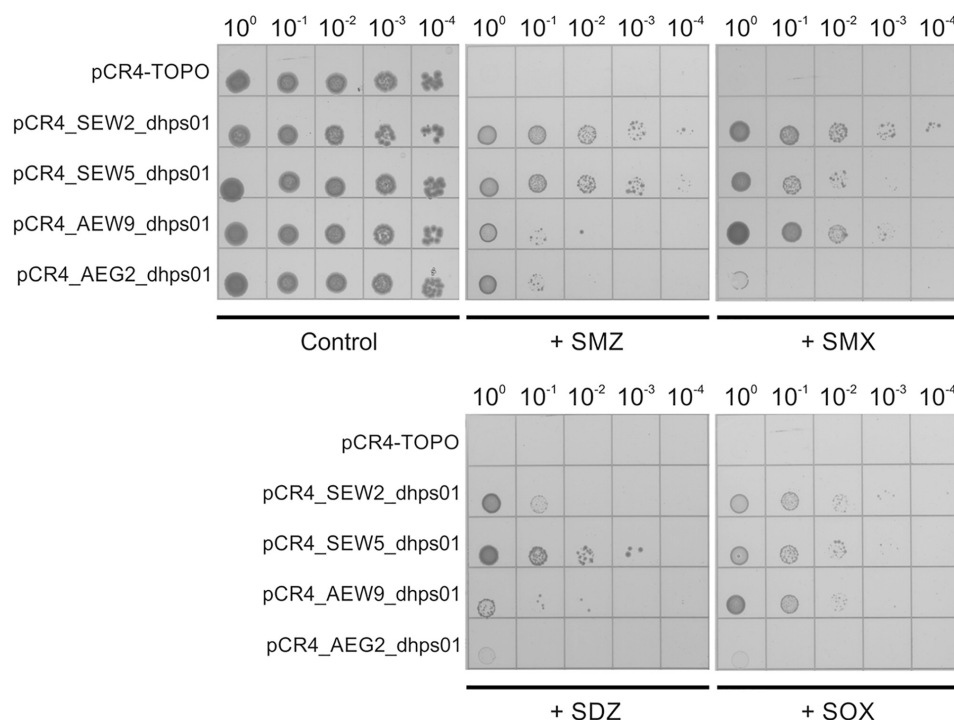


FIGURE 1 | Resistance against sulfonamide antibiotics mediated by *SEW2_dhps01*, *SEW5_dhps01*, *AEW9_dhps01*, and *AEG2_dhps01*. Five microliters of serially diluted *E. coli* TOP10 cultures with starting OD₆₀₀ of 0.5 were spotted onto Iso-Sensitest agar plates supplemented with 1000 mg/L sulfamethazine (+ SMZ), 250 mg/L sulfamethoxazole (+ SMX), 250 mg/L sulfadiazine (+ SDZ) or 500 mg/L sulfisoxazole (+ SOX). Iso-Sensitest agar plates with no sulfonamide added (control) were also included. *E. coli* TOP10 cultures carrying the cloning vector pCR4-TOPO, pCR4_SEW2_dhps01, pCR4_SEW5_dhps01, pCR4_AEW9_dhps01 or pCR4_AEG2_dhps01 were considered.

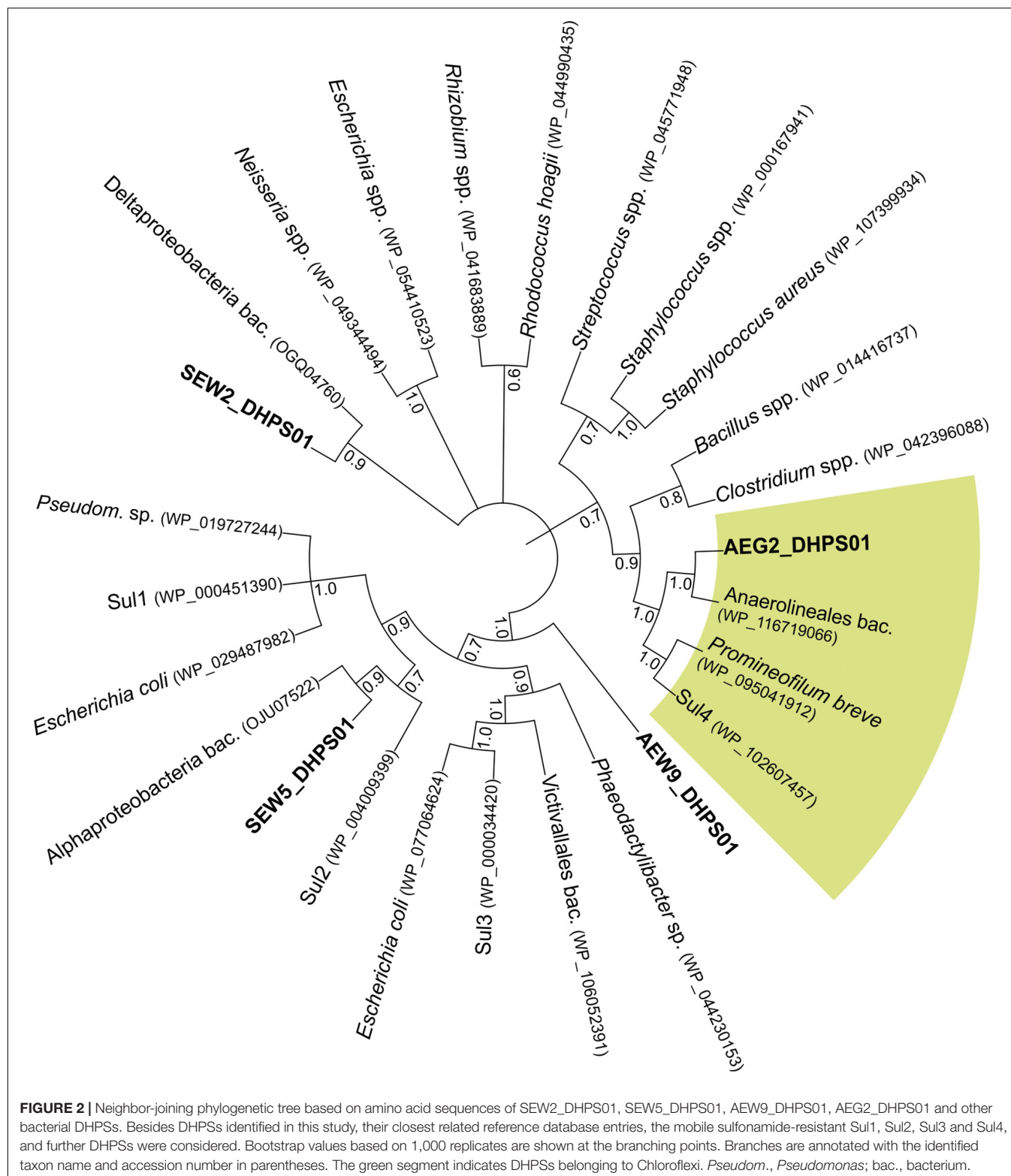
(Phuong Hoa et al., 2008; Wang et al., 2014), but also in clinical isolates (Grape et al., 2003). To our knowledge, we report here for the first time the presence of functional non-mobile sulfonamide-resistant DHPSs in forest soil ecosystems. The deduced gene products of *AEW9_dhps01*, *SEW2_dhps01*, and *SEW5_dhps01* showed only 46 to 58% amino acid sequence identities to the closest known DHPSs over the full length proteins (Table 5). Furthermore, *AEW9_dhps01* harbors the alternative start codon GTG (all other detected *dhps* genes harbored the start codon ATG).

Phylogenetic analysis revealed that *SEW2_DHPS01* exhibits homology with a putative DHPS affiliated to Deltaproteobacteria (Figure 2). Nevertheless, it has so far not been analyzed if this putative enzyme represents a functional DHPS, which can confer resistance to sulfonamides. In contrast to *SEW2_DHPS01*, *AEW9_DHPS01* showed low identity (46%) to a DHPS with confirmed sulfonamide resistance, but branched separately from this enzyme affiliated to the Lentisphaerae (family Victivallales), in a phylogenetic tree (Figure 2). The remaining sulfonamide resistance-conferring enzyme identified in forest soil, *SEW5_DHPS01*, was most similar (58% identity) to a DHPS from Alphaproteobacteria. Strikingly, no mobile genetic elements were predicted with respect to the inserts comprising *AEW9_dhps01*, *SEW2_dhps01*, and *SEW5_dhps01*. This indicates that different bacterial phyla colonizing forest soil ecosystems harbor DHPSs, which are naturally insensitive to the inhibitory

effects of sulfonamides. Furthermore, our results show that forest soil-derived DHPSs can provide high-level resistance in *E. coli* TOP10 (Figures 1, 3) and therefore potentially also in clinically relevant Enterobacteriaceae. As sulfonamides are used to treat gastrointestinal or urinary infections in human and belong to the most commonly sold and administered veterinary antibiotics (De Briyne et al., 2014; Santman-Berends et al., 2014), mobilization and spread of so far unknown genes conferring resistance to these synthetic compounds would have severe consequences, especially for the animal sector. In particular, *SEW2_DHPS01* and *SEW5_DHPS01* exhibited high-level resistance toward sulfamethazine (Figure 1), which is widely used in food animal production (Lau et al., 2017).

Discovery of a Grassland Soil-Derived DHPS Affiliated to Chloroflexi

Recently, a fourth mobile sulfonamide resistance gene (*sul4*), encoding a DHPS phylogenetically related to representatives of the phylum Chloroflexi, has been discovered in polluted Indian river sediment (Razavi et al., 2017). This gene is flanked by an ISCR element, which is known to be involved in horizontal gene transfer (Razavi et al., 2017). In this study, we identified an enzyme (*AEG2_DHPS01*) with reduced susceptibility toward sulfonamides (Figure 1 and Table 6), showing similarity to DHPSs from Chloroflexi, in a fertilized grassland soil.



AEG2_DHPS01 shares 76% sequence identity with a DHPs from a member of the Anaerolineae (Table 5) and clusters with different Chloroflexi DHPs including Sul4 in a phylogenetic tree (Figure 2).

As *sul4* is flanked by a partial *folK* ORE, it might have been decontextualized from a set of chromosomal genes involved in folate synthesis (Razavi et al., 2017). Nevertheless, Razavi et al. (2017) pointed out that further investigations on Chloroflexi

could provide additional hints about the original host of *sul4* and how it has been decontextualized. With respect to the insert carrying *AEG2_dhps01*, no genes potentially involved in folate synthesis were identified. Instead, *AEG2_dhps01* is flanked by an ORF encoding a putative gene product with low similarity (23% identity) to a primosomal protein N' (replication factor Y) – superfamily 2 helicase from an *Anaerolineae* bacterium (Supplementary Table S2). It is possible that this gene product can contribute to horizontal gene transfer between Chloroflexi and other bacterial taxa as helicases play a major role in replication, recombination, and repair of nucleic acid substrates (Flechsigt et al., 2011; Byrd and Raney, 2012). Besides the potential helicase gene, *AEG2_dhps01* is flanked by an ORF encoding a gene product with similarity to a hypothetical protein of an *Anaerolineales* bacterium.

Taxonomic analysis of the complete insert carrying *AEG2_dhps01* confirmed that its original host belongs to the Chloroflexi (Supplementary Table S1). Thus, besides *Sul4*, *AEG2_DHPS01* represents the so far only identified DHPS showing reduced susceptibility toward sulfonamides (Table 6), which is affiliated to the Chloroflexi. In order to analyze if sulfonamide resistance is a common characteristic of Chloroflexi, isolates belonging to this phylum should be analyzed with respect to susceptibility toward synthetic drugs in future surveys. Apart from sulfonamides, no decreased susceptibility toward other tested antibiotics was detected with respect to *E. coli* TOP10 carrying the subcloned *dhps* genes (Figure 3 and Table 6).

An Efflux Protein Conferring Reduced Tetracycline and Lincomycin Susceptibility

We identified four plasmids, pLAEG3_tet01, pLSEG6_tet01, pLSEG8_tet01, and pLSEG8_tet02, conferring efflux-mediated tetracycline resistance. All of these plasmids encode gene products with similarity to major facilitator superfamily (MFS) efflux proteins (Table 5). MFS efflux systems are widely distributed in both Gram-positive and Gram-negative bacteria (Sun et al., 2014). Accordingly, Wang et al. (2017) reported that 21 out of 24 tetracycline resistance genes, identified by functional

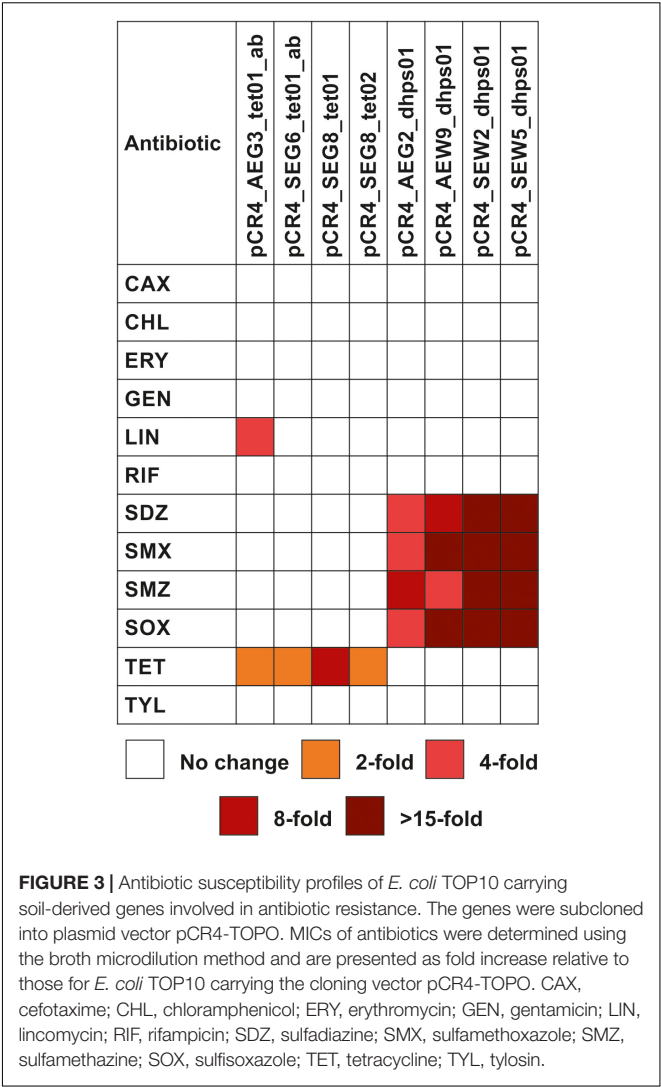


FIGURE 3 | Antibiotic susceptibility profiles of *E. coli* TOP10 carrying soil-derived genes involved in antibiotic resistance. The genes were subcloned into plasmid vector pCR4-TOPO. MICs of antibiotics were determined using the broth microdilution method and are presented as fold increase relative to those for *E. coli* TOP10 carrying the cloning vector pCR4-TOPO. CAX, cefotaxime; CHL, chloramphenicol; ERY, erythromycin; GEN, gentamicin; LIN, lincomycin; RIF, rifampicin; SDZ, sulfadiazine; SMX, sulfamethoxazole; SMZ, sulfamethazine; SOX, sulfisoxazole; TET, tetracycline; TYL, tylosin.

metagenomics in Chinese soils, were affiliated to the MFS. The proteins encoded by these 21 genes showed identities $\geq 78\%$ to

TABLE 6 | Antibiotic susceptibility of plasmid-carrying *E. coli* clones.

Plasmid	Minimal inhibitory concentration (µg/ml)											
	CAX	CHL	ERY	GEN	LIN	RIF	SDZ	SMX	SMZ	SOX	TET	TYL
Cloning vector	<0.125	2	1024	4	512	8	15.625	7.8125	62.5	15.625	1	512
pCR4_AEG2_dhps01	<0.125	2	1024	4	512	8	62.5	31.25	500	62.5	1	512
pCR4_AEW9_dhps01	<0.125	2	1024	4	512	8	125	500	250	1000	1	512
pCR4_SEW2_dhps01	<0.125	2	1024	4	512	8	500	500	>1000	1000	1	512
pCR4_SEW5_dhps01	<0.125	2	1024	4	512	8	>1000	500	>1000	1000	1	512
pCR4_AEG3_tet01ab	<0.125	2	1024	4	2048	8	15.625	7.8125	62.5	15.625	2	512
pCR4_SEG6_tet01ab	<0.125	2	1024	4	512	8	15.625	7.8125	62.5	15.625	2	512
pCR4_SEG8_tet01	<0.125	2	1024	4	512	8	15.625	7.8125	62.5	15.625	8	512
pCR4_SEG8_tet02	<0.125	2	1024	4	512	8	15.625	7.8125	62.5	15.625	2	512

CAX, cefotaxime; CHL, chloramphenicol; ERY, erythromycin; GEN, gentamicin; LIN, lincomycin; RIF, rifampicin; SDZ, sulfadiazine; SMX, sulfamethoxazole; SMZ, sulfamethazine; SOX, sulfisoxazole; TET, tetracycline; TYL, tylosin. Bold values indicate an increase in minimal inhibitory concentration compared to the control strain carrying the cloning vector pCR4-TOPO.

the closest related reference database entries (Wang et al., 2017). In contrast, three out of four MFS representatives identified in this study shared $\leq 67\%$ identity with their closest related proteins (Table 5). Besides an MFS representative, two insert sequences (corresponding plasmids, pLAEG3_tet01 and pLSEG6_tet01) encoded proteins with similarity to members of the TetR family of regulators (Table 5). These regulators are associated with antibiotic resistance and are known to control expression of MFS members (Cuthbertson and Nodwell, 2013). Noteworthy, the insert of plasmid pLtetSEG8_02 encodes a protein with similarity to an endonuclease (Supplementary Table S2), which might contribute to horizontal gene transfer.

McGarvey et al. (2012) identified a tetracycline-resistant metagenomic library clone, harboring a MFS representative, with reduced susceptibility toward rifampicin. Here, no resistance toward rifampicin was detected with respect to recombinant MFS producing *E. coli* clones (Figure 3). Nevertheless, the tetracycline-resistant clone carrying plasmid pCR4_AEG3_tet01ab showed reduced susceptibility toward lincomycin (Figure 3 and Table 6). The gene product AEG3_Tet01a encoded by this plasmid shows 98% identity to a soil-derived MFS from an uncultured bacterium (Table 5), which confers resistance to chloramphenicol. So far, it has not been analyzed if this chloramphenicol resistance mediating MFS identified by Forsberg et al. (2014) also encodes lincomycin resistance.

CONCLUSION

Our findings highlight the vast potential of functional metagenomics for the discovery of so far unknown antibiotic resistance determinants in environmental resistomes. We recovered several soil-derived target genes and proteins with low similarity to reference database entries from hardly as well as intensively managed forest and grassland, indicating that the resistance reservoir of the uncultured microbial majority is far from being extensively explored. As we detected here for the first time non-mobile DHPs conferring resistance to sulfonamides in forest soil with no history of exposure to these synthetic drugs, it is possible that this characteristic naturally occurs in complex bacterial communities. Most of the detected antibiotic resistance determinants were not flanked by potential mobile genetic elements. Nevertheless, the recent finding of a fourth mobile sulfonamide resistance gene indicates ongoing forces that introduce, mobilize and maintain antibiotic resistance determinants in bacterial communities (Razavi et al., 2017). Considering, that several ARGs reported here conferred high-level resistance to non-pathogenic *E. coli*, it can be assumed that this could also be the case with respect to clinically

relevant Enterobacteriaceae. In order to predict the emergence of antibiotic resistance, an extensive knowledge on environmental resistomes will be required, which might also direct the design of novel antibiotics that are less susceptible to resistance.

DATA AVAILABILITY

The datasets generated for this study can be found in GenBank, MK159018 to MK159025.

AUTHOR CONTRIBUTIONS

HN designed the study. IW, AK, NA, DK, SB, FF, and HN carried out field and laboratory work. IW and HN prepared and analyzed the data. All authors interpreted the results and wrote the paper.

FUNDING

This work was funded by the DFG Priority Program 1374 “Infrastructure-Biodiversity-Exploratories” (NA 848/2-1) and the Open Access Publication Funds of the Göttingen University.

ACKNOWLEDGMENTS

We thank the managers of the three Exploratories, Kirsten Reichel-Jung, Iris Steitz, Sandra Weithmann, Florian Straub, Katrin Lorenzen, Juliane Vogt, Miriam Teuscher and all former managers for their work in maintaining the plot and project infrastructure; Christiane Fischer for giving support through the central office, Andreas Ostrowski for managing the central data base, and Markus Fischer, Eduard Linsenmair, Dominik Hessenmöller, Daniel Prati, Ingo Schöning, François Buscot, Ernst-Detlef Schulze, Wolfgang W. Weisser, and the late Elisabeth Kalko for their role in setting up the Biodiversity Exploratories project. Field work permits were issued by the responsible state environmental offices of Baden-Württemberg, Thüringen, and Brandenburg. We thank Melissa Kocatuerk who contributed to the performance of the MIC assays.

SUPPLEMENTARY MATERIAL

The Supplementary Material for this article can be found online at: <https://www.frontiersin.org/articles/10.3389/fmicb.2019.00460/full#supplementary-material>

REFERENCES

- Allen, H. K., Moe, L. A., Rodbumrer, J., Gaarder, A., and Handelsman, J. (2009). Functional metagenomics reveals diverse beta-lactamases in a remote Alaskan soil. *ISME J.* 3, 243–251. doi: 10.1038/ismej.2008.86
- Altschul, S. F., Gish, W., Miller, W., Myers, E. W., and Lipman, D. J. (1990). Basic local alignment search tool. *J. Mol. Biol.* 215, 403–410. doi: 10.1016/S0022-2836(05)80360-2
- Blüthgen, N., Dormann, C. F., Prati, D., Klaus, V. H., Kleinebecker, T., Hölzel, N., et al. (2012). A quantitative index of land-use intensity in grasslands: integrating

- mowing, grazing and fertilization. *Basic Appl. Ecol.* 13, 207–220. doi: 10.1016/j.baae.2012.04.001
- Byrd, A. K., and Raney, K. D. (2012). Superfamily 2 helicases. *Front. Biosci.* 17:2070–2088. doi: 10.2741/4038
- Cheng, J., Romantsov, T., Engel, K., Doxey, A. C., Rose, D. R., Neufeld, J. D., et al. (2017). Functional metagenomics reveals novel β -galactosidases not predictable from gene sequences. *PLoS One* 12:e0172545. doi: 10.1371/journal.pone.0172545
- Cuthbertson, L., and Nodwell, J. R. (2013). The TetR family of regulators. *Microbiol. Mol. Biol. Rev.* 77, 440–475. doi: 10.1128/MMBR.00018-13
- Davies, J., and Davies, D. (2010). Origins and evolution of antibiotic resistance. *Microbiol. Mol. Biol. Rev.* 74, 417–433. doi: 10.1128/MMBR.00016-10
- D'Costa, V. M., Griffiths, E., and Wright, G. D. (2007). Expanding the soil antibiotic resistome: exploring environmental diversity. *Curr. Opin. Microbiol.* 10, 481–489. doi: 10.1016/j.mib.2007.08.009
- De Briyne, N., Atkinson, J., Pokludová, L., and Borriello, S. P. (2014). Antibiotics used most commonly to treat animals in Europe. *Vet. Rec.* 175:325. doi: 10.1136/vr.102462
- Delmont, T. O., Robe, P., Cecillon, S., Clark, I. M., Constancias, F., Simonet, P., et al. (2011). Accessing the soil metagenome for studies of microbial diversity. *Appl. Environ. Microbiol.* 77, 1315–1324. doi: 10.1128/AEM.01526-10
- Fischer, M., Bossdorf, O., Gockel, S., Hänsel, F., Hemp, A., Hessenmöller, D., et al. (2010). Implementing large-scale and long-term functional biodiversity research: the biodiversity exploratories. *Basic Appl. Ecol.* 11, 473–485. doi: 10.1016/j.baae.2010.07.009
- Fleischig, H., Popp, D., and Mikhailov, A. S. (2011). In silico investigation of conformational motions in superfamily 2 helicase proteins. *PLoS One* 6:e21809. doi: 10.1371/journal.pone.0021809
- Forsberg, K. J., Patel, S., Gibson, M. K., Lauber, C. L., Knight, R., Fierer, N., et al. (2014). Bacterial phylogeny structures soil resistomes across habitats. *Nature* 509, 612–616. doi: 10.1038/nature13377
- Forsberg, K. J., Reyes, A., Wang, B., Selleck, E. M., Sommer, M. O., and Dantas, G. (2012). The shared antibiotic resistome of soil bacteria and human pathogens. *Science* 337, 1107–1111. doi: 10.1126/science.1220761
- Gibson, M. K., Forsberg, K. J., and Dantas, G. (2015). Improved annotation of antibiotic resistance determinants reveals microbial resistomes cluster by ecology. *ISME J.* 9, 207–216. doi: 10.1038/ismej.2014.106
- Grape, M., Sundström, L., and Kronvall, G. (2003). Sulphonamide resistance gene *sul3* found in *Escherichia coli* isolates from human sources. *J. Antimicrob. Chemother.* 52, 1022–1024. doi: 10.1093/jac/dkg473
- Kaiser, K., Wemheuer, B., Korolkow, V., Wemheuer, F., Nacke, H., Schöning, I., et al. (2016). Driving forces of soil bacterial community structure, diversity, and function in temperate grasslands and forests. *Sci. Rep.* 6:33696. doi: 10.1038/srep33696
- Kumar, S., Stecher, G., and Tamura, K. (2016). MEGA7: molecular evolutionary genetics analysis version 7.0 for bigger datasets. *Mol. Biol. Evol.* 33, 1870–1874. doi: 10.1093/molbev/msw054
- Landers, T. F., Cohen, B., Wittum, T. E., and Larson, E. L. (2012). A review of antibiotic use in food animals: perspective, policy and potential. *Public Health Rep.* 127, 4–22. doi: 10.1177/003335491212700103
- Lau, C. H., van Engelen, K., Gordon, S., Renaud, J., and Topp, E. (2017). Novel novel antibiotic resistance determinants from agricultural soil exposed to antibiotics widely used in human medicine and animal farming. *Appl. Environ. Microbiol.* doi: 10.1128/AEM.00989-17 [Epub ahead of print].
- Leplae, R., Lima-Mendez, G., and Toussaint, A. (2010). ACLAME: a classification of mobile genetic elements, update 2010. *Nucleic Acids Res.* 38, D57–D61. doi: 10.1093/nar/gkp938
- Llorens, C., Futami, R., Covelli, L., Domínguez-Escribá, L., Viu, J. M., Tamarit, D., et al. (2011). The gypsy database (GyDB) of mobile genetic elements: release 2.0. *Nucleic Acids Res.* 39, D70–D74. doi: 10.1093/nar/gkq1061
- Martínez, J. L. (2008). Antibiotics and antibiotic resistance genes in natural environments. *Science* 321, 365–367. doi: 10.1126/science.1159483
- McGarvey, K. M., Queitsch, K., and Fields, S. (2012). Wide variation in antibiotic resistance proteins identified by functional metagenomic screening of a soil DNA library. *Appl. Environ. Microbiol.* 78, 1708–1714. doi: 10.1128/AEM.06759-11
- Menzel, P., Ng, K. L., and Krogh, A. (2016). Fast and sensitive taxonomic classification for metagenomics with Kaiju. *Nat. Commun.* 7:11257. doi: 10.1038/ncomms11257
- Nacke, H., and Daniel, R. (2014). “Approaches in metagenome research: progress and challenges,” in *Encyclopedia of Metagenomics*, ed. K. Nelson (New York, NY: Springer).
- Nacke, H., Thürmer, A., Wollherr, A., Will, C., Hodac, L., Herold, N., et al. (2011a). Pyrosequencing-based assessment of bacterial community structure along different management types in German forest and grassland soils. *PLoS One* 6:e17000. doi: 10.1371/journal.pone.0017000
- Nacke, H., Will, C., Herzog, S., Nowka, B., Engelhaupt, M., and Daniel, R. (2011b). Identification of novel lipolytic genes and gene families by screening of metagenomic libraries derived from soil samples of the German Biodiversity Exploratories. *FEMS Microbiol. Ecol.* 78, 188–201. doi: 10.1111/j.1574-6941.2011.01088.x
- Nesme, J., and Simonet, P. (2015). The soil resistome: a critical review on antibiotic resistance origins, ecology and dissemination potential in telluric bacteria. *Environ. Microbiol.* 17, 913–930. doi: 10.1111/1462-2920.12631
- Perreten, V., and Boerlin, P. (2003). A new sulfonamide resistance gene (*sul3*) in *Escherichia coli* is widespread in the pig population of Switzerland. *Antimicrob. Agents Chemother.* 47, 1169–1172. doi: 10.1128/AAC.47.3.1169-1172.2003
- Perron, G. G., Whyte, L., Turnbaugh, P. J., Goordial, J., Hanage, W. P., Dantas, G., et al. (2015). Functional characterization of bacteria isolated from ancient arctic soil exposes diverse resistance mechanisms to modern antibiotics. *PLoS One* 10:e0069533. doi: 10.1371/journal.pone.0069533
- Phuong Hoa, P. T., Nonaka, L., Hung Viet, P., and Suzuki, S. (2008). Detection of the *sul1*, *sul2*, and *sul3* genes in sulfonamide-resistant bacteria from wastewater and shrimp ponds of north Vietnam. *Sci. Total Environ.* 405, 377–384. doi: 10.1016/j.scitotenv.2008.06.023
- Piddock, L. J. (2006). Multidrug-resistance efflux pumps - not just for resistance. *Nat. Rev. Microbiol.* 4, 629–636. doi: 10.1038/nrmicro1464
- Razavi, M., Marathe, N. P., Gillings, M. R., Flach, C. F., Kristiansson, E., and Joakim Larsson, D. G. (2017). Discovery of the fourth mobile sulfonamide resistance gene. *Microbiome* 5:160. doi: 10.1186/s40168-017-0379-y
- Rutherford, K., Parkhill, J., Crook, J., Horsnell, T., Rice, P., Rajandream, M. A., et al. (2000). Artemis: sequence visualization and annotation. *Bioinformatics* 16, 944–945. doi: 10.1093/bioinformatics/16.10.944
- Santman-Berends, I., Luttikholt, S., Van den Brom, R., Van Schaik, G., Gonggrijp, M., Hage, H., et al. (2014). Estimation of the use of antibiotics in the small ruminant industry in The Netherlands in 2011 and 2012. *PLoS One* 9:e105052. doi: 10.1371/journal.pone.0105052
- Siguier, P., Perochon, J., Lestrade, L., Mahillon, J., and Chandler, M. (2006). ISfinder: the reference centre for bacterial insertion sequences. *Nucleic Acids Res.* 34, D32–D36. doi: 10.1093/nar/gkj014
- Simon, C., and Daniel, R. (2009). Achievements and new knowledge unraveled by metagenomic approaches. *Appl. Microbiol. Biotechnol.* 85, 265–276. doi: 10.1007/s00253-009-2233-z
- Sköld, O. (2000). Sulfonamide resistance: mechanisms and trends. *Drug Resistance Updates* 3, 155–160. doi: 10.1054/drup.2000.0146
- Sun, J., Deng, Z., and Yan, A. (2014). Bacterial multidrug efflux pumps: mechanisms, physiology and pharmacological exploitations. *Biochem. Biophys. Res. Commun.* 453, 254–267. doi: 10.1016/j.bbrc.2014.05.090
- Thaker, M., Spanogiannopoulos, P., and Wright, G. D. (2010). The tetracycline resistome. *Cell. Mol. Life Sci.* 67, 419–431. doi: 10.1007/s00018-009-0172-6
- Thompson, J., Higgins, D., and Gibson, T. (1994). CLUSTAL W: improving the sensitivity of progressive multiple sequence alignment through sequence weighting, position-specific gap penalties and weight matrix choice. *Nucleic Acids Res.* 22, 4673–4680. doi: 10.1093/nar/22.22.4673
- Walsh, F. (2013a). Investigating antibiotic resistance in non-clinical environments. *Front. Microbiol.* 4:19. doi: 10.3389/fmicb.2013.00019
- Walsh, F. (2013b). The multiple roles of antibiotics and antibiotic resistance in nature. *Front. Microbiol.* 4:255. doi: 10.3389/fmicb.2013.00255
- Walsh, F., and Duffy, B. (2013). The culturable soil antibiotic resistome: a community of multi-drug resistant bacteria. *PLoS One* 8:e65567. doi: 10.1371/journal.pone.0065567

- Wang, N., Yang, X., Jiao, S., Zhang, J., Ye, B., and Gao, S. (2014). Sulfonamide-resistant bacteria and their resistance genes in soils fertilized with manures from Jiangsu Province, Southeastern China. *PLoS One* 9:e112626. doi: 10.1371/journal.pone.0112626
- Wang, S., Gao, X., Gao, Y., Li, Y., Cao, M., Xi, Z., et al. (2017). Tetracycline resistance genes identified from distinct soil environments in china by functional metagenomics. *Front. Microbiol.* 8:1406. doi: 10.3389/fmicb.2017.01406
- Wheeler, D. L., Church, D. M., Federhen, S., Lash, A. E., Madden, T. L., Pontius, J. U., et al. (2003). Database resources of the national center for biotechnology. *Nucleic Acids Res.* 31, 28–33. doi: 10.1093/nar/gkg033

Conflict of Interest Statement: The authors declare that the research was conducted in the absence of any commercial or financial relationships that could be construed as a potential conflict of interest.

Copyright © 2019 Willms, Kamran, Aßmann, Krone, Bolz, Fiedler and Nacke. This is an open-access article distributed under the terms of the Creative Commons Attribution License (CC BY). The use, distribution or reproduction in other forums is permitted, provided the original author(s) and the copyright owner(s) are credited and that the original publication in this journal is cited, in accordance with accepted academic practice. No use, distribution or reproduction is permitted which does not comply with these terms.

4.1. Supplemental information for chapter four

Table S1. Taxonomic classification of plasmid inserts from positive clones.

Table S2. Open reading frames potentially involved in lateral gene transfer identified on plasmids and description of corresponding gene products and their observed sequence identities.

Table S1. Taxonomic classification of plasmid inserts from positive clones.

Plasmid	Taxonomic classification of insert
pLAEG2_dhps01	Cellular organisms; Bacteria; Terrabacteria group; Chloroflexi; unclassified Chloroflexi; unclassified Chloroflexi (miscellaneous); Chloroflexi bacterium OLB14
pLAEW9_dhps01	Cellular organisms; Bacteria; Terrabacteria group; Actinobacteria; Actinobacteria; Micrococcales; Microbacteriaceae; <i>Microbacterium</i> ; <i>Microbacterium</i> sp.
pLSEW2_dhps01	Cellular organisms; Bacteria; unclassified Bacteria; Bacteria candidate phyla; candidate division Zixibacteria; candidate division Zixibacteria bacterium SM23_81
pLSEW5_dhps01	Cellular organisms; Bacteria; Proteobacteria; Alphaproteobacteria; Rhizobiales; Rhodobiaceae; <i>Parvibaculum</i> ; <i>Parvibaculum lavamentivorans</i>
pLAEG3_tet01	Cellular organisms; Bacteria; environmental samples; uncultured bacterium
pLSEG6_tet01	Cellular organisms; Bacteria; Terrabacteria group; Actinobacteria; Actinobacteria; Corynebacteriales; Mycobacteriaceae; <i>Mycobacterium</i> ; <i>Mycobacterium rhodesiae</i>
pLSEG8_tet01	Cellular organisms; Bacteria
pLSEG8_tet02	Cellular organisms; Bacteria; FCB group; Bacteroidetes/Chlorobi group; Bacteroidetes; Chitinophagia; Chitinophagales

Table S2. Open reading frames potentially involved in lateral gene transfer identified on plasmids and description of corresponding gene products and their observed sequence identities.

Plasmid	ORF#	No. of encoded amino acids	Closest similar protein potentially involved in lateral gene transfer, accession no. (no. of encoded amino acids), organism	E value	Percent identity to the closest similar bacterial protein
pLAEG2_dhps01	18	445	Primosomal protein N' – superfamily II helicase, RCK75038 (471), Anaerolineae bacterium	1e-40	118/429 (28%)
pLSEG8_tet02	40	123	Endonuclease domain-containing protein, WP_068706482 (129), Paludibacter jiangxiensis	4e-35	57/115 (50%)

5. Globally abundant *Candidatus* Udaeobacter benefits from release of antibiotics in soil and potentially performs trace gas scavenging

Inka M. Willms¹, Anina Y. Rudolph¹, Isabell Göschel¹, Simon H. Bolz¹, Dominik Schneider¹, Caterina Penone², Anja Poehlein¹, Ingo Schöning³, Heiko Nacke^{1*}

¹ Department of Genomic and Applied Microbiology and Göttingen Genomics Laboratory, Institute of Microbiology and Genetics, Georg-August University of Göttingen, D-37077 Göttingen, Germany^a

² Institute of Plant Sciences, University of Bern, CH-3013 Bern, Switzerland^b

³ Max Planck Institute for Biogeochemistry, D-07745 Jena, Germany^c

Running Head: Novel features of soil-resident *Candidatus* Udaeobacter

Revised version of this manuscript published in: mSphere (2020), 5:e00186-20

Author contributions to the work

Conceptualization, I.M.W. and H.N.; formal analysis, I.M.W., C.P., A.P., D.S. and H.N.; investigation, I.M.W., A.Y.R., I.G. and S.H.B.; resources, H.N. and I.S.; data curation, I.M.W. and H.N.; writing – original draft preparation, I.M.W. and H.N.; writing – review and editing, I.M.W., H.N., D.S. and I.S.; visualization, I.M.W. and H.N.; supervision, I.M.W. and H.N.; project administration, H.N.; funding acquisition, H.N.

Abstract

Verrucomicrobia affiliated to *Candidatus* Udaeobacter belong to the most abundant soil bacteria worldwide. Although the synthesis of antibiotics presumably evolved in soil and environmental pollution with antimicrobials increases, the impact of these complex molecules on *Ca. Udaeobacter* remains to be elucidated. In this study, we demonstrate that *Ca. Udaeobacter* representatives residing in grassland as well as forest soil ecosystems show multiresistance and even take advantage of antibiotics release. Soils treated with up to six different antibiotics exhibited a higher *Ca. Udaeobacter* abundance than corresponding controls after three, eight and twenty days of incubation. In this context, we provide evidence that *Ca. Udaeobacter* utilizes nutrients which are released due to antibiotic-driven lysis of other soil microbes and thereby reduces energetically expensive synthesis of required biomolecules. Moreover, genomic analysis revealed the presence of genes conferring resistance to multiple classes of antibiotics and indicates that *Ca. Udaeobacter* representatives most likely oxidize the trace gas H_2 to generate energy. This energy might be required for long-term persistence in terrestrial habitats, as already suggested for other dominant soil bacteria. Our study illustrates for the first time that globally abundant *Ca. Udaeobacter* benefits from release of antibiotics, which confers advantages over other soil bacteria and represents a so far overlooked fundamental lifestyle feature of this poorly characterized verrucomicrobial group. Furthermore, our study suggests that *Ca. Udaeobacter* representatives can utilize H_2 as an alternative electron donor.

Importance

Soil bacteria have been investigated for more than a century, but one of the most dominant terrestrial groups on Earth, *Candidatus* Udaeobacter, remains elusive and largely unexplored. Its natural habitat is considered as a major reservoir of antibiotics, which directly or indirectly impact phylogenetically diverse microorganisms. Here, we found that *Ca. Udaeobacter* representatives exhibit multi-resistance and not only evade harmful effects of antimicrobials, but even benefit from antibiotic pressure in soil. Therefore, *Ca. Udaeobacter* evidently affects the composition of soil resistomes worldwide and might represent a winner of rising environmental pollution with antimicrobials. In addition, our study indicates that *Ca. Udaeobacter* representatives utilize H_2 and thereby contribute to global hydrogen cycling. The

here reported findings provide insights into elementary lifestyle features of *Ca. Udaeobacter*, potentially contributing to its successful global dissemination.

Introduction

Candidatus Udaeobacter representatives are encountered across soil ecosystems globally (1). Nevertheless, currently it is largely unknown, how these verrucomicrobial organisms became successful terrestrial colonizers. No *Ca. Udaeobacter* cultures, which would allow detailed physiological analyses, are available. Moreover, *Verrucomicrobia* have been under-recognized in many studies on soil bacterial communities since commonly used PCR primers widely exclude their 16S rRNA genes during amplification (2). So far, the effects of antibiotics, which can be lethal, growth-inhibiting, but also beneficial for microbial taxa, have not been analyzed with respect to *Ca. Udaeobacter*.

A recently published metagenome-assembled genome (MAG) of *Ca. Udaeobacter copiosus* indicates that this phylotype exhibits auxotrophies for numerous putative vitamin and costly amino acid synthesis pathways (1). It is hypothesized that essential metabolites, *Ca. Udaeobacter copiosus* appears incapable of synthesizing, are taken up from the environment, as the MAG is enriched with amino acid transporter and protease genes (1). Being dependent on extracellular metabolites in a densely colonized habitat like soil might entail increased influx and thus vulnerability to toxic agents secreted by microorganisms competing for scarce nutrients (3). Therefore, an efficient strategy for protection against harmful substances such as antibiotics seems likely and potentially contributed to the successful global dissemination of *Ca. Udaeobacter*. This theory is supported by an enriched abundance of beta-lactamase genes within the phylum *Verrucomicrobia*, identified through function-based screening of soil metagenomic libraries (4).

In this study, for the first time, impacts of antibiotics on the ubiquitous soil bacterium *Ca. Udaeobacter*, a member of the *Chthoniobacterales*, were investigated. To enable robust assessment of its response to antibiotic treatment in a microcosm experiment, topsoil samples from forests and grasslands of two different geographic regions were considered. We monitored the abundance of *Ca. Udaeobacter* relative to other bacterial taxa during microcosm incubation via amplicon sequencing of 16S rRNA genes. Since primers specifically targeting this poorly characterized verrucomicrobial group are not available, we designed and evaluated oligonucleotides, which we subsequently used for qPCR-based estimation of its absolute 16S rRNA gene abundance in microcosm samples. Furthermore, a MAG of *Ca. Udaeobacter* was reconstructed from metagenomic sequences in order to identify antibiotic

resistance genes (ARGs) and additional characteristics potentially contributing to its dominance in soil ecosystems.

We hypothesized that the abundance of *Ca. Udaeobacter* representatives is not reduced by an elevated concentration of the broad-spectrum antibiotic amoxicillin, as it has been indicated that beta-lactamases are enriched within *Verrucomicrobia* (4). Taking into account that numerous antimicrobial compounds are produced and released in soil, we further hypothesized that these globally abundant bacteria are not solely resistant to a single class of antibiotics but exhibit multi-drug resistance.

Results

Antibiotics evoke elevated *Ca. Udaeobacter* relative abundance

A microcosm experiment was performed to investigate how antibiotics release affects soil bacteria representing *Ca. Udaeobacter*. For this experiment, initial concentrations of 77 antibiotics were determined in all considered forest and grassland soil samples derived from two geographic regions (Hainich-Dün and Schwäbische Alb, Germany) (Table S1). Except chlortetracycline (0.011 mg/kg in forest sample AEW2), which was not applied during the microcosm experiment, each of the antimicrobial compounds exhibited a concentration below the detection limit (Table S2). Soils were treated with one antibiotic (amoxicillin), three antibiotics (amoxicillin, oxytetracycline and sulfadiazine) and six antibiotics (amoxicillin, oxytetracycline, sulfadiazine, trimethoprim, tylosin and ciprofloxacin) in high as well as low concentration (corresponding controls, not treated with antibiotics, were also considered). Subsequently, we assessed the relative abundances of bacterial taxonomic groups in soil microcosms via 16S rRNA gene-based high-throughput amplicon sequencing over a period of 20 days. Prior to antibiotic treatment, strong variations of *Ca. Udaeobacter* relative abundances between the microcosm samples were determined. For example, the relative abundance of *Ca. Udaeobacter* accounted for approximately 15% in beech forest soil from the Schwäbische Alb (sample AEW7), whereas only about 3% of the bacterial community in a grassland soil from the Hainich-Dün region (sample HEG7) represented *Ca. Udaeobacter* (Figure S1).

Strikingly, grassland as well as forest soil microcosms treated with antibiotics exhibited significantly higher relative abundances of *Ca. Udaeobacter* than corresponding controls ($p\text{-value} < 2 \times 10^{-16}$) (Fig. 1,

Fig. S1). This pattern was detected when a single antibiotic was added, but also when three or six antibiotics were applied in both, high and low concentration (Table S3). After three days of incubation, the treatment with six antibiotics in high concentration led to the most pronounced rise of *Ca. Udaeobacter* relative abundance (~50-100%). Furthermore, the treatment with one antibiotic and three antibiotics in high concentration evoked a similar increase in *Ca. Udaeobacter* relative abundance after three days of incubation (~50-80%) (Fig. 1). With increasing days of incubation we determined a statistically significant reduction of the antibiotic treatment effect on *Ca. Udaeobacter* relative abundance ($p\text{-value} < 2 \times 10^{-16}$).

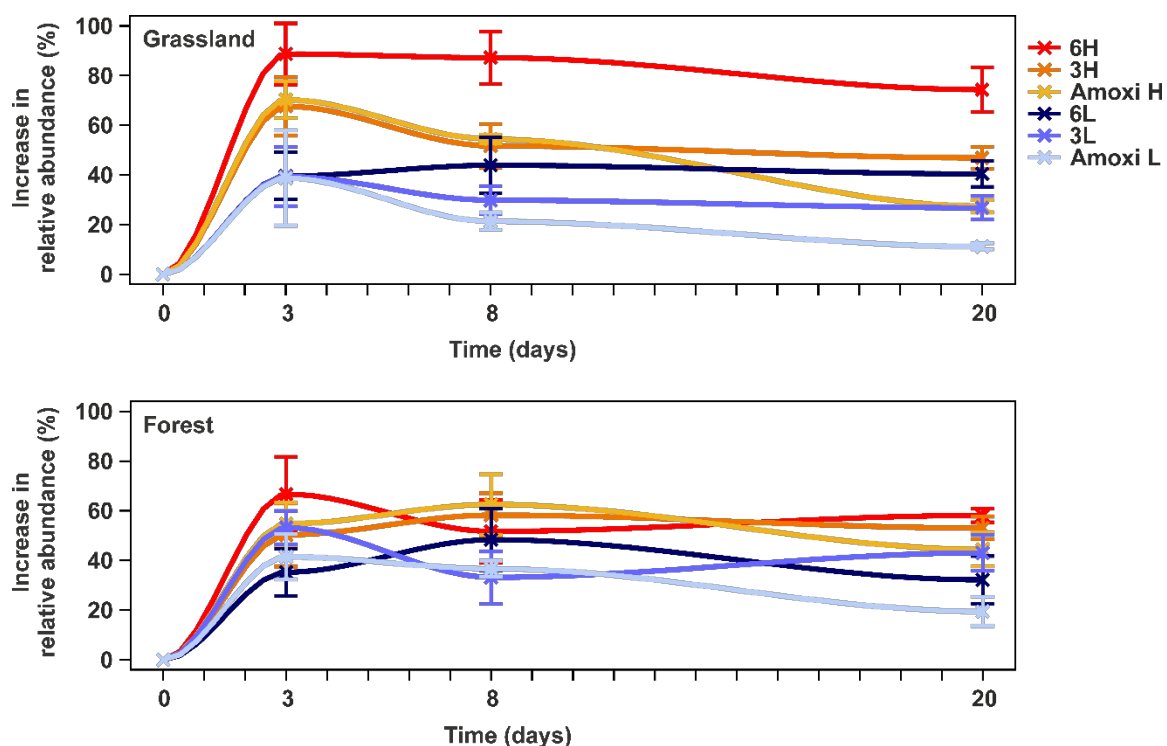


Figure 1. Increase in relative abundance of *Ca. Udaeobacter* upon antibiotic treatment across grassland and forest soil microcosms. To determine the increase in *Ca. Udaeobacter* relative abundance, samples treated with antibiotics were compared with corresponding controls. The increase in abundance relative to these controls is depicted. Abbreviations: Amoxi L, treatment with amoxicillin in low concentration; 3L, treatment with three antibiotics in low concentration; 6L, treatment with six antibiotics in low concentration; Amoxi H, treatment with amoxicillin in high concentration; 3H, treatment with three antibiotics in high concentration; 6H, treatment with six antibiotics in high concentration. Standard errors are indicated by vertical bars. Barplots depicting abundances of *Ca. Udaeobacter* relative to other bacterial groups with respect to the single samples analyzed in this study are presented in Fig. S1.

First primer pair for targeted detection of *Ca. Udaeobacter*

To verify if the abundance of *Ca. Udaeobacter* remains stable or even rises upon antibiotic treatment, we designed and evaluated a primer pair (UDBAC_F/UDBAC_R) for targeted detection of this verrucomicrobial group. An *in silico* analysis indicated that the primer pair covers approximately 97.14% of the *Ca. Udaeobacter* 16S rRNA gene sequences deposited in the SILVA SSU database (release 132). Within the evaluation process, the primer pair was used to generate amplicons based on DNA extracted from soils used to prepare the microcosms, as well as corresponding samples, incubated for three days after treatment with six antibiotics in high concentration. These amplicons were subsequently subjected to high-throughput sequencing and, as expected, the generated data revealed a high preference of the UDBAC primers for *Ca. Udaeobacter*. Its relative abundance accounted for 99.0 ± 0.4 and $98.9 \pm 0.4\%$ of the amplicon sequences derived from untreated and treated forest soils, respectively, of both geographic regions (Fig. 2). Furthermore, with respect to Schwäbische Alb grassland soils, 96.2 ± 3 (untreated soils) and $95.6 \pm 3.9\%$ (treated soils) of the generated amplicons represented *Ca. Udaeobacter* (Fig. 2). The major fraction of amplicon sequences, derived from Hainich-Dün grassland soils (untreated soil, $79.4 \pm 1\%$; treated soil, $84.8 \pm 0.9\%$), was also assigned to *Ca. Udaeobacter* (Fig. 2), but mainly due to a higher proportion of detected uncultured *Verrucomicrobiaceae*, its relative abundance was lower in Hainich-Dün grassland soils compared to the other considered soils. Based on this analysis, we utilized the UDBAC primers for targeted detection and quantification of *Ca. Udaeobacter* 16S rRNA genes in microcosm samples.

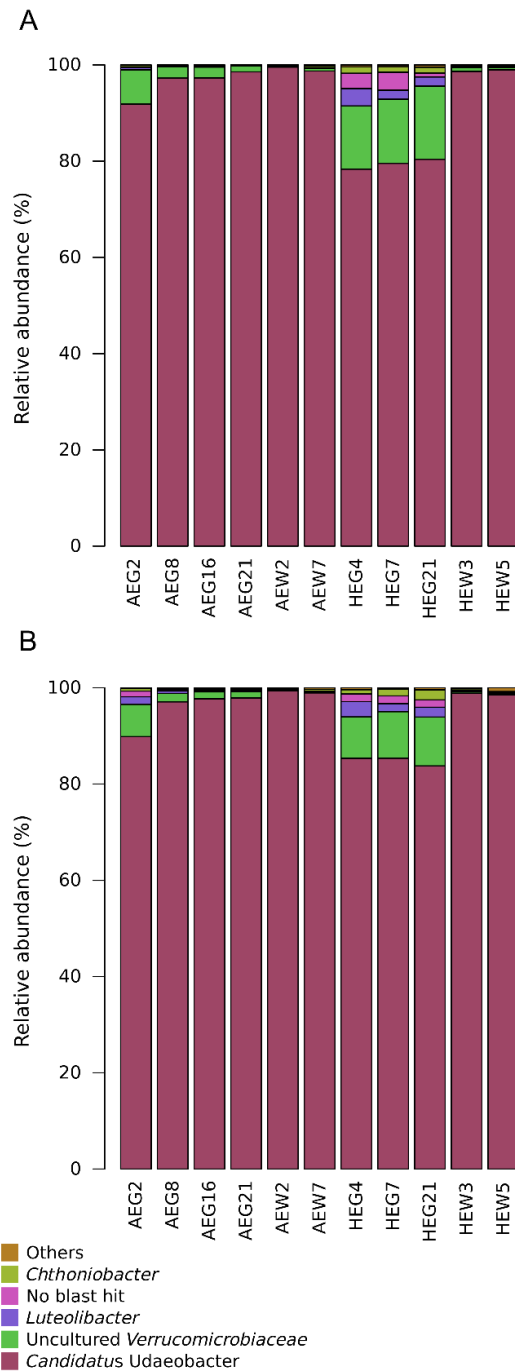


Figure 2. Relative 16S rRNA gene abundance of bacterial groups detected with the UDBAC primer pair designed in this study. Grassland and forest soils used for microcosm preparation were considered (A). In addition, samples incubated for three days upon treatment with six different antibiotics in high concentration (B) were considered. “Others”: bacterial groups showing less than 1% relative abundance.

Ca. Udaeobacter benefits from antibiotics release in soil

The increase of *Ca. Udaeobacter* abundance upon antibiotic treatment, as assessed by amplicon sequencing-based analysis, was verified via qPCR in combination with the UDBAC primers described above. This verification revealed a statistically significant rise (p-value 1.84×10^{-7}) of 16S rRNA gene abundance in soil microcosms incubated for three days upon antibiotic treatment (Fig. 3, Table S3). Since we found during our primer evaluation that mainly *Ca. Udaeobacter* is covered by the UDBAC primers in these microcosms, the rise of 16S rRNA gene abundance is to a high degree evoked by this verrucomicrobial group. Furthermore, similar to the amplicon sequencing-based analysis, the qPCR data also showed that the effect of antibiotic treatment on *Ca. Udaeobacter* abundance decreased in the course of the microcosm experiment.

Within our qPCR-based verification, soils from both geographic regions, treated with six different antibiotics in high concentration, and corresponding controls were analyzed. In this way, we could prove that even after extensive release of multiple classes of antibiotics, *Ca. Udaeobacter* abundance showed no decline in forest as well as grassland soil. Moreover, our target soil bacterial group even takes advantage of antibiotics release since its 16S rRNA gene abundance was significantly higher in treated compared to control microcosms with respect to the amplicon sequencing as well as the qPCR-based data.

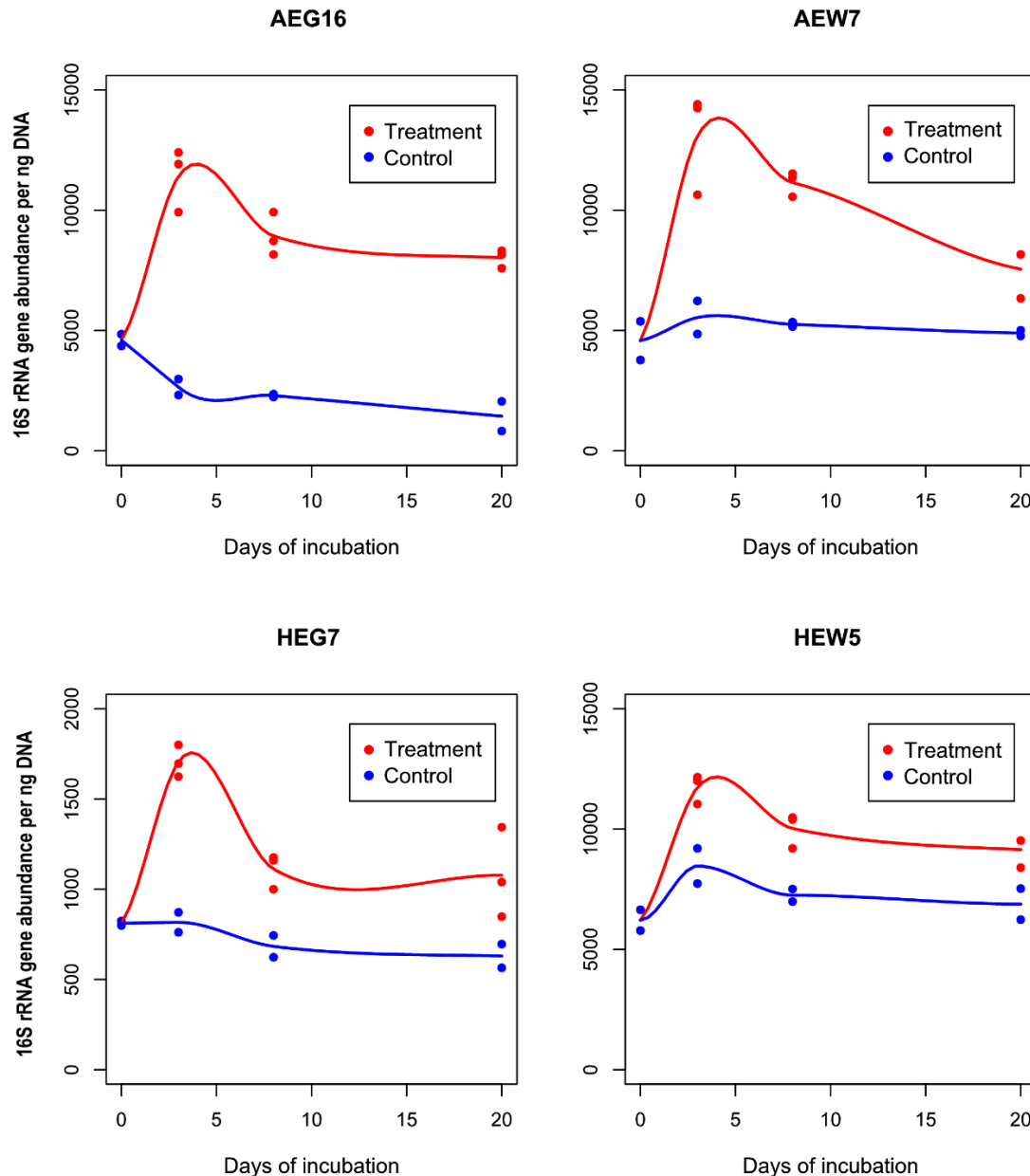


Figure 3. UDBAC primer pair-based determination of 16S rRNA gene abundance via qPCR. The 16S rRNA genes were quantified with respect to a grassland soil from each geographic region (samples AEG16 and HEG7) as well as a forest soil from each geographic region (samples AEW7 and HEW5). Untreated control samples (“Control”) and samples treated with six different antibiotics in high concentration (“Treatment”) were considered.

Ca. Udaeobacter sp. MAG harbors several antibiotic resistance genes

Soil-derived shotgun metagenomic sequencing data, including Oxford Nanopore and Illumina MiSeq reads, was generated to assemble a MAG of a *Ca. Udaeobacter* representative. In this context, we selected a forest soil sample (AEW3), extracted cells from the soil matrix, and subsequently sequenced

DNA isolated from these cells. A forest soil sample was selected, as a *Ca. Udaeobacter* MAG from a grassland soil has already been reported (1). Additionally, several other verrucomicrobial MAGs were recently isolated from grassland soils (5). To extend the knowledge on verrucomicrobial representatives, we focused on genomic features of a *Ca. Udaeobacter* species inhabiting forest soil.

We assembled a 3.22 Mbp MAG comprising 145 scaffolds with an average GC content of 55.2% and an average length of 22.22 kbp (size of the longest scaffold, 92.97 kbp). It exhibited a 31-fold average Illumina MiSeq read coverage and a 64.6-fold average Oxford Nanopore read coverage. 3,341 open reading frames (ORFs), one partially complete 16S rRNA gene (1,139 bp), located on a contig with a 33.7-fold average Illumina MiSeq read coverage, one 5S rRNA gene and 38 tRNA genes are encoded by this MAG. The Illumina MiSeq contig coverage indicates that the 16S rRNA gene occurs once in the genome, which is consistent with previous findings (6) and further validates its correct assignment to the genome bin. The 16S rRNA gene shows 98.83% identity to amplicon sequence variant 6 (ASV 6) (query coverage: 100%), which is the fourth most abundant ASV in all microcosm samples and increases significantly upon antibiotic treatment (p-value of 1.68×10^{-6}). Overall, domain-specific single-copy housekeeping gene analysis predicted 87.3% genome bin completeness with a potential contamination of 3.7%. This estimation of completeness and contamination is categorized as substantially complete with low contamination (7). The affiliation of the here assembled genome bin to *Ca. Udaeobacter* was validated based on phylogenetic analysis of the nucleotide sequence of 16S rRNA genes as well as the occurrence and amino acid sequence of 120 marker genes. Regarding the 16S rRNA gene, our MAG clusters together with the ribosomal clone DA101, affiliated to *Ca. Udaeobacter*, and is clearly phylogenetically distinct from *Chthoniobacter* and *Xiphinematobacter*, which also represent *Chthoniobacterales* (Fig. 4).

Furthermore, the phylogenetic analysis based on the occurrence and amino acid sequence of 120 marker gene sequences of all *Chthoniobacterales* used for phylogenetic analysis (Table S4), assigned our MAG together with *Ca. Udaeobacter copiosus* to the GTDB genus AV55 (Fig. 5). As the 16S rRNA gene of our MAG is a representative of the genus *Ca. Udaeobacter* (Fig. 4) and *Ca. Udaeobacter copiosus* also clusters in the GTDB genus AV55 (Fig. 5), AV55 most likely represents the genus *Ca. Udaeobacter*. The closest relative of our MAG is, based on FastANI analysis, AV55 sp003218915.1 with an average nucleotide identity (ANI) of 90% over 74.6% of the genome. These

values are below the ANI species threshold (8) and therefore the here assembled MAG represents a novel species within *Ca. Udaeobacter*, which we designate *Ca. Udaeobacter* sp. in this manuscript.

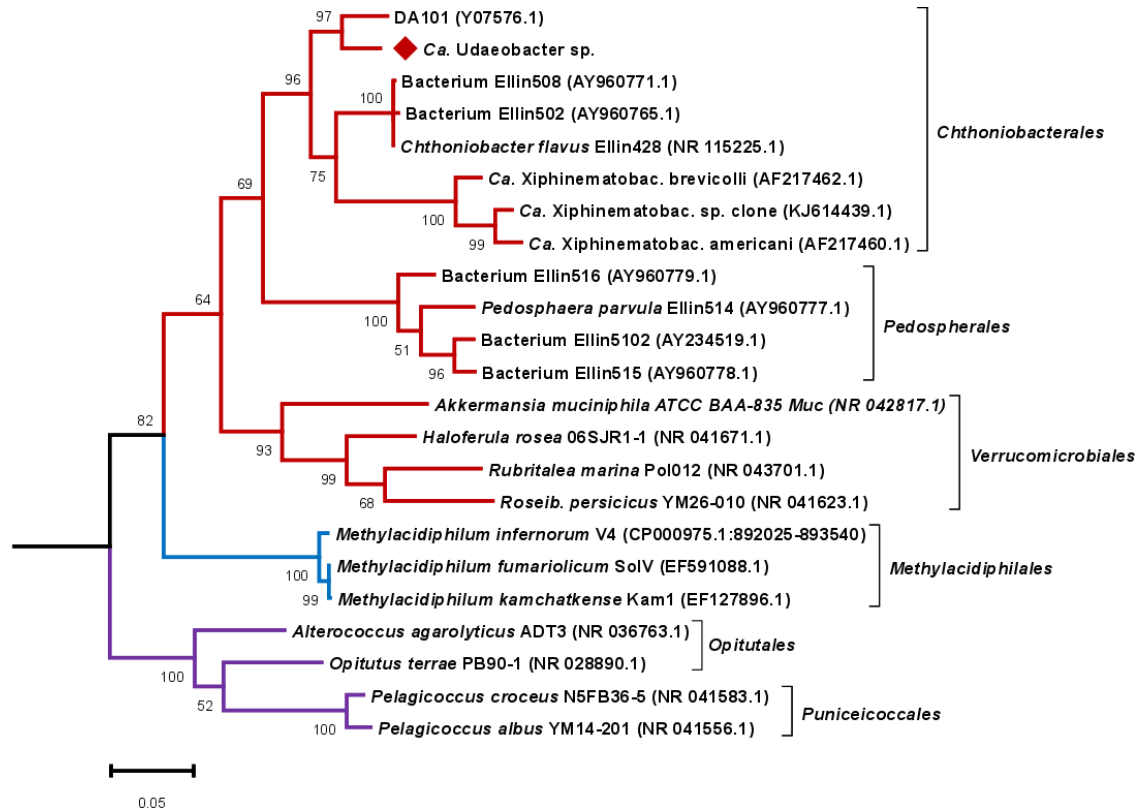


Figure 4. Phylogenetic analysis based on 16S rRNA gene sequences of verrucomicrobial representatives. The 16S rRNA gene sequence of the here assembled *Ca. Udaeobacter* sp. MAG is highlighted with a red diamond and clusters together with the ribosomal clone DA101, affiliated to *Ca. Udaeobacter*. Besides the 16S rRNA gene sequence of the MAG assembled in this study, the 16S rRNA gene sequences of 22 other verrucomicrobial representatives were considered. The tree was rooted on the 16S rRNA gene sequence of *Escherichia coli* K-12 MG 1655 (NC_000913.3:4035531-4037072). Red, blue and purple colored branches indicate the verrucomicrobial classes *Verrucomicrobiae*, *Methylocidiphilae* and *Opitutae*, respectively. Accession numbers are given in parentheses. Bootstrap values based on 500 replicates are shown at the branching points and the bar represents 0.05 changes per nucleotide position. All positions with less than 90% site coverage were eliminated. Abbreviations: *Ca. Xiphinematobac.*, *Candidatus Xiphinematobacter*; *Roseib.*, *Roseibacillus*.

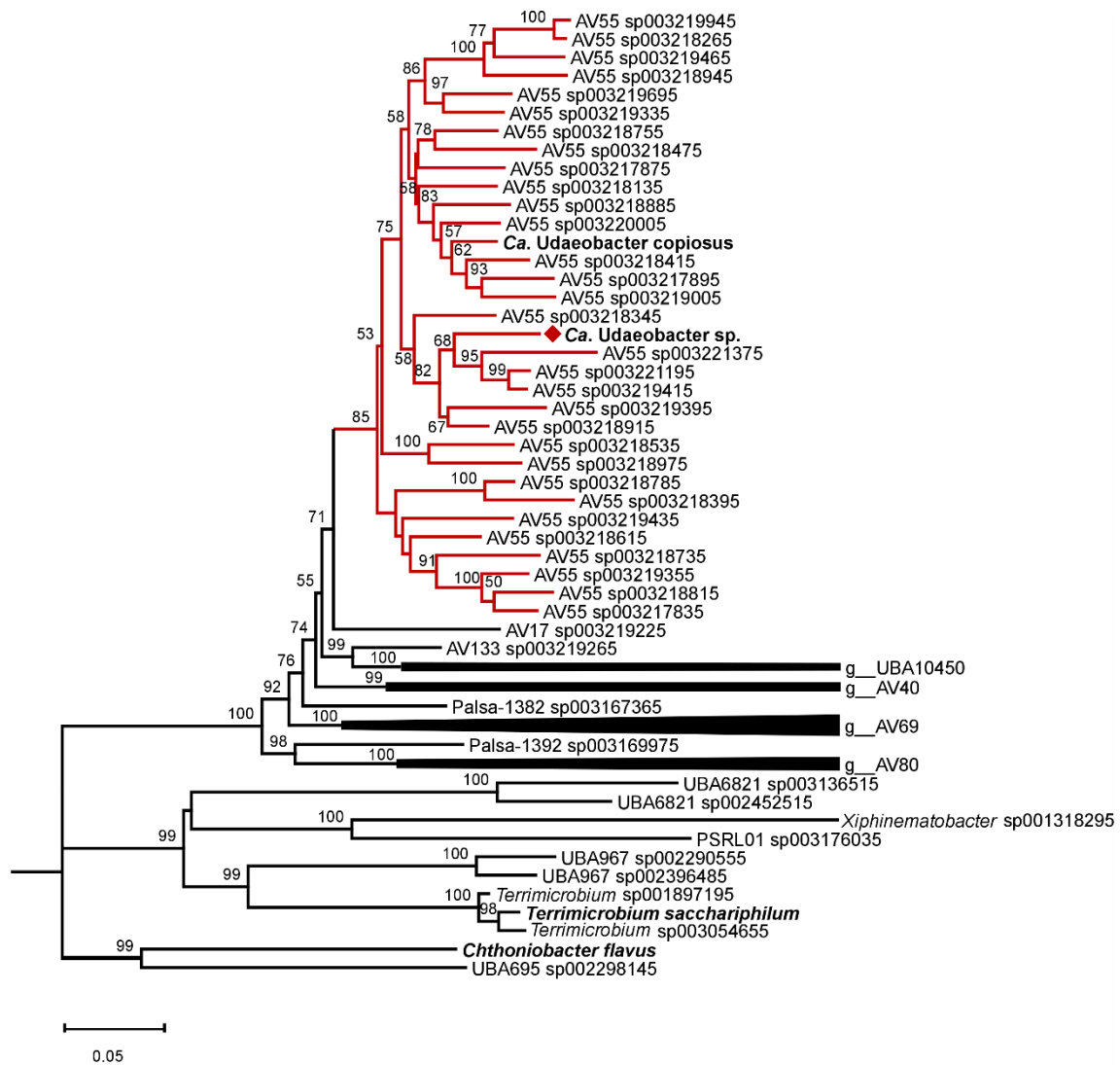


Figure 5. Phylogenetic tree based on the occurrence and amino acid sequence of 120 marker genes from *Chthoniobacterales*. MAGs available at GTDB as well as the *Ca. Udaeobacter copiosus* and the here assembled MAG were considered. The neighbor-joining tree was rooted on *Escherichia coli* UMN026 marker gene sequences. Red colored branches indicate the verrucomicrobial genus AV55 classified by GTDB and the red diamond highlights the here assembled *Ca. Udaeobacter* sp. MAG. Bootstrap values ≥ 50 calculated based on 500 iterations are shown at the branching points and the bar represents 0.05 changes per amino acid position. All positions with less than 90% site coverage were eliminated.

Our MAG enabled insights into the ARG and MGE repertoire of *Ca. Udaeobacter* (Table S5). Based on our analysis, 55 potential ARGs and 14 MGEs were identified. Highly abundant are genes coding for multidrug resistance mechanisms, especially subunits of resistance nodulation division (RND) MdtABC multidrug efflux systems and multidrug ABC transporters. On contig 74, a complete mdtABC efflux

system is encoded including the two RND pump genes *mdtB* and *mdtC* as well as the periplasmic adaptor protein gene *mdtA* (Fig. 6).

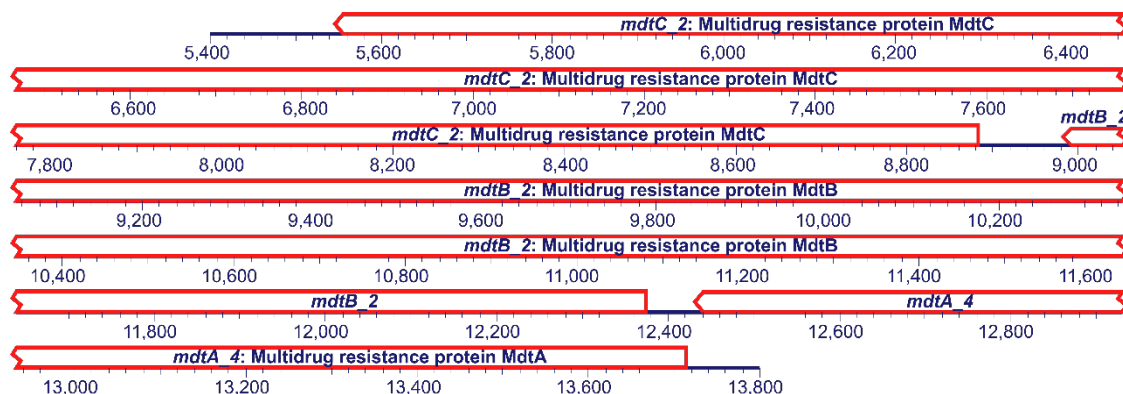


Figure 6. Genes potentially encoding a complete *mdtABC* multidrug efflux pump carried by contig 74 of the here reported *Ca. Udaeobacter* sp. MAG. An excerpt of the contig from 5,400 to 13,800 bp is depicted (total contig length: 16,800 bp).

Furthermore, the draft genome is enriched with genes coding for macrolide efflux pump subunits as two MacA periplasmic adaptor, four MacB-like periplasmic core domain and five inner membrane ATP transporter (MacB) genes are present. On contig 99, a MacB efflux pump subunit including its periplasmic adaptor protein and an outer membrane secretion protein HlyD are encoded. Additionally, the organism seems to be well protected from beta-lactam antibiotics, due to six encoded beta-lactamases. Regarding MGEs, the MAG harbors five XerC and two XerD tyrosine recombinase as well as five insertion sequence family transposase genes. A co-location of ARGs and MGEs was not detected as the space between the only ARG (putative chloramphenicol resistance gene) and MGE (*xerC*, encoding a tyrosine recombinase), located on one contig, is 81.675 kbps.

We also analyzed *Ca. Udaeobacter* sp. for the production of secondary metabolites such as antibiotics and identified a potential phosphonate synthesis cluster. From this cluster, only four percent of the genes show similarity to the known and validated thioplatensimycin biosynthetic gene cluster from *Streptomyces platensis*. Besides this, four gene clusters were identified which are potentially involved in terpene, arylpolyene and ladderane, and phosphonate synthesis. However, this similarity comprised

only 18%, 16%, 8% and 15% of the respective genes in the corresponding clusters and these clusters have not been confirmed to produce a synthesis product.

Ca. Udaeobacter sp. MAG reveals potential H₂-based energy generation

Regarding the central metabolism encoded by the *Ca. Udaeobacter* sp. MAG, only one glycolysis gene is missing (the phosphoglycerate kinase gene), the pentose phosphate pathway is completely encoded and the TCA cycle includes the glyoxylate bypass enzymes. The here identified species can probably oxidize hydrogen aerobically with a small and large subunit of a Ni-Fe-S hydrogenase and an additional soluble hydrogenase, which has so far not been reported with respect to *Ca. Udaeobacter*. Regarding vitamin biosynthesis, vitamin B₁₂ (cobalamin) is most likely imported from outside of the cell indicated by five encoded vitamin B₁₂ import ATP-binding proteins (BtuD) and two B₁₂ transporter proteins (BtuB) and further converted into its active form via the completely encoded adenosylcobalamin salvage pathway. The pathway for vitamin B₉ (tetrahydrofolate) biosynthesis is only partially encoded as the tetrahydrofolate reductase is missing. However, *Ca. Udaeobacter* is probably capable to salvage it from 5,10-methenyltetrahydrofolate as the respective pathway is completely encoded. Furthermore, a salvage pathway to generate thiamine (vitamin B₁) from its degradation product and a partially complete pathway to synthesize vitamin B₆ (four genes required for 3-amino-1-hydroxyacetone-1-phosphate synthesis from D-erythrose-4-phosphate are missing) are present in the assembled MAG.

A copper/zinc superoxide dismutase and a catalase-peroxidase gene potentially allow protection from reactive oxygen species. Furthermore, *Ca. Udaeobacter* sp. encodes for arginine dependent acid resistance and the biosynthesis of cadaverine from L-lysine, which protect against acidic conditions. Regarding proteinogenic amino acid biosynthesis, *Ca. Udaeobacter* sp. encodes complete synthesis pathways for glycine, alanine, aspartate, glutamate, glutamine, methionine and threonine. The synthesis pathways for asparagine (1/4 enzymes missing), leucine (1/3 enzymes missing), cysteine (1/2 enzymes missing), isoleucine (3/5 enzymes missing), arginine (3/8 enzymes missing), phenylalanine (2/3 enzymes missing), tryptophan (1/12 enzymes missing), proline (2/3 enzymes missing), serine (2/3 enzymes missing) and valine (3/4 enzymes missing) are incomplete. The amino acid synthesis pathways for histidine, lysine and tyrosine could not be identified. However, genes for

two putative amino acid permeases (YdhG), which are predicted to be importers for H⁺ and an undefined amino acid, as well as for three serine/threonine exchangers (SteT) which pump out threonine into the periplasm in exchange for serine, were detected.

Discussion

The here reported experiments clearly demonstrate that *Ca. Udaeobacter* representatives show multi-resistance and even benefit from the release of antibiotics in soil. This pattern was consistently detected although we considered samples from distinct ecosystems (beech forest, spruce forest, meadows, and pastures) of two different geographic regions. Besides the MAG reported in this study (estimated size, ~3.67 Mbp; derived from a forest soil), another relatively small MAG (estimated size, ~2.81 Mbp; derived from a prairie soil) of a *Ca. Udaeobacter* representative (*Ca. Udaeobacter copiosus*), which indicates multiple amino acid and vitamin auxotrophies, has been described (1, 9). Ubiquitous soil bacteria are generally known to have larger genomes in order to cope with the highly variable and rapidly changing environmental conditions in their terrestrial habitat (1, 10–12). According to Brewer et al. (1), *Ca. Udaeobacter copiosus* might undergo streamlining processes to reduce the metabolic expense for synthesizing costly amino acids and vitamins, which are potentially acquired from the soil environment. The here assembled MAG of *Ca. Udaeobacter* sp. is missing enzymes of 13 amino acid synthesis pathways. On the other hand, 7 amino acid synthesis pathways are completely encoded. Nevertheless, it remains questionable, whether the missing enzymes of the respective biosynthetic pathways infer an amino acid auxotrophy, as Price et al. (13) have shown, that many missing enzymes from amino acid synthesis pathways can be filled and are predicted due to knowledge gaps in this field. However, the detected amino acid permeases and serine/threonine exchangers imply a dependency on extracellular amino acids or at least advantages of amino acid uptake for the growth of the *Ca. Udaeobacter* representative described in this study. Regarding vitamin biosynthesis, *Ca. Udaeobacter* sp. encodes salvage pathways for vitamin B₁, B₁₂ and B₉, as well as transporter proteins for the import of vitamin B₁₂. These indications, together with our experimental findings, showing that the abundance of *Ca. Udaeobacter* strongly increased in microcosms treated with antibiotics, points to an efficient utilization of nutrients from soil (e.g. vitamins and amino acids) upon release of antimicrobial

substances. In this context, a scavenging lifestyle of antibiotic resistant cheater cells, proposed by Leisner, et al. (3), for environmental bacteria residing in nutrient-deprived habitats, appears quite likely with respect to members of *Ca. Udaeobacter*. This would explain the strong increase of *Ca. Udaeobacter* abundance in coniferous and deciduous forest as well as grassland soil microcosms, treated with antibiotics. Notably, the treatment of soil with one and three antibiotics in high concentration evoked a similar increase in *Ca. Udaeobacter* abundance after three days of incubation (Fig. 1 and Fig. S1). This might be due to the fact that in both cases only one bactericidal antibiotic (amoxicillin) was applied, which in contrast to bacteriostatic antibiotics kills bacteria. When a second bactericidal antibiotic was added (ciprofloxacin), a stronger increase in *Ca. Udaeobacter* abundance could be identified after an incubation period of three days. This observation supports our theory that *Ca. Udaeobacter* acquires nutrients released from cells, which are killed and consequently lysed by antimicrobial compounds. With respect to treatment of soil with antibiotics in low concentration, a similar pattern was observed after a period of eight days. Moreover, it can be assumed that the treatment effect, inducing elevated *Ca. Udaeobacter* abundance, declined after prolonged incubation, as added antibiotics are degraded and therefore antimicrobial-driven cell lysis decreased over time.

For protection against the variety of antimicrobials, released by antibiotic producers, and to maintain efficient scavenging in soil, multi-resistance can be considered as elementary feature of cheater cells, taking advantage of lysed cells. Accordingly, the *Ca. Udaeobacter* sp. MAG reported in this study encodes many multi-drug efflux pumps (mostly MdtABC efflux system and ABC transporter subunits), macrolide efflux pumps (MacB ABC transporter subunits), and beta-lactam as well as other resistance genes (Table S5). This finding is supported by Forsberg et al. (4), who reported an enrichment of beta-lactam resistance genes within *Verrucomicrobia*. With respect to *Ca. Udaeobacter*, its ARG repertoire in combination with efficient uptake of nutrients, released by antimicrobial-driven cell lysis, potentially enables the proposed scavenging lifestyle and confers advantages over other soil bacteria upon antibiotics release.

As we could only identify few putative genes associated with secondary metabolite biosynthesis encoded in the *Ca. Udaeobacter* sp. MAG, it seems unlikely that *Ca. Udaeobacter* representatives produce different antibiotics, which require large polyketide and nonribosomal peptide biosynthetic gene clusters. This theory is supported by potential genome streamlining and the so far described relatively

small *Ca. Udaeobacter* genomes. It seems much more plausible that *Ca. Udaeobacter* obtains nutrients from cell lysis evoked by antibiotic producers without high energetic cost associated with the synthesis of antimicrobial compounds.

Regarding the central metabolism, the encoded glyoxylate bypass might be advantageous with respect to bactericidal antibiotics as it provides a means against oxidative stress. Bactericidal drugs cause a higher production of NADH through the TCA cycle which results in a higher proportion of superoxide, formed as a consequence of respiratory chain oxidation driven by oxygen and the conversion of NADH to NAD⁺ (14, 15). Superoxides on the other hand cause iron leaching from iron-sulfur clusters and iron participates in the conversion of superoxide to hydroxyl radicals in the Fenton reaction (14). Hydroxyl radicals are extremely toxic and damage cellular proteins, lipids and DNA which leads to cell death and lysis (14). Bypassing the complete TCA cycle by the glyoxylate shunt reduces NADH production and causes a reduced sensitivity towards bactericidal antibiotics (16). *Ca. Udaeobacter* encodes for two enzymes (A copper/zinc superoxide dismutase and a catalase-peroxidase) that convert superoxide to oxygen, which might also have a positive effect on the sensitivity towards bactericidal antibiotics. Another potential feature of *Ca. Udaeobacter* sp. is the aerobic oxidation of hydrogen indicated by genes for an Ni-Fe-S hydrogenase enzyme complex and an additional soluble hydrogenase. Thus, *Ca. Udaeobacter* sp. probably has the ability to scavenge atmospheric H₂ for energy production. This feature has been observed for *Acidobacteria* as well and was proposed as “*general mechanism for dominant soil phyla to generate the maintenance energy required for long-term survival*” (17). As approximately 30% of the world's soils are acidic (18), the acid resistance mechanisms (biosynthetic arginine decarboxylase and putative lysine decarboxylase) that were detected in the here assembled MAG might contribute to the global dissemination of *Ca. Udaeobacter*. These mechanisms could increase the tolerance against acidic conditions, for example in some forest soils, and provide an advantage over other soil bacteria.

Our study illustrates that a group of ubiquitous soil bacteria, *Ca. Udaeobacter*, thrives upon release of multiple classes of antibiotics. These bacteria evade growth-inhibiting and lethal effects of antimicrobials, supporting our hypotheses, and, importantly, even take advantage of antibiotic pressure. Thus, steadily increasing global antibiotic consumption and an associated rising environmental pollution with antimicrobials might be advantageous for *Ca. Udaeobacter* representatives. Furthermore, we

found that a representative of *Ca. Udaeobacter* encodes enzymes for hydrogen oxidation, supporting the hypothesis that trace gas scavenging might be a general mechanism of ubiquitous soil bacteria, to generate energy for a stable maintenance in soil. To more specifically target this verrucomicrobial group in future studies, the 16S rRNA gene-based primer pair described here will be valuable. For example, insights into the *Ca. Udaeobacter* phylotype composition in various soil ecosystems can be gained via sequencing of amplicons generated using the UDBAC primers. Another important step with respect to the analysis of *Ca. Udaeobacter* will be the cultivation of representatives belonging to this dominant group of soil bacteria. For instance, cultivates could be used to analyze potential hydrogenase activity of *Ca. Udaeobacter*. Moreover, the findings presented in our study indicate that application of antibiotics can contribute to a successful enrichment of *Ca. Udaeobacter* representatives.

Materials and Methods

Sampling and soil characteristics

Soil samples (the upper 10 cm of the mineral soil) were derived from plots of the German Biodiversity Exploratories Hainich-Dün (central Germany) and Schwäbische Alb (southwestern Germany) (19) in May 2017, as described by Solly et al. (20). Each study region covers the land use types forest and grassland. Grassland plots are 50 m × 50 m and forest plots are 100 m × 100 m in size. Detailed information on land use, dominant tree species and fertilization for every plot is provided in Table S1. The gravimetric water content of the soil was determined by drying 10 g at 105°C for 24 h. The pH of each soil was determined as described by Solly et al. (20). For soil incubations, water contents of fresh soil samples were adjusted with deionized water to 60% water holding capacity (WHC) as the optimum water content for carbon mineralization usually falls in this range (21). The total WHC (equal to 100% WHC) was determined in the laboratory by means of disturbed soil samples. Fifteen g of fresh soil was filled in 10 cm high funnels which were placed in deionized water overnight until the soil was saturated with water by capillary rise. After the soil samples have been drained on sand for several hours, the soil was oven-dried at 105°C to a constant weight and the soil water content at total WHC was determined. Taking into account the water contents of fresh soil samples, the amount of water that had to be added to the incubated samples to reach 60% WHC was then calculated.

All soils for the microcosm experiment were chromatographically analyzed for residues of 77 different antibiotics by JenaBios company (Jena, Germany) (Table S2).

Microcosm incubations

The water content of soil derived from the selected plots was adjusted to 60% of its water holding capacity and subsamples were frozen at -80°C in order to enable analysis of soil bacterial communities at the beginning of the microcosm experiment. Subsequently, the soil was treated with six antibiotics, three antibiotics or one antibiotic in high and low concentration. This procedure was performed in triplicate. The concentrations of the used antibiotics were selected based on previous microcosm experiments (22–26). Concentrations of 10 and 100 mg/kg soil of amoxicillin (Sigma-Aldrich, Steinheim, Germany), oxytetracycline dihydrate (Sigma-Aldrich), sulfadiazine (Sigma-Aldrich), trimethoprim (Sigma-Aldrich) and tylosin tartrate (Sigma-Aldrich), as well as concentrations of 5 and 50 mg/kg soil of ciprofloxacin (Sigma-Aldrich) were used for treatment with six different antibiotics. For the treatment with three antibiotics (amoxicillin, oxytetracycline dihydrate and sulfadiazine) or one antibiotic (amoxicillin), we also used concentrations of 10 and 100 mg/kg soil. Due to insufficient solubility in water, all antibiotics, except tylosin, were spiked onto soil in solid form. Tylosin was dissolved in sterile H₂O prior to soil treatment. Organic solvents were avoided as they can potentially impact soil microbial communities (23). The antibiotics were distributed in soil by vigorous mixing. Subsequently, microcosms containing 10 g of soil were prepared in 100 ml bulk flasks and incubated in the dark at 20°C. Flasks containing 10 g of soil, which was not treated with antibiotics, served as control (set up in duplicate). The microcosms were aerated every third day to ensure oxygen supply and the water content was ascertained to be stable via regular weighing. After 3, 8 and 20 days, samples were taken (1.25 g) and stored at -80°C for subsequent analysis.

DNA extraction and sequencing of 16S rRNA gene amplicons

Soil microbial community DNA was isolated from a total of 628 microcosm samples by using the DNeasy PowerSoil Kit (Qiagen, Hilden, Germany) according to the manufacturer's instructions. Subsequently, the DNA concentration was measured by employing the *Qubit dsDNA Broad-Range* Assay Kit (Thermo

Fisher Scientific, Braunschweig, Germany) and a Qubit 3.0 Fluorometer (Thermo Fisher Scientific) following the manufacturer's instructions.

The V3-V4 region of the 16S rRNA genes was amplified by PCR, using the extracted DNA from the 628 microcosm samples and the primer pair Bact-0341-b-S-17 and S-D-Bact-0785-a-A-21 (27) with modifications for Illumina MiSeq sequencing described by Schneider et al. (28). Each PCR reaction (50 µl) contained 10 µl 5 x Phusion GC buffer (Thermo Fisher Scientific), 25 ng template DNA, 0.2 µM of each primer, 0.2 mM of each deoxynucleoside triphosphate, 0.15 mM MgCl₂ and 1 U Phusion High-Fidelity DNA Polymerase (Thermo Fisher Scientific). PCR reactions were initiated at 98°C for 1 min, followed by 25 cycles of 98°C for 45 s, 66°C for 45 s and 72°C for 30 s. The reaction ended with a final elongation step at 72°C for 5 min.

Amplicons were purified with a magnetic bead purification by the automated work station Janus (PerkinElmer, Downers Grove, IL, USA) with a bead (MagSi-NGS^{PREP} Plus – Magnetic Beads, Steinbrenner, Wiesenach, Germany) to sample ratio of 1:1. Subsequently, indexes were added at both ends of the amplicons as described by Schneider et al. (28). Sequencing of the V3-V4 region of the 16S rRNA genes was carried out using an Illumina MiSeq sequencer in paired-end mode and the MiSeq Reagent Kit v3 (600 cycles).

Amplicon sequence data processing and statistical analysis

The raw sequences were demultiplexed and sequencing adapters clipped by employing the data analysis software CASAVA (Illumina, San Diego, CA, USA). PEAR v.0.9.10 (29) was used for merging of paired-end reads, and sequences with a lower quality score than 20 or with unresolved bases were removed by applying the *split_library_fastq.py* script provided by QIIME 1.9.1 (30). Remaining forward and reverse primer sequences were removed using cutadapt 1.10 (31) with default settings. Reads ≥ 380 bp were clustered into amplicon sequence variants (ASVs) (32) with the UNOISE2 algorithm (33) of USEARCH (34), which includes sequence error correction and de-novo chimera removal. Additional chimera removal was conducted via UCHIME (35) using the SILVA SSU database (36) (release 132) as reference. Subsequently, all quality-filtered sequences were mapped on the ASVs to determine the respective read abundance. For taxonomic classification, the ASVs were blasted against the SILVA SSU database (release 132) using the QIIME script *parallel_assign_taxonomy_blast.py*. Extrinsic

domain ASVs, mitochondria, chloroplasts and unclassified ASVs were removed by employing the QIIME script *filter_otu_table.py*. Datasets rarefied via QIIME script *single_rarefaction.py* to 10,000 sequences per sample were utilized for linear mixed effect regression analysis.

The effect of antibiotic treatment on *Ca. Udaeobacter* was statistically analyzed using linear mixed effect models, constructed with the R version 3.5.3 (37) and the R library lme4 (38). In this context, the logarithm of the abundance of *Ca. Udaeobacter* served as response variable, the concentration of antibiotics for treatment and the days of incubation as fixed effects, and the microcosm ID as well as the sample plot ID represented nested random effects. Furthermore, six additional models were constructed to test for significance of each treatment variation (treatment with one antibiotic, three antibiotics and six antibiotics in high and low concentration), whereat each of the six treatments served as independent fixed effect along with the days of incubation and the nested random effects. The residuals were tested for normality and constant variance with quantile-quantile plots and residual plots using the diagnostics plots function in R. Independent variables were selected by considering collinearity, significance and explanatory power based on p-values, R^2_m and R^2_c , calculated with the lmerTest library (39) and the r.squaredGLMM function of the MuMIn library (40). The p-values of the fixed and random effects were calculated with the Satterthwaite's method and the Chi square test of the anova function, respectively. All model formulas, sample sizes, corresponding p-values, estimates, degrees of freedom and R^2 of the conducted linear regressions are listed in Table S3.

Design and evaluation of *Ca. Udaeobacter*-specific primers

Primers for targeted detection of bacteria belonging to *Ca. Udaeobacter* were designed based on the 16S rRNA gene of the verrucomicrobial phylotype DA101 (41) using primer blast (42). An *in silico* PCR analysis was conducted using TestPrime 1.0 and the SILVA SSU database (27,36) (release 132) as reference to evaluate the specificity of designed primers. The primer pair comprising UDBAC_F (5'-CCAGAAGAGGAAGAGACGGC-3') and UDBAC_R (5'-GTCCTCAAGCACGGCAGTAT-3') was used for further validation of specificity via multiplex sequencing. In this context, MiSeq overhangs described by Schneider et al. (28) were attached to each primer and amplicons for MiSeq sequencing were produced via PCR.

Each PCR reaction (50 µl) was set up in triplicate and contained 10 µl 5 x Phusion HF buffer (Thermo Fisher Scientific), 25 ng template DNA, 0.2 µM of each primer, 0.2 mM of each deoxynucleoside triphosphate, 1 mM MgCl₂ and 1 U Phusion High-Fidelity DNA Polymerase (Thermo Fisher Scientific). DNA extracted from all soils used for microcosm preparation and samples incubated for three days upon treatment with six antibiotics in high concentration served as templates within the PCR. The cycling program started with an initial denaturation at 98°C for 1 min followed by 25 cycles of denaturation for 10 s at 98°C, annealing at 58°C for 30 s and elongation at 72°C for 10 s. The final elongation step was carried out at 72°C for 5 min. Generated amplicons were purified and indexed as described above. Sequencing was carried out using an Illumina MiSeq sequencer in paired-end mode and the MiSeq Reagent Kit v3 (600 cycles).

Bioinformatic processing of the raw data was performed as described above, except that reads shorter than 113 bp and longer than 153 bp were discarded with cutadapt 1.10.

Quantification of *Ca. Udaeobacter* 16S rRNA genes

Quantitative real-time PCR (qPCR) using primer pair UDBAC was conducted to estimate the absolute abundance of *Ca. Udaeobacter* 16S rRNA genes in microcosms. In a first step, a DNA fragment obtained via PCR using the UDBAC primer set was cloned into vector pCR4-TOPO (Thermo Fisher Scientific) as recommended by the manufacturer, to serve as standard for qPCR. To confirm that a partial *Ca. Udaeobacter* 16S rRNA gene has been cloned into this vector, the insert sequence was determined by Microsynth SeqLab (Göttingen, Germany) using Sanger sequencing technology. The 16S rRNA genes of *Ca. Udaeobacter* representatives were quantified using an icycler iQ5 (Bio-Rad, Hercules, CA, USA), with the QuantiNova SYBR Green PCR kit (Qiagen). Each reaction had a final volume of 20 µl with 10 µl of 2 x QuantiNova SYBR Green RT-PCR Master Mix, 0.7 µM of each primer and 12.5 ng DNA template. DNA from untreated control samples and samples treated with six different antibiotics in high concentration served as template. The amplification was conducted as recommended by the manufacturer with an initial activation step at 95°C for 2min, followed by 40 cycles of denaturation at 95°C for 5 s and combined annealing and extension at 60°C for 10 s. Subsequently, melting curve analysis was conducted to ensure specific amplification.

Scatterplots depicting the 16S rRNA gene abundance of *Ca. Udaeobacter* per ng DNA in response to antibiotic treatment and sampling days were produced by employing R. In this context, a smoothed curve was generated using the `loess.smooth` function. The effect of the antibiotic treatment on the absolute 16S rRNA gene abundance after three days of incubation was statistically analyzed with a linear mixed effect model, as described above, whereat the logarithm of the 16S rRNA gene copies per ng DNA served as response variable, the antibiotic treatment as fixed effect and the sample plot ID as random effect.

Cell extraction, sequencing and hybrid assembly of a *Ca. Udaeobacter* MAG

A frozen (-20°C) forest soil sample (AEW3) was chosen as target for *Ca. Udaeobacter* genome bin assembly. Cells were extracted from the soil matrix prior to DNA extraction and sequencing. For this purpose, 100 g frozen soil was added to 200 ml MES buffer (pH 5.5), supplemented with 0.24 M NH_4Cl and 100 mg/kg amoxicillin. Subsequently, the suspension was vigorously mixed with a hand mixer for eight minutes. After an incubation of 20 h at 160 rpm and 20°C , mixing was repeated and soil particles were separated from the dissociated cells by centrifugation at $1,000 \times g$ for 10 min at 4°C . Afterwards, the cells in the supernatant were pelleted at $10,000 \times g$ for 30 min at 4°C and resuspended in 10 ml MES buffer. The cell suspension was pipetted onto 10 ml OptiPrepTM Density Gradient Medium (Sigma-Aldrich) (1.32 g/ml iodixanol) for a density gradient centrifugation at $3,000 \times g$ for 90 min at 4°C . In this way, the living cells were separated from dead cell particles and other (in-)organic contaminants. A thin layer above the OptiPrep layer, containing the living cells, was carefully transferred into a new vial and washed twice with 8 ml MES buffer at $10,000 \times g$ for 30 min at 4°C . Finally, the cell suspension was pelleted at $10,000 \times g$ for 1 h at 4°C , resuspended in 500 μl MES buffer and stored at 4°C . High molecular weight DNA was isolated with the MasterPure Complete DNA & RNA Purification Kit (Biozym, Hessisch Oldendorf, Germany) following the instructions in the manual. Quality of isolated DNA was initially checked by agarose gel electrophoresis and validated by using an Agilent Bioanalyzer 2100 and an Agilent DNA 12000 Kit as recommended by the manufacturer (Agilent Technologies, Waldbronn, Germany). Purity of the isolated DNA was checked with a Nanodrop ND-1000 (PeqLab Erlangen, Germany) and subsequently the concentration was determined using the Qubit[®] dsDNA HS Assay Kit (Life Technologies GmbH, Darmstadt, Germany) and a Qubit 3.0 Fluorometer (Thermo Fisher

Scientific). Illumina shotgun libraries were prepared using the Nextera DNA Sample Preparation Kit and subsequently sequenced on a MiSeq system with the reagent kit v3 with 600 cycles (Illumina, San Diego, CA, USA). With respect to Oxford Nanopore sequencing, 1.5 µg DNA was used for library preparation using the Ligation Sequencing Kit 1D (SQK-LSK109). Sequencing was performed for 72 h on a MinION device Mk1B using a SpotON Flow Cell R9.4.1, resulting in 16.5 million reads. Low-quality MiSeq reads and sequencing adapters were trimmed by employing trimmomatic version 0.36 in paired-end mode (43). After sequencing and trimmomatic-based quality filtering, 40.8 million MiSeq reads with an average length and paired-end insert size of 222 and 330.5 bp, respectively, were available for further processing.

Assembly was conducted by HybridSPades (44) in meta mode with automatically assessed kmer lengths. The resulting contigs were binned into MAGs with MaxBin2 (45) and checked for completeness and contamination with CheckM v1.0.12 (7). The received MAG was reassembled with HybridSPades using automatically assessed kmer lengths and the assembly was reevaluated with CheckM and QualiMap v.2.2.1 (46, 47).

Open Reading Frames (ORFs) were predicted and annotated using PROKKA version 1.13.4 (48). The relative abundance of an ASV, closely related to the PROKKA annotated 16S rRNA gene in the assembled MAG, was tested for significant rise in relative abundance upon antibiotic treatment over the time course of the microcosm experiment with a linear mixed model, where the ASV abundance served as response variable, the concentration of antibiotics for treatment and the days of incubation as fixed effects, and the microcosm ID as well as the sample plot ID represented nested random effects (Table S3). Subsequently, the MAG was analyzed in terms of energy metabolism, amino acid auxotrophies and environmental stress response via the PathoLogic (49) component of the Pathway Tools software (50) version 23.5 and the MetaCyc database (51). The encoded proteins were screened for annotated ARGs and MGEs. In addition, putatively novel resistance mechanisms were identified with deepARG (52) using a minimal sequence identity of 30% and a probability of over 90% as thresholds. Additional MGEs were identified via DIAMOND blastx (-e 0.00001 --id 50 --subject-cover 50) against the MGE database of nanoARG (53). Furthermore, the MAG was screened for secondary metabolite biosynthesis clusters via antiSMASH 5.1 (54).

Phylogenetic analysis

A phylogenetic tree was constructed using MEGA X (55) based on 16S rRNA gene sequences of the here assembled MAG and other verrucomicrobial representatives. A total of 23 nucleotide sequences were aligned with MUSCLE (56) and the tree was calculated with 500 iterations by using the Maximum Likelihood method and the Tamura-Nei model (57). Furthermore, the partial deletion option with a site coverage cutoff of 90% was used and the tree was rooted with the 16S rRNA gene sequence of *Escherichia coli* K-12 MG1655.

The phylogenetic relation of the here assembled MAG to other draft genomes stored in the GTDB database (58) as well as *Ca. Udaeobacter copiosus* was calculated based on the occurrence and amino acid sequence of 120 marker genes. The marker gene sequences identified by GTDB-tk (59) of all *Chthoniobacterales* included in the analysis (Table S4), were aligned with MUSCLE and used for calculation of a phylogenetic tree with 500 iterations by using the Neighbor-Joining Method (60). Evolutionary distances were computed using the JTT matrix-based method (61) and the partial deletion option with a site coverage cutoff of 90% was applied. Finally, the tree was rooted based on the 16S rRNA gene sequence of *E. coli* UMN026 (GCA_000026325.2).

Additionally, the closest relative of our MAG was identified via FastANI based on whole-genome average nucleotide identity (62).

Data availability

The 16S rRNA gene-based amplicon sequencing data generated in this study were deposited in the Sequence Read Archive (SRA) of the NCBI under the accession number SRP226057 (bioproject accession: PRJNA576637). The *Ca. Udaeobacter* sp. genome bin is publicly available at the NCBI under bioproject accession number PRJNA605948 (SUB6956007). Raw sequences from which the *Ca. Udaeobacter* sp. genome bin was assembled are available at the SRA under accession number SRP249494 (bioproject accession: PRJNA605948).

References

1. Brewer T, Handley K, Carini P, Gibert J, Fierer N. 2016. Genome reduction in an abundant and ubiquitous soil bacterium '*Candidatus* Udaeobacter copiosus'. *Nat Microbiol* 2: 16198.
2. Bergmann GT, Bates ST, Eilers KG, Lauber CL, Caporaso JG, Walters WA, Knight R, Fierer N. 2011. The under-recognized dominance of *Verrucomicrobia* in soil bacterial communities. *Soil Biol Biochem* 43:1450–1455.
3. Leisner JJ, Jørgensen NOG, Middelboe M. 2016. Predation and selection for antibiotic resistance in natural environments. *Evol Appl* 9:427–434.
4. Forsberg KJ, Patel S, Gibson MK, Lauber CL, Knight R, Fierer N, Dantas G. 2014. Bacterial phylogeny structures soil resistomes across habitats. *Nature* 509:612–616.
5. Crits-Christoph A, Diamond S, Butterfield CN, Thomas BC, Banfield JF. 2018. Novel soil bacteria possess diverse genes for secondary metabolite biosynthesis. *Nature* 558:440–444.
6. Větrovský T, Baldrian P. 2013. The Variability of the 16S rRNA Gene in Bacterial Genomes and Its Consequences for Bacterial Community Analyses. *PLoS One* 8:e57923.
7. Parks DH, Imelfort M, Skennerton CT, Hugenholtz P, Tyson GW. 2015. CheckM: assessing the quality of microbial genomes recovered from isolates, single cells, and metagenomes. *Genome Res* 25:1043–55.
8. Konstantinidis KT, Tiedje JM. 2005. Genomic insights that advance the species definition for prokaryotes. *Proc Natl Acad Sci U S A* 102:2567–2572.
9. Delgado-Baquerizo M, Oliverio AM, Brewer TE, Benavent-González A, Eldridge DJ, Bardgett RD, Maestre FT, Singh BK, Fierer N. 2018. A global atlas of the dominant bacteria found in soil. *Science* 359:320–325.
10. Fierer N. 2017. Embracing the unknown: disentangling the complexities of the soil microbiome. *Nat Rev Microbiol* 15:579–590.
11. Cobo-Simón M, Tamames J. 2017. Relating genomic characteristics to environmental preferences and ubiquity in different microbial taxa. *BMC Genomics* 18:499.
12. Land M, Hauser L, Jun S-R, Nookaew I, Leuze MR, Ahn T-H, Karpinets T, Lund O, Kora G, Wassenaar T, Poudel S, Ussery DW. 2015. Insights from 20 years of bacterial genome sequencing. *Funct Integr Genomics* 15:141–61.

13. Price MN, Zane GM, Kuehl J V., Melnyk RA, Wall JD, Deutschbauer AM, Arkin AP. 2018. Filling gaps in bacterial amino acid biosynthesis pathways with high-throughput genetics. *PLOS Genet* 14:e1007147.
14. Kohanski MA, Dwyer DJ, Hayete B, Lawrence CA, Collins JJ. 2007. A Common Mechanism of Cellular Death Induced by Bactericidal Antibiotics. *Cell* 130:797–810.
15. Vinogradov AD, Grivennikova VG. 2016. Oxidation of NADH and ROS production by respiratory complex i. *Biochim Biophys Acta* 1857:863-871.
16. Ahn S, Jung J, Jang IA, Madsen EL, Park W. 2016. Role of glyoxylate shunt in oxidative stress response. *J Biol Chem* 291:11928–11938.
17. Greening C, Carere CR, Rushton-Green R, Harold LK, Hards K, Taylor MC, Morales SE, Stott MB, Cook GM. 2015. Persistence of the dominant soil phylum *Acidobacteria* by trace gas scavenging. *Proc Natl Acad Sci U S A* 112:10497–10502.
18. Uexküll HR, Mutert E. 1995. Global extent, development and economic impact of acid soils, p 5-19. In Date RA, Grundon NJ, Raymet GE, Probert ME (ed), *Plant-Soil Interactions at low pH: Principles and Management*. Kluwer Acad. Publ, Dordrecht, Netherlands.
19. Fischer M, Bossdorf O, Gockel S, Hänsel F, Hemp A, Hessenmöller D, Korte G, Nieschulze J, Pfeiffer S, Prati D, Renner S, Schöning I, Schumacher U, Wells K, Buscot F, Kalko EKV, Linsenmair KE, Schulze E-D, Weisser WW. 2010. Implementing large-scale and long-term functional biodiversity research: The Biodiversity Exploratories. *Basic Appl Ecol* 11:473–485.
20. Solly EF, Schöning I, Boch S, Kandeler E, Marhan S, Michalzik B, Müller J, Zscheischler J, Trumbore SE, Schrumpf M. 2014. Factors controlling decomposition rates of fine root litter in temperate forests and grasslands. *Plant Soil* 382:203–218.
21. Rey A, Petsikos C, Jarvis PG, Grace J. 2005. Effect of temperature and moisture on rates of carbon mineralization in a Mediterranean oak forest soil under controlled and field conditions. *Eur J Soil Sci* 56:589–599.
22. Binh CTT, Heuer H, Gomes NCM, Kotzerke A, Fulle M, Wilke B-M, Schlöter M, Smalla K. 2007. Short-term effects of amoxicillin on bacterial communities in manured soil. *FEMS Microbiol Ecol* 62:290–302.

23. Vaclavik E, Halling-Sørensen B, Ingerslev F. 2004. Evaluation of manometric respiration tests to assess the effects of veterinary antibiotics in soil. *Chemosphere* 56:667-76.
24. Ding G-C, Radl V, Schlöter-Hai B, Jechalke S, Heuer H, Smalla K, Schlöter M. 2014. Dynamics of Soil Bacterial Communities in Response to Repeated Application of Manure Containing Sulfadiazine. *PLoS One* 9:e92958.
25. Čermák L, Kopecký J, Novotná J, Omelka M, Parkhomenko N, Plháčková K, Ságová-Marečková M. 2008. Bacterial communities of two contrasting soils reacted differently to lincomycin treatment. *Appl Soil Ecol* 40: 348-358.
26. Liu F, Ying G, Tao R, Zhao J, Yang J, Zhao L. 2009. Effects of six selected antibiotics on plant growth and soil microbial and enzymatic activities. *Environ Pollut* 157:1636–1642.
27. Klindworth A, Pruesse E, Schweer T, Peplies J, Quast C, Horn M, Glöckner FO. 2013. Evaluation of general 16S ribosomal RNA gene PCR primers for classical and next-generation sequencing-based diversity studies. *Nucleic Acids Res* 41:e1.
28. Schneider D, Thürmer A, Gollnow K, Lugert R, Gunka K, Groß U, Daniel R. 2017. Gut bacterial communities of diarrheic patients with indications of *Clostridioides difficile* infection. *Sci Data* 4:170152.
29. Zhang J, Kobert K, Flouri T, Stamatakis A. 2014. PEAR: a fast and accurate Illumina Paired-End read mergeR. *Bioinformatics* 30:614–620.
30. Caporaso JG, Kuczynski J, Stombaugh J, Bittinger K, Bushman FD, Costello EK, Fierer N, Peña AG, Goodrich JK, Gordon JI, Huttley GA, Kelley ST, Knights D, Koenig JE, Ley RE, Lozupone CA, McDonald D, Muegge BD, Pirrung M, Reeder J, Sevinsky JR, Turnbaugh PJ, Walters WA, Widmann J, Yatsunenko T, Zaneveld J, Knight R. 2010. QIIME allows analysis of high-throughput community sequencing data. *Nat Methods* 7:335–336.
31. Martin M. 2011. Cutadapt removes adapter sequences from high-throughput sequencing reads. *EMBnet J* 17:10.
32. Callahan BJ, McMurdie PJ, Holmes SP. 2017. Exact sequence variants should replace operational taxonomic units in marker-gene data analysis. *ISME J* 11:2639–2643.
33. Edgar RC. 2016. UNOISE2: improved error-correction for Illumina 16S and ITS amplicon sequencing. *bioRxiv* 21.

34. Rognes T, Flouri T, Nichols B, Quince C, Mahé F. 2016. VSEARCH: a versatile open source tool for metagenomics. *PeerJ* 4:e2584.
35. Edgar RC, Haas BJ, Clemente JC, Quince C, Knight R. 2011. UCHIME improves sensitivity and speed of chimera detection. *Bioinformatics* 27:2194–2200.
36. Yilmaz P, Parfrey LW, Yarza P, Gerken J, Pruesse E, Quast C, Schweer T, Peplies J, Ludwig W, Glöckner FO. 2014. The SILVA and “All-species Living Tree Project (LTP)” taxonomic frameworks. *Nucleic Acids Res* 42:D643–D648.
37. R Core Team. 2016. R: A Language and Environment for Statistical Computing. 3.3.1. Vienna, Austria. <http://www.r-project.org/index.html>. Retrieved 6 Dec 2019.
38. Bates D, Mächler M, Bolker B, Walker S. 2015. Fitting Linear Mixed-Effects Models Using lme4. *J Stat Softw* 67.
39. Kuznetsova A, Brockhoff PB, Christensen RHB. 2017. lmerTest Package: Tests in Linear Mixed Effects Models. *J Stat Softw* 82.
40. Bartoń K. 2018. MuMIn: Multi-Model Inference. <https://cran.r-project.org/web/packages/MuMIn/>. Retrieved 6 Dec 2019.
41. Felske, Akkermans. 1998. Prominent occurrence of ribosomes from an uncultured bacterium of the Verrucomicrobiales cluster in grassland soils. *Lett Appl Microbiol* 26:219–223.
42. Ye J, Coulouris G, Zaretskaya I, Cutcutache I, Rozen S, Madden TL. 2012. Primer-BLAST: A tool to design target-specific primers for polymerase chain reaction. *BMC Bioinformatics* 13:134.
43. Bolger AM, Lohse M, Usadel B. 2014. Trimmomatic: a flexible trimmer for Illumina sequence data. *Bioinformatics* 30:2114–2120.
44. Antipov D, Korobeynikov A, McLean JS, Pevzner PA. 2016. hybridSPAdes: an algorithm for hybrid assembly of short and long reads. *Bioinformatics* 32:1009–1015.
45. Wu YW, Simmons BA, Singer SW. 2015. MaxBin 2.0: An automated binning algorithm to recover genomes from multiple metagenomic datasets. *Bioinformatics* 32: 605–607.
46. García-Alcalde F, Okonechnikov K, Carbonell J, Cruz LM, Götz S, Tarazona S, Dopazo J, Meyer TF, Conesa A. 2012. Qualimap: evaluating next-generation sequencing alignment data. *Bioinformatics* 28:2678–2679.

47. Okonechnikov K, Conesa A, García-Alcalde F. 2015. Qualimap 2: advanced multi-sample quality control for high-throughput sequencing data. *Bioinformatics* 32:btv566.
48. Seemann T. 2014. Prokka: rapid prokaryotic genome annotation. *Bioinformatics* 30:2068–9.
49. Karp PD, Latendresse M, Caspi R. 2011. The pathway tools pathway prediction algorithm. *Stand Genomic Sci* 5:424–429.
50. Karp PD, Latendresse M, Paley SM, Krummenacker M, Ong QD, Billington R, Kothari A, Weaver D, Lee T, Subhraveti P, Spaulding A, Fulcher C, Keseler IM, Caspi R. 2016. Pathway tools version 19.0 update: Software for pathway/genome informatics and systems biology. *Brief Bioinform* 17:877–890.
51. Caspi R, Billington R, Keseler IM, Kothari A, Krummenacker M, Midford PE, Ong WK, Paley S, Subhraveti P, Karp PD. 2019. The MetaCyc database of metabolic pathways and enzymes - a 2019 update. *Nucleic Acids Res* 48:D445-D453.
52. Arango-Argoty G, Garner E, Pruden A, Heath LS, Vikesland P, Zhang L. 2018. DeepARG: a deep learning approach for predicting antibiotic resistance genes from metagenomic data. *Microbiome* 6:23.
53. Arango-Argoty GA, Dai D, Pruden A, Vikesland P, Heath LS, Zhang L. 2019. NanoARG: a web service for detecting and contextualizing antimicrobial resistance genes from nanopore-derived metagenomes. *Microbiome* 7:88.
54. Blin K, Shaw S, Steinke K, Villebro R, Ziemert N, Lee SY, Medema MH, Weber T. 2019. antiSMASH 5.0: updates to the secondary metabolite genome mining pipeline. *Nucleic Acids Res* 47:W81–W87.
55. Kumar S, Stecher G, Li M, Knyaz C. 2018. MEGA X: Molecular Evolutionary Genetics Analysis across computing platforms. *Mol Biol Evol* 35:1547–1549.
56. Edgar RC. 2004. MUSCLE: multiple sequence alignment with high accuracy and high throughput. *Nucleic Acids Res* 32:1792–7.
57. Tamura K, Nei M. 1993. Estimation of the number of nucleotide substitutions in the control region of mitochondrial DNA in humans and chimpanzees. *Mol Biol Evol* 10:512–526.

58. Parks DH, Chuvochina M, Waite DW, Rinke C, Skarshewski A, Chaumeil P-A, Hugenholtz P. 2018. A standardized bacterial taxonomy based on genome phylogeny substantially revises the tree of life. *Nat Biotechnol* 36:996.
59. Chaumeil P-A, Mussig AJ, Hugenholtz P, Parks DH. 2019. GTDB-Tk: a toolkit to classify genomes with the Genome Taxonomy Database. *Bioinformatics*.
60. Saitou N, Nei M. 1987. The neighbor-joining method: A new method for reconstructing phylogenetic trees. *Mol Biol Evol* 4:406–25.
61. Jones DT, Taylor WR, Thornton JM. 1992. The rapid generation of mutation data matrices from protein sequences. *Bioinformatics* 8:275–282.
62. Jain C, Rodriguez-R LM, Phillippy AM, Konstantinidis KT, Aluru S. 2018. High throughput ANI analysis of 90K prokaryotic genomes reveals clear species boundaries. *Nat Commun* 9.

Acknowledgements

We thank the managers of the three Exploratories, Kirsten Reichel-Jung, Iris Steitz, Sandra Weithmann, Florian Straub, Katrin Lorenzen, Juliane Vogt, Miriam Teuscher and all former managers for their work in maintaining the plot and project infrastructure; Christiane Fischer and Jule Mangels for giving support through the central office, Andreas Ostrowski for managing the central data base, and Markus Fischer, Eduard Linsenmair, Dominik Hessenmöller, Daniel Prati, François Buscot, Ernst-Detlef Schulze, Wolfgang W. Weisser and the late Elisabeth Kalko for their role in setting up the Biodiversity Exploratories project.

The work has been funded by the DFG Priority Program 1374 "Infrastructure-Biodiversity-Exploratories" (NA 848/2-1). Field work permits were issued by the responsible state environmental offices of Baden-Württemberg, Thüringen, and Brandenburg.

We acknowledge support by the Open Access Publication Funds of the University of Göttingen. Furthermore, we would like to thank Dr. Sascha Dietrich for bioinformatic support and Dr. Lauren Alteio for correspondence regarding metagenome assembled genomes.

Author contributions: Conceptualization, I.M.W. and H.N.; formal analysis, I.M.W., C.P., A.P., D.S. and H.N.; investigation, I.M.W., A.Y.R., I.G. and S.H.B.; resources, H.N. and I.S.; data curation, I.M.W. and

H.N.; writing - original draft preparation, I.M.W. and H.N.; writing - review and editing, I.M.W., H.N., D.S. and I.S.; visualization, I.M.W. and H.N.; supervision, I.M.W. and H.N.; project administration, H.N.; funding acquisition, H.N.

Competing interests

The authors declare no competing interests.

5.1. Supplemental information for chapter five

Figure S1. Relative abundance of *Ca. Udaeobacter* and other bacterial groups for all soil microcosms.

Table S1. Description of plot characteristics and properties of the soils used to set up the microcosms and for cell extraction.

Table S2. List of antibiotics that have been chromatographically analyzed for residues in all grassland and forest soils used for the microcosm experiment.

Table S3. Model formulas and results from linear mixed model regression analysis.

Table S4. Attributes of all *Chthoniobacterales* MAGs used to construct the Neighbor-joining tree.

Table S5: Antibiotic resistance genes (ARGs) and mobile genetic elements (MGE) encoded in the MAG of *Ca. Udaeobacter* sp.

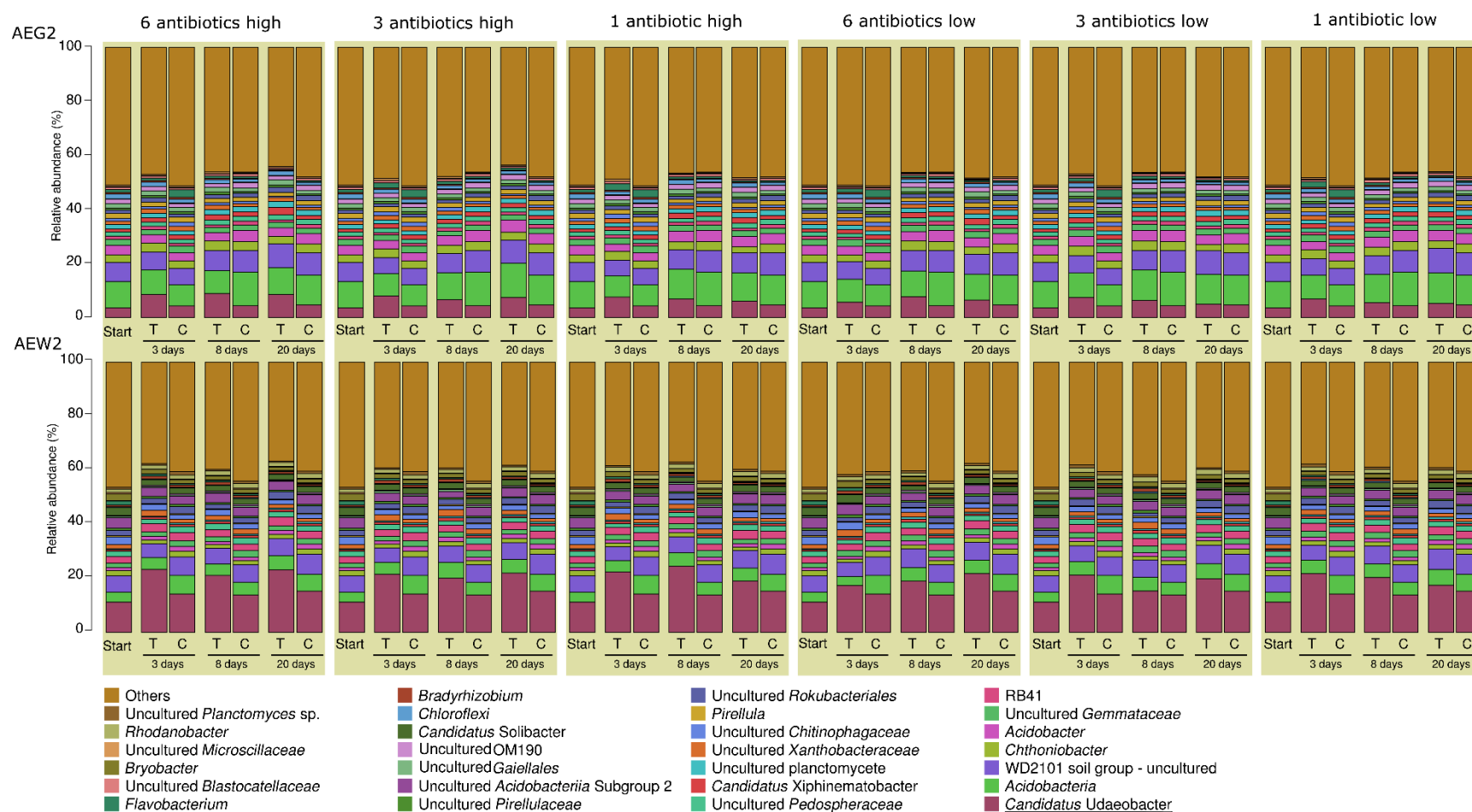


Figure S1. Relative abundance of *Ca. Udaeobacter* and other bacterial groups for all soil microcosms. Untreated control samples, “C”, as well as samples treated with antibiotics in high or low concentration, “T”, were analyzed. Others: bacterial groups accounting for < 2% relative abundance. Results are presented as mean of replicates. With respect to all of the four forest soil samples, treatment with one antibiotic, three antibiotics and six antibiotics in high as well as low concentration was performed. Four of the seven grassland soil samples were also subjected to this antibiotic treatment procedure. In addition, the remaining three grassland soil samples (AEG16, AEG21 and HEG21) were treated with three antibiotics and six antibiotics in high as well as low concentration to further verify the effect of antibiotics release on *Ca. Udaeobacter*.

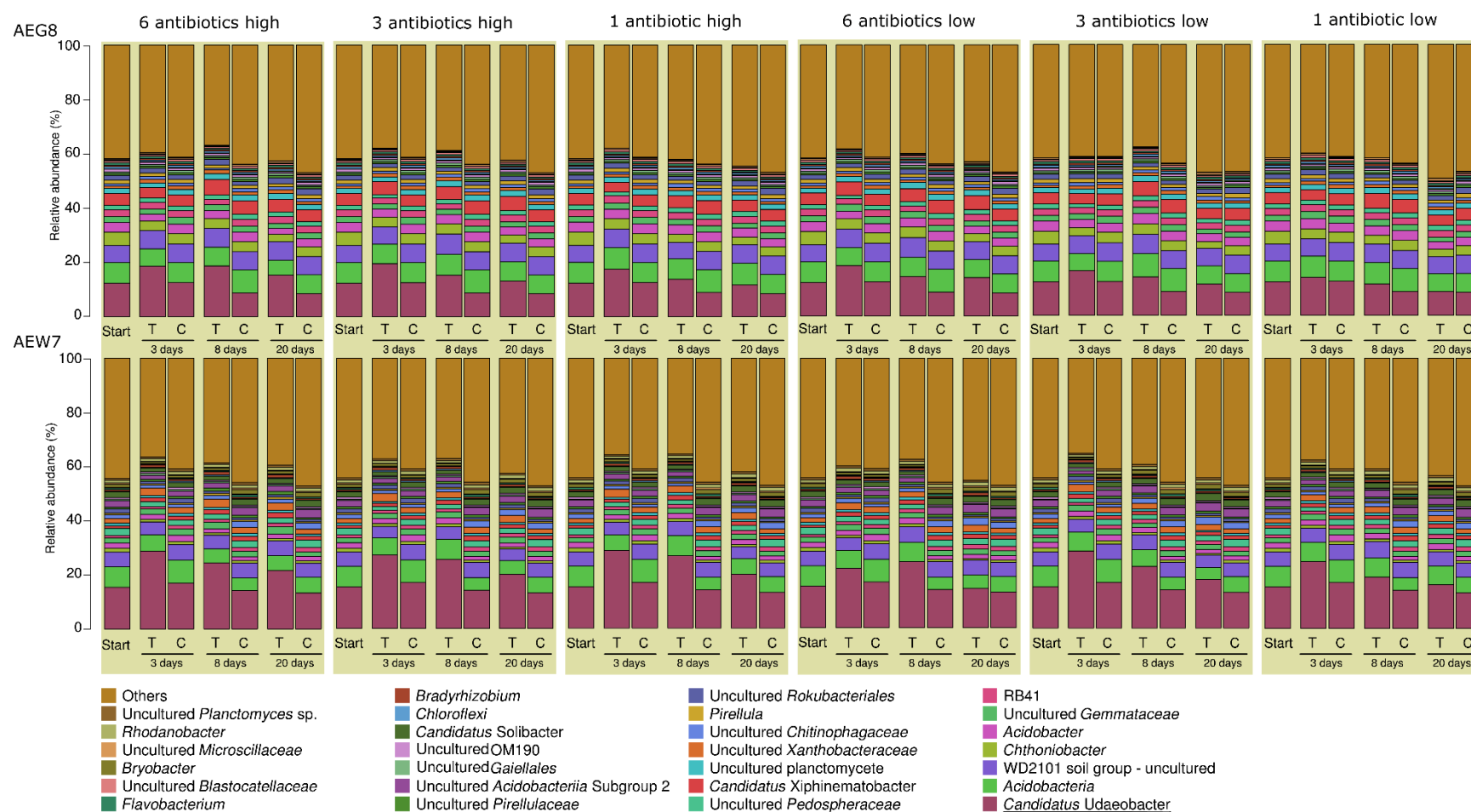


Figure S1. continued

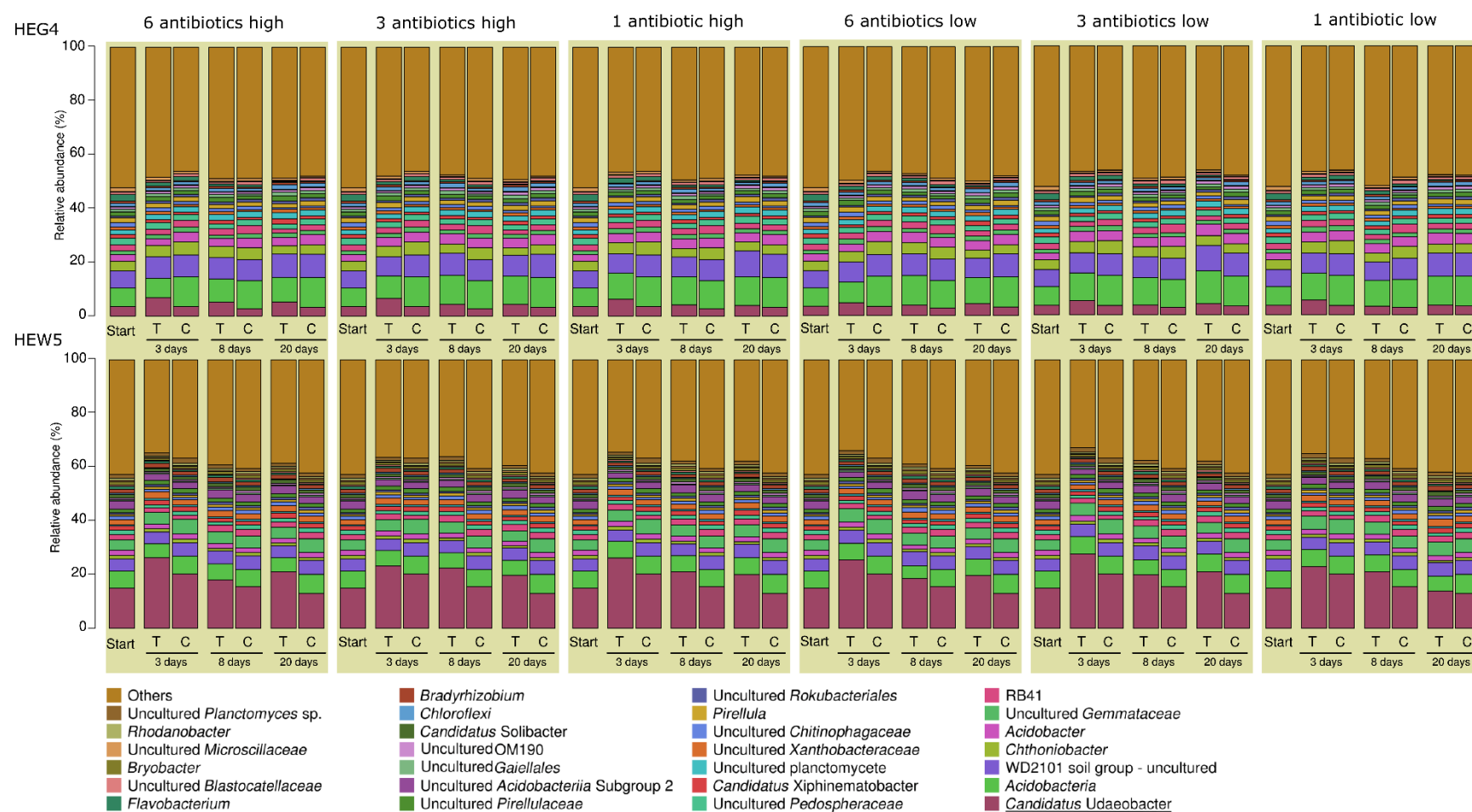


Figure S1. continued

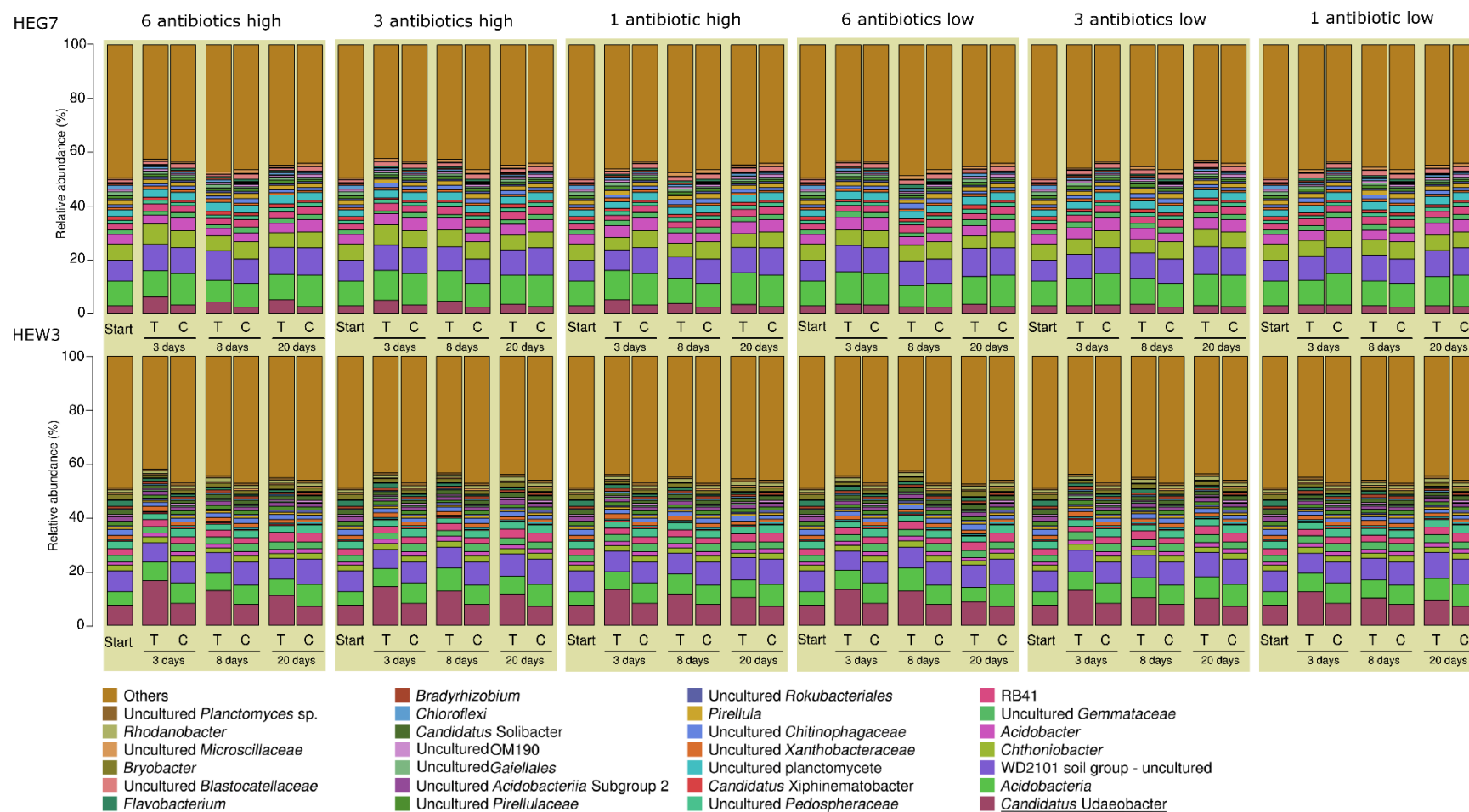


Figure S1. continued

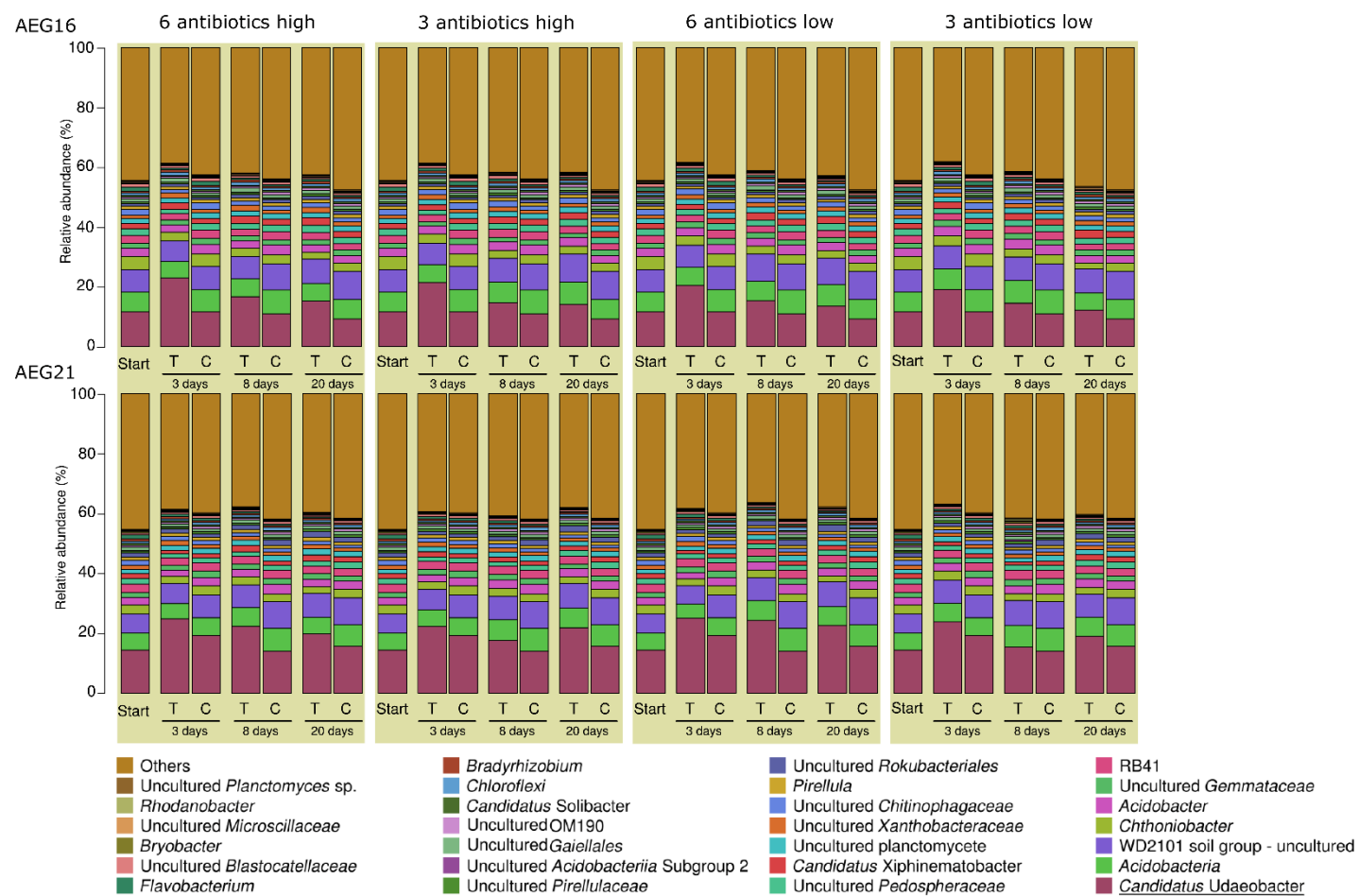


Figure S1. continued

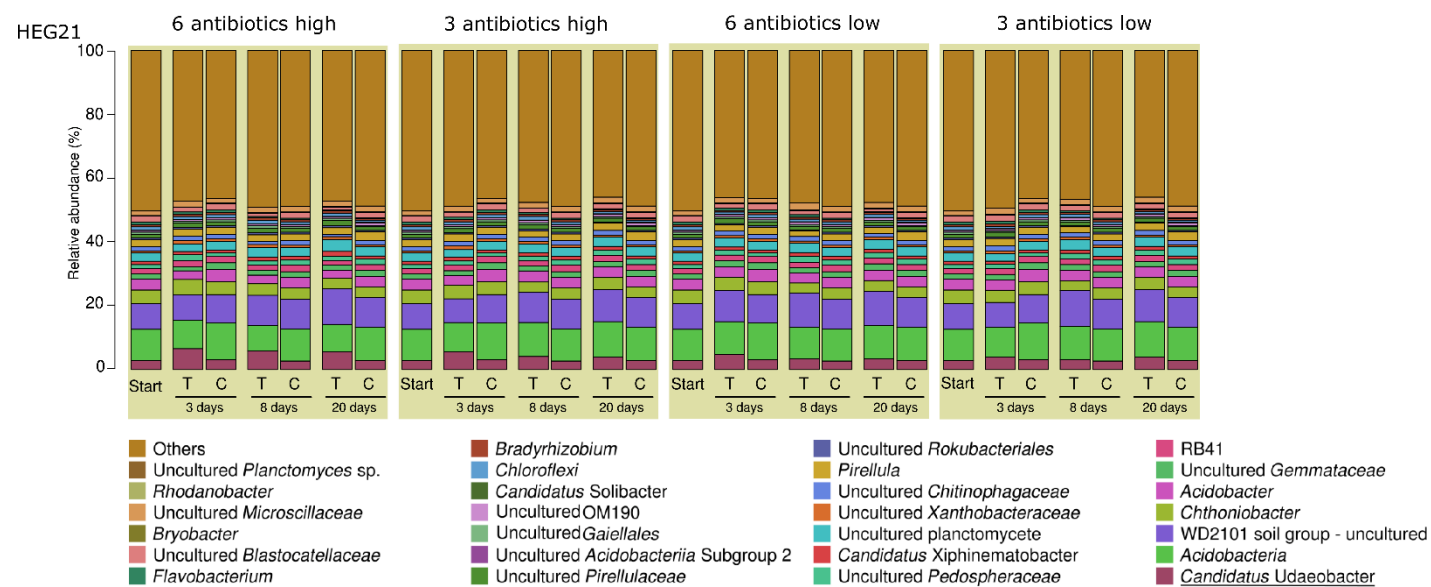


Figure S1. continued

Table S1. Description of plot characteristics and properties of the soils used to set up the microcosms and for cell extraction. Pasture: grassland with grazing livestock, meadow: grassland without grazing livestock. AEW3 is not used for the set up of the microcosms but for cell extraction.

Plot ID	Exploratory	Plot characteristics	LUI/SMI	pH	% water	C:N ratio
HEG4	HAI	Mown, fertilized meadow	2.1	6.5	35.8	10.7
HEG7	HAI	Pasture	1.7	7	25.2	9.5
HEG21	HAI	Mown pasture	0.7	7.3	26.5	10.4
HEW3	HAI	Spruce forest	0.5	5.1	39.8	16.5
HEW5	HAI	Beech forest	0.2	5.3	52.5	13.1
AEG2	ALB	Mown, fertilized meadow	3.1	6.9	59.7	9.5
AEG8	ALB	Mown pasture	1.3	6.6	70.4	10.9
AEG16	ALB	Mown, fertilized pasture	1.7	6.0	54.7	10.2
AEG21	ALB	Mown, fertilized pasture	3.9	5.8	52.9	10.0
AEW2	ALB	Spruce forest	0.6	4.8	38.3	13.9
AEW7	ALB	Beech forest	0.2	5.0	64.9	12.9
AEW3	Alb	Spruce forest	0.5	5.6	52.7	13.6

Abbreviations: HAI, exploratory Hainich-Dün; ALB, exploratory Schwäbische Alb; LUI, land use intensity index; SMI, silvicultural management index, % water, gravimetric water content; C:N ratio, organic carbon divided by total N.

Table S2. List of antibiotics that have been chromatographically analyzed for residues in all grassland and forest soils used for the microcosm experiment.

Tested antibiotics	Detection limit (mg/kg soil)	Soil sample (concentration of antibiotic)
Sulfonamides		
Acetylsulfadiazine	<0.001	-
Acetylsulfadimethoxine	<0.001	-
Acetylsulfamethazine	<0.001	-
Acetylsulfadoxine	<0.001	-
Acetylsulfamerazine	<0.001	-
Acetylsulfamethoxazole	<0.001	-
Acetylsulfathiazole	<0.001	-
Sulfadiazine	<0.001	-
Sulfadimethoxine	<0.001	-
Sulfamethazine	<0.001	-
Sulfadoxine	<0.001	-
Sulfamerazine	<0.001	-
Sulfamethoxazole	<0.001	-
Sulfathiazole	<0.001	-
Penicillins		
Amoxicillin	<0.01	-
Ampicillin	<0.01	-
Benzylpenicillin	<0.01	-
Cloxacillin	<0.01	-
Dicloxacillin	<0.01	-
Oxacillin	<0.01	-
Penethamate	<0.01	-
Penicillin V	<0.01	-
Aminoglycosides		
Apramycin	<0.01	-
Clindamycin	<0.01	-
Gentamycin C1a	<0.05	-
Lincomycin	<0.01	-
Neomycin	<0.01	-
Spectinomycin	<0.05	-
Streptomycin	<0.01	-
Polypeptides		
Bacitracin A	<0.01	-
Collistin	<0.03	-
Nafcillin	<0.01	-
Nisin	<0.01	-
Cephalosporins		
Cefadroxil	<0.01	-
Cefapirin	<0.01	-
Cefazolin	<0.01	-
Cefquinome	<0.01	-
Ceftiofur	<0.01	-
Cefuroxime	<0.01	-
Cephalexin	<0.01	-
Amphenicols		
Chloramphenicol	<0.001	-
Florfenicol	<0.001	-

Only soil samples exhibiting antibiotic concentrations above the detection limits are listed.

Table S2. continued

Tested antibiotics	Detection limit (mg/kg soil)	Soil sample (concentration of antibiotic)
Thiamphenicol	<0.001	-
Tetracyclines		
Chlortetracycline	<0.01	AEW2 (0.011 mg/kg)
Demeclocycline	<0.003	-
Doxycycline	<0.01	-
Iso-Chlortetracycline	<0.01	-
Meclocycline	<0.01	-
Metacycline	<0.01	-
Oxytetracycline	<0.01	-
Tetracycline	<0.01	-
Quinolones		
Ciprofloxacin	<0.001	-
Danofloxacin	<0.01	-
Difloxacin	<0.01	-
Enrofloxacin	<0.01	-
Marbofloxacin	<0.01	-
Ofloxacin	<0.01	-
Sarafloxacin	<0.01	-
Macrolides		
Clarithromycin	<0.01	-
Erythromycin	<0.01	-
Flavomycin	<0.01	-
Ivermectin B1a	<0.05	-
Natamycin	<0.01	-
Oleandomycin	<0.01	-
Spiramycin S-I	<0.05	-
Spiramycin S-II	<0.01	-
Spiramycin S-III	<0.01	-
Tilmicosin	<0.01	-
Tylosin	<0.05	-
Nitroimidazoles		
Metronidazole	<0.01	-
Ronidazole	<0.01	-
Additional antibiotics		
Imipenem	<0.01	-
Tiamulin	<0.001	-
Trimethoprim	<0.01	-
Tylvalosin	<0.01	-
Valnemulin	<0.01	-
Virginamycin	<0.01	-

Only soil samples exhibiting antibiotic concentrations above the detection limits are listed.

Table S3. Model formulas and results from linear mixed model regression analysis. The relative abundance of *Ca. Udaeobacter*, ASV 6 upon antibiotic treatment and the rise in absolute 16S rRNA gene abundance per ng DNA upon antibiotics release after 3 days of incubation, assessed via qPCR, was analyzed.

Model formula	N	R ² m/ R ² c	p treat.	Df treat.	Est. treat.	p day	Df day	Est. day
lmer(log(<i>Ca. Udaeobacter</i>)~Concentr+Days+(1 plotID/sampleID))	606	0.04/ 0.96	< 2 e ⁻¹⁶	190	6.0 e ⁻⁴	< 2 e ⁻¹⁶	403	-0.01
lmer(log(<i>Ca. Udaeobacter</i>)~SixAntib.High+Days+(1 plotID/sampleID))	83	0.15/ 0.96	< 2 e ⁻¹⁶	38	9.8 e ⁻⁴	1.8 e ⁻⁴	66	-0.01
lmer(log(<i>Ca. Udaeobacter</i>)~SixAntib.Low+Days+(1 plotID/sampleID))	79	0.06/ 0.96	1.4 e ⁻¹³	66	0.01	6.9 e ⁻⁴	66	-0.01
lmer(log(<i>Ca. Udaeobacter</i>)~ThreeAntib.High+Days+(1 plotID/sampleID))	87	0.08/ 0.95	< 2 e ⁻¹⁶	74	1.4 e ⁻³	7.4 e ⁻⁴	74	-0.01
lmer(log(<i>Ca. Udaeobacter</i>)~ThreeAntib.Low+Days+(1 plotID/sampleID))	88	0.04/ 0.96	8.4 e ⁻¹⁴	75	0.01	9.9 e ⁻⁴	75	-0.01
lmer(log(<i>Ca. Udaeobacter</i>)~OneAntib.High+Days+(1 plotID/sampleID))	65	0.1/ 0.97	1.67 e ⁻¹¹	25	4.5 e ⁻³	2.5 e ⁻⁵	50	-0.01
lmer(log(<i>Ca. Udaeobacter</i>)~OneAntib.Low+Days+(1 plotID/sampleID))	66	0.04/ 0.96	4.22 e ⁻⁷	53	0.02	3.0 e ⁻⁵	52	-0.01
lmer(ASV 6~Concentr+Days+(1 plotID/sampleID))	606	0.02/0.90	1.68 e ⁻⁶	593	0.04	< 2 e ⁻¹⁶	593	-1.73
lmer(log(16S rRNA genes per ng DNA after 3 days)~Concentr+(1 plotID))	30	0.02/ 0.90	1.84 e ⁻⁷	23	1.6 e ⁻³	NA.	NA	NA

Abbreviations: p, p-value ; treat., antibiotic treatment; Df, degrees of freedom; Est., estimates; N, sample size.

Table S4. Attributes of all *Chthoniobacterales* MAGs used to construct the Neighbor-joining tree. The yellow highlighted MAGs cluster together with the here assembled MAG of *Ca. Udaeobacter* sp.

GBK assembly accession	GTDB Phylogeny starting with the family	Compl.	Cont.	Size in Mbp	GC
GCA_003221405.1	f__UBA10450;g__AV69;s__AV69 sp003221405	66.6%	2.0%	1.94	55.4%
GCA_003218375.1	f__UBA10450;g__AV80;s__AV80 sp003218375	100.0%	2.7%	3.96	58.8%
GCA_003218735.1	f__UBA10450;g__AV55;s__AV55 sp003218735	72.0%	2.6%	1.49	54.5%
GCA_003218615.1	f__UBA10450;g__AV55;s__AV55 sp003218615	88.3%	0.5%	2.29	55.3%
GCA_003219225.1	f__UBA10450;g__AV17;s__AV17 sp003219225	70.5%	0.7%	2.04	58.4%
GCA_003219215.1	f__UBA10450;g__AV40;s__AV40 sp003219215	90.8%	1.7%	2.33	55.3%
GCA_003219095.1	f__UBA10450;g__AV69;s__AV69 sp003219095	71.4%	3.2%	2.38	55.1%
GCA_003244145.1	f__UBA10450;g__AV80;s__AV80 sp003244145	92.9%	5.1%	3.63	58.4%
GCF_001613545.1	f__Terrimicrobiaceae;g__Terrimicrobium;s__Terrimicrobium sacchariphilum	100.0%	2.7%	4.75	60.2%
GCA_003219465.1	f__UBA10450;g__AV55;s__AV55 sp003219465	89.1%	6.6%	4.19	55.2%
GCA_003134785.1	f__UBA10450;g__AV80;s__AV80 sp003134785	100.0%	3.4%	4.39	57.8%
GCA_003218885.1	f__UBA10450;g__AV55;s__AV55 sp003218885	88.0%	2.4%	2.30	55.4%
GCF_000173075.1	f__Chthoniobacteraceae;g__Chthoniobacter;s__Chthoniobacter flavus	97.3%	2.9%	7.85	61.1%
GCA_003221295.1	f__UBA10450;g__AV69;s__AV69 sp003221295	90.2%	3.7%	2.98	55.3%
GCA_003219175.1	f__UBA10450;g__AV69;s__AV69 sp003219175	98.0%	5.7%	3.24	55.0%
GCA_003220155.1	f__UBA10450;g__AV69;s__AV69 sp003220155	96.3%	3.0%	3.35	55.3%
GCA_003167555.1	f__UBA10450;g__AV80;s__AV80 sp003167555	100.0%	3.4%	4.20	58.5%
GCA_003219195.1	f__UBA10450;g__UBA10450;s__UBA10450 sp003219195	95.3%	2.2%	2.82	55.8%
GCA_003219925.1	f__UBA10450;g__AV69;s__AV69 sp003219925	81.2%	3.0%	2.10	55.3%
GCA_003219355.1	f__UBA10450;g__AV55;s__AV55 sp003219355	88.4%	6.4%	2.23	54.5%
GCA_003445855.1	f__UBA10450;g__UBA10450;s__UBA10450 sp003445855	78.0%	1.7%	2.10	55.9%
GCA_003219995.1	f__UBA10450;g__UBA10450;s__UBA10450 sp003219995	82.6%	2.5%	2.10	55.3%
GCA_003221375.1	f__UBA10450;g__AV55;s__AV55 sp003221375	73.9%	1.4%	2.17	54.1%
GCA_003218535.1	f__UBA10450;g__AV55;s__AV55 sp003218535	92.6%	4.4%	2.69	54.5%
GCA_003167365.1	f__UBA10450;g__Palsa-1382;s__Palsa-1382 sp003167365	100.0%	1.4%	3.13	55.2%
GCA_003219495.1	f__UBA10450;g__AV40;s__AV40 sp003219495	72.9%	1.5%	2.11	56.3%
GCA_003218305.1	f__UBA10450;g__AV80;s__AV80 sp003218305	92.9%	4.6%	3.60	59.0%
GCA_003169695.1	f__UBA10450;g__AV80;s__AV80 sp003169695	99.7%	4.7%	4.14	57.2%
GCA_001897195.1	f__Terrimicrobiaceae;g__Terrimicrobium;s__Terrimicrobium sp001897195	96.6%	3.8%	5.06	60.8%
GCA_003219125.1	f__UBA10450;g__AV69;s__AV69 sp003219125	92.3%	4.6%	3.20	55.0%

Table S4 continued:

GBK assembly accession	GTDB Phylogeny starting with the family	Compl.	Cont.	Size in Mbp	GC
GCA_003219435.1	f__UBA10450;g__AV55;s__AV55 sp003219435	86.4%	2.4%	2.73	55.2%
GCA_003220055.1	f__UBA10450;g__AV40;s__AV40 sp003220055	81.8%	0.2%	2.08	55.5%
GCA_003219335.1	f__UBA10450;g__AV55;s__AV55 sp003219335	83.0%	4.1%	3.71	55.0%
GCA_002290555.1	f__ <i>Terrimicrobiaceae</i> ;g__UBA967;s__UBA967 sp002290555	81.1%	0.2%	1.82	56.6%
GCA_003136515.1	f__UBA6821;g__UBA6821;s__UBA6821 sp003136515	85.1%	4.1%	2.36	53.2%
GCA_002298145.1	f__ <i>Chthoniobacteraceae</i> ;g__UBA695;s__UBA695 sp002298145	92.6%	0.7%	4.11	60.5%
GCA_003218415.1	f__UBA10450;g__AV55;s__AV55 sp003218415	83.7%	3.4%	2.05	55.3%
GCA_003219005.1	f__UBA10450;g__AV55;s__AV55 sp003219005	87.8%	1.1%	2.69	55.2%
GCA_003218975.1	f__UBA10450;g__AV55;s__AV55 sp003218975	98.0%	2.9%	3.06	55.1%
GCA_003218785.1	f__UBA10450;g__AV55;s__AV55 sp003218785	85.6%	0.7%	2.78	54.9%
GCA_003218705.1	f__UBA10450;g__AV40;s__AV40 sp003218705	76.5%	0.8%	1.70	55.4%
GCA_003218945.1	f__UBA10450;g__AV55;s__AV55 sp003218945	87.8%	3.1%	2.80	55.0%
GCA_003219265.1	f__UBA10450;g__AV133;s__AV133 sp003219265	78.4%	1.4%	2.09	56.2%
GCA_003218135.1	f__UBA10450;g__AV55;s__AV55 sp003218135	91.2%	3.7%	2.75	54.9%
GCA_003169975.1	f__UBA10450;g__Palsa-1392;s__Palsa-1392 sp003169975	100.0%	2.7%	4.47	59.9%
GCF_001318295.1	f__ <i>Xiphinematobacteraceae</i> ;g__ <i>Xiphinematobacter</i> ;s__ <i>Xiphinematobacter</i> sp001318295	89.9%	0.0%	0.92	47.7%
GCA_003244125.1	f__UBA10450;g__AV69;s__AV69 sp003244125	66.0%	2.3%	2.50	58.7%
GCA_003217965.1	f__UBA10450;g__AV69;s__AV69 sp003217965	90.3%	3.7%	2.64	55.2%
GCA_003218475.1	f__UBA10450;g__AV55;s__AV55 sp003218475	94.7%	3.6%	3.16	54.8%
GCA_003134765.1	f__UBA10450;g__AV80;s__AV80 sp003134765	96.0%	2.7%	4.05	58.7%
GCA_003221195.1	f__UBA10450;g__AV55;s__AV55 sp003221195	89.6%	4.1%	3.10	54.3%
GCA_003218345.1	f__UBA10450;g__AV55;s__AV55 sp003218345	82.5%	3.2%	2.39	54.5%
GCA_003218915.1	f__UBA10450;g__AV55;s__AV55 sp003218915	88.7%	3.3%	2.91	54.6%
GCA_003220075.1	f__UBA10450;g__AV69;s__AV69 sp003220075	87.4%	4.5%	2.79	55.2%
GCA_003176035.1	f__ <i>Xiphinematobacteraceae</i> ;g__PSRL01;s__PSRL01 sp003176035	70.4%	3.4%	1.92	48.5%
GCF_003054655.1	f__ <i>Terrimicrobiaceae</i> ;g__ <i>Terrimicrobium</i> ;s__ <i>Terrimicrobium</i> sp003054655	100.0%	2.0%	4.75	60.7%
GCA_003218265.1	f__UBA10450;g__AV55;s__AV55 sp003218265	66.6%	2.2%	2.25	55.0%
GCA_003218815.1	f__UBA10450;g__AV55;s__AV55 sp003218815	77.1%	2.3%	1.85	54.6%
GCA_003218395.1	f__UBA10450;g__AV55;s__AV55 sp003218395	90.7%	4.4%	2.95	54.9%
GCA_003219695.1	f__UBA10450;g__AV55;s__AV55 sp003219695	92.8%	3.4%	3.14	55.6%
GCA_003219115.1	f__UBA10450;g__AV69;s__AV69 sp003219115	82.4%	1.0%	2.67	55.3%

Table S4 continued:

GBK assembly accession	GTDB Phylogeny starting with the family	Compl.	Cont.	Size in Mbp	GC
GCA_003219395.1	f__UBA10450;g__AV55;s__AV55 sp003219395	69.3%	2.2%	2.82	54.5%
GCA_003219415.1	f__UBA10450;g__AV55;s__AV55 sp003219415	97.8%	3.2%	3.62	54.4%
GCA_003217875.1	f__UBA10450;g__AV55;s__AV55 sp003217875	86.8%	2.1%	2.45	54.6%
GCA_003220005.1	f__UBA10450;g__AV55;s__AV55 sp003220005	82.4%	0.7%	2.53	55.0%
GCA_002396485.1	f__ <i>Terrimicrobiaceae</i> ;g__UBA967;s__UBA967 sp002396485	98.7%	0.0%	2.77	56.2%
GCA_003217835.1	f__UBA10450;g__AV55;s__AV55 sp003217835	74.3%	0.7%	1.75	54.6%
GCA_003218525.1	f__UBA10450;g__AV69;s__AV69 sp003218525	78.0%	3.5%	2.43	55.3%
GCA_002452515.1	f__UBA6821;g__UBA6821;s__UBA6821 sp002452515	90.2%	1.4%	2.35	54.0%
GCA_003219945.1	f__UBA10450;g__AV55;s__AV55 sp003219945	81.5%	2.3%	2.24	54.9%
GCA_003218755.1	f__UBA10450;g__AV55;s__AV55 sp003218755	88.5%	3.2%	2.63	54.9%
GCA_003217895.1	f__UBA10450;g__AV55;s__AV55 sp003217895	94.3%	2.7%	2.74	55.0%
2651869889 (IMG Taxon ID)	not listed in the GTDB database (ncbi taxonomy: <i>Chthoniobacteraceae</i> ; <i>Candidatus</i> Udaeobacter; <i>Candidatus</i> Udaeobacter copiosus)	80.0%	4.0%	2.66	54.3%

Abbreviations: Compl, completeness estimated by Checkm; Cont, contamination estimated by Checkm; GC, GC content

Table S5: Antibiotic resistance genes (ARGs) and mobile genetic elements (MGE) encoded in the MAG of *Ca. Udaeobacter* sp.

Detection strategy	Contig/scaffold	Annotation	Product	deepARG predicted resistance
deepARG	1	rlmN	Dual-specificity RNA methyltransferase RlmN	Phenicol
Prokka annotation	1	xerC_1	Tyrosine recombinase XerC	
Prokka annotation	3	xerC_2	Tyrosine recombinase XerC	Multidrug
deepARG	5	Udae02_04600	multi-drug expRT ATP binding/permease protein	
deepARG	6	phoP	Alkaline phosphatase synthesis transcriptional regulatory protein PhoP	Glycopeptide
Prokka annotation	6	ybhF_1	putative multidrug ABC transporter ATP-binding protein YbhF	
Prokka annotation	6	ybhR	putative multidrug ABC transporter permease YbhR	
Prokka annotation	7	Udae02_06040	Beta-lactamase	multidrug
deepARG	8	mdtA_1	multidrug resistance protein MdtA	
Prokka annotation	8	mdtC_1	Multidrug resistance protein MdtC	
Prokka annotation	9	fabI	Enoyl-[acyl-carrier-protein] reductase [NADH] FabI	
deepARG	11	macA_1	macrolide export protein	MLS
Prokka annotation	11	yknY_1	putative ABC transporter ATP-binding protein YknY	
Prokka annotation	11	macB_1	Macrolide export ATP-binding/permease protein MacB	Aminoglycoside
deepARG	11	rsmA	ribosomal RNA small subunit methyltransferase A	
deepARG	12	ybhF_2	multidrug ABC transporter ATP-binding protein	Bacitracin
deepARG	14	czcR	Transcriptional activator protein	Glycopeptide
Prokka annotation	14	macA_2	Macrolide export protein MacA	
deepARG	17	nreC	Oxygen regulatory protein NreC	Unclassified
deepARG	19	kdpD	sensor protein	Unclassified
Prokka annotation	21	mdtA_2	Multidrug resistance protein MdtA	
Prokka annotation	22	Udae02_12270	Beta-lactamase superfamily domain protein	
Diamond	23	Udae02_12390	IS5 family transposase IS1355	
Prokka annotation	27	Udae02_13820	IS110 family transposase ISGme8	
Prokka annotation	28	mdtA_3	Multidrug resistance protein MdtA	

Table S5 continued:

Detection strategy	Contig/scaffold	Annotation	Product	deepARG predicted resistance
deepARG	28	ybaL	Putative cation/proton antiporterI YbaL	Fosmidomycin
Prokka annotation	30	vanB	Vancomycin B-type resistance protein VanB	
deepARG	40	spoVD	Stage V sporulation protein D	Beta-lactam
Diamond	42	xerD_1	Tyrosine recombinase XerD	
deepARG	46	bepE	Efflux pump membrane transporter	Multidrug
deepARG	46	srpA	Solvent efflux pump periplasmatic linker SrpA	Multidrug
Prokka annotation	49	Udae02_20030	IS110 family transposase ISGme8	
Diamond	49	Udae02_20040	IS3 family transposase ISStau1	
Diamond	61	xerD_2	Tyrosine recombinase XerD	
Prokka annotation	64	Udae02_23300	Beta-lactamase	
Prokka annotation	69	macB_2	Macrolide export ATP-binding/permease protein MacB	
Prokka annotation	69	macB_3	Macrolide export ATP-binding/permease protein MacB	
deepARG	69	Udae02_24310	Putative multidrug export ATP-binding/permease protein	Multidrug
Prokka annotation	74	mdtA_4	Multidrug resistance protein MdtA	
Prokka annotation	74	mdtB_1	Multidrug resistance protein MdtB	
Prokka annotation	74	mdtB_2	Multidrug resistance protein MdtB	
Prokka annotation	74	mdtC_2	Multidrug resistance protein MdtC	
Prokka annotation	78	xerC_3	Tyrosine recombinase XerC	
Prokka annotation	80	xerC_4	Tyrosine recombinase XerC	
Prokka annotation	89	InrL	Linearmycin resistance ATP-binding protein	
Prokka annotation	89	InrN	Linearmycin resistance permease protein LnrN	
deepARG	89	syrM1	HTH-type transcriptional regulator SyrM 1	
deepARG	92	Udae02_28300	Putative multidrug export ATP-binding/permease protein	Multidrug
Diamond	94	recA	Protein RecA	
deepARG	98	tcrA	Transcriptional regulatory protein	Glycopeptide

Table S5 continued:

Detection strategy	Contig/scaffold	Annotation	Product	deepARG predicted resistance
Prokka annotation	99	Udaeo2_29330	macB: subunit of efflux pump conferring antibiotic resistance	
Prokka annotation	99	Udaeo2_29350	macB-like periplasmic core domain protein	
Prokka annotation	99	yknY_4	putative ABC transporter ATP-binding protein YknY	
Prokka annotation	99	Udaeo2_29370	HlyD family secretion protein	
Prokka annotation	106	mdtA_5	Multidrug resistance protein MdtA	
Prokka annotation	106	mdtC_3	Multidrug resistance protein MdtC	
Prokka annotation	109	Udaeo2_30640	Metallo-beta-lactamase superfamily protein	
Prokka annotation	110	macB_4	Macrolide export ATP-binding/permease protein MacB	
Prokka annotation	110	Udaeo2_30740	MacB-like periplasmic core domain protein	
Prokka annotation	110	Udaeo2_30700	MacB-like periplasmic core domain protein	
Prokka annotation	110	Udaeo2_30690	MacB-like periplasmic core domain protein	
Prokka annotation	110	Udaeo2_30660	macB: subunit of efflux pump conferring antibiotic resistance	
Prokka annotation	110	Udaeo2_30670	macB: subunit of efflux pump conferring antibiotic resistance	
deepARG	112	stp	Multidrug resistance protein Stp	Tetracenomycin_C
deepARG	116	blaP	Beta-lactamase	Beta-lactam
deepARG	125	Udaeo2_32650	Metallo-beta-lactamase superfamily protein	Beta-lactam
Prokka annotation	131	Udaeo2_33250	Transposase IS116/IS110/IS902 family protein	
Diamond	132	xerC_5	Tyrosine recombinase XerC	

6. Discussion

Before antibiotics were discovered, bacterial infections were difficult to treat and often ended with the death of the patient. Due to the current antibiotic resistance crisis, notorious diseases that finally became treatable with the discovery of antibiotics in the 20th century, such as tuberculosis (caused by *Mycobacterium tuberculosis*), diphtheria (caused by *Corynebacterium diphtheriae*), typhoid fever (caused by *Salmonella enterica* serovar Typhi) or leprosy (caused by *Mycobacterium leprae*), can today become problematic again. In fact, infections with antibiotic resistant strains of all mentioned bacteria have already been reported (predominantly with respect to developing countries) (Zignol et al. 2016; Mina et al. 2011; Zaki and Karande 2011; Cambau et al. 2018). Especially nosocomial infections with multidrug resistant (MDR) pathogens occur frequently and pose a serious threat to human health (Santajit and Indrawattana 2016; Partridge et al. 2018; Spigaglia, Mastrantonio, and Barbanti 2018). In future, this development may worsen considerably, if antibiotic misuse and environmental pollution with antimicrobials is not properly addressed. As a matter of fact, predictions suggest that we may even find ourselves in a post-antibiotic era where common bacterial infections can no longer be treated adequately (Runcie 2015; Reardon 2014).

The soil bacterial resistome is most likely the origin of many pathogen encoded antibiotic resistance genes (ARGs), due to the circulation of ARGs between soil, human and livestock, fostered by the evolutionary pressure from antibiotic application and pollution (Bengtsson-Palme, Kristiansson, and Larsson 2018). However, a comprehensive understanding about properties and factors influencing the soil resistome which possibly affect the development of antibiotic resistant pathogens, is still lacking. To improve this fragmentary knowledge, three different aspects with respect to the soil resistome were addressed in this thesis. First, information on how human practices and existing soil characteristics affect the soil resistome was gathered. On this account, medically relevant ARGs and mobile genetic elements (MGEs) were quantified in soil DNA from 300 forest and grassland sample plots from the Biodiversity Exploratories. Second, knowledge about the still widely untapped variety of ARGs within the soil resistome was extended via functional screenings of grassland and forest soil metagenomic libraries. As previous findings indicate that the soil bacterial community represents the major driver for the soil ARG content (Forsberg et al. 2014), the third research focus was placed on a globally abundant

but so far poorly characterized soil bacterial genus designated *Candidatus* Udaeobacter. In this context, the response of *Ca. Udaeobacter* towards antibiotic exposure was investigated to gain knowledge about the resistance properties of these organisms.

6.1. Anthropogenic and natural effectors of the soil resistome

The aminoglycoside resistance genes *aac(6')-Ib* and *aacC1*, the beta-lactamase genes *bla_{IMP-12}* and *bla_{IMP-5}*, the MLS (macrolide, lincosamide and streptogramin) resistance gene *ermB*, the macrolide resistance gene *mefA*, the tetracycline resistance gene *tetA* as well as IncP-1 plasmids and class 1 integrons were quantified based on grassland and forest soil DNA from all 300 EPs of the Biodiversity Exploratories. Land use practices and soil features that influence the abundance of these target ARGs and MGEs were identified with a combination of two statistical analyses. First, binomial regression analysis was conducted to determine parameters influencing the occurrence of the mentioned targets. For this purpose, C_T values (the number of cycles within a real-time quantitative PCR reaction required for the fluorescent signal to cross a fixed threshold) were transformed into binary data. More precisely, non-detects (C_T values ≥ 37) and detects (C_T values < 37) were represented by “0” and “1”, respectively. Additionally, left censored regression analyses were carried out to estimate shifts in the abundance of the selected targets without having to substitute or discard non-detects.

This combined statistical approach enabled the acquisition of valid results, despite low detection frequencies. This is due to the left censored regression approach which addresses the issue of non-detects in real-time quantitative PCR data, also referred to as censored values. In many studies, non-detects are substituted or discarded, to be able to use the remaining abundance data (Karkman et al. 2016; Dungan, Strausbaugh, and Leytem 2019). However, this can lead to false conclusions, as non-detects do not imply that the target sequence does not occur or is present at similar levels in all samples. It merely implies that its concentration lies below the detection threshold and is, thus, not measurable (McCall et al. 2014). Deleting non-detects, can also notably falsify statistical outcomes, as the proportion of censored values and uncensored values is a statistically important information (Helsel 2011). In fact, ignoring data points from non-detects has led to severe consequences in the past. For instance, NASA statisticians failed to include censored data in their analysis on the correlation between temperature and O-ring (component of the rocket booster necessary for sealing in gas) failure, which

contributed to the death of seven people (Helsel 2011; Rogers et al. 1986). However, as non-detects were addressed properly in the present study, the results on land use practices and soil properties, affecting the abundance of medically relevant ARGs and MGEs in soil are robust and provide reliable information about effectors of the soil resistome. Due to the fact that three different geographic regions (located up to 700 km apart) were considered, the determined effectors potentially do not solely apply to specific environments, but rather influence the soil resistome in general. The identified effectors include land use type (grassland or forest), nitrogen input from organic fertilization, mowing frequency, soil pH and water content, forest soil fungal diversity as well as dominant tree type in forests.

It was found that the abundance of all target ARGs and MGEs, except the two beta-lactamase genes, were significantly elevated in grassland soils in comparison to forest soils. This may be explained by a higher pH (Chapter 3.2 Table S1), and a concomitant shift in microbial community composition in grassland soils, which is considered, as stated previously, the primary driver of the soil resistome (Forsberg et al. 2014). However, the closer proximity of grasslands to anthropogenic activities, including the use of antibiotics in human and veterinary medicine, could also play an important role. This assumption is supported by the significantly positive impact of organic nitrogen input through organic fertilization on the abundances of *mefA* and *sul2*, identified in this thesis. The abundances of these resistance genes are most likely increased in organically fertilized soils, as elevated amounts of antibiotic resistant bacteria (ARBs) and ARGs in manure, caused by selective pressure within the gastro-intestinal system of treated livestock, get in contact with the soil microbial community (DeFrancesco et al. 2004). In fact, livestock waste contains more (pig and chicken manure) or similar (cattle manure) amounts of ARGs in comparison to hospital waste (Figure 4) (He et al. 2020). To decrease this excessive ARG concentration in livestock manure, treatment processes, such as anaerobic digestion, have previously proven effective (He et al. 2020; Sun et al. 2016) and should therefore be applied more regularly.

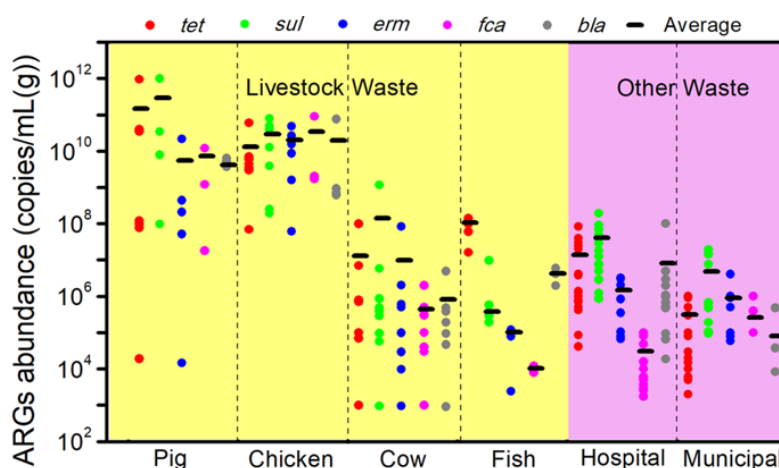


Figure 4 Abundance of selected ARGs in different livestock wastes versus hospital and municipal waste.

The figure was adopted from He et al. 2020. Further information regarding the depicted genes can be derived from tables S2 and S5 of the same study.

Abbreviations: *tet*, tetracycline resistance genes; *sul*, sulfonamide resistance genes; *erm*, MLS resistance genes; *fca*, fluoroquinolone resistance genes, *bla*, β -lactam resistance genes.

Another important aspect is that applied antibiotic substances are, to a large extent, excreted functionally by treated animals, accumulate in manure and thus potentially establish a selective pressure. This promotes the acquisition and maintenance of resistance mechanisms with respect to the soil microbiome (Berendsen et al. 2015; Holman, Yang, and Alexander 2019; United States Pharmacopeial Convention. 2007). To receive indications about veterinary practices which may be problematic in terms of accumulation of medically relevant ARGs in the soil resistome, a survey was conducted with German veterinarians dealing with commonly applied antibiotic substances for the treatment of livestock. In this context, evidence indicating that the *mefA* abundance in soil may be influenced by the application of tulathromycin, used for treatment of bovine respiratory diseases in calves and young cattle, was gathered. The long elimination half-life of this antibiotic appears particularly problematic, as it implies that it persists for longer times in subinhibitory concentrations in the system of the treated animal, which is suspected to promote the development of antibiotic resistance (Blondeau 2005). Additionally, metaphylactic treatment, where an entire group of newly purchased calves is treated when one animal falls sick, is common practice in German conventional cattle farms and probably contributes notably to the amount of utilized tulathromycin. It is therefore reasonable to investigate resistance development upon treatment with antibiotics exhibiting long elimination half-lives more deeply in the future, likely leading to further restrictions for the usage of these antibiotics.

The elevated abundance of *sul2* in organically fertilized soils may be linked to the wide prescription range for sulfonamide antibiotics, as this leads to the application of these substances against a huge variety of different conditions in cattle. Sulfonamide resistances usually apply to all substances of this antibiotic family (Werckenthin and Schwarz 2003). Therefore, it is advisable to reconsider the prescription range for a selection of these substances in order to prevent the development of sulfonamide resistant human pathogens. Generally, the input of veterinary antibiotics, ARGs and ARBs into the soil microbial community could be limited best by decreasing the practice of factory farming which is associated with a higher risk of infection and thus a more frequent application of antibiotics (Anomaly 2015; Pluhar 2010). Furthermore, less factory farming would additionally decrease the amount of produced manure which is applied onto fields. At the same time, this would limit changes in the soil microbial community which could potentially be evoked through contact with the gut microbial bacteria of untreated animals (Udikovic-Kolic et al. 2014).

With respect to the abundance of the aminoglycoside resistance gene *aac(6')-Ib*, we determined a positive correlation with mowing frequency. A possible explanation for this correlation could be the uptake and accumulation of antibiotics by plants and the resulting development of resistant endophytes that may come into contact with the soil microbial community when plants are cut (Lillenberg et al. 2010; Hu, Zhou, and Luo 2010). Additionally, plants can release toxic aromatic compounds, root exudates, signaling molecules and antimicrobial substances upon mowing, which possibly induce elevated expression of ARGs by the soil microbial community (Alonso, Sanchez, and Martinez 2001; Yergeau et al. 2014). Antibiotic substances, distributed in the environment via surface water run offs, dust or wild animals, may also be involved in resistance development in areas which are not directly exposed to manure, and could therefore contribute to an increase in the abundance of *aac(6')-Ib* and other ARGs (Allen et al. 2010).

Looking at the forest samples, it was determined that the beta-lactamase gene *bla_{IMP-12}* is more abundant at sites with beech trees and a high fungal diversity. The gene product of *bla_{IMP-12}* is an enzyme that cleaves aminopenicillins, carbapenems and cephalosporins (Docquier et al. 2003), the latter being synthesized by the filamentous fungus *Acremonium chrysogenum* (Burton and Abraham 1951; Pöggeler, Hoff, and Kück 2008). The natural synthesis of antibiotics by soil fungi as a means to take up nutrients from lysed bacterial cells when many competitors for resources are on site, evidently

contributes to an increased *bla*_{IMP-12} abundance. Furthermore, the connectedness between the soil fungal community and the dominant tree species (Goldmann et al. 2015) is indicated, as both, beech trees and a high fungal diversity, affect *bla*_{IMP-12} abundance.

In summary, this study investigates how abundances of genes conferring antibiotic resistance vary between soils affected by different land use types and practices. This includes antibiotics, such as aminoglycosides, macrolides, aminopenicillins, carbapenems and cephalosporins, all classified as critically important antibiotics for human health, as well as tetracyclines and sulfonamides, classified as highly important for human health (World Health Organisation 2019). In future studies, genes conferring resistances to further critically important antibiotics, such as glycopeptides (e.g. vancomycin) or phosphonic acid antibiotics (e.g. fosfomycin), should be investigated comprehensively. Glycopeptide and phosphonic acid antibiotics are generally not authorized in veterinary medicine for food producing animals in Germany (Silley and Stephan 2017), yet their abundance may still be elevated due to organic fertilization. The integration of intestinal bacteria of untreated livestock through application of manure into the soil microbiome has previously been shown to increase the abundance of genes conferring resistance against a variety of antibiotics, including vancomycin (Udikovic-Kolic et al. 2014; Hu et al. 2016). Furthermore, antibiotic treatment of livestock with a specific antibiotic could still elevate the abundance of genes conferring resistances against other antimicrobials, as MGEs, such as the IncP-1 plasmids can accumulate ARGs of many different classes (Popowska and Krawczyk-Balska 2013). In the light of our findings, the mentioned effect is particularly relevant since the abundance of the quantified IncP-1 plasmids and class 1 integrons was significantly elevated in grasslands.

6.2. Novel sulfonamide and tetracycline resistance genes from forest and grassland soils

Function-based metagenomic screenings are still the only means to identify entirely novel classes of genes and do not depend on prior information about related gene products, as it is the case for sequence-based approaches (Simon and Daniel 2011). Therefore, forest and grassland soil metagenomic libraries from sampling sites of the Schorfheide-Chorin and Schwäbische-Alb exploratories were subjected to function-based screenings for novel sulfonamide and tetracycline resistance genes. Four sulfonamide and four tetracycline resistance determinants showing only 46-

76% identity to known proteins from a variety of different taxa were identified. The respective range of taxa includes dominant gram-negative and gram-positive phyla (*Proteobacteria*, *Bacteroidetes* and *Actinobacteria*) previously detected in soils of the sampling sites by Kaiser et al. (2016). This underlines the efficiency of *Escherichia coli* as host for expression of ARGs from distinct origins. Nevertheless, a different expression host could potentially lead to the identification of some specific candidates that cannot be expressed by *E. coli*. The gram-positive *Bacillus subtilis* would be a promising candidate, as it is an established heterologous expression host (Cui et al. 2018) and belongs to the phylum of the *Firmicutes*, which includes the human pathogenic species *Staphylococcus aureus* and *Clostridium difficile*. Even though Forsberg et al. (2014) previously found that *E. coli* can express ARGs from *Firmicutes*, it remains doubtful that all possible resistance determinants can be found when functional screenings are performed exclusively with this species. Thus, considering other expression strains during metagenomic library screening potentially contributes to the development of a more holistic picture of the unexplored parts of the soil resistome.

The identified tetracycline resistance genes all code for major facilitator superfamily (MFS) efflux pumps which are mostly monomeric transporters that can extrude harmful substances out of the bacterial cell (Pasqua et al. 2019). Another study, in which soil metagenomic libraries were screened for tetracycline resistance genes, also identified MFS pumps as main resistance determinants (Wang et al. 2017). Together with our findings this indicates that these efflux pumps are a common tetracycline resistance mechanism in soil microbial communities in general. This is not surprising, as MFS pumps are the most abundant and diverse group of transporters throughout all domains of life (Du et al. 2018). They function not only as drug efflux pumps but are also extremely versatile due to a wide range of different substrates (Pasqua et al. 2019). MFS pumps can confer resistance against different classes of antibiotics and, due to their frequent occurrence on plasmids, may even spread throughout microbial communities via horizontal gene transfer (HGT) (Pasqua et al. 2019; Xian-Zhi and Nikaido 2009; Shi et al. 2018). Furthermore, specific MFS pumps can extrude several antibiotics out of the bacterial cell and are therefore classified as multidrug efflux (MDR) pumps (Du et al. 2018). Nevertheless, in this thesis, cross-resistance could only be observed for one candidate gene, where a fourfold increase in the minimal inhibitory concentration of lincomycin was measured. Other than that, the identified MFS transporters are tetracycline-specific which does not necessarily imply that they confer resistance to all

antibiotics of the tetracycline class. In fact, (semi-)synthetic substances, such as tigecycline, omadacycline and eravacycline were recently designed and are functional against strains, resistant to other tetracycline representatives (Grossman 2016). Due to the recurrent tetracycline resistance of human pathogens, these (semi-)synthetic substances are mostly applied in the clinical frame nowadays (Grossman 2016). Hence, the effectivity of the here discovered MFS pumps against these tetracyclines is of interest and would provide information regarding their medical relevance. Furthermore, functional screenings for novel resistances towards the new (semi-)synthetic tetracycline substances in soil metagenomic libraries may provide information about further potentially clinically relevant ARGs of the future. One example for such a medically relevant resistance determinant with environmental origin is a flavin-dependent monooxygenase, encoded by *tetX*, which degrades tetracyclines, including tigecycline (Moore, Hughes, and Wright 2005). Notably, *tetX* was first discovered on transposons, harbored by *Bacteroides fragilis*, which is a commensal bacterium of the human colon (Speer, Bedzyk, and Salyers 1991; Huang, Lee, and Mazmanian 2011). However, highly homologous genes are encoded by bacteria colonizing soil (*Cytophaga hutchinsonii*, *Streptomyces coelicolor*, and *Streptomyces avermitilis*) which indicates that *tetX* evolved in this habitat and has potentially been mobilized (Yang et al. 2004).

All four sulfonamide resistance genes, identified in this study, encode a dihydropteroate synthase (DHPS). DHPSs catalyze the synthesis reaction from para-aminobenzoic acid (pABA) and dihydropteroate diphosphate to dihydropteroic acid in the folic acid synthesis pathway (Bermingham and Derrick 2002). Sulfonamides are synthetic antibiotics which competitively inhibit DHPSs because they are structural analogues of pABA (Sammes and Taylor 1990). Since folic acid is a coenzyme for synthesis reactions of purines, pyrimidines, and methionine, sulfonamides lead to the impairment of vital metabolic functions, such as DNA synthesis (Tibbetts and Appling 2010; Revuelta et al. 2018; Maddison, Watson, and Elliott 2008). Resistance against these antibiotic substances develops relatively fast and is mostly conferred through alternative DHPS variants (Sköld 2000). So far, four DHPS variants (*sul1-4*) are known to confer acquired sulfonamide resistance (Jiang et al. 2019). They are encoded on mobilizable or conjugative plasmids of different incompatibility groups and class 1 integrons (Jiang et al. 2019). Previous findings suggest that *sul1-2*, *sul3* and *sul4* were decontextualized by mobilizing the corresponding chromosomally encoded DHPS gene (*folP*) from *Rhodobiaceae*, *Leptospiraceae* and

Chloroflexi, respectively (Sánchez-Osuna et al. 2019; Razavi et al. 2017). The mobilization events most likely took place upon selective pressure established through pollution with antimicrobials, as shown for *sul4* (Razavi et al. 2017). Interestingly, the resistance of the *folP* variants which potentially represent the origin of *sul1-3*, is suspected to predate the discovery of antibiotics, suggesting that bacterial pan-genomes also encode for resistance mechanisms against synthetic antibiotics, prior to their discovery and application (Sánchez-Osuna et al. 2019). Sánchez-Osuna et al. (2019) explain this observation with other fitness benefits that are provided by the mutational changes which confer resistance as a side effect. The here reported findings substantiate this theory, as non-mobile sulfonamide resistance genes with distinct phylogenetic relation were identified in metagenomic DNA from forest soil without history of exposure to these synthetic drugs (Chapter 4 Figure 2, chapter 4.1 Table S1). This further underlines the relevance of functional screenings for genes conferring resistance against synthetic or semi-synthetic antimicrobial substances in soil metagenomic libraries. In addition to tigecycline, the synthetic fluoroquinolones or semi-synthetic derivatives of chloramphenicol (e.g. florfenicol) would be a logical choice for screening agents, as corresponding resistances against these critically important antibiotics are especially relevant (World Health Organisation 2019).

The inserts, harboring one MFS pump and one DHPS, encode potential gene products which show similarity to an endonuclease and a superfamily 2 helicase, respectively. It is possible that these gene products contribute to HGT, yet the evidence is vague and requires further investigations. To receive more stable evidence for possible mobilization of the resistance determinants, it would, therefore, be reasonable to perform functional screenings with fosmid or cosmid vectors, in addition to plasmid libraries. These vectors can integrate much larger DNA fragments (up to ~ 40 kb), rendering the investigation of genes flanking ARGs for evidence of mobilization more promising (Taupp, Mewis, and Hallam 2011). Furthermore, large-insert metagenomic libraries would provide an opportunity to identify resistance determinants which cannot be detected by applying functional screenings of plasmid libraries. One reason for this is that regulator genes often control the expression of the resistant phenotype and can easily be lost in plasmid libraries, possibly rendering ARGs dysfunctional (Depardieu et al. 2007; Du et al. 2018). Furthermore, multimeric resistance determinants which are encoded by more than one open reading frame, like MDR pumps of the resistance nodulation division (RND) superfamily, could potentially be identified more frequently (Du et al. 2018).

6.3. Antibiotic resistance properties and lifestyle features of

Ca. Udaeobacter

As Forsberg et al. (2014) determined that the composition of the soil resistome correlates with the taxonomic structure of the corresponding microbial community, in this study, a globally abundant soil verrucomicrobial genus was analyzed to deepen our understanding of this correlation. The respective genus, *Ca. Udaeobacter*, can make up more than 30% of 16S rRNA gene sequences present in soil, with particularly high abundances in grassland soils (Figure 5) (Brewer et al. 2016).

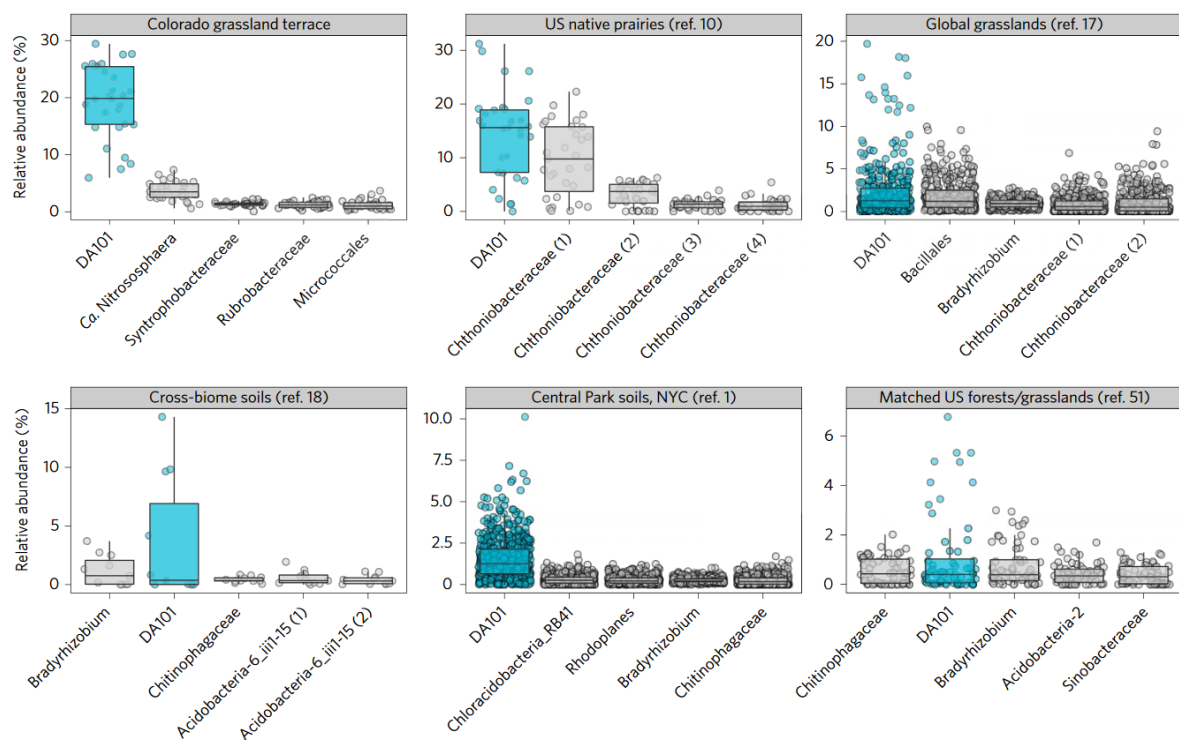


Figure 5 relative 16S rRNA gene abundance of the major five bacterial phylotypes across >1000 soils. *Ca. Udaeobacter* representatives sharing 99% 16S rRNA gene sequence identity with the ribosomal clone “DA101” are colored blue and labeled as DA101. Other taxa are indicated in grey. Taxa are listed on the x axis in decreasing order of their median value (mid-line of each box). The upper and lower edge of the box represent the 25th and 75th percentiles, respectively and the whiskers indicate the range of points, excluding outliers. The figure was adapted from Brewer et al. (2016). Information on considered data sets from previously published studies are provided in Supplementary Table 1 of Brewer et al. (2016) and in the respective references in the publication.

In general, *Verrucomicrobia* have long been under-recognized in studies dealing with the composition of soil microbial communities, as the majority of commonly used PCR primers do not match

their 16S rRNA genes during amplification (Bergmann et al. 2011). This, and the fact that no isolate is available for detailed physiological analysis, are the reasons for the limited amount of information about this bacterial genus. Current knowledge is primarily based on a single reconstructed genome of a phylotype termed *Ca. Udaeobacter copiosus* (Brewer et al. 2016). Conspicuously, this genome is, based on the current state of studies, unusually small (estimated size, ~2.81 Mbp) in comparison to other cosmopolitan soil bacteria (Brewer et al. 2016). It was therefore hypothesized that *Ca. Udaeobacter* species might have undergone genome streamlining whereby they have reduced energetically expensive metabolic pathways to increase efficiency for a life dependent on extracellular metabolites (Brewer et al. 2016).

Our investigation has provided more specific information regarding the previously proposed lifestyle of *Ca. Udaeobacter* species. We found that representatives of *Ca. Udaeobacter* benefit from release of antibiotics in soil, as they are multi-resistant and most likely utilize nutrients released by antibiotic-driven cell lysis, without having to bear the metabolic cost of antibiotic synthesis themselves.

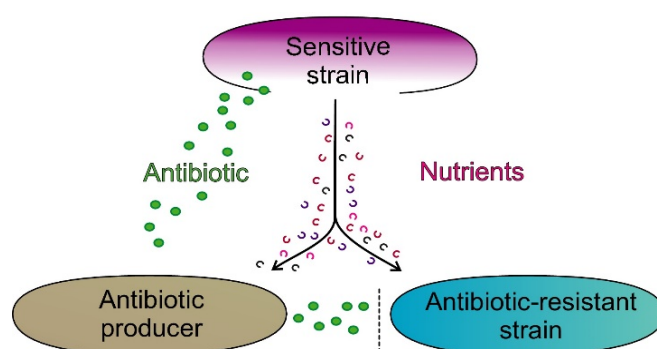


Figure 6 Overview of nutritional effect by antibiotic-driven predation on antibiotic-resistant cheater cells.

The figure was adapted from Leisner et al. (2016).

Bacteria, pursuing such a scavenging lifestyle are designated as antibiotic-resistant cheater cells (Figure 6) (Leisner, Jørgensen, and Middelboe 2016). With respect to *Ca. Udaeobacter* this hypothetical lifestyle is supported by significant growth of bacteria belonging to this genus, as a response to treatment of soil with highly concentrated mixtures of up to six different antibiotics.

Moreover, amino acid permeases and serine/threonine exchangers, vitamin B1, B12 and B9 salvage pathways and vitamin B12 importer proteins were identified upon investigation of a MAG derived from a representative of *Ca. Udaeobacter*, (referred to as *Ca. Udaeobacter* sp. in the following), which shows increased abundance after antibiotic treatment. These salvage pathways and transporter proteins support the hypothesis that *Ca. Udaeobacter* benefits from nutrients (e.g. vitamins and amino acids) released from antibiotic-driven cell lysis. Furthermore, several ARGs were detected, providing protection against released antibiotics. Especially MDR pumps, macrolide efflux pumps and beta-

lactam resistance genes are enriched in the genome of this organism (Chapter 5.1 Table S5). This finding is consistent with results of Forsberg et al. (2014), according to which soil-dwelling *Verrucomicrobia* encode a variety of beta-lactam resistance genes. Another protective mechanism against antibiotics, encoded by the MAG, constitutes the glyoxylate bypass, copper/zinc superoxide dismutase and the catalase-peroxidase as means against oxidative stress caused by bactericidal antibiotics (Chapter 5) (Kohanski et al. 2007; Vinogradov and Grivennikova 2016; Ahn et al. 2016). The glyoxylate bypass also enables *Ca. Udaeobacter* to grow exclusively on substrates such as acetate, fatty acids, or ketogenic amino acids by skipping the oxidative decarboxylation steps of the TCA cycle (Dolan and Welch 2018) and thereby contributes to survival in the highly variable soil environment. Other features, which potentially contribute to survival in soils globally, are the biosynthetic arginine decarboxylase and putative lysine decarboxylase, conferring protection against acidic conditions. These two mechanisms may explain why the microcosms with acidic forest soils harbored a higher *Ca. Udaeobacter* abundance than those based on neutral grassland soils (Chapter 5.1 Figure S1 and Table S1). Contrary to this finding, Brewer et al. (2016) previously reported that *Ca. Udaeobacter* occurs in higher abundance in grassland than in forest soils (Brewer et al. 2016). Therefore, it would be interesting to analyze this trend more carefully in the future. This will be possible through the use of the quantitative real-time PCR primers, specifically targeting *Ca. Udaeobacter*, designed and validated in this study.

A further probable lifestyle feature of *Ca. Udaeobacter* sp., is the aerobic oxidization of atmospheric H₂ to sustain electron input into the respiratory chain at nutrient deprived conditions. This was found in the here reported MAG, and may also contribute to the high abundance of the corresponding genus in soils globally. In this context, *Ca. Udaeobacter* sp. encodes two machineries, a membrane bound NiFeS-hydrogenase, consisting of a small and large subunit, which is coupled to electron transport chains, and a soluble cytoplasmic bidirectional NAD-reducing hydrogenase (Friedrich and Schwartz 1993; Greening et al. 2016) (Chapter 5). It was recently validated that H₂ scavenging is performed by several soil-dwelling species of *Actinobacteria* (Greening, Constant, et al. 2015). In addition, this has also been described for verrucomicrobial methanotrophs colonizing geothermally influenced surface soils (Carere et al. 2017). Based on the identification of membrane bound NiFe-hydrogenases encoded by genomes of a variety of different soil bacteria it was hypothesized, that H₂-

oxidation is a widely distributed attribute of soil-dwelling prokaryotes (Greening et al. 2015). However, until now the here provided information is, to our knowledge, the first evidence linking hydrogenase genes specifically to the genus *Ca. Udaeobacter*.

The 16S rRNA gene coverage of *Ca. Udaeobacter* sp. indicates that a single gene copy is present in the genome, which is consistent with previous predictions (Brewer et al. 2016; Větrovský and Baldrian 2013). Hence, the high fraction of *Ca. Udaeobacter* 16S rRNA genes in soil seems to derive from a high cell density instead of a high 16S rRNA gene copy number per cell. This is particularly relevant with respect to the global soil resistome as it consequently can be assumed that a high proportion of ARGs is encoded by *Ca. Udaeobacter* representatives. Even if the true average genome size of *Ca. Udaeobacter* representatives lies somewhere between ~ 2.81 Mbp (*Ca. Udaeobacter copiosus*) and ~3.67 Mbp (*Ca. Udaeobacter* sp.), the size difference compared to the estimated average genome size of soil bacteria (4.74 Mbp) (Brewer et al. 2016) does not relativize the here assumed huge proportion of *Ca. Udaeobacter* ARGs in the global soil resistome. In fact, *Ca. Udaeobacter* relative abundance is frequently more than two times higher than of other phylotypes and can even increase 100-fold upon addition of antibiotics (Chapter 5.1 Figure S1 and Table S3; Figure 5).

Regarding the clinical relevance of ARGs carried by *Ca. Udaeobacter*, no resistance gene of pathogenic bacteria with a phylogenetic relation to this genus has been identified so far. However, absence of evidence does not mean evidence of absence. In fact, even though the ARGs encoded by *Ca. Udaeobacter* sp. are not encoded in synteny with MGEs, mobilization upon environmental antibiotic pollution and spread to pathogenic strains is possible, as it was likely the case for *sul1-4* (Chapter 6.2) (Sánchez-Osuna et al. 2019; Razavi et al. 2017). Moreover, our results indicate that proximity to antibiotic usage entails a higher abundance of IncP-1 plasmids and class 1 integrons (Chapter 4 and 6.1), increasing the chance for gene mobilization. Additionally, antibiotics release in soil lead to a significant increase in *Ca. Udaeobacter* abundance in our microcosm experiment, suggesting that these organisms likely represent winners of antimicrobial pollution. Taken together, antibiotic pollution of the soil environment leads to a high probability for mobilization of ARGs from *Ca. Udaeobacter* species, underlining the importance for in-depth studies of these organisms along with their resistance genes. Overall, the here presented lifestyle features along with the designed real-time quantitative PCR primers

will be valuable for future investigations and may contribute to the successful development of a cultivation approach for members of this genus.

6.4. Literature

- Ahn S, Jung J, Jang IA, Madsen EL, Park W. 2016. Role of Glyoxylate Shunt in Oxidative Stress Response. *J Biol Chem* 291:11928–11938.
- Allen HK, Donato J, Wang HH, Cloud-Hansen KA, Davies J, Handelsman J. 2010. Call of the wild: antibiotic resistance genes in natural environments. *Nat Rev Microbiol* 8:251–259.
- Alonso A, Sanchez P, Martinez JL. 2001. Environmental selection of antibiotic resistance genes. *Environ Microbiol* 3:1–9.
- Anomaly J. 2015. What's Wrong With Factory Farming? *Public Health Ethics* 8:246–254.
- Bengtsson-Palme J, Kristiansson E, Larsson DGJ. 2018. Environmental factors influencing the development and spread of antibiotic resistance. *FEMS Microbiol Rev* 42: fux053.
- Berendsen BJA, Weh RS, Memelink J, Zuidema T, Stolker LAM. 2015. The analysis of animal faeces as a tool to monitor antibiotic usage. *Talanta* 132:258–268.
- Bergmann GT, Bates ST, Eilers KG, Lauber CL, Caporaso JG, Walters WA, Knight R, Fierer N. 2011. The under-recognized dominance of *Verrucomicrobia* in soil bacterial communities. *Soil Biol Biochem* 43:1450–1455.
- Bermingham A, Derrick JP. 2002. The Folic Acid Biosynthesis Pathway in Bacteria: Evaluation of Potential for Antibacterial Drug Discovery. *Bioessays* 24:637-648.
- Blondeau J. 2005. Differential impact of macrolide compounds in the selection of macrolide nonsusceptible *Streptococcus pneumoniae*. *Therapy* 2:813–818.
- Brewer TE, Handley KM, Carini P, Gilbert JA, Fierer N. 2016. Genome reduction in an abundant and ubiquitous soil bacterium '*Candidatus Udaeobacter copiosus*'. *Nat Microbiol* 2:16198.
- Burton HS, Abraham EP. 1951. Isolation of antibiotics from a species of *Cephalosporium*. Cephalosporins P₁, P₂, P₃, P₄ and P₅. *Biochem J* 50:168–174.
- Cambau E, Saunderson P, Matsuoka M, Cole ST, Kai M, Suffys P, Rosa PS, Williams D, Gupta UD, Lavania M, Cardona-Castro N, Miyamoto Y, Hagge D, Srikantam A, Hongseng W, Indropo A,

- Vissa V, Johnson RC, Cauchoix B, Pannikar VK, Cooreman EAWD, Pemmaraju VRR, Gillini L, WHO surveillance network of antimicrobial resistance in leprosy. 2018. Antimicrobial resistance in leprosy: results of the first prospective open survey conducted by a WHO surveillance network for the period 2009–15. *Clin Microbiol Infect* 24:1305–1310.
- Carere CR, Hards K, Houghton KM, Power JF, McDonald B, Collet C, Gapes DJ, Sparling R, Boyd ES, Cook GM, Greening C, Stott MB. 2017. Mixotrophy drives niche expansion of verrucomicrobial methanotrophs. *ISME J* 11:2599–2610.
- Cui W, Han L, Suo F, Liu Z, Zhou L, Zhou Z. 2018. Exploitation of *Bacillus subtilis* as a robust workhorse for production of heterologous proteins and beyond. *World J Microbiol Biotechnol* 34:145.
- DeFrancesco KA, Cobbold RN, Rice DH, Besser TE, Hancock DD. 2004. Antimicrobial resistance of commensal *Escherichia coli* from dairy cattle associated with recent multi-resistant salmonellosis outbreaks. *Vet Microbiol* 98:55–61.
- Depardieu F, Podglajen I, Leclercq R, Collatz E, Courvalin P. 2007. Modes and Modulations of Antibiotic Resistance Gene Expression. *Clin Microbiol Rev* 20: 79–114.
- Docquier J-D, Riccio ML, Mugnaioli C, Luzzaro F, Endimiani A, Toniolo A, Amicosante G, Rossolini GM. 2003. IMP-12, a New Plasmid-Encoded Metallo- β -Lactamase from a *Pseudomonas putida* Clinical Isolate. *Antimicrob Agents Chemother* 47:1522–1528.
- Dolan SK, Welch M. 2018. The Glyoxylate Shunt, 60 Years On. *Annu Rev Microbiol* 72:309–330.
- Du D, Wang-Kan X, Neuberger A, van Veen HW, Pos KM, Piddock LJV, Luisi BF. 2018. Multidrug efflux pumps: structure, function and regulation. *Nat Rev Microbiol* 16:523-539.
- Dungan RS, Strausbaugh CA, Leytem AB. 2019. Survey of selected antibiotic resistance genes in agricultural and non-agricultural soils in south-central Idaho. *FEMS Microbiol Ecol* 95:fiz071.
- Forsberg KJ, Patel S, Gibson MK, Lauber CL, Knight R, Fierer N, Dantas G. 2014. Bacterial phylogeny structures soil resistomes across habitats. *Nature* 509:612–616.
- Friedrich B, Schwartz E. 1993. Molecular Biology of Hydrogen Utilization in Aerobic Chemolithotrophs. *Annu Rev Microbiol* 47:351–383.

- Goldmann K, Schöning I, Buscot F, Wubet T. 2015. Forest Management Type Influences Diversity and Community Composition of Soil Fungi across Temperate Forest Ecosystems. *Front Microbiol* 6:1300.
- Greening C, Biswas A, Carere CR, Jackson CJ, Taylor MC, Stott MB, Cook GM, Morales SE. 2016. Genomic and metagenomic surveys of hydrogenase distribution indicate H₂ is a widely utilised energy source for microbial growth and survival. *ISME J* 10:761–777.
- Greening C, Carere CR, Rushton-Green R, Harold LK, Hards K, Taylor MC, Morales SE, Stott MB, Cook GM. 2015. Persistence of the dominant soil phylum *Acidobacteria* by trace gas scavenging. *Proc Natl Acad Sci U S A* 112:10497–10502.
- Greening C, Constant P, Hards K, Morales SE, Oakeshott JG, Russell RJ, Taylor MC, Berney M, Conrad R, Cook GM. 2015. Atmospheric Hydrogen Scavenging: from Enzymes to Ecosystems. *Appl Environ Microbiol.* 81:1190-1199.
- Grossman TH. 2016. Tetracycline Antibiotics and Resistance. *Cold Spring Harb Perspect Med* 6:a025387.
- He Y, Yuan Q, Mathieu J, Stadler L, Senehi N, Sun R, Alvarez PJJ. 2020. Antibiotic resistance genes from livestock waste: occurrence, dissemination, and treatment. *npj Clean Water* 3:4.
- Helsel DR. 2011. *Statistics for Censored Environmental Data Using Minitab® and R*, 2nd ed. John Wiley & Sons, Inc., Hoboken, NJ, USA.
- Holman DB, Yang W, Alexander TW. 2019. Antibiotic treatment in feedlot cattle: a longitudinal study of the effect of oxytetracycline and tulathromycin on the fecal and nasopharyngeal microbiota. *Microbiome* 7:86.
- Hu H-W, Han X-M, Shi X-Z, Wang J-T, Han L-L, Chen D, He J-Z. 2016. Temporal changes of antibiotic-resistance genes and bacterial communities in two contrasting soils treated with cattle manure. *FEMS Microbiol Ecol* 92:fiv169.
- Hu X, Zhou Q, Luo Y. 2010. Occurrence and source analysis of typical veterinary antibiotics in manure, soil, vegetables and groundwater from organic vegetable bases, northern China. *Environ Pollut* 158:2992–2998.

- Huang JY, Lee SM, Mazmanian SK. 2011. The human commensal *Bacteroides fragilis* binds intestinal mucin. *Anaerobe* 17:137–141.
- Jiang H, Cheng H, Liang Y, Yu S, Yu T, Fang J, Zhu C. 2019. Diverse Mobile Genetic Elements and Conjugal Transferability of Sulfonamide Resistance Genes (*sul1*, *sul2*, and *sul3*) in *Escherichia coli* Isolates From *Penaeus vannamei* and Pork From Large Markets in Zhejiang, China. *Front Microbiol* 10:1787.
- Kaiser K, Wemheuer B, Korolkow V, Wemheuer F, Nacke H, Schöning I, Schrumpf M, Daniel R. 2016. Driving Forces of Soil Bacterial Community Structure, Diversity, and Function in Temperate Grasslands and Forests. *Sci Rep* 6:33696.
- Karkman A, Johnson TA, Lyra C, Stedtfeld RD, Tamminen M, Tiedje JM, Virta M. 2016. High-throughput quantification of antibiotic resistance genes from an urban wastewater treatment plant. *FEMS Microbiol Ecol* 92:fiw014.
- Kohanski MA, Dwyer DJ, Hayete B, Lawrence CA, Collins JJ. 2007. A Common Mechanism of Cellular Death Induced by Bactericidal Antibiotics. *Cell* 130:797–810.
- Leisner JJ, Jørgensen NOG, Middelboe M. 2016. Predation and selection for antibiotic resistance in natural environments. *Evol Appl* 9:427–434.
- Lillenberg M, Litvin SV, Nei L, Roasto M, Sepp KI. 2010. Enrofloxacin and ciprofloxacin uptake by plants from soil. *Agron. Res.* 8:807-814.
- Maddison JE, Watson ADJ, Elliott J. 2008. Antibacterial drugs, p. 148–185. *In* *Small Animal Clinical Pharmacology*, 2nd ed. Saunders.
- McCall MN, McMurray HR, Land H, Almudevar A. 2014. On non-detects in qPCR data. *Bioinformatics* 30:2310–2316.
- Mina N V., Burdz T, Wiebe D, Rai JS, Rahim T, Shing F, Hoang L, Bernard K. 2011. Canada's first case of a Multidrug-Resistant *Corynebacterium diphtheriae* strain, Isolated from a Skin Abscess. *J Clin Microbiol* 49:4003–4005.
- Moore IF, Hughes DW, Wright GD. 2005. Tigecycline is modified by the flavin-dependent

- monooxygenase TetX. *Biochemistry* 44:11829–11835.
- Partridge SR, Kwong SM, Firth N, Jensen SO. 2018. Mobile Genetic Elements Associated with Antimicrobial Resistance. *Clin Microbiol Rev* 31:e00088-17.
- Pasqua M, Grossi M, Zennaro A, Fanelli G, Micheli G, Barras F, Colonna B, Prosseda G. 2019. The Varied Role of Efflux Pumps of the MFS Family in the Interplay of Bacteria with Animal and Plant Cells. *Microorganisms* 7:285.
- Pluhar EB. 2010. Meat and Morality: Alternatives to Factory Farming. *J Agric Environ Ethics* 23:455–468.
- Pöggeler S, Hoff B, Kück U. 2008. Asexual Cephalosporin C Producer *Acremonium chrysogenum* Carries a Functional Mating Type Locus. *Appl Environ Microbiol* 74:6006–16.
- Popowska M, Krawczyk-Balska A. 2013. Broad-host-range IncP-1 plasmids and their resistance potential. *Front Microbiol* 4:44.
- Razavi M, Marathe NP, Gillings MR, Flach C-F, Kristiansson E, Joakim Larsson DG. 2017. Discovery of the Fourth Mobile Sulfonamide Resistance Gene. *Microbiome* 5:160.
- Reardon S. 2014. WHO warns against “post-antibiotic” era. *Nature News*.
- Revuelta JL, Serrano-Amatriain C, Ledesma-Amaro R, Jiménez A. 2018. Formation of Folates by Microorganisms: Towards the Biotechnological Production of This Vitamin. *Appl Microbiol Biotechnol* 102: 8613–8620.
- Rogers WP, Armstrong NA, Acheson DC, Covert EE, Feynman RP, Hotz RB, Kutyna DJ, Ride SK, Rummel RW, Sutter JF, Walker ABCJ, Wheelon AD, Yeager CE. 1986. Report to the President By the Presidential Commission On the Space Shuttle Challenger Accident. Washington D.C.
- Runcie H. 2015. Infection in a Pre-Antibiotic Era. *J Anc Dis Prev Rem* 3:2.
- Sammes, P.G., and J.B. Taylor, eds. 1990. *Comprehensive Medicinal Chemistry*. p. 255–270. Oxford, Oxford: Pergamon Press, Oxford, New York.
- Sánchez-Osuna M, Cortés P, Barbé J, Erill I. 2019. Origin of the Mobile Di-Hydro-Pteroate Synthase Gene Determining Sulfonamide Resistance in Clinical Isolates. *Front Microbiol* 10:3332.

- Santajit S, Indrawattana N. 2016. Mechanisms of Antimicrobial Resistance in ESKAPE Pathogens. *Biomed Res Int* 2016: 2475067.
- Shi L, Liang Q, Feng J, Zhan Z, Zhao Y, Yang W, Yang H, Chen Y, Huang M, Tong Y, Li X, Yin Z, Wang J, Zhou D. 2018. Coexistence of Two Novel Resistance Plasmids, *bla*_{KPC-2}-carrying p14057A and *tetA* (A) -carrying p14057B, in *Pseudomonas aeruginosa*. *Virulence* 9:306–311.
- Silley P, Stephan B. 2017. Prudent use and regulatory guidelines for veterinary antibiotics—politics or science? *J Appl Microbiol* 123:1373-1380.
- Simon C, Daniel R. 2011. Metagenomic Analyses: Past and Future Trends. *Appl Environ Microbiol* 77:1153–1161.
- Sköld O. 2000. Sulfonamide Resistance: Mechanisms and Trends. *Drug Resist Updat* 3:155–160.
- Speer BS, Bedzyk L, Salyers AA. 1991. Evidence that a novel tetracycline resistance gene found on two *Bacteroides* transposons encodes an NADP-requiring oxidoreductase. *J Bacteriol* 173:176–183.
- Spigaglia P, Mastrantonio P, Barbanti F. 2018. Antibiotic resistances of *Clostridium difficile*. *Adv in Exp Med* 1050:137-159.
- Sun W, Qian X, Gu J, Wang XJ, Duan ML. 2016. Mechanism and Effect of Temperature on Variations in Antibiotic Resistance Genes during Anaerobic Digestion of Dairy Manure. *Sci Rep* 6:30237.
- Taupp M, Mewis K, Hallam SJ. 2011. The Art and Design of Functional Metagenomic Screens. *Curr Opin Biotechnol* 22:465-72.
- Tibbetts AS, Appling DR. 2010. Compartmentalization of Mammalian Folate-Mediated One-Carbon Metabolism. *Annu Rev Nutr* 30:57–81.
- Udikovic-Kolic N, Wichmann F, Broderick NA, Handelsman J. 2014. Bloom of resident antibiotic-resistant bacteria in soil following manure fertilization. *Proc Natl Acad Sci U S A* 111:15202–15207.
- United States Pharmacopeial Convention. 2007. The United States pharmacopeia 31 ; The national formulary 26. United States Pharmacopeial Convention, Rockville MD.

- Větrovský T, Baldrian P. 2013. The Variability of the 16S rRNA Gene in Bacterial Genomes and Its Consequences for Bacterial Community Analyses. *PLoS One* 8:e57923.
- Vinogradov AD, Grivennikova VG. 2016. Oxidation of NADH and ROS production by respiratory complex I. *Biochim Biophys Acta* 1857:863-71.
- Wang S, Gao X, Gao Y, Li Y, Cao M, Xi Z, Zhao L, Feng Z. 2017. Tetracycline Resistance Genes Identified From Distinct Soil Environments in China by Functional Metagenomics. *Front Microbiol* 8:1406.
- Werckenthin C, Schwarz S. 2003. Kreuzresistenzen: Beurteilung von Antibiotogrammen, Auswahl von antimikrobiellen Wirkstoffen für die in-vitro Empfindlichkeitsprüfung und molekulare Grundlagen. Manuskript zur 22. Arbeits- und Fortbildungstagung Bakteriologie des Arbeitskreises Veterinärmedizinischer Infekt der DVG.
- World Health Organization. 2019. Critically important antimicrobials for human medicine, 6th revision. WHO.
- Xian-Zhi L, Nikaido H. 2009. Efflux-mediated drug resistance in bacteria: an update. *Drugs* 69:1555–623.
- Yang W, Moore IF, Koteva KP, Bareich DC, Hughes DW, Wright GD. 2004. TetX is a flavin-dependent monooxygenase conferring resistance to tetracycline antibiotics. *J Biol Chem* 279:52346–52352.
- Yergeau E, Sanschagrin S, Maynard C, St-Arnaud M, Greer CW. 2014. Microbial expression profiles in the rhizosphere of willows depend on soil contamination. *ISME J* 8:344–358.
- Zaki SA, Karande S. 2011. Multidrug-resistant typhoid fever: A review. *J Infect Dev Ctries* 5:324-337.
- Zignol M, Dean AS, Falzon D, van Gemert W, Wright A, van Deun A, Portaels F, Laszlo A, Espinal MA, Pablos-Méndez A, Bloom A, Aziz MA, Weyer K, Jaramillo E, Nunn P, Floyd K, Raviglione MC. 2016. Twenty Years of Global Surveillance of Antituberculosis-Drug Resistance. *N Engl J Med* 375:1081–1089

7. Appendix

7.1. Declaration of plagiarism

I, Inka Marie Willms, hereby confirm that I wrote the here presented doctoral thesis “**Assessment of antibiotic resistance in soil and its link to different land use types and intensities**” independently, without using any means others than those mentioned in the respective chapters. I did neither seek unauthorized assistance nor did I submit this thesis in any form for another degree at any institution or university. All contributions by other authors to the here included publications are listed before the corresponding manuscripts.

Inka Marie Willms

7.2. Danksagung

Zu aller Erst möchte ich Dr. Heiko Nacke für die Möglichkeit danken in diesem interessanten Projekt promovieren zu können und dafür, dass er mir ständig mit gutem Rat zur Seite stand. Vielen Dank für die zahlreichen Korrekturen, die ständige Bereitschaft zum wissenschaftlichen Austausch und die Unterstützung und das Verständnis bei Problemen aller Art! Ich bin mir sehr bewusst, dass ich großes Glück hatte einen so großartigen Betreuer gehabt zu haben, der mir genug Freiheit gegeben hat meine eigenen Ideen in die Tat umzusetzen und mir genug Halt gegeben hat um mich nicht in der großen weiten Wissenschaft zu verlieren.

Weiterer Dank geht an PD. Dr. Michael Hoppert für die Bereitschaft Co-referent dieser Arbeit zu sein und für sein Interesse an den Ergebnissen. Außerdem möchte ich Prof. Rolf Daniel für die fachliche und verwaltungsbezogene Unterstützung danken, die er diesem Projekt entgegengebracht hat. Natürlich danke ich ebenfalls der restlichen Prüfungskommission für die Durchsicht und Beurteilung meiner Arbeit.

Ohne meine Studenten Anina, Isabell, Jingyue, Melissa, Lisa und Simon, hätte ich die Laborarbeit nicht bewältigen können, die nötig war um die hier analysierten Daten zu erheben. Vielen Dank für eure Arbeit!

Ich danke der kompletten Abteilung der Genomischen und Angewandten Mikrobiologie, für die gute Arbeitsatmosphäre, was die drei Jahre meiner Doktorarbeit zu einem großen Vergnügen gemacht hat! Diesbezüglich möchte ich besonders Dr. Dominik Schneider hervorheben, der diese Arbeit, genauso wie ein weiteres Manuskript korrigiert hat und für bioinformatische Probleme immer ein hervorragender Ansprechpartner war! Lieber Dank geht außerdem an Dr. Birgit Pfeiffer für die emotionale und wissenschaftliche Unterstützung in Form von vielen Gesprächen, die mir durch so manches Doktorarbeitstief geholfen haben! Dr. Anja Poehlein möchte ich für ihre bioinformatische Unterstützung danken und dafür, eine aufmunternde Seele im Büro vorzufinden, die einen das Arbeiten an vielen Tagen um manches erleichtert hat. Ein weiterer, großer Dank geht an Dr. Robert Hertel, ohne den ich gar nicht erst an dieser Stelle stehen würde.

Ganz lieben Dank an Avi, Miriam, Dirko, Tati, Stefani und Ines, für eine schöne Zeit und den großartigen Doktorhüten, die wir zusammen gebastelt haben. Wenigstens haben wir uns nicht nehmen lassen, die Doktorarbeiten angemessen zu zelebrieren, bei denen es möglich war!

Diese Arbeit wäre ebenfalls nie zustande gekommen, wenn ich nicht eine so tolle Familie hätte, die trotz gelegentlicher kleiner und großer Uneinigkeiten immer zusammenhält und sich unterstützt. Besonders möchte ich meiner Mama und Achim, meinen Geschwistern, Antje, Lisa und Anton, mit Florian und Christof, meinem Vater und Andrea, Oma & Opa und Elke & Claus dafür danken ein Teil von mir und dementsprechend dieser Arbeit zu sein.

Zuletzt möchte ich mich von ganzem Herzen bei Oleg bedanken, dass er mich gelehrt hat, dass das Leben keinen Plänen folgt und man sich wegen Angst und Zweifel nicht für Geringeres entscheiden sollte. Außerdem danke ich ihm für den festen Halt, den er mir fortwährend gibt, egal wie rau die See ist.

7.3. Curriculum Vitae of Inka Marie Willms

EDUCATION

May 2017- presumably May 2020	Doctorate student at the Georg-August-University (Göttingen) Department of Genomic and Applied Microbiology First supervisor: Dr. Heiko Nacke
Oct. 2014 - Jan. 2017	Masters degree at the Georg-August-University (Göttingen) Master of Science in "Microbiology and Biochemistry" <ul style="list-style-type: none">• Module Highlights: General and Applied Microbiology, Structural Biochemistry, Biochemistry and Biophysics• Degree: Master of Science – Final Grade 1.3• Thesis: "Physiologic and genomic analysis of <i>Bacillus</i> phages vB- BsuM_Goe2 and vB-BsuM_Goe3" – Grade 1.0
Oct. 2011 - Oct. 2014	Bachelors degree at the Carl von Ossietzky University (Oldenburg) Bachelor of Science in "Environmental Sciences" – Final Grade 1.9 <ul style="list-style-type: none">• Module Highlights: General Microbiology, Environmental Microbiology, Genetics, Bio- and Geochemistry• Thesis: "Generierung dreidimensionaler Darstellungen am Rasterelektronenmikroskop mit Hilfe von Z-Stapeln" – Grade 1.5

ADDITIONAL WORK EXPERIENCE

June 2017- Jan. 2020	Project design for two bachelor and one master thesis projects as well as supervision of four bachelor and two master students in the context of the dissertation
Sept. 2016 Dec. 2016	Internship – Identification of <i>Campylobacter jejuni</i> phage receptor binding proteins University of Copenhagen; Department of Veterinary and Disease Biology
May 2016 - July 2016	Student Research Assistant Georg-August-University; Department of General Microbiology <ul style="list-style-type: none">• Support in teaching and correction of student protocols throughout the bachelor course "General Microbiology"

PUBLICATIONS & CONFERENCE PARTICIPATIONS

Feb. 2020	Submission of first author paper “Globally abundant <i>Candidatus</i> Udaeobacter benefits from release of antibiotics in soil and potentially performs trace gas scavenging” to mSphere.
Jan. 2020	Willms, Yuan, Penone, Goldmann, Vogt, Wubet, Schöning, Schruppf, Buscot, Nacke. 2020. Distribution of Medically Relevant Antibiotic Resistance Genes and Mobile Genetic Elements in Soils of Temperate Forests and Grasslands Varying in Land Use. <i>Genes</i> 11:150.
March 2019	Willms IM, Kamran A, Aßmann NF, Krone D, Bolz SH, Fiedler F, Nacke H. 2019. Discovery of Novel Antibiotic Resistance Determinants in Forest and Grassland Soil Metagenomes. <i>Front Microbiol</i> 10:460.
Feb. 2019	Biodiversity Exploratories Assembly (Wernigerode, Germany) Oral presentation: “Antibiotic resistance and its link to land use” Presentation of poster: “Antibiotic resistance and its link to land use”.
Aug. 2018	ISME17 (Leipzig, Germany) Presentation of poster: “Exploring a cradle of multi-resistant bacteria- antibiotic resistance in soil and its link to different land use types and intensities”.
May 2017	Willms IM, Hoppert M, Hertel R. 2017. Characterization of <i>Bacillus subtilis</i> viruses vB_BsuM-Goe2 and vB_BsuM-Goe3. <i>Viruses</i> 9:146.
Feb. 2018	Biodiversity Exploratories Assembly (Wernigerode, Germany) Oral presentation: “Antibiotic resistance and its link to land use” Presentation of poster: “Antibiotic resistance and its link to land use”.
Sep. 2016	Willms IM, Hertel R. 2016. Phage vB_BsuP-Goe1: The smallest identified lytic phage of <i>Bacillus subtilis</i> . <i>FEMS Microbiol Lett</i> 363: fnw208.
March 2016	VAAM-Conference (Jena, Germany) Presentation of poster: “ <i>Bacillus subtilis</i> phages: new isolates and insights”